Cardiff
Catalysis Institute

Sefydliad Catalysis
Caerdydd

Using Hydrogen Peroxide Derived *In-situ* for Oxidation Reactions: Applications in Greywater Sterilisation and the Development of New Pd-SnO_2 Catalysts

Thesis submitted in accordance with the requirements of Cardiff University for the degree of doctor of philosophy by

Jonathan Huw Harrhy

School of Chemistry

Cardiff University

2017

DECLARATION

This work has not been submitted in substance for any other degree or award at this or any other university or place of learning, nor is being submitted concurrently in candidature for any degree or other award.

Signed …… (candidate) Date ……..……..……

STATEMENT 1

This thesis is being submitted in partial fulfillment of the requirements for the degree of ……(insert MCh, MD, MPhil, PhD etc, as appropriate)

Signed ……..…… (candidate) Date ……..……

STATEMENT 2

This thesis is the result of my own independent work/investigation, except where otherwise stated, and the thesis has not been edited by a third party beyond what is permitted by Cardiff University's Policy on the Use of Third Party Editors by Research Degree Students. Other sources are acknowledged by explicit references. The views expressed are my own.

Signed ……..……..…… (candidate) Date ……..……

STATEMENT 3

I hereby give consent for my thesis, if accepted, to be available online in the University's Open Access repository and for inter-library loan, and for the title and summary to be made available to outside organisations.

Signed ……..…….. (candidate) Date ……

STATEMENT 4: PREVIOUSLY APPROVED BAR ON ACCESS

I hereby give consent for my thesis, if accepted, to be available online in the University's Open Access repository and for inter-library loans **after expiry of a bar on access previously approved by the Academic Standards & Quality Committee.**

Signed ……..…… (candidate) Date ……..……

Summary

This thesis explores a new use for the direct synthesis of hydrogen peroxide (H_2O_2), water sterilisation. The first part of this work seeks to identify if *in-situ* derived H_2O_2 can be used to sterilise household greywater (GW). It was found that H_2O_2 synthesised via the direct synthesis reaction in a continuous flow reactor can remove concentrations of up to 10^9 CFU ml^{-1} of *Escherichia Coli* after only a single pass through the reactor. The effectiveness of *in-situ* generated H_2O_2 was then compared with various *ex-situ* H_2O_2 sources and it was found that:

In-situ ≥ pre-synthesised > commercial unstabilised > commercial stabilised.

The next part of this thesis builds on the findings of the initial work, investigating whether *in-situ* generated H_2O_2 is effective as an antimicrobial agent against recognised standard strains of *Staphylococcus Aureus*, *Escherichia Coli* and *Pseudomonas Aeruginosa*. It was found that a 2-log reduction of *Staphylococcus Aureus* is possible after a single pass through the flow reactor and this can be increased to a maximum of a 3-log reduction by optimising the reaction conditions and using a 1 wt.% AuPd/TiO_2 catalyst. The same result was found for *Escherichia Coli* but only a 1-log reduction was possible in the case of *Pseudomonas Aeruginosa*. Incorporating iron (Fe^{2+} and Fe^{3+}) into the catalyst led to greater antimicrobial activity but catalyst instability was an issue.

In the final part of this thesis, the use of a novel palladium catalyst supported on tin oxide (Pd-SnO_2) for the direct synthesis of H_2O_2 was investigated. It was found that catalysts prepared by impregnation are active for the direct synthesis but in using a novel sol-gel preparation, the catalyst activity is greatly increased. Selectivity towards H_2O_2 was found to be less than PdSn bimetallic catalysts and an ORO heat treatment led to some morphological changes in the sol-gel catalysts but only small changes in the activity and selectivity were observed.

Acknowledgements

I would first like to thank Prof. Graham J. Hutchings FRS for his invaluable guidance and support and giving me the opportunity to work on such an interesting and rewarding PhD project.

I extend my deepest thanks to my co-supervisors. Firstly, Dr Simon J. Freakley for mentoring me throughout my entire PhD and for his corrections of this thesis. Dr Jennifer K. Edwards for her supervision and advice. This thesis would not have been possible without both of your help.

I would like to thank Dr Qian He for the fantastic STEM and EELS analysis of my catalysts. I would also like to gratefully acknowledge Prof. Jean-Yves Maillard for the opportunity to work in his lab for the final year of my project and helping me to get to grips with basic microbiology. I gratefully acknowledge the help of Dr. E. Joel Loveridge for his help and assistance in performing the initial greywater sterilisation tests. I gratefully acknowledge the school of chemistry workshop staff, particularly Steve Morris.

I would like to thank all the PhD students and postdoc's that I have worked with in the CCI, you have all made this experience thoroughly enjoyable. Special thanks go to all of team H_2O_2: Buddha (who I spent more time impersonating than I would care to admit), Rich, Dave, Adeeba and Ouardia, thank you for all your help, working with you all was a pleasure.

I thank all my school friends and team Nike Cardiff for all the great times over the last few years. Team Ironman Wales 2016 for making summer 2016 one of the best I've ever had. Thank you to Giulia for everything you have done over the past months, I really don't think I could have finished this without you. I will look back over the last few years knowing that I have made some amazing memories and you have all played a part in that.

I would like to thank my family: My Granny and Grampy who have always supported me. Mum and Dad, your love and support have kept me going when I really wanted to give up and I will be forever indebted to you for that. Finally, to my Grandma who won't get to see me graduate but always told me how proud she was, this is for you all.

Table of Contents

Chapter 1

Introduction

1. Literature Review

1.1 Catalysis Background and Concepts

Catalysis underpins all aspects of modern society, from transportation to food. It is estimated that over 75% of the world's population owes its existence to catalysis and this is due to what is possibly the greatest scientific breakthrough of the 21st century, the Haber-Bosch process[1]. Without the Haber-Bosch process it would be impossible to synthesise the 130 million tonnes of liquid ammonia that is produced worldwide, most of which is used in the agricultural industry. Indeed, without catalysis society today would be extremely different. The catalyst employed in the Haber-Bosch process is an iron (Fe) based catalyst that is cheap and highly active, it has been shown that ruthenium (Ru) can facilitate the reaction at lower pressures, however these catalysts suffer from poisoning problems and are far costlier, therefore the iron catalysts are still used today.

The accepted definition of a catalyst is a material or substance that provides an increase in the rate of a chemical reaction without modifying the overall standard Gibbs energy change in the reaction[2]. An illustration of this can be seen in figure 1.1 below:

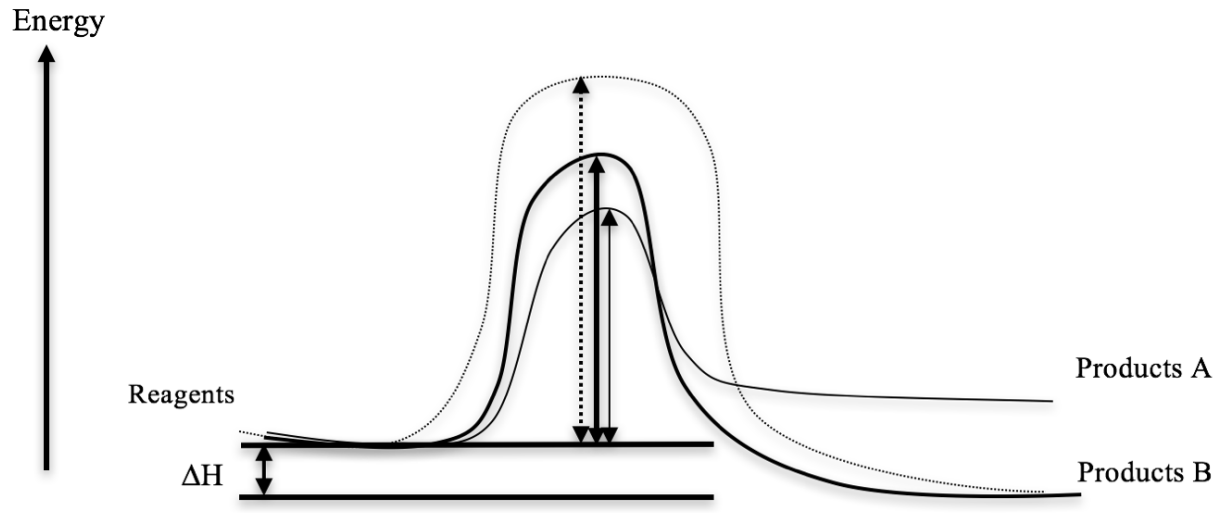

Figure 1.1: Energy diagram showing the difference in energy barriers and product distribution of a chemical reaction.

All chemical reactions have an energy barrier that must be overcome by the system to form the products of the reaction. The dotted line in figure 1.1 illustrates this, there is clearly a large energy barrier which needs to be overcome for the reagents to be transformed into products (A), this energy barrier is described as the activation energy and is denoted E_a. A catalyst facilitates an alternative reaction pathway with a considerably lower activation energy, meaning that the reagents can be transformed into products at a much greater rate of reaction under similar operating conditions, this is illustrated in figure 1.1 by the bold line. Another positive to catalysed processes is that they often modify the product distribution and can therefore be used to tailor the selectivity of a chemical reaction towards desired products. figure 1.1 shows a new reaction pathway for the catalysed reaction leading to product B, this product may have not been attainable under non-catalysed conditions due to a high activation energy barrier for the product formation. However, the selectivity of the reaction can only be manipulated to give high concentrations of product B when the reaction is run under kinetic control, such that the reaction is stopped before it reaches equilibrium. Somorjai *et al*[3] reviewed how the advancements in spectroscopic and surface science techniques are influencing the selectivity in heterogeneous catalysis and concluded that the advancement of *in-situ* techniques allows researchers to work with an attainable goal of achieving 100% activity and selectivity when designing heterogeneous catalysts.

Catalysts can be separated into two main categories, heterogeneous and homogeneous. Heterogeneous catalysts are in a different physical state to the reactants, most commonly this involves a solid catalyst and either gaseous or liquid reactants. Homogeneous catalysts are in the same physical state as the reactants and homogeneously catalysed reactions occur most commonly in the liquid phase. Homogeneously catalysed reactions occur in only one phase whereas heterogeneously catalysed reactions occur at/near an interface between two different physical phases. It is often easier to achieve higher turnovers and greater product selectivity using a homogeneous catalyst as there is a single active site i.e. the whole catalytic material can act as an active site, whereas heterogeneous catalysts have many different sites due to the heterogeneity of surface sites. Despite the greater performance benefits of homogeneous catalysts, it is heterogeneous catalysts that are favoured by industry due to the ease of catalyst recovery and separation of products when compared to a homogeneous catalyst. The activity of a heterogeneous catalyst is a function of the number of active sites, catalysts must therefore be designed to incorporate the highest number of active sites possible. It is common for heterogeneous catalysts to contain small amounts of precious metals which have been dispersed and supported on a solid support, however this is not always the case, other examples can include zeolites, mixed metal oxides etc. When precious metals are used it is highly desirable to produce a catalyst with a high dispersion of metal particles that are generally on a nanoscale, this is to maximise the number of active sites across the catalyst surface.

1.2 Hydrogen Peroxide

Hydrogen peroxide (H_2O_2) is an extremely useful commodity chemical and as such is produced on large scales every year. Discovered in 1818 by French chemist Louis Jacques Thénard[4] the initial synthesis was based on the reaction of barium peroxide (BaO_3) with nitric acid (HNO_3), the process was later refined by using hydrochloric acid (HCl) to increase the acidity of the reaction medium and therefore decrease the decomposition of H_2O_2. Thénard also noted that it was possible to slow down the rate of decomposition by adding noble metals and that the rate of decomposition could be further controlled by altering the noble metal used. It was not until 1853 that the next major development came, when Meidinger developed a process for forming H_2O_2 via electrolysis[5] from sulphuric acid (H_2SO_4), the reaction scheme for this electrolytic process is shown below in scheme 1.1.

$$2H_2SO_4 \rightarrow H_2S_2O_8 + H_2$$
$$H_2S_2O_8 + H_2O \rightarrow H_2SO_5 + H_2SO_4$$
$$H_2SO_5 + H_2O \rightarrow H_2O_2 + H_2SO_4$$
$$2H_2O \rightarrow H_2O_2 + H_2$$

Scheme 1.1: Reaction scheme for Meidinger's electrolytic route to H_2O_2 from H_2SO_4.

The next breakthrough came in 1934 following research by Hans-Joachim Riedl and George Pfleiderer[6,7] who developed the anthraquinone/auto-oxidation (AO) process which is still today the industrially used method for H_2O_2 production. The anthraquinone process builds on the work of Manchot[8] who reported that, when under alkaline conditions, auto-oxadisable compounds such as hydrazobenzenes and hydroquinones react quantitatively, forming peroxides. The AO process can be summarized in a few important reaction steps; a working solution is made by dissolving a 2-alkylanthraquinone into a solvent system, the working solution is subjected to a hydrogenation reaction over a suitable catalyst at reaction conditions of 40-50 °C and a partial pressure of 4 bar hydrogen (H_2), historically using a raney nickel (Ni) catalyst. This hydrogenation step produces a 2-alkylanthrahydroquinone which can be separated from the hydrogenation catalyst and aerated to reform the original 2-alkylanthraquinone and H_2O_2. Deionised water (H_2O) is used to separate the H_2O_2 (aqueous phase) from the 2-alkylanthraquinone (organic phase). The chemistry of the AO process is also summarised in the reaction scheme shown below in figure 1.2[9].

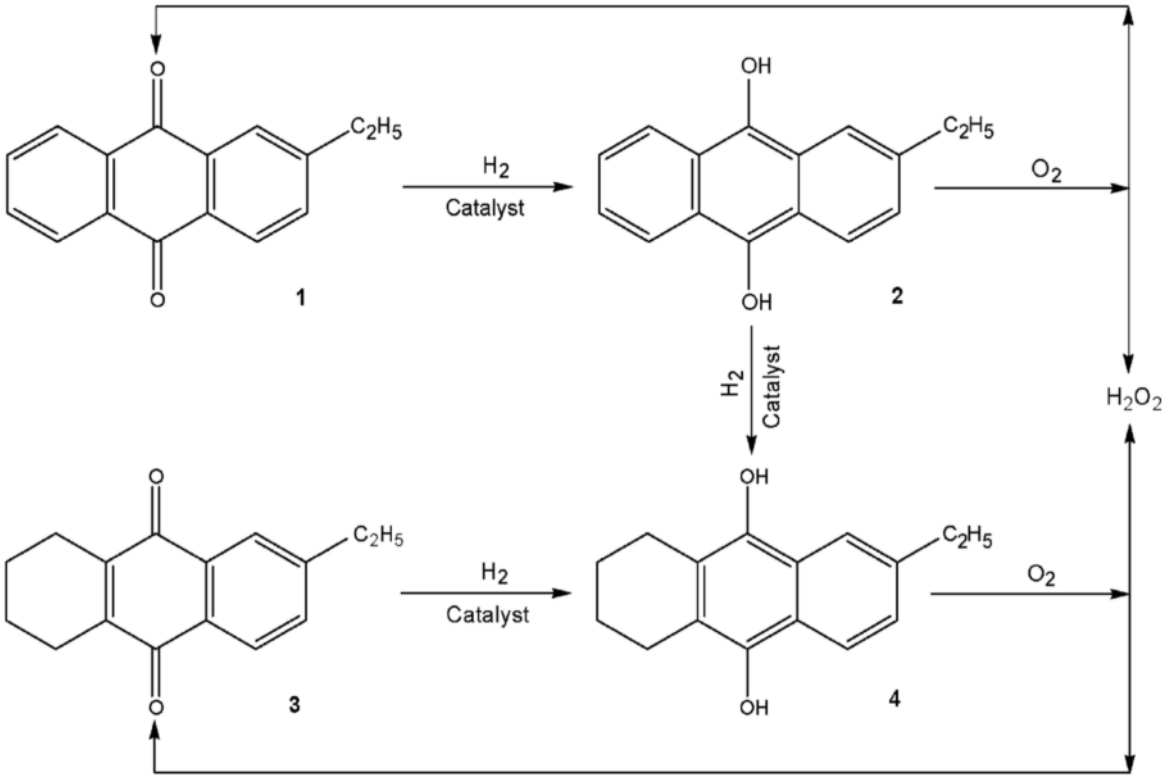

Figure 1.2: Reaction scheme of the AO process to produce H_2O_2[9].

Although the AO process is a highly productive industrial synthesis it is not without its drawbacks[10]. Firstly, it is a multi-step process, figure 1.3 demonstrates the number of steps and complexity of the overall process. The multi-step nature of the AO process means that it is energy intensive, costly and generates large amounts of waste products such as quinone decomposition products formed during the hydrogenation step which must in turn be disposed of appropriately accruing yet more costs both in an economical and environmental sense. There are four key steps in the AO process, these are; hydrogenation, oxidation, separation and finally, purification. Since the development of the first industrial plant in the 1940's there have been several minor improvements made to each of these reaction stages however the principles remain untouched, much like the Haber-Bosch process.

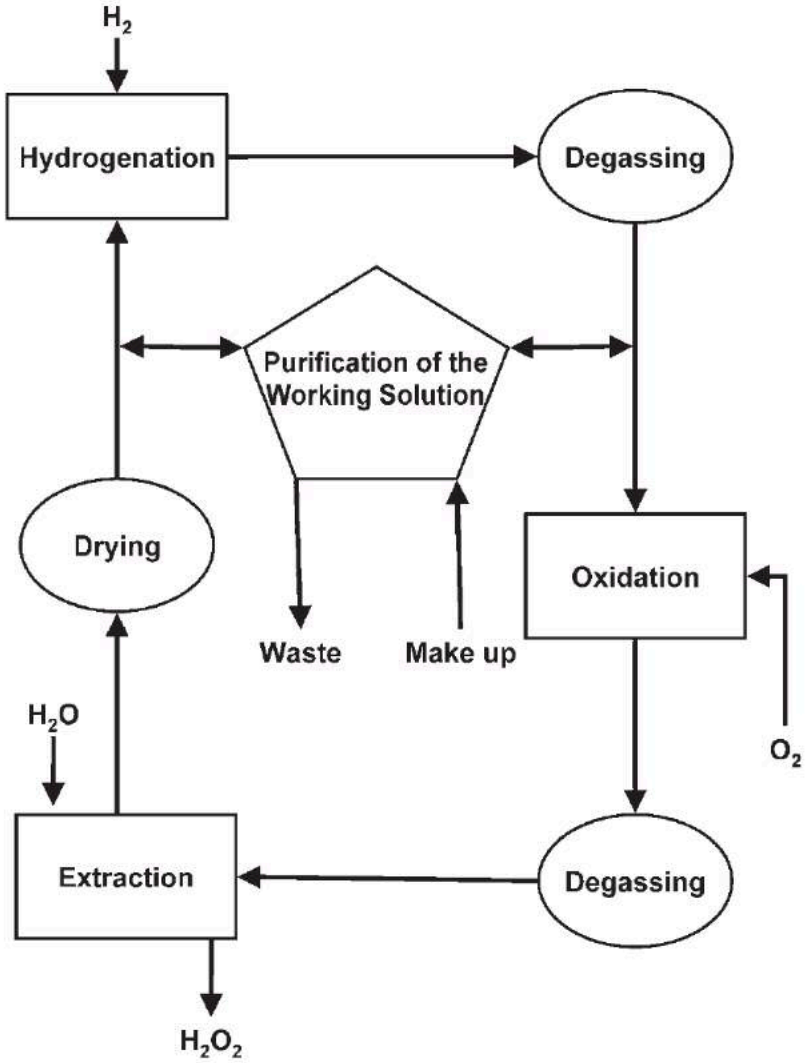

Figure 1.3: Block diagram showing the steps involved in the AO process for the synthesis of H_2O_2[10].

As is a problem with nearly all catalytic hydrogenations, selectivity is a concern in the initial hydrogenation, side reactions can lead to the formation of 5, 6, 7, 8-tetrahydroanthrahydroquinone (THAQ) via the hydrogenation of the unsubstituted aromatic ring in the starting material. The original Ni catalyst was both unselective and prone to deactivation[11]. This lead to the investigation of palladium (Pd) based catalysts but activity towards undesired side reactions was again an issue. The academic search for a catalyst which could selectively hydrogenate the carbonyl group on the anthraquinone and not the unsubstituted aromatic ring leads to the development of Ni-B alloys[12]. These catalysts are nanosized amorphous materials which show significantly better catalytic performance than their predecessors. Further tuning of the catalysts can be achieved by the incorporation of

chromium (Cr)[12, 13] and lanthanum (La)[14], which increases stability and activity respectively. The hydrogenation reaction is now most commonly performed using Pd catalysts supported on either alumina (Al_2O_3), silica (SiO_2) or carbon (C)[10], employed in a fixed bed reactor. The use of monolith type systems has also been developed, having the benefits of a large surface area and high degree of uniformity meaning they are highly suitable for processes using a high flow rate.

1.2.1 Direct Synthesis of H_2O_2

The 12 principles of green chemistry set out by Anastas *et al*[15] highlight the steps that chemists should consider when designing a "green" chemical process. The second principle states that "synthetic methods should be designed to maximise the incorporation of all materials used in the process into the final product", this is known as the atom economy of a reaction. The direct synthesis of H_2O_2 from H_2 and oxygen (O_2) represents an alternative to the AO process which is 100% atom efficient, it also uses greener solvents (H_2O and MeOH), minimises the amount of reaction and separation steps and is far less energy intensive. Another drawback of the AO process is that it is only economically viable on large scales due to the significant energy requirements and multi-step nature of the process. Solutions of 40 wt.% H_2O_2 are typically produced. This presents another issue in the transportation of concentrated solutions of H_2O_2 which can be hazardous; furthermore, most applications require much lower concentrations and the solutions are subsequently diluted down at the point of use, making the transportation an unnecessary risk. Whilst the direct synthesis removes the need to dilute concentrated solution of H_2O_2 the reaction does suffer from poor yields of H_2O_2.

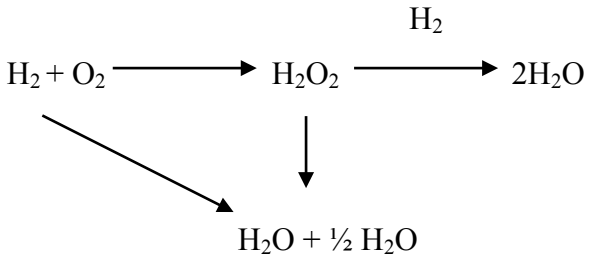

Scheme 1.2: Reaction scheme for the direct synthesis of H_2O_2.

The direct synthesis of H_2O_2 has been studied for many years with the first patent dating back as early as 1914[16]. Despite this extensive period of study selectivity remains an issue. This is

due to the competing reaction pathways for hydrogenation and decomposition, shown in scheme 1.2, being more thermodynamically favourable than the desired synthesis route, which results in low yields of H_2O_2 and poor selectivity towards the desired product.

1.2.1.1 Palladium Catalysts for the Direct Synthesis of H_2O_2

The use of Pd catalysts for the direct synthesis of H_2O_2 was first reported by Henkel and Webber[16]. Since then the direct synthesis of H_2O_2 using noble metal catalytic materials has been area of great research interest, Pd catalysts have been at the heart of this research and in fact arguably the most important developments in noble metal catalytic materials for the direct synthesis of H_2O_2 have been based upon supported Pd catalysts. Whilst the direct synthesis of H_2O_2 appears to be an attractive alternative to the AO process, it is yet to be fully commercialised. DuPont developed a pilot plant whereby a supported Pd-based catalyst was used however, an explosion meant that it never reached commercialisation. The flammable range of concentrations of H_2 in air is the widest of all popular fuel gases, not only that but it exhibits a high rate of diffusion in air. These factors mean that, when contained in a pressurised autoclave, a local explosive environment can be created at the head and in dead spots of the reactor, giving a high risk of explosion. A method of avoiding such risks is working outside of the explosive region: typical reaction conditions involve gas feed streams of 5% H_2 diluted in an inert gas and an O_2/H_2 of 2:1[17]. The limited amount of H_2 present in the feed stream and the challenge of H_2 solubility means relatively low concentrations of H_2O_2 are generally obtained from the direct synthesis. A 5 wt.% Pd/TiO_2 catalyst is known to only produce concentrations of 0.06 wt.% H_2O_2 under such conditions. However, many authors have reported concentrations much higher than this by still working in the explosive region manipulating the reactor design.

Selinsek *et al*[18] have recently reported a novel reactor which combines membrane and micro reaction technology. The authors report that the reactor design consists of two cover plates with an exchangeable microreactor channel plate in between. The channel plate has a cooling side allowing for rapid heating upon entry into the reactor channel, good control of temperature throughout the whole reaction channel and finally, fast quenching upon exit. It is also noted that the curvilinear design of the reactor channel is specifically to increase transversal mass transfer and therefore prevent the suspended catalyst particles causing a blockage due to sedimentation. For direct synthesis reactions, a commercially available 5

wt.% Pd/C catalyst was used with a commercially available woven PTFE membrane having a pore size consisting of 100 x 500 μm. The authors report H_2O_2 concentrations of 0.09 mmol l^{-1}.

The mechanism of the direct synthesis of H_2O_2 over a supported Pd catalyst was first postulated by Pospelova *et al* in 1967[19-21]. It was suggested that it is a three-part mechanism in which H_2 is dissociated on the surface of the Pd catalyst; O_2H is then formed via reaction of O_2 molecules with the adsorbed H atoms, this intermediate O_2H adsorbed species can then further react with adsorbed H atoms to form H_2O_2. This mechanism is illustrated below in scheme 1.3:

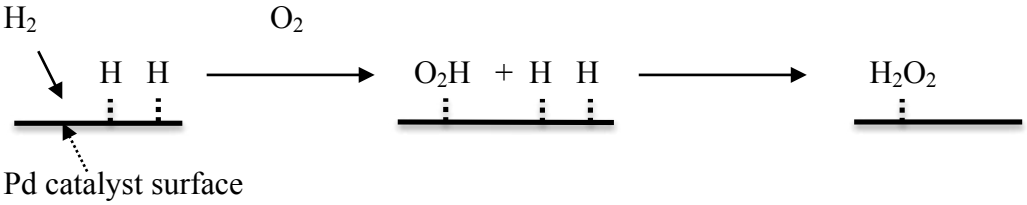

Scheme 1.3: Scheme showing the mechanism for the direct synthesis of H_2O_2 on Pd surfaces as proposed by Pospelova[19-21]

One parameter that is known to be highly influential in heterogeneous catalyst design is the support. Choudhary and co-workers investigated the direct synthesis using Pd catalysts on a variety of supports, including alumina (Al_2O_3), zirconia (ZrO_2), gallia (Ga_2O_3), ceria (CeO_2), yttria (Y_2O_3) and thoria (ThO_2)[22]. Catalysts were prepared by incipient wetness and wet impregnation, supports were then modified by fluorination, chlorination and sulfatation to further investigate the effect of additives which have been shown to promote the direct synthesis of H_2O_2. Sulfatation and fluorination were found to lead to a dramatic increase in selectivity for Pd catalysts supported on Al_2O_3 and ZrO_2 but a decrease in selectivity was observed for CeO_2, Y_2O_3 and ThO_2. It was also concluded that the formation of H_2O_2 and H_2O from the reduction of O_2 is likely to occur from parallel reactions for CeO_2, Al_2O_3 and Ga_2O_3 supported Pd catalysts as they displayed low H_2O_2 decomposition activity, indicating that the formation of H_2O through a consecutive reaction pathway is highly unlikely. The opposite was found for ZrO_2, Y_2O_3 and ThO_2 supported catalysts, as a high H_2O_2 decomposition was observed.

Melada *et al*[23] reported that a Pd catalyst supported on ZrO_2 was active for the direct synthesis of H_2O_2 under mild conditions. ZrO_2 was chosen as a support as it is tuneable, with additives being known to affect the acidity/basicity, porosity and surface area. ZrO_2 was prepared by precipitation from zirconyl chloride ($ZrOCl_2$), ZrO_2 was then modified by impregnation with a variety of anions including halides and sulphates, finally the modified ZrO_2 was impregnated with Pd to give a total weight loading of 2.5 wt.%. Direct synthesis reactions were performed outside of the explosive range but inside the flammable range using a total gas composition of H_2:O_2:N_2 = 10:10:80 and the solvent used was a weak H_2SO_4 (0.03 M) ethanolic, methanolic or aqueous mixture. Despite the undesirable reaction conditions just mentioned, the authors state that all catalytic reactions were performed using a mild pressure and temperature, 1 bar and 20 °C respectively. In the aqueous solution, a H_2O_2 concentration of 4.4 mM was produced within 2 hours of reaction when using a 2.5 wt.% Pd/ZrO_2 catalyst, when an analogous reaction was performed in an ethanolic solvent mixture the amount of H_2O_2 produced increased with concentrations ranging from 9 – 12.2 mM, the non-promoted 2.5 wt.% Pd/ZrO_2 catalyst gave the lowest productivity and the sulphate promoted catalyst led to the highest productivity. Using a methanolic solvent mixture gave a further increase in catalyst productivity and after 2 hours of reaction a maximum concentration of 36 mM of H_2O_2 was observed, surprisingly, the unmodified Pd/ZrO_2 catalyst was equally as active as the catalysts which had been modified by sulphate and fluorine addition, although the fluorine doped catalyst did give a better selectivity. The similar activities observed between the sulphate modified and unmodified catalysts is reasoned due to the adsorption of sulphate ions in the reaction medium onto the unmodified zirconia surface essentially yielding a sulphate modified catalyst, this is confirmed via TPR. The findings here are in accordance of those recorded by other authors including Lunsford[24].

Blanco-Brieva *et al*[25] reported that Pd^{2+} ions could be anchored into mesoporous ion exchange resins which have been functionalised with sulphonic groups. A palladium acetate ($Pd(OAc)_2$) solution was added dropwise to a variety of commercial resins that had been functionalised with sulphonic groups to prepare the catalysts. Direct synthesis reactions were performed using the resin catalysts and reaction conditions of 40 °C, 100 bar and a gas mixture ratio of 2:48:50, H_2:O_2:N_2. After 2 hours of reaction a H_2O_2 concentration ranging from 4.8 – 5.9 wt.% was recorded and the best performing catalyst was found to have the highest surface density of sulphonic-acid groups. XPS analysis further revealed that the lower

the proportion of PdO, the greater the amount of H_2O_2 produced and the greater the selectivity observed. The authors therefore reason that the Pd^{2+} species interacting with the SO_3H groups is the site responsible for H_2O_2 formation. Whilst the concentration of H_2O_2 produced from these experiments is significant, it must be noted that several undesirable conditions were used to achieve this. The reactions were performed in a methanol (MeOH) solvent including the presence of a bromide promotor and the pressure is much higher than a lot of the other work reported in the literature.

The active component of Pd catalysts has long been a subject of investigation in the literature and in a seminal research paper Sheldon *et al*[26] addressed the fact that little attention is paid to leaching when developing and investigating new heterogeneous solid catalysts for liquid phase reactions, where in fact a leachate may be responsible for the observed catalytic activity. Lunsford and co-workers have performed several in-depth investigations in to the direct formation of H_2O_2 over colloidal Pd catalysts[27-36]. When investigating a 5 wt.% Pd/SiO_2 catalyst[27] for the direct synthesis of H_2O_2 it was found that the catalytic activity was largely due to colloidal Pd metal. The formation of the Pd metal colloid is proposed to occur through the oxidation of supported Pd^0 in the presence of HCl, leading the presence of $PdCl_4^{2-}$ in the solution. These ions are reduced by H_2 back to metallic palladium some of which is present as a palladium metal colloid. The authors note a key observation, after a period of reaction the supported catalyst was removed and the rate of H_2O_2 production was unaffected. It was also observed that when unsupported $PdCl_2$ was present the rate of H_2O_2 formation was substantially higher when compared to the supported Pd/SiO_2 catalyst. Further studies by Lunsford[28] showed that a linear relationship was observed between colloid concentration and the rate of H_2O_2 formation, these results are shown in figure 1.4[28], these data provided further indication that the predominant activity was due to colloidal Pd. It must be noted that in these investigations high concentrations of halides are used in the reaction media and in the absence of halides the formation of H_2O_2 is greatly diminished. The dissolution of Pd from the supported catalyst and subsequent formation of Pd colloids in the reaction medium is also thought to be due to the high concentrations of HCl (0.1 – 1 M).

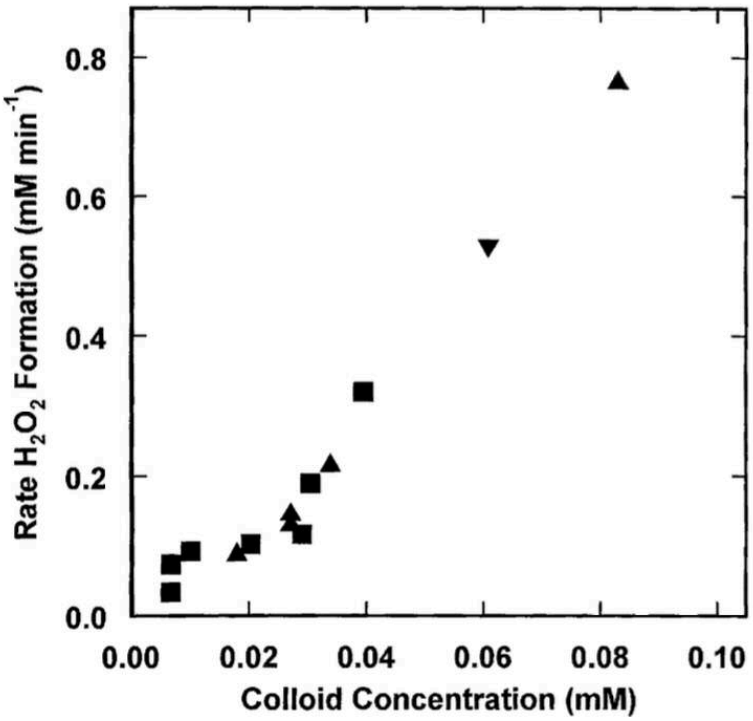

Figure 1.4: Rate of H_2O_2 synthesis as a function of Pd metal colloid concentration. Where: squares indicate colloids derived from 10^{-3} M $PdCl_2$ and triangles indicate colloids derived from 5 wt.% Pd/SiO_2 (both upwards and downwards facing)[28].

Isotopic labelling experiments were used to determine whether O_2 is dissociated in the formation of H_2O_2 or if it remains in the diatomic form as previously suggested by Pospelova[19-21]. Isotopically labelled H_2O_2 was prepared by reacting $^{18}O_2$ (6.6 psi) and $^{16}O_2$ (7.7 psi) with H_2 (7.7 psi) in 10 ml of 1M HCl using a Pd/SiO_2 catalyst, the reaction was left to stir for 8 hours and the H_2O_2 was further concentrated by pumping on the system for 30 minutes at 30 °C. Results obtained by Raman spectroscopy did not show the presence of any ^{16}O - ^{18}O cross coupled products, consolidating the previously proposed mechanism where molecular O_2 is thought to be absorbed on the Pd surface undergoing a reaction with absorbed H atoms to form O_2H.

Whilst from an academic standpoint it is interesting to investigate the use of a metallic colloidal Pd catalyst it is highly undesirable for industry as, for the reasons previously stated in this chapter, heterogeneous catalysts are far preferred. The literature on supported Pd catalysts for the direct synthesis of H_2O_2 is extensive, Pd catalysts are productive for this

reaction due to their ability to readily disassociate H_2. However, to achieve a high selectivity, it is desirable for O_2 to be absorbed on the catalyst surface and not disassociated.

Efforts to tune the selectivity of supported Pd catalysts have been led by Choudhary and co-workers[37-39]. The effect of halide promotors in the reaction medium was investigated for various reduced, supported Pd catalysts[39]. It was found that for all reduced Pd catalysts investigated, in the presence of H_2SO_4 and H_3PO_4 acid promotors but the absence of halide, a high H_2 conversion is achieved. However, selectivity is poor with most of the H_2 being converted to H_2O. When both acidic and halide promotors (particularly Cl) are present, both high selectivity towards H_2O_2 formation and H_2 conversion is seen. Interestingly, it is only Cl^- and Br^- promoters that have a positive effect on the reaction, F^- anions had no effect on H_2 conversion or selectivity and I^- acted as a catalyst poison. Previous studies[37-39] by this group showed that when using non-reduced supported Pd catalysts, high H_2 conversions and selectivity's towards H_2O_2 can be achieved through the addition of mineral acids to the reaction medium without any halide promotors. The authors[39] draw the conclusion that the increased selectivity towards H_2O_2 and higher yields of H_2O_2 in the presence of mineral acids and Cl^- and Br^- is due to the poisoning of active sites responsible for the H_2O_2 decomposition reactions on reduced Pd catalysts. The information presented above can lead one to draw the conclusion that whilst supported Pd catalysts are active for the direct synthesis of H_2O_2 without the addition of a promoter in either the reaction medium or in pre-treatment of the catalyst, supported Pd catalysts suffer from several drawbacks including poor selectivity and leaching of metal into the reaction solution. This is an issue which has meant the academic research has shifted to find new methods in catalyst design that will retain the superior activity of supported Pd species but minimise the drawbacks listed above.

1.2.1.2 Gold Catalysts for the Direct Synthesis of H_2O_2

Since the discovery that nanoparticulate gold (Au) is an active catalyst for several important reactions, this has been an area of significant interest, particularly for researchers working in the field of heterogeneous catalysis.

In a seminal research paper, Haruta *et al*[40] first showed that Au could in fact be highly active as a catalyst, contrary to thinking that Au was too noble to be active. They showed that Au nanoparticles dispersed on a variety of supports were highly active for the oxidation of

carbon monoxide (CO). This discovery led to a surge of research into Au catalysis and supported Au catalysts were shown to be active for a range of epoxidations, selective oxidations and hydrogenations.

In a theoretical study by Olivera *et al*[41] it was predicted that Au would be more active for the direct synthesis of H_2O_2 than other noble metals such as Pd, platinum (Pt) and silver (Ag). A reaction scheme which shows the steps necessary for either the formation of H_2O or H_2O_2 over metallic catalysts is shown in figure 1.5. The authors determined that the optimal heterogeneous catalyst for this reaction would destabilise surface adsorbed hydroxyls (OH), block the reactions which produce OH via O_2 and the decomposition of both OOH and H_2O_2 must also be blocked. Au was determined to have the highest activation energy barrier for both O_2 dissociation and the reactions which yield OH, moreover, Au displayed the lowest activation energy barrier for the reactions involved in the proposed H_2O_2 channel.

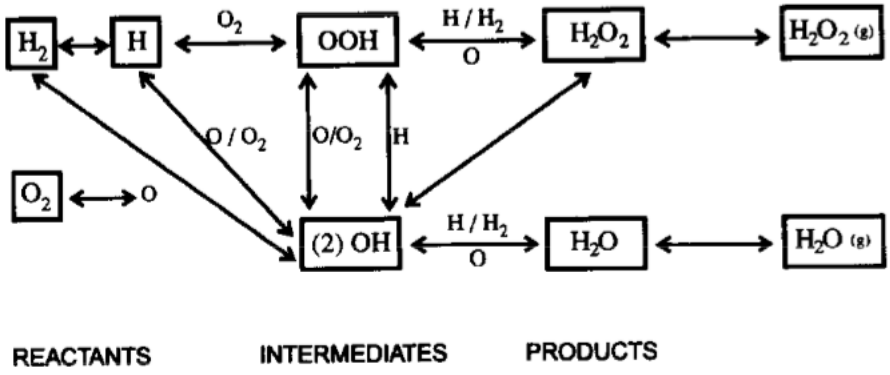

Figure 1.5: Reaction scheme for the formation of H_2O_2 and H_2O over supported metallic catalysts[41].

It was Landon *et al*[42] who first investigated supported Au catalysts for the direct synthesis of H_2O_2. Initial experiments reported the use of supercritical CO_2 as a reaction solvent to overcome the limitations of H_2 solubility. However, both Au and Pd catalysts demonstrated very low yields of H_2O_2 and in fact, only H_2O was formed when using the Pd catalyst, these results highlight the instability of H_2O_2 and led the authors to redesign the experiment, using lower temperatures of 2 °C and also MeOH solvent to try and stabilise any H_2O_2 that is formed. Au catalysts were found to perform very well under these conditions and were more

active for the direct synthesis than Pd counterparts. The results are summarised below in table 1.1:

Catalyst	Solvent[a]	Temperature/ °C	Pressure/ MPa	O_2/H_2 mol ratio	H_2O_2[b] mmol g(catalyst)$^{-1}$ h^{-1}
Au/Al_2O_3	CH_3OH	2	3.7	1.2	1530
$Au:Pd\ (1:1)/Al_2O_3$	CH_3OH	2	3.7	1.2	4460
Pd/Al_2O_3	CH_3OH	2	3.7	1.2	370
Au/ZnO	$SCCO_2$	35	9.2	1.0	9
Au:Pd (1:3)/ZnO	$SCCO_2$	35	9.2	1.1	7
Au:Pd (1:1)/ZnO	$SCCO_2$	35	9.2	0.8	12
Au:Pd (3:1)/ZnO	$SCCO_2$	35	9.2	0.9	8
Pd/ZnO	$SCCO_2$	35	9.2	1.3	0

[a] $SCCO_2$ = supercritical CO_2, details of experimental methods given in refs. 16 and 18 [b] Rate of H_2O_2 formation averaged over 30 min experiment.

Table 1.1: Direct synthesis of H_2O_2 using supported Pd, Au and AuPd catalysts[42].

These findings led to a new era of catalyst design for the direct synthesis of H_2O_2. Following this important discovery, a range of studies utilising supported Au catalysts for the direct synthesis of H_2O_2 were reported in the literature. Au/SiO_2 catalysts prepared by wet impregnation were notably studied by Ishihara *et al*[43]. These catalysts were shown to be active in the absence of halide promoters, the key step in the formation of H_2O_2 over the supported Au catalysts was thought to be the activation of H_2 as a proportional increase in H_2O_2 formation was seen with increasing partial pressure of H_2. These findings are compounded by the work of the Haruta group, who investigated a range of supported Au catalysts including Au/SiO_2 and Au/MCM-41 for both the vapour phase epoxidation of propylene (C_3H_6)[45, 46] and the direct synthesis of H_2O_2[44]. Findings from these studies show that the activity of Au catalysts is related to the particle size, with sintering leading to catalyst deactivation. Seeing as we know that particle size can greatly affect the catalytic activity of supported Au catalysts, the choice of preparation technique can be said to be an important parameter that could potentially greatly influence catalytic activity. Another common technique for preparing supported metal catalysts is deposition-precipitation. This technique, like the impregnation technique, involves mounting dissolved precursors from the aqueous phase onto a solid support. In general, the deposition-precipitation technique has a few key steps[47]; the aqueous metal precursor and support are mixed, a reactant is then added which facilitates the transformation of the metal precursor into an insoluble form (precipitate), the reaction proceeds and the concentration of the precipitate is raised, when the process of nucleation begins the metal precipitate is adsorbed exclusively onto the support. Ma *et al*[48] reported that Au/TiO_2 and Au/TS-1 catalysts were active for H_2O_2 formation when prepared via deposition-precipitation using urea. Au particle size was found to be a function of urea

concentration, an increase in urea concentration lead to a decrease in the size of Au nanoparticles. Catalysts with a smaller Au particle size had a higher catalytic activity, which was attributed to a larger surface area for chemical interactions. In a leading study, Corma *et al*[49] investigated the use of Au as a hydrogenation catalyst in the selective hydrogenation of nitro compounds. Other hydrogenation catalysts such as Pt and Pd perform this reaction with low selectivity and it is known that that alkenes and nitrogen dioxide (NO_2) will adsorb differently on a gold surface than the aforementioned metals. Monometallic Au catalysts (1.5 – 4.5 wt.%), AuPd and AuPt alloy catalysts were all tested for the hydrogenation of a variety of nitro compounds. The authors show that supported Au catalysts greatly outperform the monometallic Pd and Pt counterparts as well as the bimetallic Au containing catalysts. The chemoselective hydrogenation of 3-nitrostyrene, 4-nitrobenzaldehyde, 4-nitrobenzonitrile, 4-nitrobenzamide and 1-nitro-1-cycohexene with supported Au catalysts is reported to have conversion values between 98.5 and 99.6% whilst retaining selectivity values between 90.9 and 97.3%. Although elevated reaction temperatures of 120 °C are required to achieve such high conversions and selectivity's, these findings demonstrate the ability of Au catalysts to not only perform hydrogenation reactions with a high conversion but also with exceptional chemoselectivity.

1.2.1.3 Bimetallic AuPd Catalysts for the Direct Synthesis of H_2O_2

Following the observation that supported Au catalysts can effectively catalyse the direct synthesis of H_2O_2, it was later reported by Solsona *et al*[50] that Au could be incorporated into supported Pd catalysts to give a synergistic effect towards selectivity. The data in table 1.1 shows that supported $AuPd/Al_2O_3$ catalysts dramatically outperform their monometallic counterparts, with a rate of formation of H_2O_2 nearly four times that of Au/Al_2O_3 and greater than ten times that of Pd/Al_2O_3 under identical reaction conditions[50].

Interestingly, AuPd bimetallic catalysts can catalyse the direct synthesis reaction in absence of acid and halide promotors which are vital to achieve a desirable yield of H_2O_2 when using monometallic catalysts. Edwards *et al*[51] have also shown that when a AuPd catalyst is used with a gas stream utilising a CO_2 diluent the formation of carbonic acid (H_2CO_3) is favoured which in turn acts as an acid stabiliser and therefore leads to an increase yield of H_2O_2. Whilst the use of MeOH as a co-solvent is appropriate for research purposes it is not

desirable from an industrial standpoint, where the dilute concentrations of H_2O_2 produced from the direct synthesis would be needed in an aqueous solution rather than an organic solvent. It is therefore an important observation that by using a selective catalyst and a 5% H_2/CO_2 feed stream (to stay below the explosive limit) a greater amount of H_2O_2 can be synthesised.

Building on previous work where it was shown that Pd supported on a sulphated ZrO_2 could catalyse the direct synthesis of H_2O_2, Bernardotto *et al*[52] investigated the same support material for bimetallic AuPd and PdPt catalysts. After formation of the modified ZrO_2 support by a previously reported method, the bimetallic catalysts were prepared by co-impregnation with either chloroauric acid ($HAuCl_4$), dihydrogen tetrachloropalladate (H_2PdCl_4) or chloroplatinic acid (H_2PtCl_6). Reaction conditions were kept the same as the previous investigations by the authors. PdPt bimetallic catalysts containing only a small amount of Pt (0.1 and 0.2 wt.%) were found to outperform the monometallic Pd catalyst both in terms of concentration of H_2O_2 produced and selectivity towards H_2O_2 formation over a 2 hour reaction. Interestingly, a catalyst with an approximate 1:1 ratio in terms of weight loading was found to have a decreased selectivity even when compared to the monometallic Pd catalyst. In contrast to this, the authors report that a low amount of Au (0.2 wt.%) is not enough to promote the activity of the Pd catalyst and the catalytic performance of this low loaded bimetallic catalyst is nearly identical to that of the monometallic Pd catalyst after a reaction period of 2 hours. Indeed, it was found that the selectivity is decreased when adding such a small amount of Au compared with the monometallic Pd catalyst. When a greater amount of Au is used (1.2 – 2 wt.%) then both productivity and selectivity are increased, with the highest selectivity and productivity values arising from a bimetallic AuPd catalyst with a 1:1 wt.% ratio. This catalyst was then subjected to a 12 hour reaction and it was noted that selectivity remained constant and H_2O_2 concentration increased in a near linear fashion. It should be noted however that these reactions were all performed in a MeOH solvent which containing 0.03 M H_2SO_4, which as mentioned earlier in this discussion is not ideal from a green chemistry standpoint and will also promote a higher selectivity towards H_2O_2 synthesis than in an aqueous solvent.

Nomura *et al*[53] investigated a nanocolloidal AuPd catalyst for the direct synthesis of H_2O_2, a colloidal solution was prepared by a chemical reduction technique, using $HAuCl_4$ and $PdCl_2$ as the metal precursors, polyvinylpyrrolidone (PVP) was added to control the particle size

dispersion. The authors performed the direct synthesis reactions under very mild conditions, atmospheric pressure and 10 °C temperature. Analysis via TEM revealed an average particle size of 4.7 nm and it was predicted from lattice constants that the particles were homogeneous alloys. It was found that increasing the Au concentration in the colloid led to an increase in the rate of formation of H_2O_2, with the optimal composition being approximately 25 mol.%, interestingly, the selectivity value is reported to be nearly 100% when the colloid with the optimal Au composition is used. H_2O_2 hydrogenation experiments revealed that the rate of H_2O_2 decomposition decreased with increasing Au content in the colloid and as expected the lowest rate of decomposition was seen for the colloid containing 25 mol.% Au. The authors further explain this increase in selectivity towards H_2O_2 production as XPS data showed that the colloid with the optimal Au concentration had the highest surface Au composition and therefore the suppression of undesired side reactions can be achieved by increasing the surface Au composition.

The reason for the enhanced selectivity of AuPd catalysts is not fully known. It is known that, in the direct synthesis of H_2O_2, H_2O is formed only because of O-O bond cleavage whereas it is thought that the formation of H_2O_2 is a result of O_2 interaction with H and not due to the interaction of hydroxyl radicals (OH•)[54]. Staykov *et al*[55] investigated a full first-principle treatment of the interaction between H_2 and O_2 on a Pd (111) surface. It was assumed that the reaction takes place in two steps, firstly the activation on the catalyst surface of O_2 into its superoxo state, a H atom then interacts with the superoxo species forming an intermediate hydrogen peroxo species. In the second step, the hydrogen peroxo species interacts with a second H atom, forming H_2O_2. The authors assume that the experimentally observed enhancement in selectivity of bimetallic AuPd catalysts is due to the presence of Au significantly reducing the rate of dissociation of O_2 molecules, meaning a lack of O_2 available on the surface and therefore a much lower rate of H_2O formation. O_2 dissociation over a Pd (111) surface was found to be an exothermic reaction and an energy difference of -95 kJ mol^{-1} was observed between the product and the reactant complex. In contrast, the presence of surface Au atoms led to an energy difference of 4.8 kJ mol^{-1} and reaction enthalpy remained nearly unchanged. These results illustrate that the incorporation of Au atoms onto a Pd (111) can significantly supress the dissociation of O-O bonds, therefore leading to a lower rate of H_2O formation as a by-product and in turn increasing the selectivity of the direct synthesis reaction.

Electrocatalytic formation of H_2O_2 using polymer electrolyte fuel cells is an interesting alternative to the anthraquinone process and like the direct synthesis reaction can be used to produce more dilute concentrations of H_2O_2 on site. Polymer electrolyte fuel cells are suited to the electrochemical reduction of O_2; they can minimise over reduction to H_2O, produce high current densities and can operate at low temperatures. Jirkovsky *et al*[56] describe the main difference between the electrochemical reduction of O_2 and the direct synthesis process as the ability to be able to recycle the Gibbs energy of the O_2 reduction to form H_2O_2 and the subsequent formation of H_2O to electrical energy, meaning the Gibbs energy of the reaction is fully employed. AuPd/C bimetallic catalysts were prepared by a sequential reduction method and the catalysts were employed for O_2 reduction reactions using a rotating ring disc electrode, monometallic Au/C catalysts was investigated for comparison. The authors report that the incorporation of up to 8 mol.% of Pd leads to a greater selectivity towards H_2O_2 formation and therefore a higher H_2O_2 production is sustained irrespective of the applied potential. DFT calculations were used to rationalise this observation and it is reasoned that the Pd sites are incorporated into the Au surface, this leads to a greater adsorption of O_2 onto the surface whilst still minimising the breaking of O-O bonds. In contrast to this, when a greater amount of Pd (Pd content of 15 mol.% and greater) is doped onto the Au surface, then Pd surface segregation occurs and the formation of H_2O starts to take precedence.

1.2.1.4 Effect of Preparation Method on AuPd Bimetallic Catalysts

Initial investigations of AuPd catalysts involved the use of an impregnation technique in which the support material was impregnated with precious metals via a wet impregnation method using aqueous solutions of Au and Pd precursors. AuPd bimetallic catalysts prepared via this impregnation technique are shown in the literature to comprise mainly of Au and Pd fcc nanoparticles that are highly dispersed and in the size range of 2 – 10 nm. Interestingly, Edwards *et al*[51] showed that if these AuPd catalysts are stored in the dark under ambient conditions for approximately 12 months then a bimodal particle size distribution is observed, with larger AuPd metal particles of in the size range of 35 - 50 nm present in addition to the smaller nanoparticles. It was also seen that aged catalysts displayed a far greater catalytic activity for the direct synthesis of H_2O_2 than fresh $AuPd/Al_2O_3$ catalysts. Scanning transmission electron microscopy (STEM) and x-ray electron dispersive spectroscopy (XEDS) images are shown below in figure 1.6. The analysis revealed that the nanoparticles were almost exclusively homogeneous alloys of Au and Pd with the Au content increasing as

the size of the nanoparticles increased, it should also be noted that no pure Au nanoparticles were seen further demonstrating the affinity for the formation of alloys between these two metals. The observed increase in activity is attributed to the electronic promotional effect of Au to Pd in these Pd rich alloy particles.

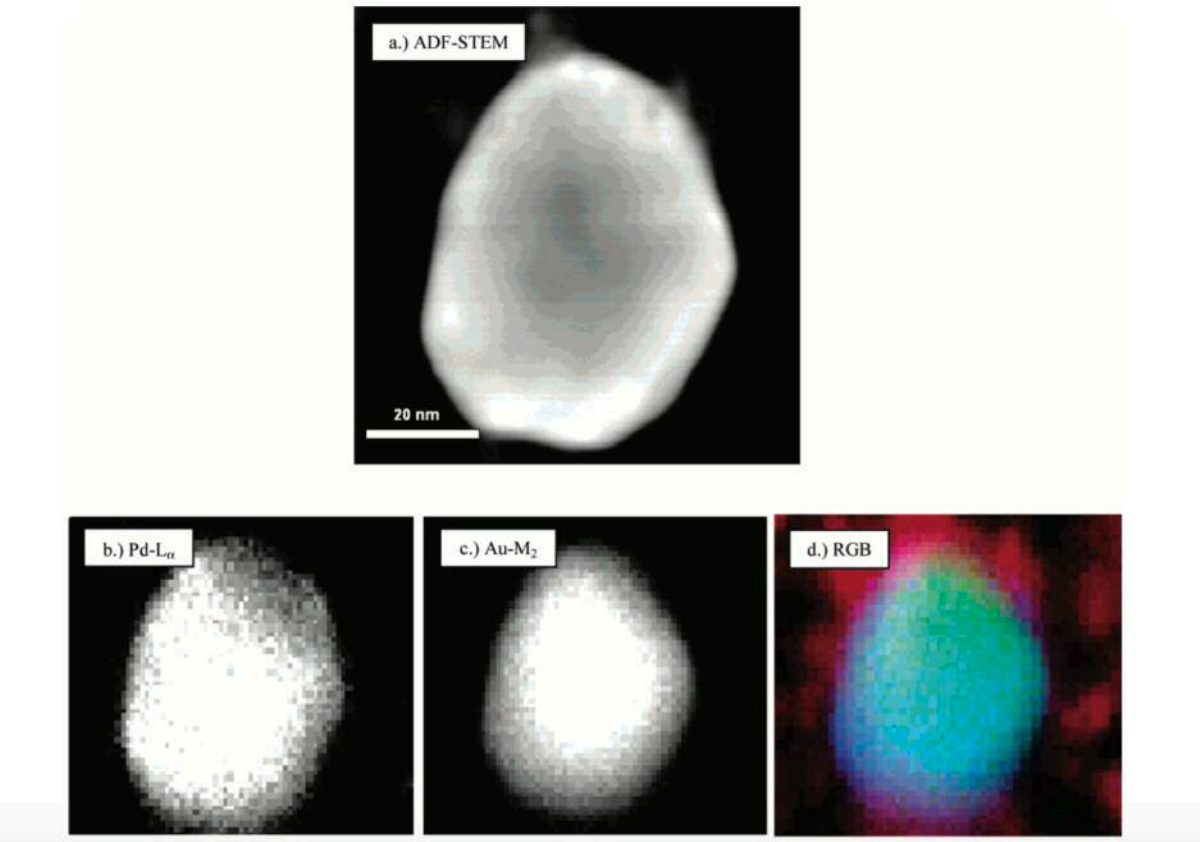

Figure 1.6: Collection of STEM-XEDS images of 25 nm particle in a 5 wt.% (1:1) $AuPd/Al_2O_3$ catalyst calcined at 500 °C in static air. (a) ADF image with corresponding XEDS maps of (b) $Pd_{L\alpha}$, (C) Au M_2 and (d) reconstructed RGB (red = Al, green = Au and blue = Pd) image showing the preferential surface enrichment of Pd[51].

One of the main issues associated with the simple wet co-impregnation technique for the preparation of supported bimetallic catalysts is particle size distribution. It is difficult to achieve a narrow particle size distribution using this simple method and as previously mentioned it is the small nanoparticles that are thought to be particularly active for the direct synthesis of H_2O_2. Pritchard[57] *et al* tried to overcome this by utilising a colloidal "sol-immobilisation" technique. In this preparation technique, colloidal nanoparticles with a very narrow size distribution are preformed through the addition of metal precursor solutions to

form a colloidal solution. A polyvinyl alcohol (PVA) solution is added to stabilise the nanoparticles and prevent agglomeration, reduction is performed by the addition of a sodium borohydride ($NaBH_4$) solution, immobilisation of the nanoparticles onto the support material (activated carbon in this case) yields the desired catalyst. Particle size data from STEM analysis showed that all bimetallic AuPd catalysts had a median particle size distribution of 2.9 - 4.6 nm and all particles were found to be random homogeneous alloys with an fcc structure. It was also observed that larger particles were Au-rich, the opposite to the observed effect when using the co-impregnation technique where larger particles are typically Pd-rich. Catalytic data for these sol-immobilised is very promising, productivity values of up to 188 $mol_{H2O2}\ kg^{-1}_{cat}\ h^{-1}$ are reported whereas the highest previously reported productivity for catalysts prepared by co-impregnation was 120 $mol_{H2O2}\ kg^{-1}_{cat}\ h^{-1}$. It is also noteworthy that these sol-immobilised catalysts only have 20% of the total metal loading compared to the most active catalysts prepared by co-impregnation. Selectivity continues to be an issue and it was reported that the sol-immobilised catalysts were also extremely active for the undesired over hydrogenation of H_2O_2 to form H_2O. These results have clearly shown that whilst small AuPd nanoparticles are the most active species for the direct synthesis, they also have an even greater affinity for the undesired side reactions.

The effect of halide and acid promotors in the reaction medium is well documented and has already been discussed at length in this chapter. In a different approach Sankar *et al*[58] investigated the effect of adding chloride (Cl^-) ions during the catalyst preparation. The conventional co-impregnation was modified by adding an excess of Cl^- anions, in the form of diluted HCl, to the $PdCl_2$ precursor solution. The "modified impregnation" technique then uses a high temperature reduction to activate the final catalyst and remove the excess Cl^- ions. The authors noted that as the concentration of the chloride increased from 0 M (standard co-impregnation) to 2.0 M the mean particle size of the smaller nanoparticles decreased from 4.7 nm to 2.6 nm. Inactive micron sized particles are also eliminated in catalysts prepared by modified impregnation. It was also noted that the particle size distribution of the modified impregnation technique is on a par with that of the sol-immobilisation technique, indicating the efficacy of this preparation method with almost all the precious metal being utilised to make catalytically active nanoparticles.

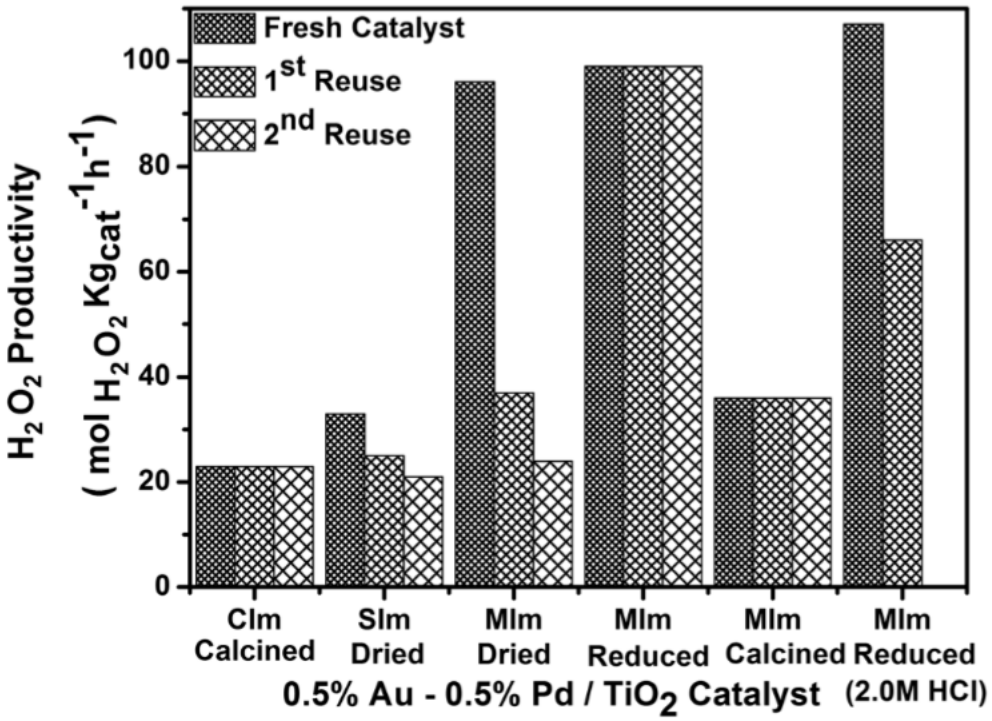

Figure 1.7: Comparison of H_2O_2 direct synthesis activity for a set of AuPd/TiO_2 catalysts prepared by different techniques and subjected to varying heat treatments[58].

A comparison of the catalytic activity of supported AuPd catalysts prepared by sol-immobilisation, co-impregnation and modified impregnation for the direct synthesis of H_2O_2 is summarised in figure 1.7. It is clear from the above data that varying the preparation method can have a profound effect of the catalytic activity of a AuPd catalyst and that even subtle changes to the preparation method can lead to a drastic increase or decrease in conversion and catalyst stability. The modified impregnation technique represents the development of a well-established preparation method (conventional co-impregnation) and fine tuning the preparation to meet the requirements of a specific reaction. Whilst the sol-immobilised catalyst is more active than the catalyst prepared by conventional impregnation, it rapidly deactivates upon reuse. When a concentration of 0.58 M HCl is used in the precursor solution and the dried powder is subjected to a reduction of 400 °C for 4 hours (2% H_2 stream), a highly active and stable catalyst is synthesised, with the authors reporting a productivity greater than 90 mol_{H2O2} kg^{-1}_{cat} h^{-1} for the fresh catalyst and for the subsequent reuses. It is also clear from the data that although an excess of Cl^- in the preparation can yield an excellent catalyst, a complete removal must be achieved during the heat treatment to

prevent catalyst poisoning, as observed with the reduced 2.0 M catalyst and the calcined 0.58 M catalyst.

1.2.1.5 Effect of Other Metals

The synergistic effect of Au and Pd is a key discovery in the design of heterogeneous catalysts for the direct synthesis of H_2O_2. However, from an industrial standpoint the cost of such precious metals is an important consideration and it would be far more desirable to utilise less expensive metals to enhance the selectivity and performance of a supported Pd catalyst. It has been very recently reported in the literature that the addition of tin (Sn) to a well-known Pd/TiO_2 heterogeneous catalyst can lead to an enhancement in selectivity for the direct synthesis of H_2O_2. Freakley *et al*[59] found that if subjected to an oxidation, reduction, oxidation (ORO) heat treatment then a $PdSn/TiO_2$ catalyst can perform a direct synthesis reaction with 100% selectivity and no net H_2O_2 degradation is observed. The authors reason this due to a strong interaction between the metals forming an alloyed species but also due to the strong interaction that is induced between the two metals and the support. STEM revealed that an amorphous layer of SnO_2 forms along the surface of the support, embedding any very small nanoparticles and covering the edge sites of larger nanoparticles, both of which are thought to be the cause of over hydrogenation and degradation reactions. Interestingly, the authors also show that this is possible to achieve with other secondary metals, including gallium (Ga) and Ni.

Kamiuchi *et al*[60] investigated the effect of a similar ORO heat treatment, however this time it was a Pd/SnO_2 catalyst which was investigated. Catalysts were prepared by an impregnation technique and subjected to a range of heat treatments. Pd/SnO_2 samples which only underwent an initial calcination showed no presence of any Pd species in the XRD pattern, the authors ascribe this to the strong metal support interaction (SMSI) and high dispersion of Pd nanoparticles on the SnO_2 support. A reduction at 200 °C led to the appearance of a weak Pd reflection in the XRD pattern, suggesting that metallic Pd had been formed and some sintering had led to the particles now being within the detection limit. Interestingly, a higher temperature reduction treatment induced reduction of not only Pd but also the top surface of SnO_2 and reflections thought to be due to an intermetallic PdSn species appeared. The presence of this intermetallic species was confirmed upon re-oxidation at 400 °C, the authors suggest that this ORO heat treatment was sufficient to change the phase and structure of the

catalyst. XPS data confirmed these results and the presence of the intermetallic species was again detected due to a shift in the binding energy of Pd $3d_{5/2}$ peak, which was located in between the known binding energies of PdO and metallic Pd, suggesting that the intermetallic species contains partially oxidised Pd, re-oxidation gave a further exaggeration of this peak shifting. STEM images showed that PdO was present as an amorphous finely dispersed layer on the SnO_2 surface in the oxidised only catalysts, an initial reduction at 200 °C led to highly crystalline metallic Pd particles of a greater size and the amorphous layer was reduced. Upon reduction at 400 °C two intermetallic species were observed, the well documented core-shell structure, known to form upon alloying between Pd and other metals such as Au. Also seen was an interesting species that the authors call a "particle intrusion structure", the authors show a crystalline Pd nanoparticle which has intruded into the SnO_2 support structure, figure 1.8 shows the TEM images of these intermetallic species:

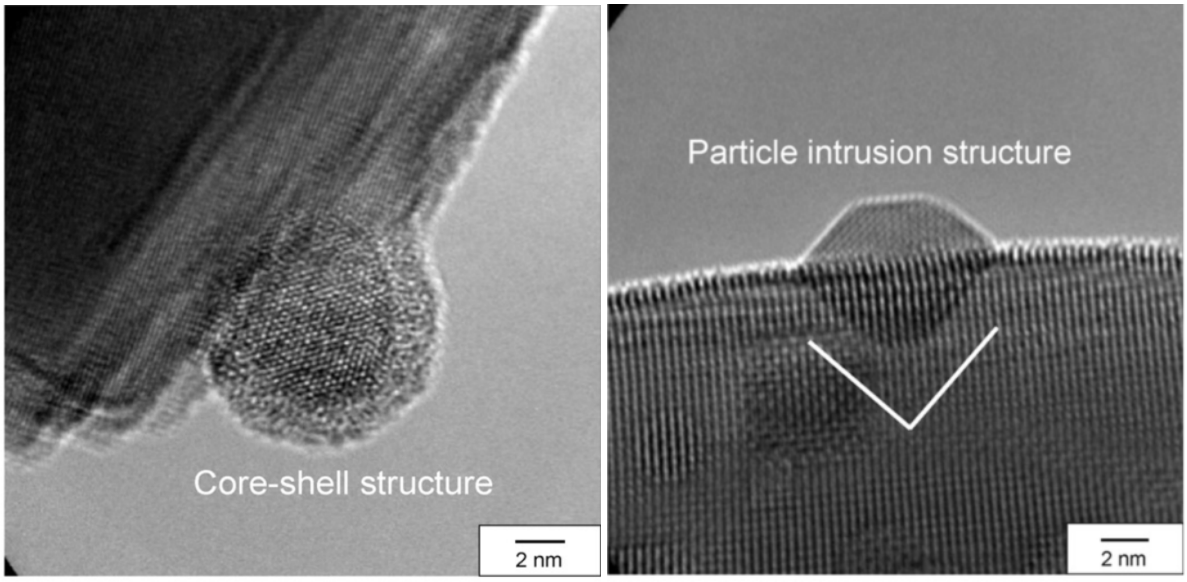

Figure 1.8: Intermetallic species formed due to an Oxidation, Reduction treatment of a model Pd/SnO_2 catalyst[60].

The authors reason this interesting observation due to the H_2 storage capacity of Pd nanoparticles along with the known SMSI between Pd and Sn. These findings show that a high catalytic activity would be expected upon the initial calcination as the Pd nanoparticles are well dispersed which should correlate with a large number of available active sites, the morphological changes induces during the induction period should cause the activity to be

diminished in comparison, however the authors show that the re-oxidation treatment could regenerate catalytic activity due to a reduction in mean particle size diameter and disappearance of the core-shell structure upon re-oxidation. These findings therefore indicate that the SMSI induced by various heat treatments can potentially influence the catalytic activity of supported Pd/SnO_2 catalysts.

1.3 Treatment of Greywater (GW)

1.3.1 Background

Greywater (GW) can be defined as any wastewater that originates from water streams which do not contain faecal contamination[61]. GW is commonly generated from households, apartment blocks or offices. Although GW does not come directly from a source with faecal contamination, such as a toilet, it still contains an abundance of hazardous components which means that it generally must be treated if it is to be suitable for reuse. Water recycling is becoming more and more important in today's modern society, as the population is expected to grow beyond 9 billion in 2050[62] and with that urban water consumption will drastically increase. Whilst there are many options to deal with the ever-growing water demands they can be split into two main categories; increasing the supply of water to urban regions and decreasing the demand for drinking water. The first option, increasing the supply of water, brings with it huge infrastructural and financial demands which are often not possible to meet, particularly in developing countries. The second option, reducing water demands, is a more feasible solution as the costs associated with it are not nearly as large. Educating the population to reduce their water consumption and the installation of water saving devices can greatly contribute to the reduction in the demand for drinking water, however, this alone will not satisfy the level of reduction that is required. Water recycling offers a decentralised solution which can greatly reduce a household's water consumption. The use of drinking water for non-potable applications such as toilet flushing or laundry is thought to be one of the biggest problems with domestic water usage, it has been reasoned that recycling of GW for such applications is beneficial both environmentally and economically.

1.3.2 Infection via GW Reuse

Waterborne bacterial and viral pathogens can be spread in many ways, most commonly by inhalation, ingestion or through topical contact[63]. The generation of aerosols from reuse applications such as toilet flushing and car washing presents a clear pathway to infection and as such governing bodies present strict guidelines of the bacterial content of GW for reuse applications. Once a waterborne pathogen such as *Pseudomonas Aeruginosa* or *Staphylococcus Aureus* has been spread through a generated aerosol they can easily be ingested via inhalation or can settle on surfaces leading to infection through topical skin contact.

Infection with pathogens such as *Staphylococcus Aureus* and *Pseudomonas Aeruginosa* generally leads to skin or respiratory infections. A healthy adult has a strong enough immune system to be able to effectively fight off this infection and therefore it does not lead to severe disease. However, when the infected person is particularly susceptible to infectious pathogens and has a weaker immune system, i.e. the elderly or infants, there is a serious risk of developing severe diseases. Further to the generation of aerosols, the reuse of GW for unintended purposes is another cause of infection, it is recommended that GW is reused for toilet flushing, crop irrigation and laundry. Using recycled GW to fill up pools is a common misuse that can easily lead to the ingestion of pathogens and therefore infection.

Before it is sent to a treatment system, GW must be separated from blackwater (BW), blackwater is in-house wastewater which includes wastewater from toilet sources and as such it is heavily contaminated. BW must be sent to an appropriate treatment centre and therefore on-site treatment is not possible. GW, however, can be treated on site, further to this GW can be separated into two sub categories; light greywater (LGW) and dark greywater (DGW), with DGW being the more heavily contaminated stream and includes wastewater from kitchen and laundry sources. The literature contains a large amount of information about the exact contents of GW and BW[64-66], unfortunately due to the number of variables involved it is difficult to exactly quantify the biological oxygen demand (BOD), chemical oxygen demand (COD) and faecal coliform values in a typical GW and BW stream. It is generally agreed that the lowest COD for BW from a household source is > 1000 mg l^{-1}, whereas GW varies between 100 mg l^{-1} for LGW and 1000 mg l^{-1} for DGW. As is expected, BW contains not only a very high concentration of faecal coliforms but also an array of enteric and

opportunistic pathogens. The high concentration of such pathogens ultimately means that it is not deemed to be safe for human health to reuse BW. Whilst GW is much less contaminated than BW it is still important to realise the level of contamination present and the mixture of different bacteria and organic matter that must be effectively treated before it is safe to reuse. Studies are often contradictory and confusing when identifying the bacteria present in GW samples. For instance, a study by Burrows *et al*[67] reported that a high concentration of *Staphylococcus Aureus* was found in GW samples collected from military camps and in another study, it was found that *Staphylococcus Aureus* was present in household GW samples. Contradictory to this, Casanova *et al*[68] did not observe any *Staphylococcus Aureus* in household GW, where the composition of GW from an individual household was investigated for seven months. These findings show that the exact composition of GW cannot be defined from a single study and that it will vary greatly depending on the variables of the household/site at which the GW is produced. The inclusion of wastewater from a kitchen source also means that bacteria such as *Salmonella* and *Campylobacter* have been seen in GW.

1.3.3 Current Technologies

1.3.3.1 Types of Treatment Systems

The complexity of GW means that treatment systems need to be efficient and often multi-stage, often relying on hazardous chemical treatments to fully decontaminate the sample before reuse. Greywater treatment systems (GTS) have been in place for many years and are generally simple, consisting primarily of a source, pre-treatment area, treatment area and a pump to send the treated GW to its non-potable end use. The composition of GW has been widely reported within the literature and it is believed that a mean composition contains approximately 10^7 CFU 100 ml^{-1}, as well as a heavy organic load. Treatment systems must therefore be highly effective at removing bacteria from an aqueous solution to ensure that contamination is not circulated into the household water system and human health is protected.

In a review of current GTS's, Pidou *et al*[69] split the current technologies into five major sections:

1. Simple treatment systems.
2. Chemical treatment systems.
3. Physical treatment systems.
4. Biological treatment systems.
5. Extensive treatment systems.

Simple treatment systems are described as a two-stage technology, where the GW is initially filtered and then once filtered it is disinfected. These systems commonly rely on a crude disinfection method to remove microorganisms such as sodium hypochlorite (NaClO), which although highly effective, carries a large environmental burden as green chemical principles look to move away from the use of stoichiometric reagents which lead to the generation of harmful waste by-products. Simple treatment systems have been found to be financially unviable as overhead and operating costs greatly outweigh the water savings from using the system. A schematic diagram of a simple GTS is shown below in figure 1.9:

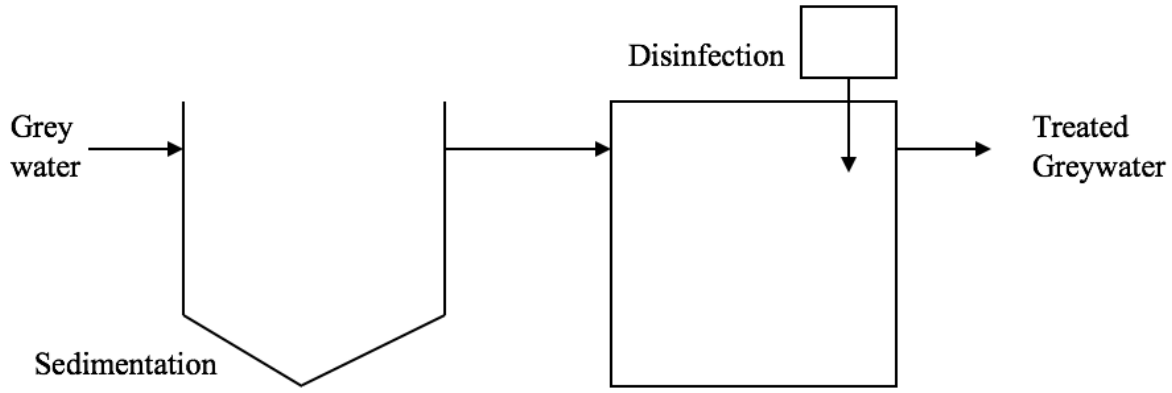

Figure 1.9: Schematic diagram showing a simple GTS.

Chemical treatment systems, like the simple treatment system, uses a chemical disinfectant to remove any microorganisms from the GW, unlike the simple treatment system, they consist

of a single treatment chamber. Although the design may sound simple as there is only a single treatment tank, the chemical treatment systems reported in the literature are surprisingly complex. Granular activated carbon (GAC) was reported to treat GW from laundry sources when used in collaboration with a sand filter[70], however this treatment system only reported to be effective for the removal of suspended solids, meaning it is not suitable for all GW sources. Another chemical treatment system utilised aluminium (Al) based electro-coagulation to good effect[71], the authors only reported this treatment for a weak GW solution, again limiting its potential use. The final example is a photocatalytic system[72] in which UV radiation is used along with TiO_2 as a photo catalyst, whilst this showed some promise in the treatment results, it relies upon a highly energy intensive and expensive technology.

Biological treatment systems are the most widely reported in the literature, with many different designs suggested, these are however seldom seen used individually, with a further disinfection step required to remove the microbiological contamination typically present in GW. The biological aspect appears in the filtration mechanism of the treatment system, with common biological treatment systems including membrane bioreactors[73], biological aerated filter systems[74], fixed film reactors[75] and rotating biological contactors[76]. As is to be expected, these devices are somewhat complex to engineer and as previously mentioned perform little to no disinfection of the GW, only removing solid matter. These treatment systems are aimed primarily at larger buildings and only prototype systems exist in the literature for much smaller scale uses.

Extensive treatment systems are described as "wetlands such as reed beds and ponds"[69] containing many different species of plants within a reed bed. Whilst these show a good removal of suspended solids, treatment of microorganisms is relatively poor, the systems also require extensive maintenance.

1.3.3.2 Chemical Disinfection of GW

Chemical disinfection can be described as the addition of a chemical to a solution containing microorganisms, the chemical added is toxic to the microorganisms present, causing them to die[77]. The most common chemical disinfectants are chlorinated disinfectants and ozone (O_3), although there is a good amount of literature on the use of H_2O_2.

The common theme with such chemical disinfectants is that they are strong chemical oxidants, it is believed that oxidation of the microorganisms DNA is the cause of cell inactivation[78]. The oxidation process can cause irreversible damage to the repair mechanisms present within the cells of the microorganisms ultimately leading to cell death. Chemical disinfection in wastewater can be difficult as there is often organic and inorganic particulate matter present too, this matter can also undergo oxidation reactions leading to the deactivation of the chemical disinfectant. The real-life effect of this is that a period where the microorganisms are effectively shielded by the particulate matter occurs and during this period only a small amount of disinfection is achieved. After this initial period and the amount of chemical disinfectant has exceeded the particulate matter present then an effective disinfection period can be achieved again.

1.3.3.3 Chlorine as a Chemical Disinfectant

The most widely used chemical disinfectant is chlorine, it can be used in many forms including gaseous chlorine (Cl_2), NaOCl and calcium hypochlorite (CaOCl). NaOCl and CaOCl are the most attractive options as they are generally safer and easier to handle and store than other chlorinated disinfectants such as chlorine dioxide (ClO_2) and Cl_2. The solubility of pelleted CaOCl does indeed make it an attractive option for the disinfection of urban wastewater, coupled with the fact that generally only small doses of hypochlorites (OCl^-) are needed to eliminate moderate concentrations of waterborne bacteria it is easy to see why this disinfectant is one of the most employed in the treatment systems previously discussed. However, there are fundamental issues with using OCl^- to treat GW. Firstly, the efficacy of the disinfectant is greatly reduced when using a GW that has an organic load or contains particulate matter[79]. For example, OCl^- will readily react with trace amounts of Fe which can be easily found in most urban wastewater, the same is true of ammonia (NH_3). March *et al*[80] demonstrated that when organic material is present, a much higher initial concentration of chlorine is needed than usual as the disinfectant undergoes deactivation. Shielding effects due to shielding or particle associate aggregation are again well documented within the literature and many studies note a so-called "tailing"[79] and the inactivation of the remaining, shielded microorganisms is independent of the disinfectant concentration.

1.3.3.4 Ozone as a Chemical Disinfectant

O_3 is another strong chemical oxidant which can be employed as a chemical disinfectant. It is a triatomic oxygen compound and its formation involves the splitting of O_2 to form radicals which subsequently undergo a recombination reaction to form O_3. Naturally occurring O_3 is formed in the upper atmosphere via a photoreaction using UV radiation from the sun. O_3 is also formed from the photoreactions of industrially emitted pollutants such as NO_x gases. O_3 is highly unstable and so it is formed at its point of use, in addition to UV generation, O_3 can be generated synthetically via a method known as the corona discharge method[81]. An oxygen containing gas, such as air, is passed across a set of electrodes which are separated by a discharge gap. A voltage is then applied to the electrodes and the discharge gap facilitates the flow of electrons which leads to the splitting of O_2 and O_3 is generated. When O_3 is added to H_2O the formation of OH• radicals is facilitated, the powerful oxidising nature of these radicals is well known and can help to explain the efficacy of O_3 as a chemical disinfectant. Like Cl_2, O_3 is thought to attack the DNA of microorganisms causing irreparable cell damage[82].

One of the main benefits to using O_3 as opposed to chlorinated chemicals is its ability to effectively deactivate protozoans and viruses such as *Cryptosporidium* and *Giardia*, an area where Cl_2 is known to not be very effective[82]. Disinfection of GW with O_3 can also vastly improve the turbidity and odour with relatively small doses, something which is again not easily achieved using chlorinated disinfectants. The short lifetime of the most active OH• radicals means that short contact times are required when using O_3, a study by Xu *et al*[83] found that increasing the contact time fivefold did not lead to a greater reduction in bacteria when investigating the disinfection of wastewaters. Unfortunately, organic loads also pose a problem for O_3, reaction with the organic matter leads to a decomposition of O_3 and therefore chemical deactivation. Problems with organic loads can be reduced by filtering the wastewater prior to treatment, however, this increases the complexity and the cost of the wastewater treatment system. Regrowth of bacteria can be a problem for wastewater treated with O_3, its short lifetime means and inherent instability can lead to a rapid deactivation and treatment with O_3 has even been shown to increase the availability of nutrients which are essential for bacterial growth, such as phosphorous.

1.3.3.5 Peracetic Acid as a Chemical Disinfectant

Peracetic Acid (CH_3CO_3H) is a simple organic molecule and is the peroxy form of acetic acid (CH_3COOH), it is known for its high oxidising potential and is often employed as an unselective oxidant in total oxidation processes. Another potential use for CH_3CO_3H is in the treatment of wastewaters. Commercially, CH_3CO_3H is obtained in an equilibrium mixture also containing H_2O_2, acetic acid (CH_3COOH) and H_2O, represented by the equation shown in scheme 1.3 below:

$$CH_3COOH + H_2O_2 \longrightarrow CH_3CO_3H + H_2O$$

Scheme 1.3: Formation of CH_3CO_3H from CH_3COOH and H_2O_2.

As the reaction equation shows, CH_3CO_3H is formed from the simple reaction between and CH_3COOH and H_2O_2, H_2SO_4 is also added to the reaction mixture as a catalyst. The CH_3CO_3H mixture is unfortunately highly unstable and so problems with storage and transport can arise, another consequence of the instability of CH_3CO_3H is that the initial starting concentration is usually very high, whilst its strong oxidising abilities mean that often only very mild doses are needed for the intended use. From a green chemistry perspective, this is not ideal.

CH_3CO_3H has been investigated as a disinfectant for many years with the earliest reports in the literature dating back to 1902[84]. As is the trend with the other antimicrobial agents examined in this chapter, CH_3CO_3H is most effective against bacteria and viruses, it is least effective against spores and protozoans. During the 1980's many studies were published on the use of CH_3CO_3H as a disinfectant to treat wastewaters. Baldry[85] reported that concentrations as low as 25 mg l^{-1} with a contact time of 5 minutes led to a 5-log reduction of *Escherichia Coli*. In a more recent study, *Rossi et al*[86] investigated the efficacy of CH_3CO_3H to treat municipal wastewaters and compared the results to those using a conventional chlorine treatment. Faecal coliforms and *Escherichia Coli* were chosen as marker bacteria and varying doses of CH_3CO_3H (1 – 15 mg l^{-1}) were investigated for contact time of 6, 12,18, 24, 36, 42 and 54 minutes, after which the post reaction effluent was plated and marker bacteria were enumerated 5 hours after the aforementioned time points. The results showed that a 4-log reduction of *Escherichia Coli* could be achieved using doses in the range of 5 to

10 mg l^{-1} for contact times ranging from 36 to 54 minutes, when the dose was increased to 15 mg l^{-1} a 5-log reduction is seen for the same contact time. This is said to be in the same range as is used for the treatment of municipal wastewater with chlorine.

Flores *et al*[87] studied the efficacy of CH_3CO_3H and the potential synergistic effect, previously eluded to in the literature, between H_2O_2 and CH_3CO_3H which is present in the commercially available CH_3CO_3H equilibrium mixture used. The effect of CH_3CO_3H alone was studied for comparison by adding small amounts of catalase enzyme (500 µl) which breaks down H_2O_2 into H_2O and O_2, whereas neutralisation of the complete mixture was achieved by a further addition of sodium thiosulphate ($Na_2S_2O_3$) (200 µl). The authors note that the CH_3CO_3H and H_2O_2 containing mixture achieves a 4-log reduction after a contact time of approximately 2 minutes. Interestingly, when H_2O_2 is inhibited the contact time must be significantly increased to achieve the same level of inactivation, a similar trend is noted when a higher concentration of 8 mg l^{-1} is used. The inhibition of H_2O_2 leads to a tailing in the inactivation, illustrated below in figure 1.10:

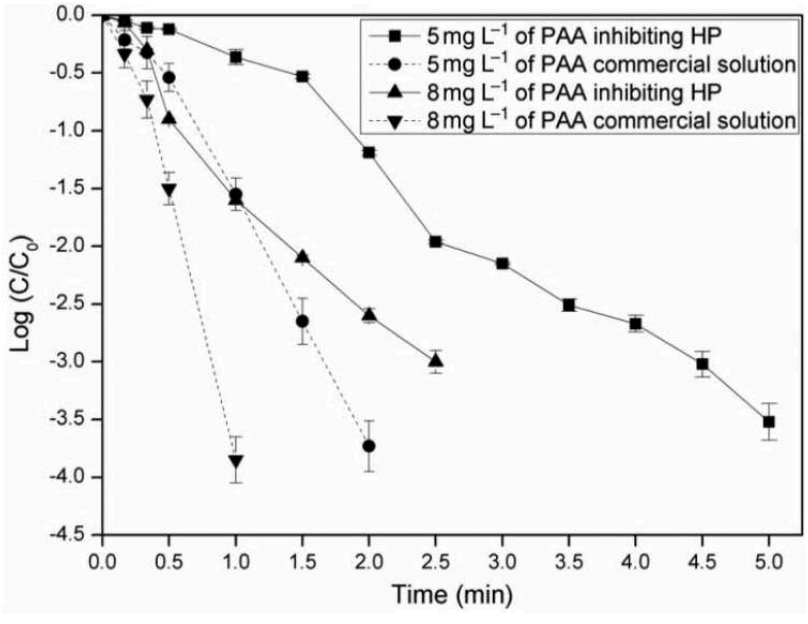

Figure 1.10: Graph showing the log reduction of *Escherichia Coli* as a function of time for varying starting concentrations of CH_3CO_3H solution with and without inhibition of H_2O_2[87].

The authors propose an interesting new reaction mechanism to explain this observed synergistic effect. The rate determining step when H_2O_2 is solely used is the initial "injuring" of the bacteria, whereby the bacteria have suffered some damage but are not considered to be dead and can still repair the damage. This is thought to be due to the defensive mechanisms of bacteria where the enzyme catalase is used, CH_3CO_3H is not affected by this and as such this step happens much faster when CH_3CO_3H is present. Once the bacteria are injured, the H_2O_2 acts rapidly, further damaging the bacteria to an irreparable level, in contrast to the initial injuring step, this happens much quicker with H_2O_2 than with CH_3CO_3H and is the rate determining step for CH_3CO_3H. The synergistic effect is therefore thought to be present as the bacteria are rapidly injured by the CH_3CO_3H and then the H_2O_2 kills the bacteria.

CH_3CO_3H suffers from the same two major drawbacks as previously discussed with chemical disinfection methods. Firstly, the presence of organic matter and other pollutants in the wastewater can cause a lag in the disinfection as the demand for the disinfectant needs to overcome the amount of organic material/inorganic pollutants that may be present before the true antimicrobial potential is seen. Secondly, the same materials can effectively shield microorganisms as they become embedded in the matter and are therefore unaffected by the antimicrobial agent.

Further to this study, Flores *et al*[88] investigated the kinetic pathway to the previously proposed mechanism. The authors studied a proposed rate mechanism for all the pathways which could lead to bacterial lysis through disinfection by CH_3CO_3H only, H_2O_2 only and a combination of both disinfectants. The pathways are summarised in the schematic shown below in figure 1.11. The authors state that the kinetic pathway is based on the assumptions that the disinfectant concentration is uniform and perfectly mixed throughout the reactor volume, the disinfectant is also assumed to be in an excess to the bacteria and constant throughout the reaction. It is reported for CH_3CO_3H acting alone that the rate limiting step is the initial attack of the biocide upon the outer cell membrane, the authors show that this is in good agreement with their computational model and with previous literature. The second step of the reaction is not rate limiting and consists of an inhibition of enzymatic reaction in the cytoplasmic membrane. Finally, once the cell has become sensitised and the biocide has penetrated the cytoplasmic membrane it rapidly causes irreversible damage in the quickest stage of the process.

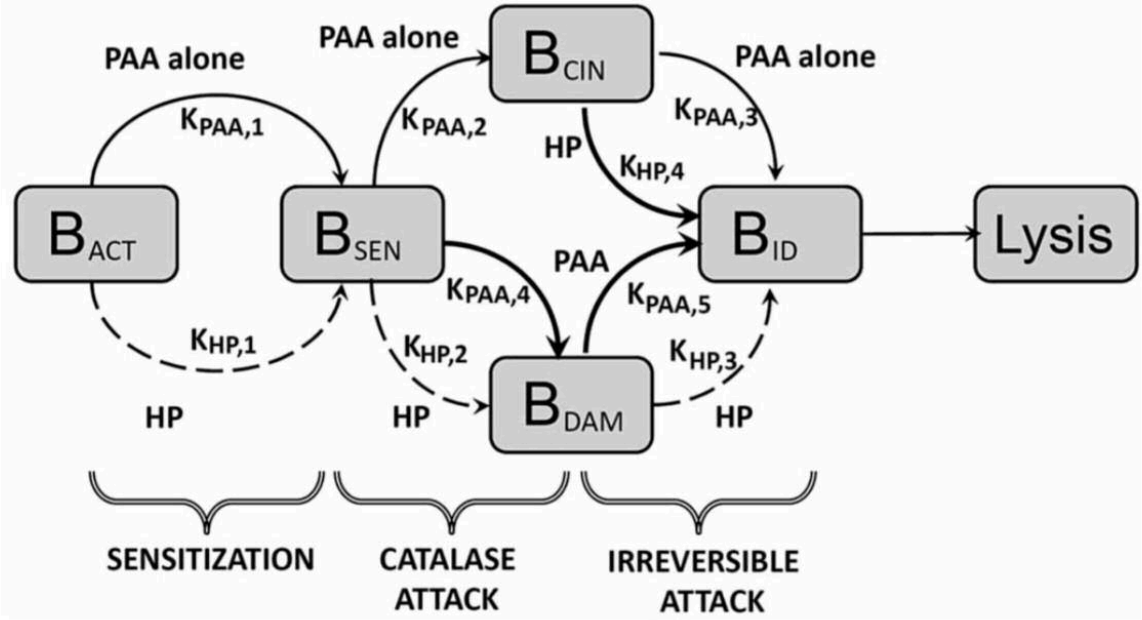

Figure 1.11: Schematic mechanism of the kinetic pathway leading to bacterial lysis using commercially available CH_3CO_3H[88].

Interestingly, when studying the kinetics of H_2O_2 acting alone, the rate constant values for the initial stage of the reaction (permeation of the cell wall) are practically the same, this is somewhat surprising considering the higher oxidation potential of CH_3CO_3H, this result is reasoned due to several factors, including the ability of H_2O_2 to permeate the cell membrane, the same chemical nature of attack between both compounds and the defence mechanism of the *Escherichia Coli* cells. The second stage of attack, sensitisation of the cell is shown to be the rate limiting step in this reaction due to the susceptibility of H_2O_2 to the catalase enzyme which must be overcome with time, unlike with CH_3CO_3H which is unaffected by this enzyme. When comparing the rate constants from the final stage of reaction, CH_3CO_3H is far superior with a much larger rate constant value, this is explained as CH_3CO_3H has a very specific free radical chain mechanism.

1.3.3.6 H_2O_2 as a Chemical Disinfectant

H_2O_2 has gained attention for its potential use as a disinfectant for wastewater for several reasons. It has a high redox potential and therefore has the promise to effectively inactivate

bacteria either by a direct interaction or by free radicals which are readily formed through decomposition reactions. Generation of hazardous by-products are avoided as mentioned earlier in this chapter, only H_2O is generated through decomposition or hydrogenation reactions, unlike chlorinated disinfectants. Furthermore, it is relatively inexpensive to use unlike treatment with O_3 and UV which are energy intensive processes.

Drogui *et al*[89] studied the production of H_2O_2 via H_2O electrolysis using a two-electrode cell and the application of this technology to water disinfection. The production of H_2O_2 was carried out in tap H_2O and disinfection experiments used municipal wastewater and *Pseudomonas Aeruginosa* (20 000 CFU ml^{-1}). In the case of the production of H_2O_2, the authors show that when using a reactor set up which included the injection of pure O_2 into the reaction and no reservoir, there was a linear increase in the production of H_2O_2 with increasing current. When applied to municipal wastewater it was found that the turbidity of the water was completely removed after electro-peroxidation and the appearance of the sample changed from brown to transparent. The removal of faecal coliforms was found to be related to the current intensity, as is to be expected, with 1 and 3-log reductions observed at 0.5 and 2.0 A respectively. Mineral H_2O (non-carbonated) was contaminated with *Pseudomonas Aeruginosa* and then subjected to two treatment methods, firstly just with treatment by H_2O_2 and the associated free radicals and secondly with the added electrical effect as electrolysis was maintained in the presence of the brass catalyst. It was seen that a greater disinfection was achieved, 3-log reduction, by using a combination of H_2O_2 and electrolysis compared with a 1-log reduction using H_2O_2 alone.

It is believed that there are several mechanisms by which H_2O_2 can cause cell inactivation. However, it is in good agreement in the literature that the presence of OH• radicals is required to cause the oxidative irreversible cell damage which leads to cell death[90]. For this to occur the H_2O_2 molecule must diffuse through the cell membrane, the size of the H_2O_2 molecule is an advantage here as it is a very simple and small molecule, meaning diffusion can be easily facilitated, although as previously mentioned in this chapter it is believed this is the rate limiting step in the process. The literature reports that the presence of Fe^{2+} cations can rapidly catalyse the decomposition of H_2O_2 into the highly reactive OH• radicals and this can be intra or extra cellular[91].

The use of H_2O_2 as the only disinfectant is not regularly reported in the literature, in fact H_2O_2 tends to be employed in collaboration with other chemical disinfectants or technologies such as O_3, UV radiation, CH_3CO_3H etc.

1.3.3.7 UV light as a chemical disinfectant

UV light has gained attention over recent years for its ability to disinfect wastewaters in what is thought to be a green and environmentally friendly process, this is reasoned as nothing is added to the wastewater and therefore there is no impact on the chemical composition. Gurzadyan *et al*[92] investigated the effect of UV laser radiation on *Escherichia Coli,* the bacteria were exposed to pulses of UV radiation of wavelength of 264, 219 and 193 nm, the authors report that photo dimers were present in the chromosomal DNA of bacteria even after exposure to 193 nm radiation. It was discussed whether protein damage has a significant effect on the deactivation of *Escherichia Coli* and the authors report that in fact protein damage does not play a role in the inactivation of the bacteria, instead its function is to shield the intracellular DNA against irradiation of UV light.

Another benefit of UV radiation for the disinfection of wastewater is that it has been shown to be effective not only against bacteria but also against viruses and protozoa, including *Giardella* and *Cryptosporidium* which are known to be resistant against disinfection with chlorine[93]. As has been discussed previously with chlorine and O_3 disinfection, the presence of organic matter and particulates has a significant effect on the inactivation of microorganisms when using UV radiation. Particulate matter containing microorganisms effectively shields from UV radiation as the radiation is absorbed by the particulate matter leaving the microorganism unscathed. The size, porosity and UV absorbing properties of the particles all influence the efficacy disinfection of UV radiation and so to effectively remove bacteria from urban wastewaters it would again be desirable to filter the wastewater prior to treatment with UV radiation.

1.4 Thesis Aims

The aims of this thesis are outlined below:

1. The use of *in-situ* generated H_2O_2 has been reported for many uses but there is no work detailing the use of *in-situ* H_2O_2 for GW sterilisation. This work aims to investigate the effectiveness of *in-situ* H_2O_2 as an antimicrobial agent in the sterilisation of GW. Firstly, establishing whether *in-situ* H_2O_2 is capable of sterilising GW. This will be investigated by using a continuous flow system and a known heterogeneous catalyst, the initial aims of the study are to prove the proof of concept as this has not yet been explored. Secondly, an investigation will be performed into how effective *in-situ* H_2O_2 is as an antimicrobial agent. To achieve this, in-situ H_2O_2 will be compared to various H_2O_2 sources using Escherichia Coli (JM109) as the bacteria, should this be successful, a detailed investigation into the antimicrobial activity of the in-situ H_2O_2 system against various other bacteria such as Staphylococcus Aureus and Pseudomonas Aeruginosa.

2. The investigation of the synergistic effect between Pd and Sn in the development of heterogeneous catalysts for the direct synthesis of H_2O_2 will be carried out via the synthesis, testing and characterisation of new Pd/SnO_2 catalysts and exploring whether a sol-gel method is an effective catalyst preparation technique for such catalysts when compared with the traditional wet impregnation. Sn presents a much cheaper alternative to other secondary metals such as Au for the enhancement of selectivity of heterogeneous Pd catalysts. Previous work within the group[52] has shown that SnO_2 strongly interacts with Pd to contribute towards the high selectivity of PdSn bimetallic catalysts. Thus, the investigation of SnO_2 as a support for Pd catalysts could potentially yield catalysts that are active, selective and cheaper than AuPd counterparts.

1.5 References

1. V. Smil, *Nature,* **1999**, *400*, 415.
2. K. J. Laidler, *Pure Appl. Chem.,* **1996**, *68*, 149 – 192.
3. G. Somorjai, C. J. Kliewer, *Reac. Kinet. Catal. Lett.*, **1987**, *35*, 191 - 208.
4. L. J. Thenard, *Ann. Chim. Phys.* **1818**, 306.
5. H. Medinger, *Ann. Chem. Pharm.* **1853**, 88.
6. H. J. Riedl, G. Pfleiderer, *US Patent No. 2158525*, **1939**
7. G. Pfleiderer, *US Patent No. 2215856*, **1940**
8. W. Manchot, *Liebigs Ann. Chim.*, **1901**, *314*, 377.
9. Q. Chen, *Chem. Eng, Process.*, **2008**, *47*, 787 - 792.
10. J. M. Campos-Martin, G. Blanco-Brieva, J. L. G. Fierro, *Ang. Chem. Int. Ed*, **2006**, *45*, 6962 – 6984.
11. C. W. Jones, *Applications of hydrogen peroxide and its derivatives*, Royal Society of Chemisty; London **1990.**
12. B. Liu, M. Qiao, J. Wang, K. Fan, *Chem. Comm.,* **2002**, 1236-1237.
13. B. Liu, M. Qiao, J. F. Deng, K. N. Fan, X. X. Zhang, B. N. Zong, *J. Catal.* **2001**, *204*, 512.
14. Y. Hou, Y. Wang, F. He, *Materials Lett.,* **2004**, *58*, 1267 – 1271.
15. P. T. Anastas, J. C. Warner, *Green Chemistry: Theory and Practice*, Oxford University Press: New York, **1998**, p.30.
16. H. Henkel, W. Weber, *US Patent No. 4410501*,**1914**.
17. J. K. Edwards, S. J. Freakley, R. J. Lewis, J. C. Pritchard, G. J. Hutchings, *Catal. Today*, **2015**, *248*, 3-9.
18. M. Selisnek, M. Bohrer, B. K. Vankayala, K. Hass-Santo, M. Kraut, R. Dittmeyer, *Catal. Today*, **2016**, *268*, 85-94.
19. T. A. Pospelova, N. I. Kobozev, E. N. Eremin, *Russian Journal of Physical Chemistry*, **1961**, *35*, 298 – 305.
20. T. A. Pospelova, N. I. Kobozev, *Russian Journal of Physical Chemistry*, **1961**, *35*, 535 – 542.
21. T. A. Pospelova, N. I. Kobozev, *Russian Journal of Physical Chemistry*, **1961**, *35*, 1192 – 1197.
22. A. G. Gaikwad, S. D. Sansare, V. R. Choudhary, *Journal of Molecular Catalysis A: Chemical* **2002**, *18*, 143 – 149.

23. S. Melada, R. Rioda, F. Menegazzo, F. Pinna, G. Strukul, *J. Catal*, **2006**, *239*, 422-430.
24. S. Chinta, J. H. Lunsford, *J. Catal,* **2004**, *225*, 249 – 255.
25. G. Blanco-Brieva, E. Cano-Serrano, J. M. Campos-Martin, J. L. G. Fierro, *Chem. Comm.*, **2004**, 1184 – 1185.
26. R. A. Sheldon, M. Wallau, I. W. C. E. Arrends, *Acc. Chem. Res.*, **1998**, *31*, 485 – 493.
27. D. P. Dissanayake, J. H. Lunsford, *Journal of Catalysis* **2002**, *206*, 173 – 176.
28. D. P. Dissanayake, J. H. Lunsford, *Journal of Catalysis* **2003**, *214*, 113 – 120.
29. J. H. Lunsford, *Journal of Catalysis* **2003**, *216*, 455 – 460.
30. S. Chinta, J. H. Lunsford, *Abstracts of Papers of the American Chemical Society* **2004**, *227*, 229.
31. Y. F. Han, J. H. Lunsford, *Catalysis Letters* **2005**, *99*, 13 – 19.
32. Y. F. Han, J. H. Lunsford, *Journal of Catalysis* **2005**, *230*, 313 – 316.
33. Q. S. Liu, J. H. Lunsford, *Journal of Catalysis* **2006**, *239*, 237 – 243.
34. Q. S. Liu, J. H. Lunsford, *Applied Catalysis A: General* **2006**, *314*, 94 – 100.
35. Q. S. Liu, J. C. Bauer, R. E. Schaak, J. H. Lunford, *Angew. Chem. Int. Ed.*, **2008**, *47*, 6221-6224.
36. Q. S. Liu, K. K. Gath, J. C. Bauer, R. E. Schaak, J. H. Lunsford, *Catal. Lett.*, **2009**, *132*, 342 – 348.
37. V. R. Choudhary, C. Samanta, T. V. Choudhary, *Appl. Catal. A.*, **2006**, *308*, 128 – 133.
38. V. R. Choudhary, C. Samanta, A. G. Gaikwad, *Chem. Comm.*, **2004**, *18*, 2054 – 2055.
39. V. R. Choudhary, C. Samanta, *J. Catal.*, **2006**, *238*, 28 – 38.
40. M. Haruta, N. Yamada, T. Kobayashi, S. Iijima, *J. Catal.*, **1989**, *115*, 301 – 309.
41. P. P. Olivera, E. M. Patrito, H. Sellers, *Surf. Sci.*, **1994**, *313*, 25-40.
42. P. Landon, P. J. Collier, A. J. Papworth, C. J. Kiely, G. J. Hutchings, *Chem Commun.*, **2002**, 2058 – 2059.
43. T. Ishihara, Y. Ohura, S. Yoshida, Y. Hata, H. Nishiguchi, Y. Takita, *Appl. Catal. A.*, **2005**, *291*, 215 – 221.
44. B. S. Uphade, T. Akita, T. Nakamura, M. Haruta, *J. Catal.*, **2002**, *209*, 331 – 340.

45. B. Chowdhury, J. J. Bravo-Suarez, N. Mimura, J. Q, Lu, K. K. Bando, S. Tsubota, M. Haruta, *J. Phys. Chem. B.*, **2006**, *110*, 22995 – 22999.
46. M. Okumura, Y. Kitagawa, K. Yamaguchi, T. Akita, S Tsubota, M. Haurta, *Chem. Lett.*, **2003**, *32*, 822 – 823.
47. G. C. Bond, D. T. Thompson, *Catal. Rev. Sci. Eng.*, **1999**, *41*, 319 – 388.
48. S. Q. Ma, G. Li, X. S. Wang, *Chem. Eng. J.*, **2008**, *156*, 532 – 539.
49. A. Corma, P. Serna, *Science*, **2006**, *313*, 332 – 334.
50. B. Solsona, J. K. Edwards, P. Landon, A. F. Carley, A. Herzing, C. J. Kiely, G. J. Hutchings, *Chem. Mater.*, **2006**, *18*, 2689 – 2695.
51. J. K. Edwards, B. Solsona, P. Landon, A. F. Carley, A. Herzing, M. Watanabe, C. J. Kiely, G. J. Hutchings, *J. Mater. Chem.*, **2005**, *15*, 4595 – 4600.
52. G. Bernadotto, F. Menegazzo, F. Pinna, M. Signoretto, G. Cruciani, G. Strukul, *Appl. Catal. A.*, **2009**, *358*, 129 – 135.
53. Y. Nomura, T. Ishihara, Y. Hata, K. Kitawaki, K. Kaneko, H. Matsumoto, *Chem. Sus. Chem.*, **2008**, *1*, 619 – 621.
54. K. Honkala, K. J. Laasonena, *Chem. Phys.*, **2001**, *115*, 2297 – 2302.
55. A. Staykov, T. Kamachi, T. Ishihara, K. Yoshizawa, *J. Phys. Chem. C.*, **2008**, *112*, 19501 – 19505.
56. J. S. Jirkovsky, I. Panas, E. Ahlberg, M. Halasa, S. Romani, D. J. Schriffin, *J. Am. Chem. Soc.*, **2011**, *103*, 19432 – 19441.
57. J. Pritchard, L. Kesavan, M. Piccinini, Q. He, R. Tiruvalam, N. Dimitratos, J. A. Lopez-Sanchez, A. F. Carley, J. K. Edwards, C. J. Kiely, G. J. Hutchings, *Langmuir*, **2010**, *26*, 16568 – 16577.
58. M. Sankar, Q. He, M. Morad, J. Pritchard, S. J. Freakley, J. K. Edwards, S. H. Taylor, D. J. Morgan, A. F. Carley, D. W. Knight, C. J. Kiely, G. J. Hutchings, *ACS Nano*, **2012**, *6*, 6600 – 6613.
59. S. J. Freakley, Q. He, J. H. Harrhy, L. Liu, D. A. Crole, D. J. Morgan, E. N. Ntainjua, J. K. Edwards, A. F. Carley, A. Y. Borisevich, C. J. Kiely, G. J. Hutchings, *Science*, **2016**, *351*, 965 – 958.
60. N. Kamiuchi, H. Muroyama, T. Matsui, R. Kikuchi, K. Eguchi, *Appl. Catal. A.*, **2010**, *379*, 148 – 154.
61. B. Jefferson, A. Palmer, P. Jeffrey, R. Stuetz, S. Judd, *Water. Sci. Technol.*, **2004**, *50*, 157 – 164.

62. P. Gerland, A. E. Raftery, H. Sevcikova, N. Li, D. Gu, T. Spoorenberg, L. Alkema, B. K. Woods, J. Chunn, N. Lalic, G. Bay, T. Buettner, G. K. Helig, J. Wilmoth, *Science*, **2014**, *346*, 234 – 237.
63. K. F. Fannin, S. C. Vana, W. Jakubowski, *Appl. Env. Microbiol.*, **1985**, *49*, 1191 – 1196.
64. H. Palmquist, J. Hanaeus, *Sci. Tot. Environ.*, **2005**, *348*, 151 – 163.
65. Y. Boyjoo, V. K. Pareek, M. Ang, *Water. Sci. Technol.*, **2013**, *67*, 1403 – 1424.
66. J. Kim, I. Song, J. Jong, J. Park, Y Choung, *Desalation*, **2009**, *238*, 347 – 357.
67. W. D. Burrows, M. O. Schmidt, R. M. Carnevale, S. A. Schaub, *Water. Sci. Technol.*, **1991**, *24*, 81 – 88.
68. L. M. Casanova, V. Little, R. J. Frye, C. P. Gerba, *J. Am. Water. Resour. Assoc.*, **2001**, *37*, 1313 – 1319.
69. M. Pidou, F. A. Memon, T. Stephenson, B. Jefferson, P. Jeffrey, *Proc. Inst. Civ. Eng. Eng. Sus.*, **2007**, *160*, 119 – 131.
70. S. Sostar-Turk, I. Pentric, M. Simonic, *Resourc. Conserv. Recy.*, **2005**, *44*, 185 – 196.
71. C. J. Lin, S. L. Lo, C. Y. Kuo, C. H. Wu, *J. Environ. Eng.*, **2005**, 491 – 495.
72. S. A. Parsons, C. Bedel, B. Jefferson, *Proceedings of the 9th International Gothenburg Symposium on Chemical Treatment*, **2000**, Istanbul, Turkey.
73. M. Andersen, G. H. Kristensen, M. Brynjolf, H. Gruttner, *Water. Sci. Technol.*, **2001**, *46*, 67 – 76.
74. S. Surendran, A. D. Wheatley, *J. CIWEM*, **1998**, *12*, 406 – 413.
75. E. Santala, J. Uotila, G. Zaitsev, R. Alasiurua, R. Tikka, J. Tengvall, *Proceedings of the 2nd International Advanced Wastewater Treatment Recycling and Reuse*, **1998**, Milan, Italy.
76. E. Nolde, *Urban Water*, **1999**, *1*, 275 – 284.
77. M. A. Shannon, P. W. Bohn, M. Elimelech, J. G. Georgiadis, B. J. Marinas, A. M. Mayes, *Nature,* **2008**, *452*, 301-310.
78. Q. Li, S. Mahendra, D. Y. Lyon, L. Brunet, M. V. Liga, D. Li, P. J. J. Alvarez, *Water Res.*, **2008**, *42*, 4591 – 4602.
79. R. W. Emerick, F. J. Lodge, T. Ginn, J. L. Darby, *Water. Environ. Res.*, **2000**, *72*, 432 – 438.
80. J. G. March, M. Gual, *Desalination*, **2009**, *249*, 317 – 322.

81. U. Kogelschatz, B. Eliasson, W. Egli, *Pure Appl. Chem.*, **1999**, *71*, 1819 – 1828.
82. J. A. Thurston- Enriquez, C. N. Haas, J. Jacangelo, C. P. Gerba, *Water Res.*, **2005**, *39*, 3650 – 3656.
83. P. Xu, M. L. Janex, P. Savoye, A. Cockx, V. Lazarova, *Water Res.*, **2002**, *36*, 1043 – 1055.
84. P. C. Freer, F. G. Novy, *Am. Chem. J.*, **1902**, *27*, 161 – 193.
85. M. G. C. Baldry, *J. Appl. Bacteriol.*, **1983**, 417 – 423.
86. S. Rossi, M. Antonelli, V. Mezzanotte, C. Nurizzo, *Water Environ. Res.*, **2007**, *79*, 341 – 350.
87. M. J. Flores, M. R. Lescano, R. J. Brandi, A. E. Cassano, M. D. Labas, *Water Sci. Technol.*, **2014**, *69*, 358 – 363.
88. M. J. Flores, R. J. Brandi, A. E. Cassano, M. D. Labas, *Water Sci. Technol.*, **2016**, *73*, 275 – 282.
89. P. Drogui, S. Elmaleh, M. Rumeau, C. Bernard, A. Rambaud, *J. Appl. Electrochem.*, **2001**, *31*, 877 – 882.
90. S. S. Block, *Disinfection, sterilization, and preservation,* 4th ed., Lea & Febiger: Philadelphia, **1991**, p.167 – 181.
91. J. A. Imlay, S. Linn, *Science*, **1988**, *240*, 640 – 642.
92. G. G. Gurzadyan, H. Gorner, D. Schulte-Frohlinde, *Radiat. Res.*, **1995**, *141*, 244 – 251.
93. W. A. M. Hijnen, E. F. Beerendonk, G. J. Medema, *Water Res.*, **2006**, *40*, 3 – 22.

Chapter 2

Experimental

In this chapter, the experimental procedures and techniques used for materials preparation, characterisation and testing are outlined. The materials discussed in this chapter are then discussed and used in detail throughout this thesis.

2.1 Materials Used

The following materials were used for all the experimental work undertaken in this thesis:

- $PdCl_2$, (ReagentPlus®, 99%, Sigma Aldrich)
- $HAuCl_4.3H_2O$ (99% > trace metal basis, Sigma Aldrich)
- $SnCl_4.5H_2O$ (98%, Sigma Aldrich)
- TiO_2 (Degussa, p25, 99.5% trace metal basis, 20 – 30 nm particle size)
- SnO_2 (99.9% trace metal basis, Sigma Aldrich)
- $Ce(SO_4)_2$ (98% >, Sigma Aldrich)
- $C_{36}H_{24}FeN_6O_4S_6$ (0.025 M, Sigma Aldrich)
- MeOH (HPLC grade, Sigma Aldrich)
- H_2O (HPLC grade, Sigma Aldrich)
- NH_4OH (28% NH_3 in H_2O, 99% > trace metal basis, Sigma Aldrich)
- 50 wt.% H_2O_2 (Sigma Aldrich)
- 30 wt.% H_2O_2 (non-stabilised, ACS Reagent, Acros Organics)
- *Escherichia Coli* (JM109)
- *Escherichia Coli* (ATCC 10536)
- *Staphylococcus Aureus* (NCTC 10788)
- *Pseudomonas Aeruginosa* (NCTC 10662)
- Nutrient Broth No. 2 (Sigma Aldrich)
- Tryptic soya broth (Oxoid)
- Tryptic soya agar (Oxoid)

2.2 Catalyst Preparation

2.2.1 Pd Catalysts Prepared by Impregnation

Monometallic Palladium (Pd) catalysts were made by impregnating the appropriate catalyst support with a requisite of Pd precursor solution to give the desired weight loading. Catalysts prepared by impregnation contained a total weight loading of 5 wt.% unless it is otherwise stated. The preparation of 2 g of a typical 5 wt.% Pd/SnO_2 catalyst follows the procedure which is well documented in the literature[1]. $PdCl_2$ (10 ml, 10 mg ml^{-1} solution) was heated to 80 °C and stirred for a few minutes, once the solution had reached the desired temperature the SnO_2 (1.90 g) support was added slowly under continuous stirring. The water (H_2O) was allowed to slowly evaporate and the heating was stopped once the mixture had reached a paste-like consistency. The resulting mixture was dried at 110 °C overnight and finally calcined in static air (500 °C, 3 hours, 20 °C min^{-1}) and the resulting brown powder was ground until a fine powder was achieved, yielding the final catalyst.

2.2.2 AuPd Bimetallic Catalysts Prepared by Modified Impregnation

Bimetallic AuPd catalysts were made by impregnating the appropriate catalyst support with a requisite amount of gold (Au) and Pd precursor solutions to give the desired weight loading. Catalysts prepared by modified impregnation contained a total weight loading of 1 wt.% unless it is otherwise stated. The preparation of 2 g of a typical 1 wt.% $AuPd/TiO_2$ catalyst follows the procedure which has been well documented in the literature[2].

A Pd precursor solution (6 mg ml^{-1}) was prepared by dissolving $PdCl_2$ into a 0.58 M HCl solution and stirred until the salt was fully dissolved. Requisite amounts of $HAuCl_4$ (8.9 mg ml^{-1}) and $PdCl_2$ (6 mg ml^{-1}, 0.58 M) were charged into a 100 ml round bottom flask and stirred vigorously (1000 rpm). The volume of the mixture was adjusted by addition of H_2O (HPLC grade) until the total volume was 16 ml. The mixture was heated from room temperature to 60 °C and after 10 minutes of heating the TiO_2 support (1.98 g, P25 Degussa) was slowly added to ensure thorough mixing between the support and aqueous metal solution. Once all the support had been added the resultant slurry was stirred at 60 °C for 30 minutes, the temperature was then raised to 95 °C and the slurry was heated overnight to evaporate the H_2O. A reddish-brown powder was finely ground and finally reduced (5% H_2/Ar atmosphere, 4 hours, 400 °C).

Once the furnace had cooled to room temperature a dark grey powder was ground to yield the final catalyst.

2.2.3 Pd Supported Catalysts Prepared by Sol-Gel.

Monometallic Pd catalysts were prepared by a sol-gel synthesis method in which the support material is synthesised via a hydrolysis reaction of a suitable precursor. Catalysts prepared by sol-gel contained a total weight loading of 5 wt.% unless it is otherwise stated. The preparation of 1.2 g of a typical 5 wt.% Pd/SnO_2 catalyst follows a method from the literature[3], whereby a high surface area tin oxide (SnO_2) material is formed with careful control of particle size depending upon the concentration and addition rate of the hydrolysis agent. This procedure was adapted to allow the formation of a Pd supported material via the addition of a Pd precursor to the SnO_2 precursor solution. $SnCl_4.5H_2O$ (2.94 g) was added to H_2O (50 ml, HPLC grade) and stirred (500 rpm) in a 100 ml round bottom flask, the requisite amount of $PdCl_2$ solution (10 mg ml^{-1}) was added to give the desired Pd loading. The mixture was heated to 30 °C and left to stir for 30 minutes. Following this an ammonium hydroxide (NH_4OH) solution (3.2 M) was added at a controlled rate of 0.1 ml min^{-1} using a HPLC pump. The resultant gel was aged overnight and then heated to 80 °C for a period of 16 hours, yielding a bright orange/red powder. The powder was washed with pure ethanol (EtOH), dried and finally calcined (static air, 500 °C, 3 hours) to give a very fine brown powder as the final catalyst product.

2.3 Catalyst Testing

2.3.1 Direct Synthesis of H_2O_2 in a Batch Reactor.

The activity of catalysts for the direct synthesis of hydrogen peroxide (H_2O_2) was tested in a stainless steel autoclave, supplied by Parr Instruments, with a nominal working volume of 100 ml and a maximum working pressure of 2030 psi. The standard working procedure for a direct synthesis reaction using such equipment has been widely reported in the literature[1]. In a typical reaction, the autoclave was charged with a reaction mixture of H_2O (2.9 g, HPLC grade), MeOH (5.6 g, HPLC grade) and 10 mg of the catalyst to be tested. MeOH is used as a co-solvent to allow reactions to be run at 2 °C and to increase hydrogen solubility. The autoclave was purged three times with 5% H_2/CO_2 (100 psi) before being pressurised with 5% H_2/CO_2

(420 psi) and then 25% O_2/CO_2 (160 psi). Reaction gases were diluted with to avoid working in the explosive region, CO_2 was chosen as carbonic acid is formed during the reaction, known to stabilise H_2O_2. Once at the desired total pressure, the autoclave was cooled to 2 °C and stirred for 30 minutes at 1200 rpm. Upon completion of the reaction, the autoclave was slowly depressurised and the reaction effluent was filtered to separate the product mixture from the catalyst. 0.5 g aliquots of the sample were taken and acidified using a 2% sulphuric acid (H_2SO_4) solution, the concentration of H_2O_2 in the solution was then determined via titration with cerium sulphate ($Ce(SO)_4$) utilising ferroin solution (0.025 M) as a redox indicator. The results of the experiment were expressed as a "productivity", that is, the average rate of H_2O_2 production which has been normalised to the catalyst mass and expressed in the unit mol_{H2O2} kg_{cat}^{-1} h^{-1}. Using productivity allows for a true comparison between different catalytic materials, the steps used in the calculation of productivity are outlined below in equations 1 - 5:

Firstly, the volume of $Ce(SO_4)_2$ required to titrate the whole reaction solution is determined:

$$\text{Volume } Ce(SO_4)_2 \text{ required to titrate reaction solution} = \frac{\text{recorded titre} \times 8.5}{\text{sample mass}} \qquad \text{Equation 1}$$

This volume is then converted to moles of $Ce(SO_4)_2$:

$$\text{Moles of } Ce(SO_4)_2 = \frac{\text{volume of } Ce(SO_4)_2 \times \text{concentration of } Ce(SO_4)_2}{1000} \qquad \text{Equation 2}$$

Using the stoichiometric ratio of the redox reaction:

$$H_2O_2 + 2Ce(SO_4)_2 \longrightarrow Ce_2(SO_4)_3 + H_2SO_4 + O_2 \qquad \text{Equation 3}$$

The molar amount of H_2O_2 in the reaction solution can be calculated:

$$\text{Moles of } H_2O_2 = \frac{\text{moles of } Ce(SO_4)_2}{2} \qquad \text{Equation 4}$$

Finally, the productivity is the calculated:

$$\text{Productivity} = \frac{\text{moles of } H_2O_2}{\text{mass of catalyst x reaction time}} \qquad \text{Equation 5}$$

2.3.2 H_2O_2 Hydrogenation in a Batch Reactor

The hydrogenation activity of catalysts towards H_2O_2 was evaluated using the same autoclave set-up as used in the direct synthesis process described above. The standard working procedure for a hydrogenation reaction using such equipment has again been widely reported in the literature[1]. In a typical reaction, the autoclave was charged with a reaction mixture of H_2O (2.22 g, HPLC grade), MeOH (5.6 g, HPLC grade), H_2O_2 (50 wt.% solution, 0.68 g) and 10 mg of the catalyst to be tested. Before the reaction mixture was charged with reaction gas, two drops of the reaction mixture were added to a titration solution of 2% H_2SO_4 and ferroin indicator, the mass of the reaction mixture was recorded and the solution was titrated with $Ce(SO_4)_2$. The autoclave was purged three times with 5% H_2/CO_2 (100 psi) before being pressurised with 5% H_2/CO_2 (420 psi). Once at the desired total pressure, the autoclave was cooled to 2 °C and stirred for 30 minutes at 1200 rpm. Upon completion of the reaction, the autoclave was slowly depressurised and the reaction effluent was filtered to separate the product mixture from the catalyst. Two drops of the sample were taken and acidified using a 2% H_2SO_4 solution, the concentration of H_2O_2 in the solution was then determined via titration with $Ce(SO)_4$ utilising ferroin solution (0.025 M) as a redox indicator. The hydrogenation activity was recorded and units of $mol_{H2O2}\ kg_{cat}^{-1}\ h^{-1}$ were used, the percentage of H_2O_2 consumed was also recorded.

2.3.3 Catalyst Re-Use in a Batch Reactor

The stability of catalysts was tested by re-using the catalyst for an additional direct synthesis reaction and recording the productivity of the second use to monitor any change in activity. As such, a direct synthesis reaction was performed using the experimental method described above, however, 70 mg of catalyst was used to ensure a sufficient amount could be easily recovered. The reaction solution was filtered and the collected catalyst was dried overnight using a vacuum desiccator to prevent any changes in oxidation state that could occur from reheating the catalyst in an oxidative atmosphere. Following this, a second synthesis reaction was performed and the catalyst performance was evaluated.

2.3.4 Direct Synthesis of H_2O_2 in a Flow Reactor

H_2O_2 synthesis reactions were performed in a continuous flow microreactor. The reactor was constructed using stainless steel Swagelok components with an internal diameter of 1/8 of an inch. Brooks gas flow controllers control the flow of 5% H_2 /CO_2, 25% O_2 /CO_2, 2% H_2/air and CO_2. Solvent was pumped through the system using an Agilent HPLC pump and the overall pressure of the reactor was controlled with a Swagelok back pressure regulator. The catalyst bed was submersed in a temperature controlled water bath and pressure gauges were positioned before and after the water bath to monitor pressure drops. Sampling was carried out using a gas liquid separator (GLS) (150 ml) fitted with a valve and positioned before the back pressure regulator. In a typical reaction, 120 mg of catalyst was pelleted (diameter ~ 425 – 350 μm) and packed into the microreactor catalyst bed supported by glass wool. The reactor was typically cooled to 2 °C in the water bath. The system was pressurised to 10 bar (unless otherwise stated) with a H_2:O_2 ratio of 1:2 unless otherwise stated. Total gas flows were kept at 42 ml min^{-1} and once the reactor was fully pressurised solvent (H_2O or H_2O/MeOH) was pumped through the system at a rate of 0.2 ml min^{-1}. The reactions conditions stated above follow those of the optimal conditions previously determined for H_2O_2 synthesis in this continuous flow system[4].

2.4. Sterilisation Tests

2.4.1 *In – situ* Sterilisation Tests in a Continuous Flow Reactor with *Escherichia Coli* (JM109)

Sterilisation tests using *in-situ* H_2O_2 were performed in the same continuous flow reactor as was used for direct synthesis investigations. The conditions were the same as for a direct synthesis reaction, unless otherwise stated, the H_2O (34%)/MeOH (66%) solvent was swapped for a solution of *Escherichia Coli* (JM109) suspended in H_2O (HPLC grade). Preparation of the working bacterial solution was achieved by the following procedure:

For model wastewater with a defined bacterial cell density, a single colony of *Escherichia Coli* (JM109) was transferred to nutrient broth no 2 (Sigma) and incubated at 37 °C, 150 rpm overnight. This culture was subcultured (1:50 dilution) into fresh nutrient broth no 2 and incubated at 37 °C, 150 rpm typically until an optical density at 600 nm of 0.6 was attained (~3 hours). 1 ml of this culture was then diluted into 40 ml of sterile H_2O to provide the model

wastewater. When an alternative cell density was required, the growth time was altered accordingly.

All sterilisation tests were evaluated using a cell counting procedure outlined below:

Cell counting was performed using nutrient broth no 2 plates containing 2% w/v agar. 50 µl aliquots of pre and post treatment samples of the model wastewater were plated directly and following 10^2 and 10^4 fold dilution. Plates were incubated at 37 °C overnight. Colonies were counted on all plates that gave non-confluent growth, and cell counts expressed as colony forming units per milliliter sample (CFU ml^{-1}). Errors between replicate plates were typically <10%. Controls showed that the number of colony forming units in the untreated model wastewater was not significantly altered by standing at room temperature for the duration of the sterilisation tests.

2.4.2 *In – situ* Sterilisation Tests Using a Continuous Flow Reactor with *Staphylococcus Aureus* (NCTC 10788)

Sterilisation tests using *in-situ* H_2O_2 were performed in the same continuous flow reactor as was used for direct synthesis investigations. The conditions were the same as for a direct synthesis reaction, unless otherwise stated, the H_2O (34%)/MeOH (66%) solvent was swapped for a solution of *Staphylococcus Aureus* (NCTC 10788) suspended in H_2O (HPLC grade). Preparation of the working bacterial solution was achieved by the following procedure:

For model wastewater with a defined bacterial cell density, a single colony of *Staphylococcus Aureus* (NCTC 10788) was transferred to tryptic soya broth (TSB) growth medium (Oxoid, 20 ml) and incubated at 37 °C, 150 rpm overnight. This culture was washed by centrifugation (1500g, 15 minutes, 23 °C) and the supernatant was removed. The bacteria were re-dispersed into sterile H_2O (HPLC grade, 20 ml) and vortexed until complete re-dispersion was achieved. The optical density of the solution was measured at 600 nm and the solution was diluted until a measurement of 0.6 was attained. 1 ml of this culture was then diluted into 40 ml of sterile H_2O to provide the model wastewater. When an alternative cell density was required, the growth time was altered accordingly.

All sterilisation tests were evaluated using a cell counting procedure outlined below:

Cell counting was performed using tryptic soya agar (TSA) plates containing 2% w/v agar. 10 μL aliquots of pre and post treatment samples of the model wastewater were plated directly and following 10 - 10^5 fold dilution. The "drop-count" method was utilised (figure 2.1), whereby 3 x 10 μl aliquots were plated for each dilution. Plates were incubated at 37 °C overnight. Colonies were counted on all plates that gave non-confluent growth, an averaged count from the 3 aliquots plated was taken and cell counts were expressed as colony forming units per milliliter sample (CFU ml^{-1}). Errors between replicate plates were typically <10%. Controls showed that the number of colony forming units in the untreated model wastewater was not significantly altered by standing at room temperature for the duration of the sterilisation tests.

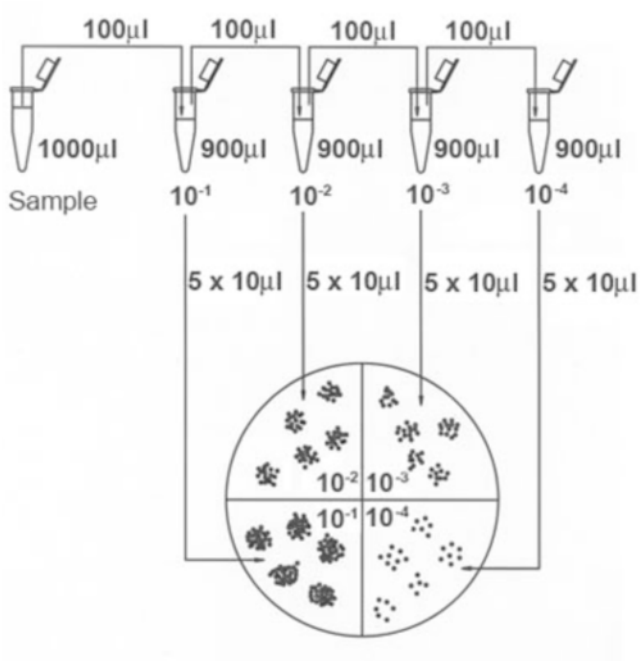

Figure 2.1: Diagram showing the dilution and subsequent plating procedures for the standard drop plating method for enumerating bacteria.

2.4.3 *Ex-situ* Sterilisation Tests in a Continuous Flow Reactor

Ex-situ sterilisation tests were performed in the continuous flow set up previously described for *in-situ* sterilisation tests, the only difference being that solutions of H_2O_2 (Sigma, Acros)

were co-fed into the flow reactor with the model wastewater solution. Reaction gases were swapped for a synthetic air and all other conditions remained the same unless it is otherwise stated.

The cell counting procedure used remained unchanged.

2.4.4 *Ex-situ* Sterilisation Tests in Glass Vials.

Ex-situ sterilisation tests were performed in glass vials using the following procedure:

Model wastewater solution (2 ml) and H_2O_2 solution (2 ml, Sigma) of a known concentration, were added simultaneously to a glass vial and magnetically stirred (100 rpm) at room temperature. Post reaction samples were taken at varying time points and the sample was immediately plated using the same methods described above for *in-situ* sterilisation tests.

2.5 Catalyst Characterisation

2.5.1 X-ray Diffraction

X-ray Diffraction (XRD) is a powerful analytical technique that allows for large amounts of information to be obtained about the crystal structure of a material. As would be expected, XRD is therefore only applicable for use on samples with a crystalline structure which is of a long range three-dimensional order, without the crystallinity there is no diffraction. XRD can give information about phase identification, unit cell size, crystallite size and information about the crystal morphology, all of which are extremely useful for heterogeneous catalysis. The detection limit is approximately a 5 nm crystallite size, XRD is a non-destructive technique so catalyst samples can be used for testing post XRD analysis. It is known that when high energy charged particles collide with solid matter, X-rays are produced. The generation of X-rays is achieved in an XRD experiment by bombarding a small copper target with electrons from an electron gun, once the high energy electrons hit the copper target they are slowed, some of this energy is converted to electromagnetic radiation. This electromagnetic radiation is white radiation and covers a wide array of wavelengths, known as *Bremsstrahlung*, taken from the german “bremsen”, literally meaning “to brake” and “strahlung” meaning “radiation”, therefore a deceleration or braking radiation. The generation of this braking radiation satisfies

the law of the conservation of energy as the kinetic energy lost by the electron is transferred into an emitted photon. When the incident high energy electron collides with the copper target it will also ionise some 1s electrons, to fill this vacancy an electron will either drop from the 2p or 3p orbitals, the energies which arise from these transitions are emitted as X-rays. The X-rays emitted from a 2p to 1s transition is denoted K_α and the 3p to 1s transition is denoted K_β. These characteristic energies are of a narrow range and be converted into a monochromatic source, i.e. of a single wavelength. Once these X-rays hit the sample they are diffracted by the lattice planes present in the crystalline sample, constructive and destructive interference between the diffracted beams can occur[5], summarised in figure 2.2 below:

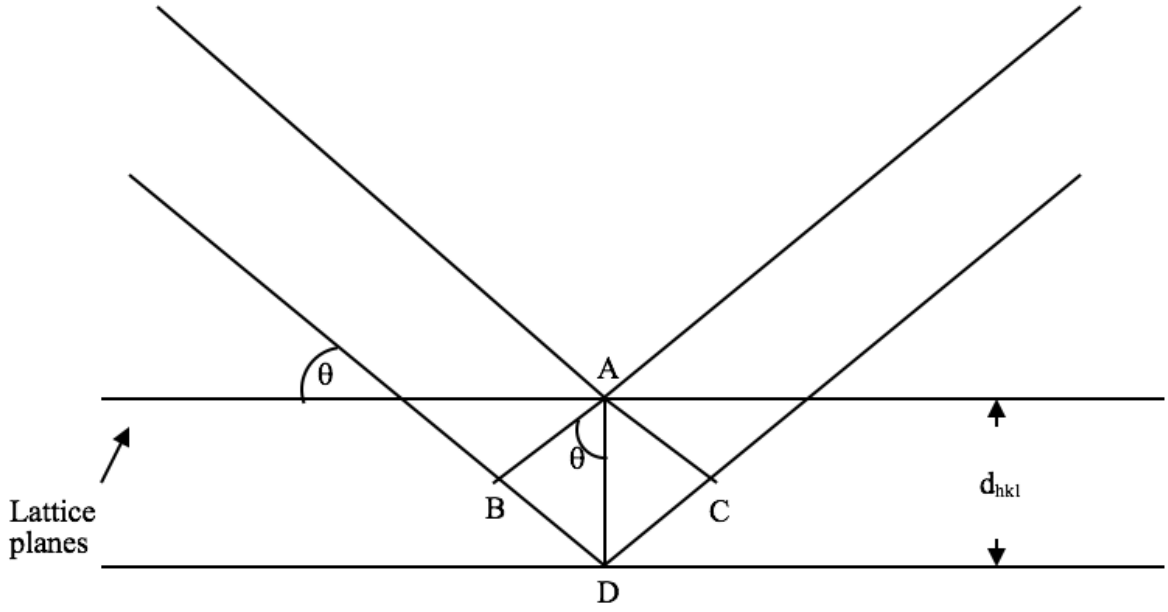

Figure 2.2: Diagram showing the diffraction of X-rays from lattice planes in a crystalline lattice, where d is the lattice spacing and θ is the angle of incidence.

If an X-ray is diffracted from A and D then to produce constructive interference, the distance travelled by the beam after it has been diffracted from D must be an integer of the wavelength. This integer is the sum of the path lengths BD and DC, which will depend on the lattice spacing, d, and the angle of incidence of the incoming X-ray beam, θ. It can therefore be shown that the Bragg equation, $n\lambda = 2d \sin\theta$, can be derived by the following steps shown in equations 6 – 8:

Integer path difference = nλ = BD +DC Equation 6

BD = DC, therefore:

nλ = 2BD Equation 7

BD = d sinθ, from trigonometry, therefore:

nλ = 2d sinθ Equation 8

Equation 8: Bragg's law for diffraction in a crystal lattice, where n = an integer, λ = the wavelength of the X-rays, d = the lattice spacing and θ = angle of incidence of the X-rays.

XRD instruments use a stationary X-ray source and a moveable detector so that the angle of diffraction at which constructive interference occurs, θ can be detected. Using Bragg's law, it is then possible to determine information regarding the lattice spacing and since different crystallite samples will have a unique set of diffraction angles XRD can be used to determine which crystal phases are present in a particular sample. It is not only the position of the reflection which can be used to determine useful information but also the shape of the reflection. It is known that reflection broadening occurs as a function of crystallite size, where smaller crystals lead to broader reflections. Equation 9 shown below describes the relationship between crystallite size and reflection broadness, this is known as the Scherrer equation.

$$\tau = \frac{K\lambda}{\beta \cos\theta}$$

Equation 9: Scherrer equation for a diffraction pattern, where, τ = crystallite size, K = dimensionless shape factor (typically 0.9), λ = X-ray wavelength, β = Full Width at Half Maximum (FWHM) and θ = Bragg angle.

Investigations into the bulk crystallite structure of supported metal heterogeneous catalysts were performed on a PANalytical X'pert Pro powder diffractometer using a Cu Kα radiation

source operating at 40 KeV and 40 mA. Standard analysis was performed using a 40 minute scan between 2θ values of 10 - 80° with the samples supported on an amorphous silicon wafer. Diffraction patterns of phases were identified using the ICDD data base.

2.5.2 *In-situ* X-ray Diffraction

The penetrating properties of X-rays means that XRD can also be used as an *in-situ* technique. XRD scans can be recorded whilst a sample is heated and/or exposed to a pressure of reaction gases, therefore mimicking the conditions present during a catalyst heat treatment or a reaction. Adaption of the XRD for such experiments requires the use of an *in-situ* cell. An Anton Parr XRK cell with an internal volume of 0.5 l was used to record 2θ values of 10 - 80° at a range of temperatures under an atmosphere of static air to mimic calcination conditions or a 10% H_2/N_2 mixture to mimic reduction conditions.

2.5.3 Temperature Programmed Reduction

Temperature programmed reduction (TPR) is an analytical technique that is widely used in the field of heterogeneous catalysis to determine information about the behaviour of catalysts when subjected to heating under a reducing atmosphere[6]. A typical TPR experiment involves a linearly increasing the temperature whilst a reducible catalyst or precursor is under a reducing atmosphere, usually a small percentage of H_2 diluted in an inert gas such as argon (Ar). From this experimental set up, the rate of reduction can be examined as the H_2 being consumed by the sample can be monitored using a thermal conductivity detector (TCD). The experiment is set up so that a positive peak in the TCD signal indicates that H_2 is being consumed and therefore that the sample is undergoing reduction. A plot of TCD signal versus temperature can then be made to elucidate at which temperatures a catalyst is undergoing reduction and this can be correlated to an active species, such as precious metal particles, or bulk reduction, such as reduction of the catalyst support. From this information, appropriate heat treatments can be designed which are specific to the catalyst. The operating procedures for a standard TPR experiment are given below:

TPR analysis was performed using a Thermo 1100 series TPDRO. Sample (approx. 0.1 g) was packed into the sample tube and quartz wool was used to hold the sample in place. An inert gas

(Ar) was used for the pre-treatment of the sample and after heating at 110 °C for 1 hour the gas was switched to a 10% H_2/Ar mixture and the gas flow rate was set to 15 ml min^{-1}. The sample oven was set to heat at a rate of 5 °C min^{-1} until a temperature of 800 °C was reached, the TPR profile was recorded using a TCD detector.

2.5.4 High Resolution Scanning Transmission Electron Microscopy

It is widely known that the active species present in supported metal catalysts, particularly those prepared by techniques such as wet impregnation, are on the nanometre scale[1]. The resolution limit of imaging techniques such as scanning electron microscopy (SEM) means that whilst the bulk structure of a catalyst can be imaged, the active metal species remains invisible. scanning transmission electron microscopy (STEM) must therefore be used to image such catalysts and determine information about the morphology, dispersion and interaction of the nanoparticles with the support.

A STEM microscope focuses a beam of electrons into a point on the material being investigated, this is achieved by passing the beam through a series of condenser lenses and an objective lens. The resultant beam is passed through an objective aperture to limit the angle of the incident beam and a set of scan coils scans the incident probe across the sample[7]. A set of detectors is positioned around the sample to form a two-dimensional image of the sample, many types of detectors are often used to provide different types of images, which can be used in connection to gain a deeper understanding of the material in question. Bright field and dark field images are typically collected in a STEM experiment. A bright field (BF) detector detects the electrons which pass directly through the sample whereas annular dark field (ADF) detectors are positioned around the sample and detects the electrons which are scattered off the sample. By positioning ADF detectors at much higher angles than just outside of the image cone, the imaging of heavy metal nanoparticles can be achieved as the atomic number is known to depend upon the image contrast, i.e. brighter portions of the image are due to heavy elements. This detector configuration is referred to as a high angle annular dark field (HAADF) configuration and is useful for the imaging of precious metal supported catalysts. In recent years, the emergence of aberration corrected microscopes have pushed the boundaries of imaging even further. Probe forming lenses have unavoidable geometric aberrations which limit the useful aperture and therefore also the image resolution, aberration correction devices

compiled with the use of an aberration correction software which measures the aberrations and subsequently adjusts the multiple lenses to the optimal settings have led to dramatic increases in the resolution of STEM apparatus and it is now possible to achieve high resolution images even at a 1 nm resolution. Figure 2.3 illustrates the detection regions of a STEM microscope:

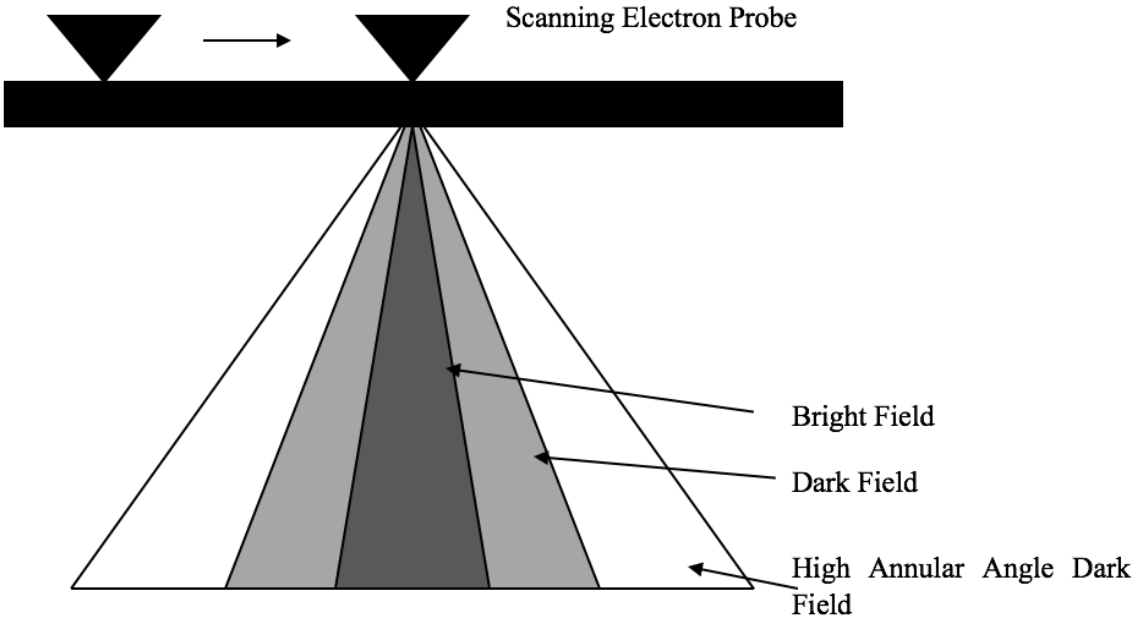

Figure 2.3: Schematic diagram showing the different detection region of a STEM microscope.

An additional technique known as electron energy loss spectroscopy (EELS) is commonly employed to give information about the chemistry of the atoms being imaged and therefore information about their electronic structure, bonding and interactions with the support. A spectrometer and detection system are used in parallel to analyse the BF electrons. Characteristic energies corresponding to inner shell excitations into the first available unoccupied states is used to give the electronic and chemical information about the sample.

2.5.5 Thermogravimetric Analysis

Thermogravimetric analysis (TGA) is a useful characterisation technique in which the mass of a sample material is monitored as a function of temperature, performed at a controlled heating rate. TGA can also be performed under different controlled atmospheres to monitor changes in sample mass due to reductions or further oxidations. A TGA curve consists of either mass or percentage mass plotted as a function of temperature, it is also useful to plot temperature as a

function of heat flow on the same graph as changes in mass can be correlated to either an exothermic or an endothermic process. A TGA experiment can give useful information to determine catalyst calcination and reduction temperatures, elucidating information about optimal temperatures and ramp rates to ensure the desired effect is achieved from the heat treatment. A schematic representation of a typical TGA instrument is shown below in figure 2.4:

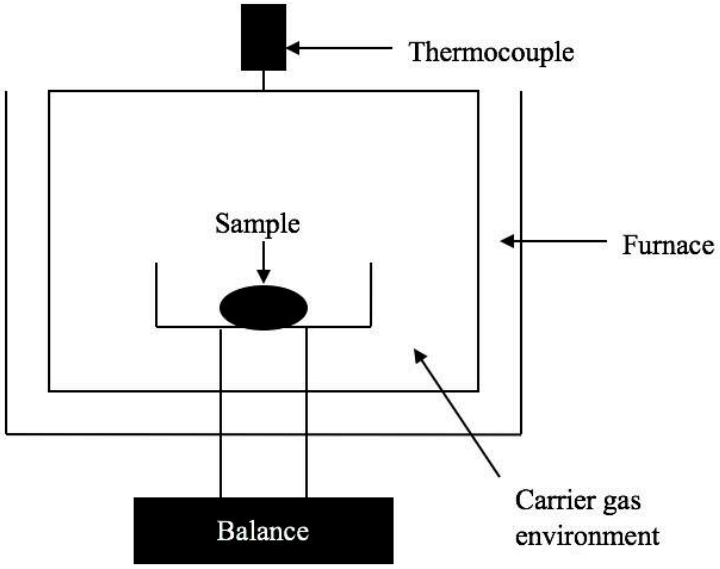

Figure 2.4: Schematic diagram of a typical TGA instrument used for thermogravimetric analysis

The operating procedures for a typical TGA experiment are given below:

Thermogravimetric analysis was performed using a Seteram TG-DTA. Sample was loaded into the aluminium sample crucible (approx. 30 – 40 mg) and heated to 600 – 800 °C at a rate of 5 °C min^{-1}, analysis was performed either under a 10% H_2/Ar or air atmosphere.

2.5.6 BET Adsorption Isotherms

The BET adsorption isotherm is a characterisation tool that has been widely used in catalysis to measure surface areas by nitrogen adsorption. It is an extension of the well-known Langmuir isotherm and makes the following assumptions[8]:

- Gas layers physisorb onto a solid in infinite layers.
- There is no interaction between the gas layers.
- The Langmuir adsorption isotherm can be applied to each layer.

Taken the above assumptions into account yields the following equation:

$$\frac{p}{v(p_0 - 1)} = \frac{c - 1}{v_m c}\left(\frac{p}{p_0}\right) + \frac{1}{v_m c}$$

Where:

p = partial pressure of gas

p_0 = saturation pressure

v = volume of the gas adsorbed

v_m = monolayer volume

c = BET constant defined by the equation: $c = \exp\left(\frac{E1-E2}{RT}\right)$

Where:

E_1 = Heat of adsorption of first layer

E_2 = Heat of adsorption of second layer

R = Gas constant

T = Temperature at which adsorption is performed

The operating procedure of a typical BET adsorption surface area analysis is outlined below:

Analysis was performed using a Quantochrome Nova Porosimeter with NovaWin analysis software. Sample was loaded into the sample tube (approx. 100 – 200 mg) and degassed for 2 hours at 120 °C prior to N_2 adsorption. Adsorption isotherms were then recorded and the surface area was analysed using a single point analysis.

2.5 References

1. J. K. Edwards, B. E. Solsona, P. Landon, A. F. Carley, A. Herzing, C. J. Kiely, G. J. Hutchings, *J. Catal.*, **2005**, *236*, 69 – 79.
2. M. Sankar, Q. He, M. Moataz, J. Pritchard, S. J. Freakley, J. K. Edwards, S. H. Taylor, D. J. Morgan, A. F. Carley, D. W. Knight, C. J. Kiely, G. J. Hutchings, *ACS Nano,* **2012**, *6*, 6600 – 6613.
3. R. Adnan, R. N. A. Razana, I. A. Rahman, M. A. Farrukh, *J. Chin. Chem. Soc.*, **2010**, *57*, 222 – 229
4. S. J. Freakley, M. Piccinini, J. K. Edwards, E. N. Ntainjua, J. A. Moulijn, G. J. Hutchings, *ACS Catal.*, **2013**, *3*, 487 – 501.
5. M. M. Woolfson, *An Introduction to X-Ray Crystallography*, 2nd Ed., **1997**, Cambridge University Press.
6. U. S. Ozkan, M. W. Kumthekar, G. Karakas, *Catal. Today*, **1998**, *40*, 3 – 14.
7. S. Amelinckx, D. V. Dyck, J. V. Landuyt, *Transmission Electron Microscopy: A Textbook for Materials Science*, **2009**.
8. S. Brunauer, P. H. Emmett, E. J. Teller, *J. Am. Chem. Soc.*, **1938**, *60*, 309 – 319.

Chapter 3

Utilisation of *In-situ* H_2O_2: Applications in Greywater Treatment

3.1 Introduction

The treatment of household greywater (GW) represents an exciting potential use for the direct synthesis of hydrogen peroxide (H_2O_2). It is widely considered that with appropriate treatment, GW could be re-used for many on-site applications including toilet flushing, garden irrigation and washing machines. These re-use applications would greatly reduce water comsuption leading to a potentially large decrease in water bills and promoting a more responsible use of urban water, a topic that is particularly relevant in today's society.

The re-use of GW can be achieved via an appropriately designed treatment infrastructure on-site using a GW Treatment System (GTS)[1]. As discussed in chapter 1, there are many current technologies on the market and in-use today for GW treatment ranging from simple filtration[2-4] to modern photocatalytic UV systems[5-8]. However, none of these are without their shortfalls; current chemical technologies utilise inorganic oxidants and bleaches which are damaging to the environment in both their synthesis and use, due largely to the by-products and waste generated. UV technologies are often energy-intensive and expensive; H_2O_2 and ozone (O_3) are commonly employed in conjunction with UV treatment systems as a source of highly active radical species[9]. The first report of a catalyst being used for the treatment of water pollutants was reported in 1977, Frank *et al*[10, 11] observed that a doped anatase TiO_2 catalyst could remove >99% of CN^- ions from a 1 mM KCN in 0.1 M KOH solution. Photo-disinfection has since received much attention in the literature and has been extensively reviewed,[12,13] however whilst high rates of disinfection can be achieved, costly UV energy is still required. The direct synthesis of H_2O_2 offers a more environmentally friendly potential solution. The only by-product from the reaction is water (H_2O) and the synthesis is a highly atom efficient reaction which takes place in a single process. The need for expensive UV treatment is removed as H_2O_2 formed via the direct synthesis is unstabilised and so will readily decompose into the required radicals, commercially available concentrated H_2O_2 contains chemical stabilisers to prevent this decomposition occurring, meaning that highly concentrated solutions can be kept for long periods of time.

A model GW treatment system using this technology would require a GW Diversion Device (GDD), where the GW is diverted to a treatment tank and blackwater (BW), wastewater containing human excrement, is sent away for appropriate treatment[1]. Figure 3.1 shows a schematic of how this potential infrastructure could look in a household setting: It can be seen that acceptable water sources from a household are the bathroom (including a basin, shower and bath) and laundry room, represented by the green ticks. The kitchen is deemed to by a questionable source, represented by the yellow colour and the question mark in figure 3.1. as it is normally heavily contaminated with fats, greases and solids. GW from these sources would pass through a GDD, where it is filtered and diverted from the drainage line for BW, and once filtered it would be sent to a GW treatment tank. The water contained in the treatment tank would then be fed through a reactor system, whereby the direct synthesis of H_2O_2 is performed and sterile re-usable GW is then stored for re-use.

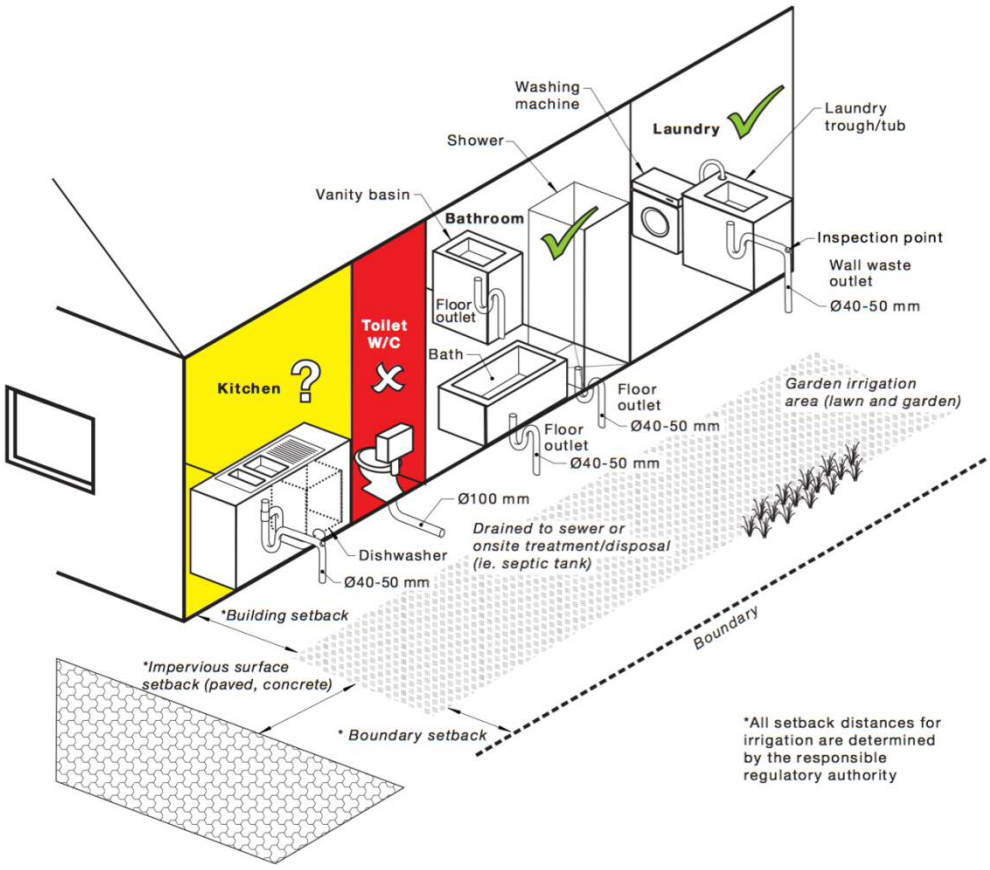

Figure 3.1: Representation of household drainage points for GW and BW which can be sent for appropriate treatment[1].

In this chapter the antimicrobial properties of *in-situ* generated H_2O_2 are investigated by using a continuous flow reactor and *Escherichia Coli* as a model wastewater microorganism contaminant. The efficacy of the *in-situ* generated H_2O_2 is then compared with commercially available H_2O_2 which is used *ex-situ*.

3.2 Results - Direct Synthesis of H_2O_2 in a Continuous Flow Reactor

3.2.1 Initial Experiments

Previous work by Freakley *et al*[14] has shown that it is possible to produce concentrations of greater than 1000 ppm of H_2O_2 using a continuous flow system under optimised conditions, as stated in Chapter 2 of this work, using a 1 wt.% $AuPd/TiO_2$ (120 mg) catalyst prepared via modified impregnation. However, these concentrations were only achieved when methanol (MeOH) was used as a co-solvent and reaction gases were diluted with carbon dioxide (CO_2). The use of CO_2 as a diluent is firstly to ensure that all experiments containing hydrogen (H_2) and oxygen (O_2) are below the explosive limit and secondly because the CO_2 dissolved in the reaction solution can form carbonic acid (H_2CO_3), which acts as an *in-situ* stabiliser to the generated H_2O_2. For the intended application, all synthesis reactions would need to be performed in H_2O only, as the introduction of MeOH into the GTS would be highly undesirable.

Initial work was performed using the same continuous flow reactor under the previously determined optimal conditions, outlined in detail in chapter 2 of this work, to investigate if H_2O_2 could be produced in a H_2O only solvent. Figure 3.2 shows the results of these initial tests:

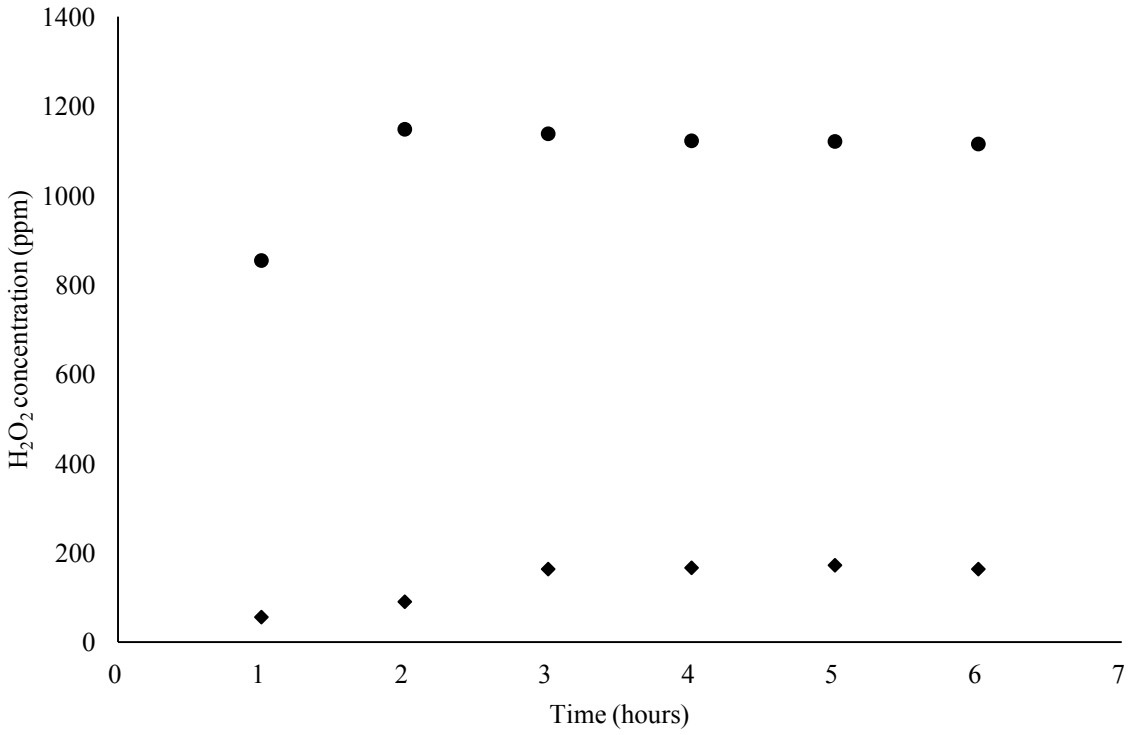

Figure 3.2: Graph showing the effect of solvent composition on the concentration of H_2O_2 produced in a continuous flow system. Diamonds indicate H_2O only, circles indicate H_2O (34%)/MeOH (66%) mixture

Reaction conditions: *10 bar pressure, 2 °C, 5% H_2/CO_2 and 25% O_2/CO_2 reactant gases, 42 ml min^{-1} gas flow, solvent H_2O (34%)/MeOH (66%) flow rate = 0.2 ml min^{-1}, 120 mg 1 wt.% $AuPd/TiO_2$ catalyst, $H_2:O_2$ ratio = 1.*

It can be seen that after an initial induction period a steady state reaction is reached and the flow system is capable of producing concentrations of up to 1200 ppm for 7 hours on stream when a 66% MeOH/34% H_2O solvent system is used, these data are in agreement with the previous findings in the group[14]. When the solvent is switched to H_2O only, the amount of H_2O_2 formed is greatly reduced, with a maximum concentration of approximately 170 ppm observed. Again, after an initial induction period a steady state reaction is reached and the system is capable of producing this for 7 hours of continuous reaction. These findings suggest two conclusions need to be considered for a GTS. Firstly, the amount of H_2O_2 produced is far less when H_2O only is used as the solvent. This is thought to be due to the limited H_2 solubility in H_2O when compared to MeOH. The solubility of H_2 in H_2O is quoted in the

literature[15] as being an order of magnitude lower than in MeOH at a temperature of 20 °C. Gemo *et al*[16] investigated the solubility of H_2 in a number of systems that included the presence of MeOH, CO_2 and O_2. They report that at a temperature of 278K, ther is a 37% increase in H_2 solubility in the presence of CO_2 in a MeOH solvent, compared to a binary H_2 and MeOH system. A negligible increase in H_2 solubility is observed withn O_2 is introduced to give a quaternary system. This further helps to explain the increase in H_2O_2 concentration when a MeOH co-solvent is used, as the H_2 solubility is additionally increased by the CO_2 present. The difference in the gas solubilities can also provide a valid hypothesis as to why there is a difference in the observed induction period for the two solvents. The solubility benefits of a MeOH co-solvent stated above mean that steady state occurs quicker when compared with a H_2O solvent. Secondly, the catalyst stability is indicated as it was observed that there was little to no decrease in the amount of H_2O_2 produced after 7 hours of continuous reaction. If an *in-situ* H_2O_2 system were to be used in a GTS, then catalyst stability would be imperative in order to ensure GW is sterile, it must also be noted that although the time period would need to be far greater than the 6h reaction discussed above. Ronen *et al*[17] have reported that commercially available, stabilised H_2O_2 concentrations of 125 ppm are as effective as 5 ppm of chlorine for the disinfection of faecal coliforms from GW. Moreover, the authors found the costs of daily disinfection for a 5 m^3 dwelling using H_2O_2 was competitive with chlorine. Based on these findings and the results reported in figure 3.2, it is feasible that enough H_2O_2 can be generated *in-situ* using H_2O as a solvent.

3.2.2 Solvent Recycling Experiments

The flow reactor was modified by adding a length of Swagelok tubing onto the back pressure regulator after the water bath and catalyst bed, this line fed directly back into the solvent reservoir, which is pumped at a controlled flow rate. This modification allowed for the effect of solvent recycling to be investigated, with the aim of steadily increasing the H_2O_2 in the solvent reservoir as the reaction is continually recycled. A direct synthesis reaction using a H_2O (34%)/MeOH (66%) solvent was carried out keeping all variables constant for a period of up to 24 hours. The results are shown in figure 3.3:

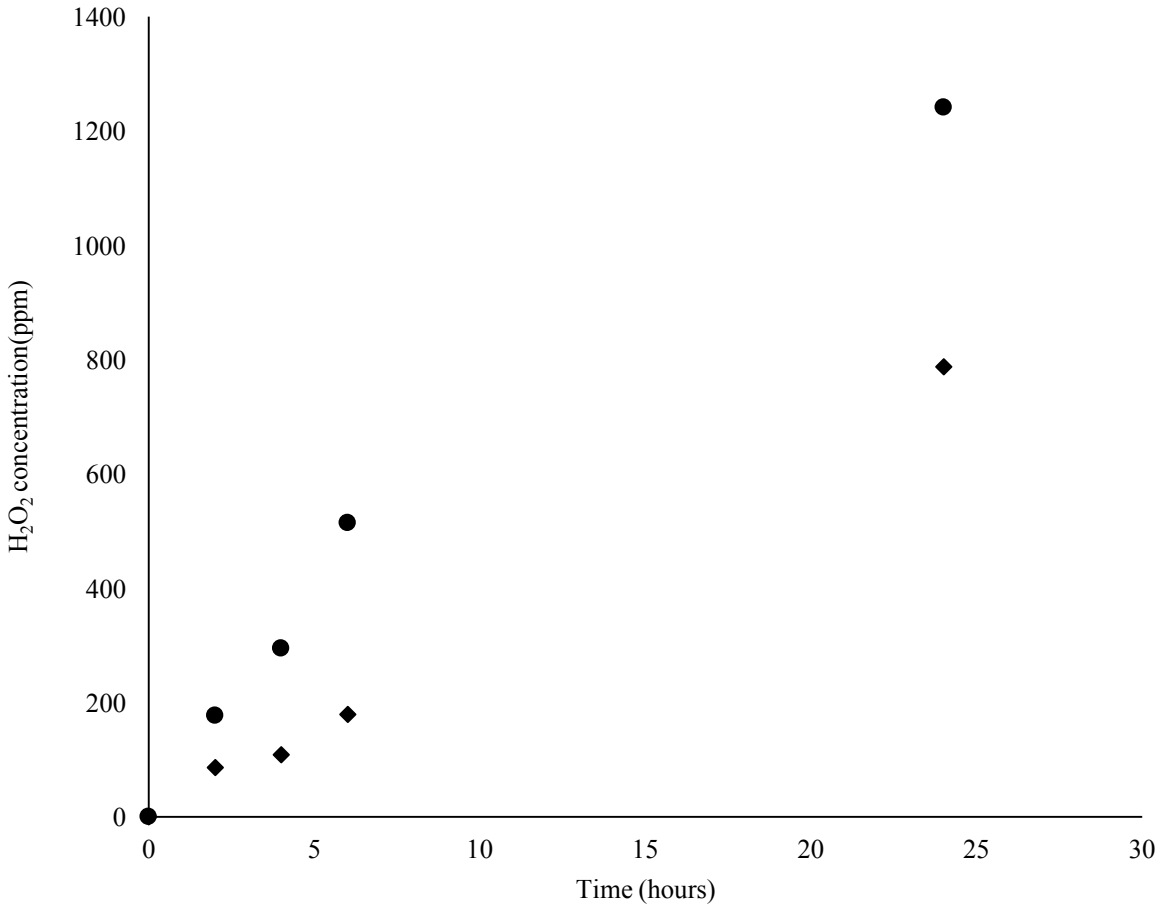

Figure 3.3: Results obtained from solvent recycling experiment using a H_2O (34%)/MeOH (66%) solvent mixture. Diamonds indicate tap data, circles indicate reservoir data.

Reaction conditions: *10 bar pressure, 2 °C, 5% H_2/CO_2 and 25% O_2/CO_2 reactant gases, 42 ml min^{-1} gas flow, solvent H_2O (34%)/MeOH (66%) flow rate = 0.2 ml min^{-1}, 120 mg 1 wt.% $AuPd/TiO_2$ catalyst, $H_2:O_2$ ratio = 1.*

These data show a near-linear increase in the concentration of H_2O_2 in the reservoir as a function of time. After a period of 24 hours the solvent reservoir had reached a concentration of approximately 800 ppm and the concentration H_2O_2 in the reaction solution measured directly from the tap was greater than 1200 ppm. These findings demonstrate that it is indeed possible to build up a concentration of H_2O_2 in a solvent reservoir kept at room temperature in the absence of stabilisers by recycling the reaction solution. In the context of a GTS this may be an important point as a tank of GW will need to be kept sterile for extended periods

of time without the addition of further reaction promoters or stabilisers and a steady production of H_2O_2 in the tank could be needed.

The same reaction was then carried out using a H_2O only solvent, as is to be expected the concentration of H_2O_2 produced is far lower than for the H_2O (34%)/MeOH (66%) system. The results can be seen in figure 3.4. After 2 hours of reaction the concentration in the reservoir was still extremely low whilst greater than 140 ppm H_2O_2 was measured from the tap. However, once the reaction reached 4 hours the concentration of the reservoir was much higher and started to echo the results observed in the H_2O (34%)/MeOH (66%) experiment. A concentration of 160 ppm was measured in the reservoir after 24 hours of reaction.

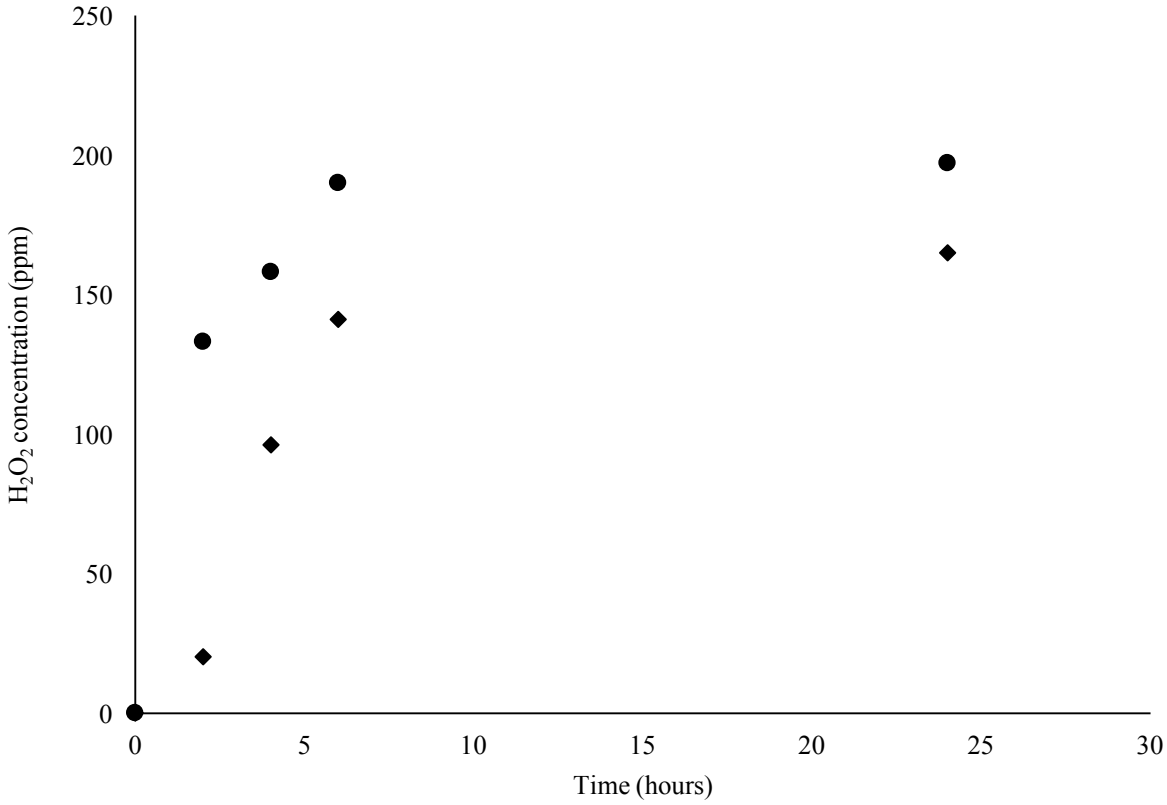

Figure 3.4: Results obtained from solvent recycling experiment using a H_2O solvent. Diamonds indicate tap data, circles indicate reservoir data.

Reaction Conditions: *10 bar pressure, 2 °C, 5% H_2/CO_2 and 25% O_2/CO_2 reactant gases, 42 ml min^{-1} gas flow, solvent H_2O flow rate = 0.2 ml min^{-1}, 120 mg 1 wt.% AuPd/TiO_2 catalyst, $H_2:O_2$ ratio = 1.*

A recent study by Crole *et al*[15] has shown that H_2O_2 degradation is significantly higher in a H_2O only solvent when compared with a H_2O (34%)/MeOH (66%) solvent in the presence of a 5 wt.% AuPd/TiO_2 catalyst. Furthermore, the limited solubility of H_2 in H_2O compared to MeOH means that the over hydrogenation to H_2O becomes less of a factor, as net H_2O_2 hydrogenation is actually reported as lower in a H_2O only solvent than the H_2O (34%)/MeOH (66%) mixture. The data in figure 3.4 show that despite these more challenging conditions, it is still possible to build up a steady concentration of H_2O_2 in the reservoir when performing a recycling reaction in the flow reactor.

It has been previously shown by Freakley *et al*[14] that the concentration of H_2O_2 produced in the continuous flow system can be significantly increased by increasing the overall pressure. The authors attribute this to higher solubility of the reaction gases and a decrease in the gas bubble size improving diffusion rates. The effect of pressure was investigated for both H_2O (34%)/MeOH (66%) and H_2O only solvents, a recycling reaction was performed using a total pressure of 20 bar, keeping all variables constant. The results for the H_2O (34%)/MeOH (66%) and H_2O only experiments are shown in figures 3.5 and 3.6 respectively.

Examining the H_2O (34%)/MeOH (66%) experiment, there is a similar trend to the analogous experiment that was performed at a total pressure of 10 bar. As is to be expected, the tap concentration exceeded that of the reservoir throughout the experiment and the highest concentrations seen were 1530 ppm and 1415 ppm for the tap and reservoir respectively. A noticeable difference between the 20 bar and 10 bar results is that the reservoir concentration is more closely matched to the tap data, with the largest gap coming at the 6 hour time point and by the time 24 hours of reaction is reached, the concentration of the tap and the reservoir are similar.

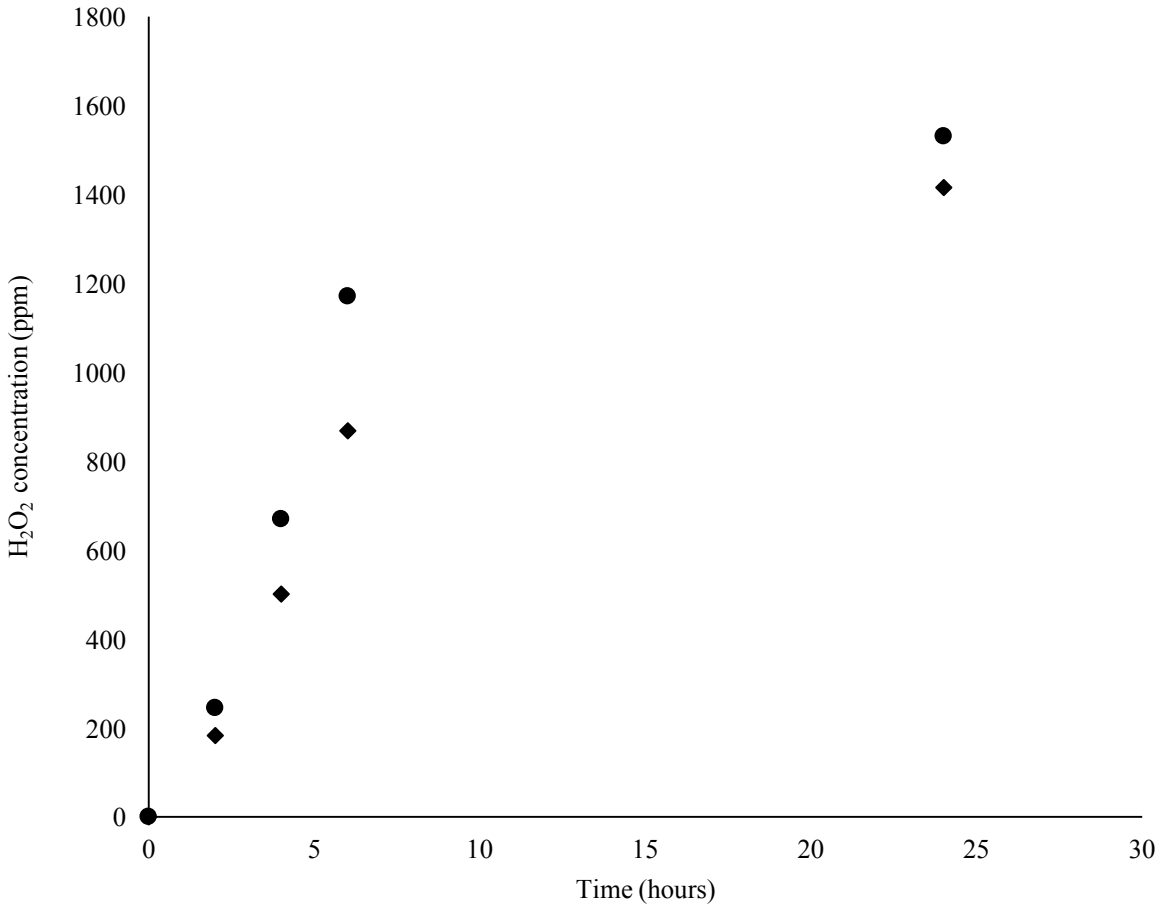

Figure 3.5: Results obtained from solvent recycling experiment using a H_2O (34%)/MeOH (66%) solvent. Diamonds indicate tap data, circles indicate reservoir data.

Reaction conditions: *20 bar pressure, 2 °C, 5% H_2/CO_2 and 25% O_2/CO_2 reactant gases, 42 ml min^{-1} gas flow, solvent H_2O (34%)/MeOH (66%) flow rate = 0.2 ml min^{-1}, 120 mg 1 wt.% $AuPd/TiO_2$ catalyst, $H_2:O_2$ ratio = 1.*

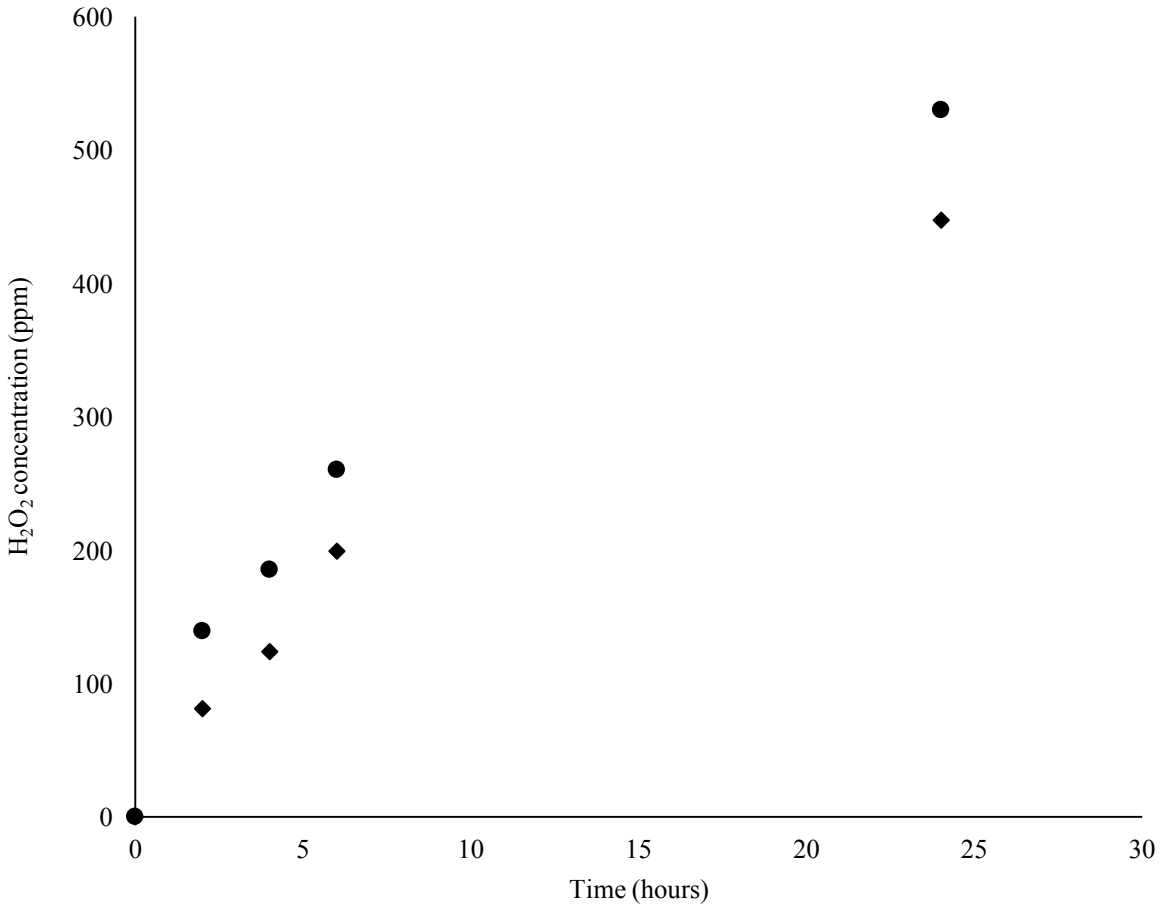

Figure 3.6: Results obtained from solvent recycling experiment using a H_2O only solvent. Diamonds indicate tap data, circles indicate reservoir data.

Reaction conditions: *20 bar pressure, 2 °C, 5% H_2/CO_2 and 25% O_2/CO_2 reactant gases, 42 ml min^{-1} gas flow, solvent H_2O flow rate = 0.2 ml min^{-1}, 120mg 1 wt.% $AuPd/TiO_2$ catalyst, $H_2:O_2$ ratio = 1.*

The same trend is observed for the H_2O only experiment, figure 3.6 shows that unlike the analogous H_2O only experiment that was performed at 10 bar, where a large difference is observed between the tap and the reservoir, the two sets of data are close throughout, with a small difference in concentration of 40 – 80 ppm maintained throughout the experiment.

3.3 *In-situ* Sterilisation Tests

3.3.1 Crude Experiment

An initial experiment was carried out to investigate the potential of the *in-situ* H_2O_2 system to remove bacteria from a contaminated H_2O stream. A 5% glucose solution was left open to the air for 2 days to collect any airborne bacteria that may land in the liquid as a basic model of harvested rain water. Figure 3.7a shows that after 2 days incubation this solution contained a high number of bacteria (no dilutions were carried out to determine the accurate cell density). This solution was then used as a reaction medium to generate H_2O_2 in the continuous microreactor. Figure 3.7b shows that after one pass through the reactor under the standard reaction conditions, no colony forming units (CFUs) were detected in the treated sample and no H_2O_2 was detected in the effluent indicating that the contaminants and bacteria in the H_2O had enhanced the H_2O_2 decomposition rate. This treated H_2O sample was recycled through the reactor for a further 3 days and no CFUs were detected indicating that it was possible to keep the H_2O free from bacteria for extended periods of time. These results demonstrate the small-scale feasibility of treating contaminated H_2O streams using *in-situ* formed H_2O_2.

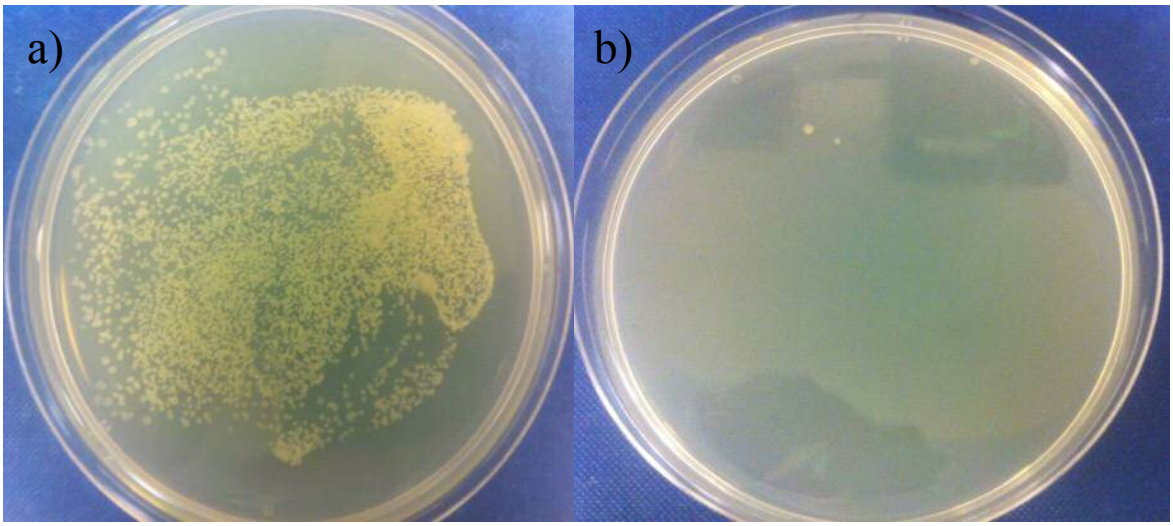

Figure 3.7: Agar plate of 5% glucose solution exposed to air for 2 days before (a) and after (b) passage through the H_2O_2 reactor system.

3.3.2 Initial Experiments Using *Escherichia Coli.*

Escherichia Coli is widely used in the literature as a model bacterium for wastewater and antimicrobial studies[18-20]. It is particularly relevant in a study with an intended use being the treatment of GW, this is because of the source of the wastewater has a large impact upon its contents. Household GW is made up of approximately 50% bathroom GW, 30% laundry GW and 20% kitchen GW. If we consider the two main streams which make up a typical GW sample, bathroom and laundry, it is most likely that the bacteria will be present due to faecal contamination from things such as body washing or soiled garments. In addition to this, the microbiological protocols for culturing *Escherichia Coli* are simple and the requisite nutrients are cheap and readily available.

The first set of reactions were carried out using laboratory grown *Escherichia Coli* (JM109) of known concentrations. An initial cell density of 10^7 CFU ml^{-1} was chosen and cultured via the methods set out in the experimental chapter of this work. Blank experiments were first performed to gauge if the reactor system itself had any antibacterial properties that would need to be accounted for. The model wastewater solution was passed through an empty reactor using a variety of reaction gases which could potentially be present during an *in-situ* H_2O_2 experiment. The results can be seen below in figure 3.8: a 2-log reduction is observed simply by passing the bacteria through the reactor in the absence of any catalyst, meaning that no *in-situ* H_2O_2 was generated. This reduction could be due either to the effect of pressurising the bacteria or the mild acidification caused by the H_2CO_3 known to be formed under such conditions. The experiment was repeated with the introduction of a 1 wt.% $AuPd/TiO_2$ catalyst, the results of which are also included in figure 3.8: These data show that simply by introducing the AuPd catalyst into the reaction gives a further log reduction when the reaction is run under a 5% H_2/CO_2 or CO_2 atmosphere, indicating that the catalyst itself may have some intrinsic antibacterial properties. This is not surprising as the use of metal nanoparticles has been widely reported in the literature for antimicrobial studies, although silver (Ag) is usually the metal of choice[21, 22]. Interestingly, a 4-log reduction is observed when a 25% O_2/CO_2 atmosphere is used, suggesting that the bacteria may be particularly susceptible to oxidative environments. When the reaction is performed under H_2O_2 synthesis conditions the post reaction plates show no growth, even when plated without dilution. This important result highlights the efficacy of *in-situ* generated H_2O_2 for the removal of bacteria from wastewater streams. The data shown in figure 3.8 clearly shows that the elimination of

bacteria is facilitated by the *in-situ* generating conditions, this could be due to the H_2O_2 itself or the highly active, however short-lived, peroxy and hydroperoxy radicals generated during the synthesis and subsequent decomposition and hydrogenation reactions through the activation of O_2 and H_2.

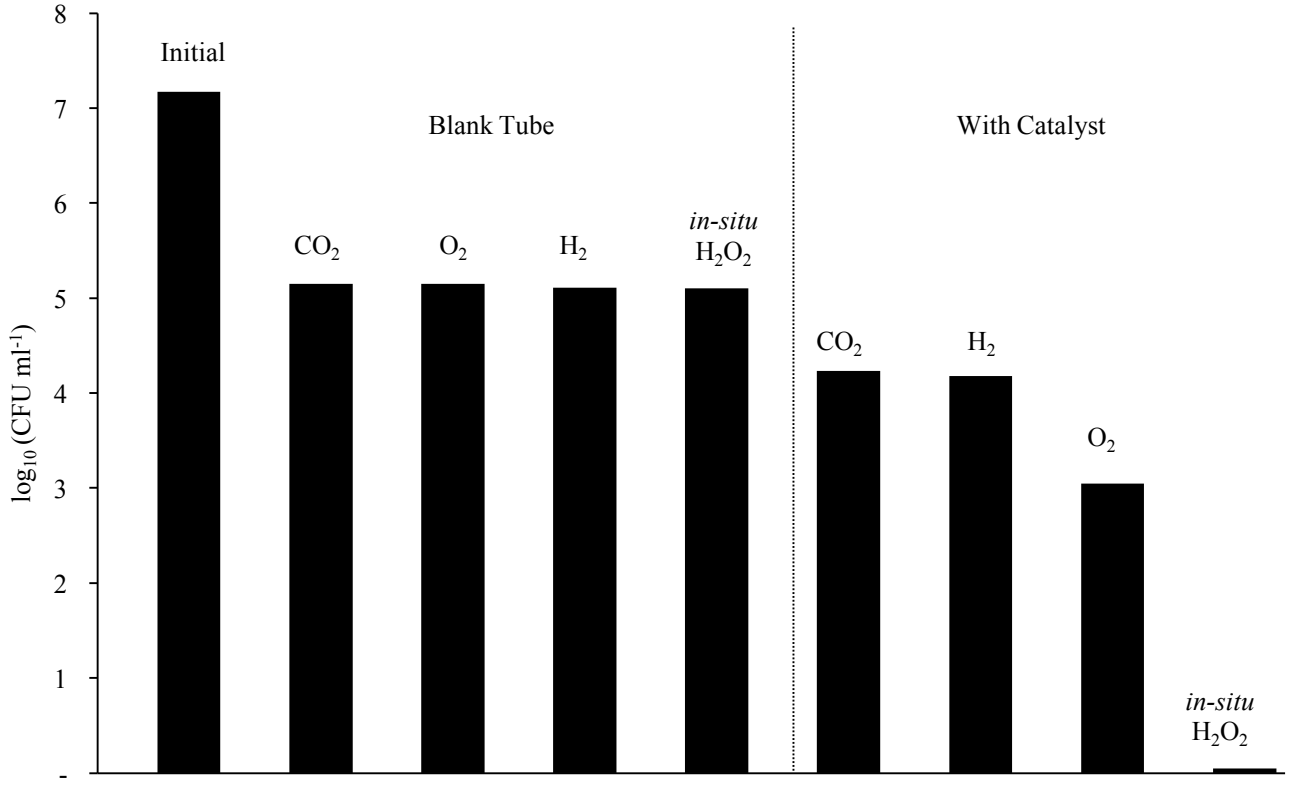

Figure 3.8: Cell density measured after a single pass through the reactor under varying atmospheres in the absence and presence of catalyst.

Reaction conditions: *10 bar pressure, 2 °C, varying reactant gases, 42 ml min^{-1} gas flow, solvent flow rate = 0.2 ml min^{-1}, 120 mg 1 wt.% AuPd/TiO$_2$ catalyst, H$_2$:O$_2$ ratio = 1.*

3.3.3 Increasing Concentration of *Escherichia Coli.*

Following the observation that *in-situ* generated H_2O_2 could successfully remove concentrations of up to 10^7 CFU ml^{-1} *Escherichia Coli* it was decided to increase the starting concentration whilst keeping the reaction conditions the same to identify the limit of the system. Reactions were performed increasing the starting concentration by an order of magnitude each time, keeping all other variables the same. Figure 3.9 shows the results:

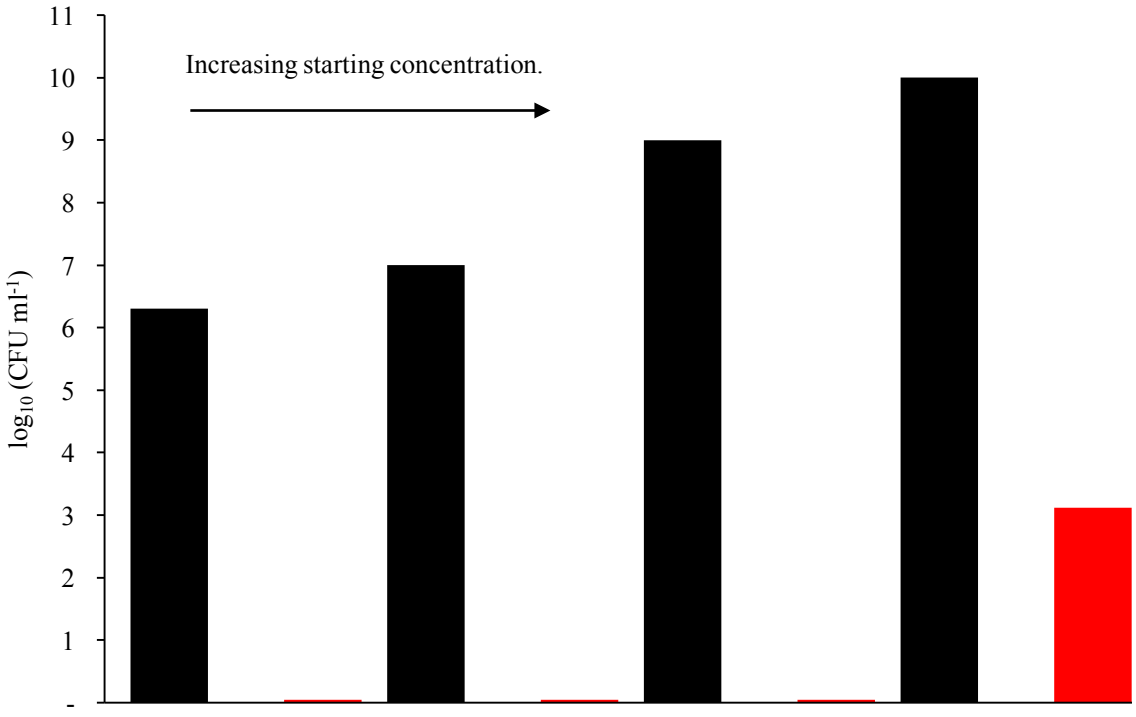

black bars = initial concentration, red bars = measured final concentration

Figure 3.9: Increasing starting concentration of *Escherichia Coli* and cell density measured after a single pass.

Reaction conditions: *10 bar pressure, 2 °C, 5% H_2/CO_2 and 25% O_2/CO_2 reactant gases, 42 ml min^{-1} gas flow, solvent flow rate = 0.2 ml min^{-1}, 120 mg 1 wt.% $AuPd/TiO_2$ catalyst, $H_2:O_2$ ratio = 1.*

It can be seen that *in-situ* generated H_2O_2 is capable of removing up to 10^9 CFU ml^{-1} *Escherchia Coli* after just a single pass through the reactor, however, a limit was reached when the initial starting concentration was increased to 10^{10} and a 100% conversion was not observed. Whilst the exact amount of *in-situ* H_2O_2 that is reacting with the bacteria is not known, it can be thought to be in the region of 140 ppm given the results reported earlier in this chapter for the direct synthesis of H_2O_2 in a water only solvent under the same reaction condiaitons. Regulations surrounding the re-use of GW require that, for domestic re-use applications such as toilet flushing and laundry, no faecal coliforms are to be present. However, the concentration of faecal coliforms such as *Escherichia Coli* present in typical GW streams are significantly lower than those tested above (typically 10^4 – 10^5 CFU 100 ml^{-}

[1]). Therefore, it is clear to see that *in-situ* generated H_2O_2 demonstrates the efficiency required as an antimicrobial agent for the intended purpose.

3.3.4 Addition of H_2O_2 Compared with *In-situ* Experiments.

Once it had been established that *in-situ* generated H_2O_2 was capable of removing high concentrations of *Escherichia Coli* a comparison with the direct addition of H_2O_2 was needed. As shown previously in this chapter concentrations of approximately 140 ppm are typically produced under the optimised reaction conditions and when H_2O is used as the solvent. Solutions of 50, 100 and 200 ppm were prepared using commercial stabilised H_2O_2, these solutions were then added in equal quantity to the *Escherichia Coli* solutions with a cell density of 10^7 CFU ml^{-1} and agitated at room temperature, the reactions were then plated at set time points. Figure 3.10 shows the results obtained:

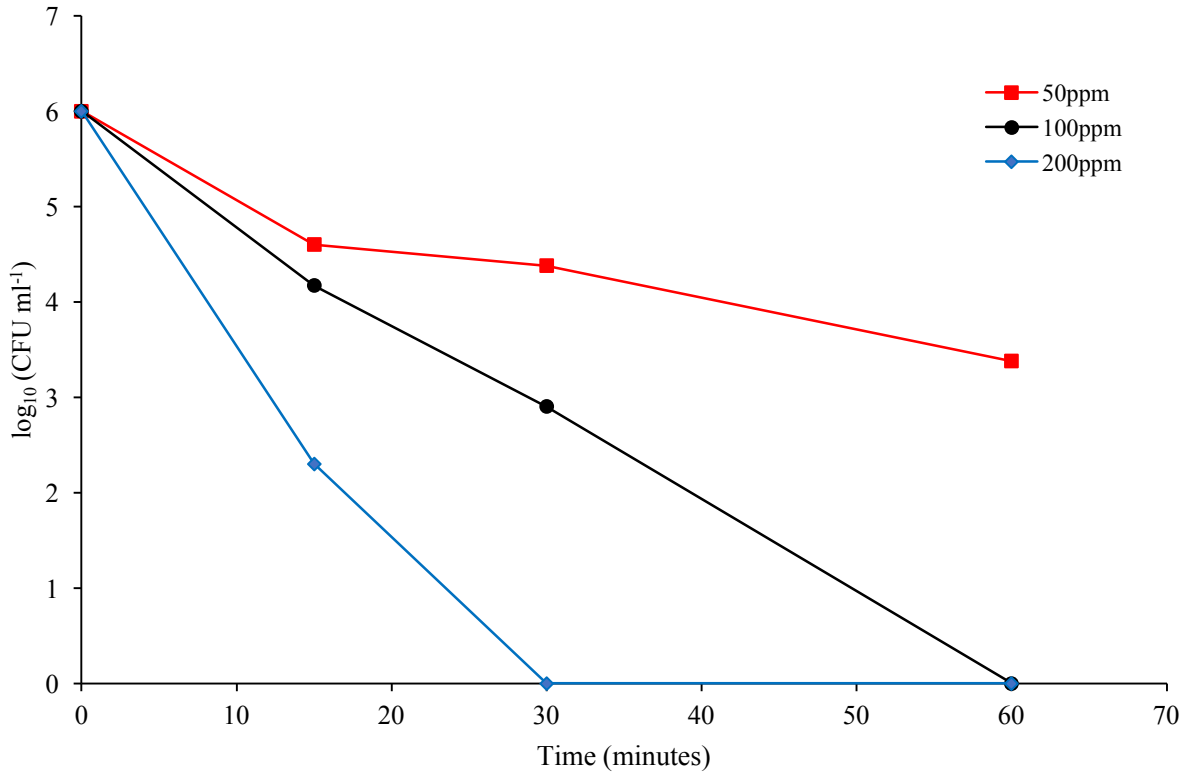

Figure 3.10: Removal of *Escherichia Coli* via the addition of H_2O_2 solutions of varying concentrations with varying contact times.

Reaction conditions: *2 ml H_2O_2 solution, 2 ml Escherichia Coli solution before dilution, varying reaction times, no catalyst or reaction gases, room temperature and constant agitation.*

These data highlight the efficiency of the *in-situ* generated H_2O_2, it is clear that a minimum concentration of 100 ppm H_2O_2 is needed to completely eliminate all of the bacteria from the solution, even after 60 minutes exposure with 50 ppm H_2O_2 there is still 10^3 CFU ml^{-1} *Escherichia Coli* remaining in the reaction solution. Under ambient conditions, the results of the 100 ppm experiment show that a minimum of 60 minutes exposure to the H_2O_2 is needed to remove all of the bacteria and after 30 minutes exposure there is still approximately 10^3 CFU ml^{-1} remaining. Finally, the 200 ppm solution is the most effective as is to be expected and the *Escherichia Coli* is successfully eliminated after an exposure of 30 minutes. When comparing the results of these experiments to those of the ones performed in the continuous flow system, it is important to consider the contact time with the antimicrobial agent. In the H_2O_2 addition experiments a minimum contact time of 30 minutes is required to bring the reaction to completion. When we consider the contact time of the bacteria passing over the catalyst bed under *in-situ* generating conditions it is markedly shorter, this is calculated below:

V_{liquid} = empty volume fraction x reactor volume

= 0.4 x 0.2 x reactor volume

Reactor volume = $\pi \times r^2 \times h = \pi \times 0.317^2 \times 10 = 3.16\ cm^3$

$V_{liquid} = 0.4 \times 0.2 \times 3.16\ cm^3 = 0.253\ cm^3$

Residence time liquid = $0.253\ cm^3$ / liquid flow rate = $0.253\ cm^3 / 0.2\ cm^3\ min^{-1}$ = 75.9 seconds

The calculations above are based upon the assumptions reported by Freakley *et al*[14] who investigated the direct synthesis of H_2O_2 using the same continuous flow reactor. It is assumed that the empty volume in the reactor was 40% and that the liquid hold up was 80% of the empty volume.

These findings demonstrate that *in-situ* generated H_2O_2 is potentially several orders of magnitude more effective for the removal of *Escherichia Coli* from wastewater streams than stabilised commercially available H_2O_2. Furthermore, the amount of H_2O_2 measured in the solution that is sampled from the flow reactor after an *in-situ* direct synthesis reaction will be lower than the local concentration of H_2O_2 over the catalyst bed. This is due to the subsequent

decomposition that occurs through the reactor and over the catalyst, indeed, it was noted earlier in this chapter how decomposition of H_2O_2 becomes more of a factor than over hydrogenation when using a H_2O only solvent. Taking these factors into account helps to explain the observation of why the *in-situ* generated H_2O_2 is more effective than simply adding commercially available H_2O_2. The *in-situ* efficiency was only investigated in a continuous flow reactor and not a batch system so as to model a GTS that could be implemented into a household for the treatment of GW. Whilst a batch process could have potentially enabled a more detailed investigation of *in-situ* H_2O_2. The introduction of reaction parameters such as a high stirring speeds that would not be present in a GTS or a flow process make their use unsuitable for this purpose.

It is widely known that a 1 wt.% $AuPd/TiO_2$ catalyst can catalyse the breakdown of H_2O_2, forming H_2O and also leading to the generation of radical species through O_2 and H_2 activation[23] A small amount of the aforementioned catalyst was added into the reaction solutions and an identical experiment to the one previously discussed was performed to investigate the effect of catalyst on the antibacterial properties of H_2O_2 solutions. The results are displayed below in figure 3.11:

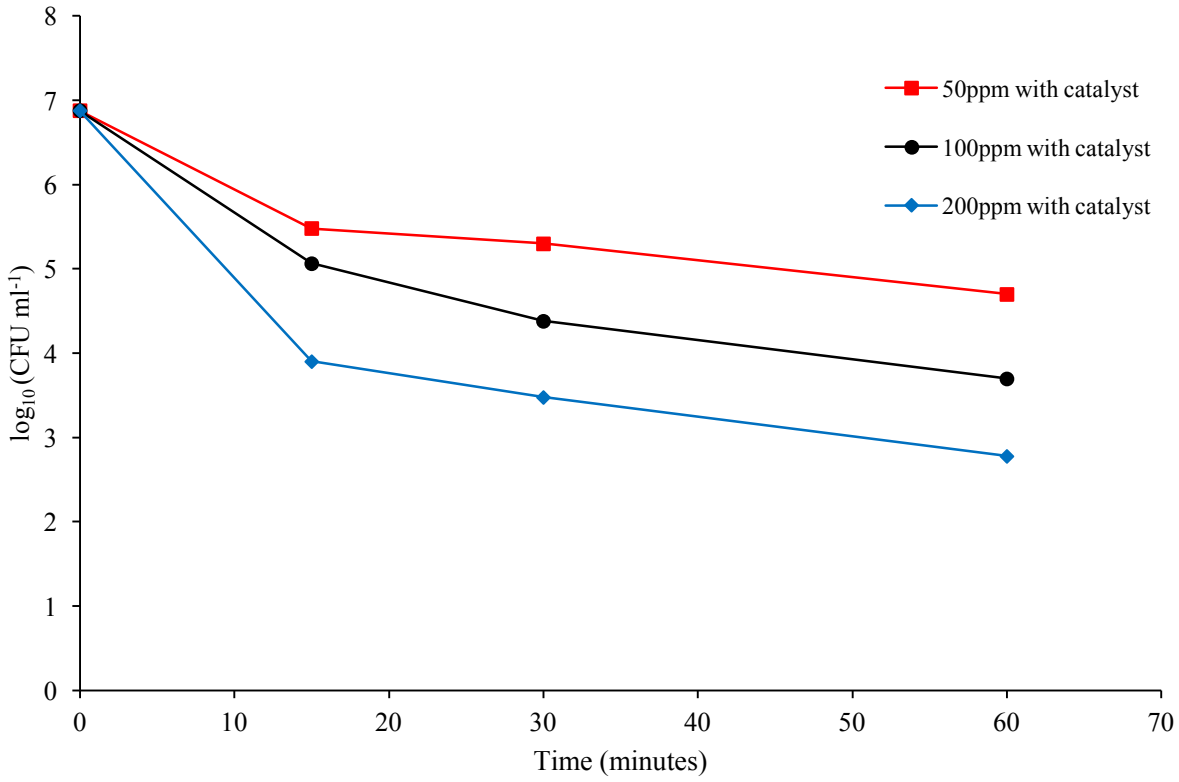

Figure 3.11: Removal of *Escherichia Coli* via the addition of H_2O_2 solutions of varying concentrations with varying contact times.

Reaction conditions: *2 ml H_2O_2 solution, 2 ml Escherichia Coli solution, varying reaction times, 10 mg 1 wt.% AuPd/TiO_2, no reaction gases, room temperature and constant agitation.*

Surprisingly, the addition of catalyst actually inhibits the reaction in this case, contradictory to what is observed in the flow system, where the catalyst itself appeared to display some antimicrobial properties. This could be reasoned in two ways, firstly, the catalyst may be hindering the decomposition reaction by selectively forming H_2O via the over hydrogenation pathway, leading to a decrease in the amount of free radical species formed that are thought to be key to killing the bacteria. Secondly, the catalyst my be mopping up any radical species that are formed, again leading to less of a log reduction. These data suggest that the addition of the AuPd catalyst to the reaction solution inhibits the decomposition pathways that lead to a greater removal of CFU. It should also be noted that the commercial H_2O_2 used in these experiments contains stabilisers, preventing the H_2O_2 from readily decomposing, which is not the case for *in-situ* generated H_2O_2. This may be further reducing the amount of free radicals that are produced in these reactions.

3.3.5 Effect of Reaction Gases

Whilst it has been shown so far in this chapter that the microreactor can effectively synthesise H_2O_2 *in-situ* which can subsequently be used to eradicate *Escherichia Coli* from wastewater streams it should be noted that all experiments have involved the use of pressurised gases with a CO_2 diluent. The intended purpose for this system is to treat GW in a GTS, however, it is undesirable for such a system to use pressurised cylinders containing CO_2. A more viable option would be to obtain the H_2 via H_2O electrolysis and to utilise air as a diluent gas in order to keep the reactions gases below the explosive limit. Air would then also act as the source of O_2 to enable H_2O_2 generating conditions. In order to simulate this, a set of tests were performed using a 2% H_2/air gas feed stream. Switching the gas supply does however present some challenges; by doing this the H_2:O_2 ratio is adjusted from 1:1 to 1:10 and the stabilisation effect due to formation of H_2CO_3 during a reaction is removed. Freakley *et al*[14] have previously shown that as the H_2:O_2 ratio is altered from a stoichiometric ratio the concentration of H_2O_2 produced is decreased. When the ratio was altered so that 10 times the

amount of O_2 was present compared with H_2, the authors reported a drop in the observed concentration of H_2O_2 from 750 ppm to 300 ppm. The authors also state that as the solvent solution can be considered to be saturated with CO_2 under operating conditions then this effect can be attributed solely to the change in the H_2:O_2 ratio. Whilst it is true that the H_2O_2 formed will not be stabilised by H_2CO_3 when a 2% H_2/air environment is used, this may not be a negative. This application may require the presence of reactive intermediates to effectively remove the bacteria from the working solution. The results of these experiments are shown below in table 3.1:

Initial concentration (CFU ml^{-1})	**Final concentration (CFU ml^{-1})**
~1 x 10^6	0
~1 x 10^7	0
~1 x 10^8	~1 x 10^3

Table 3.1: Effect of using a 2% H_2/air reaction gas on the removal of *Escherichia Coli* (JM109) after a single pass through the continuous flow microreactor.

Reaction conditions: *10 bar pressure, 2 °C, 42 ml min^{-1} gas flow, solvent flow rate = 0.2 ml min^{-1}, 120 mg 1 wt.% AuPd/TiO_2 catalyst, 2% H_2/air gas stream.*

Even when using a 2% H_2/air feed stream, the *in-situ* H_2O_2 is able to effectively remove concentrations of up to 10^7 CFU ml^{-1} from the working solution. An estimate of the maximum amount of H_2O_2 that could be produced on the catalyst surface can be made by using previous hydrogen selectivity data for the same flow reactor and catalyst. Freakley *et al*[14] recorded that in a H_2O only solvent and using identical operating conditions, a hydrogen conversion of 5% was achieved. It can be calculated that based off a H_2 conversion of 5% as previously reported by Freakley *et al*[14], and assuming that the all of the H_2 is then utilised to produce H_2O_2, then under the above operating conditions, the maximum concentration of H_2O_2 that would be produced is approximately 250 ppm. However, this would be the maximum concentration of H_2O_2 that it is possible to produce under these reaction conditions, due to the competing H_2O_2 degradation reactions the observed H_2O_2 value is reported as approximately 140 ppm. Limitations with H_2 solubility and competing reactions mean that the amount of H_2O_2 produced during a reaction is likely to be far less than this.

These results again highlight the efficacy of the *in-situ* for the removal of bacteria from wastewater solutions when compared with the addition of stabilised H_2O_2.

3.3.6 Effect of Pressure

Once it had been established that using a more desirable gas stream could still effectively remove high concentrations of *Escherichia Coli* in the microreactor the effect of pressure was investigated. For a GTS the lower the pressure at which the system can operate the better as a lower pressure means the process is less energy intensive, in addition to this from a health and safety standpoint a lower pressure is always preferred particularly in a domestic setting. A series of experiments was performed using 2% H_2/air and the total pressure of the system was decreased from 10 – 2.5 bar. The results are presented below in figure 3.12:

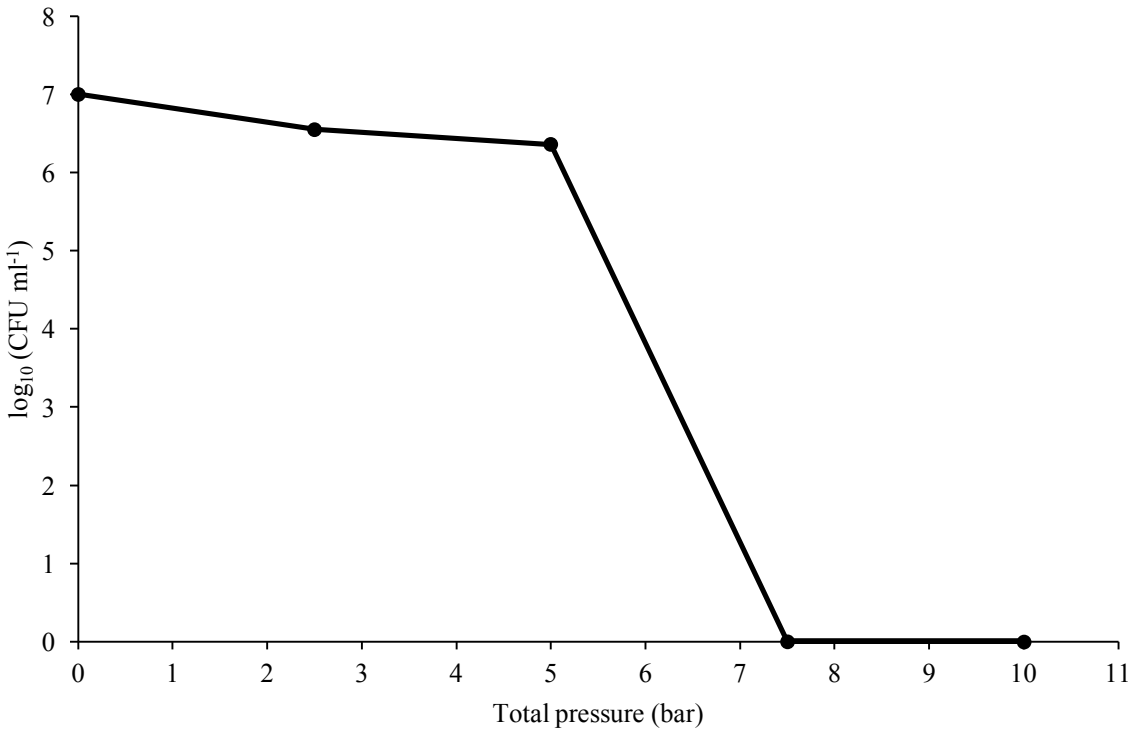

Figure 3.12: Measured cell density after a single pass through the micro reactor under varying total pressures.

Reaction conditions: *Varying pressure, 2 °C, 42 ml min^{-1} gas flow, solvent flow rate = 0.2 ml min^{-1}, 120 mg 1 wt.% AuPd/TiO$_2$ catalyst, 2% H$_2$/air.*

Freakley *et al*[14] previously reported that the concentration of H_2O_2 produced depends linearly on the pressure of the reactor. This observation has also been noted by other researchers, Huerta *et al*[24] recently reported a near linear increase in the concentration of H_2O_2 produced from a trickle bed reactor as the total pressure of the system was raised from 5 to 28 bar. Based on these observations, we would expect that the amount of H_2O_2 produced at lower pressures will be significantly lower than when a total pressure of 10 bar is used and subsequently, the CFU reduction to decrease at lower pressures. The results in figure 3.12 echo this, it is clear that at a total pressure of 10 bar and 7.5 bar enough H_2O_2 is produced *in-situ* to remove all of the *Escherichia Coli* from the working solution. This is promising as even under mild conditions the system is still operating effectively. However, when the pressure is lowered to 5 bar only a 1-log reduction is achieved. Given the relationship between total reaction pressure and concentration of H_2O_2 produced, these data suggest that the lower concentrations of H_2O_2 produced when the reaction is run below 7.5 bar lead to the observed drop in antimicrobial activity. Whilst the quantities of *in-situ* H_2O_2 produced at these reaction pressures are not known, a similar observation was noted earlier in this chapter for the data displayed in figure 3.10. Following the addition of stabilised H_2O_2 to an aqueous *Escherichia Coli* solution in glass vials, a minimum H_2O_2 of 100 ppm was required to kill all the bacteria.

3.3.7 Effect of Gas Flow Rate

Similarly, to the observed effect of reducing total pressure leading to a decrease in the concentration of H_2O_2 produced, the effect of gas flow rate has been shown to be influential with a lower flow rate yielding a lower concentration of H_2O_2. However, for the intended use of a GTS a greater contact time may be beneficial as the antimicrobial agent has longer to interact with the cells. The results of the solvent flow experiment are shown below in figure 3.13:

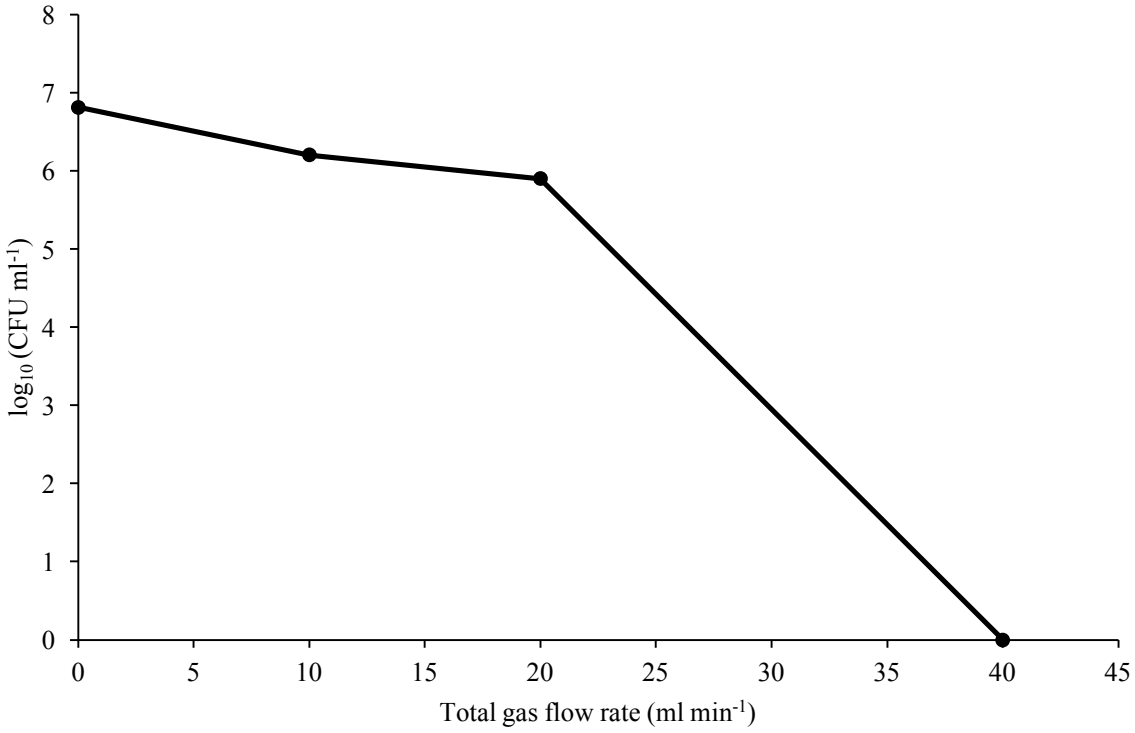

Figure 3.13: Measured cell density after a single pass through the micro reactor under varying gas flow.

Reaction conditions: *10 bar pressure, 2 °C, varying gas flow, solvent flow rate = 0.2 ml min^{-1}, 120 mg 1 wt.% AuPd/TiO_2 catalyst, 2% H_2/air.*

For all gas flows, lower than 42 ml min^{-1}, there is a high concentration of *Escherichia Coli* remaining post reaction. These data suggest that at higher gas flow rates a higher mass transfer between the liquid and the gas is achieved, specifically a higher mass transfer through the liquid layer which surrounds the catalyst surface.

3.3.8 *In-situ* H_2O_2 vs *Ex-situ* H_2O_2

Whilst not yet fully proven, the data so far presented in this chapter has indicated that *in-situ* generated H_2O_2 is far more effective for the removal of *Escherichia Coli* than comparative concentrations of stabilised, commercially available H_2O_2. These tests were not a true comparison between the sources of H_2O_2 due to the differences in experimental set up, the stabilised H_2O_2 was simply added in a glass vial, whereas the *in-situ* process involves using the microreactor. To try and get a true comparison between the two sources of H_2O_2 a series

of tests were performed using the microreactor system. A mixture of the *Escherichia Coli* and H_2O_2 solutions were co-fed through the reactor under identical operating conditions to those of an *in-situ* experiment. The only difference being that synthetic air was used in the gas feed stream. This should account for any differences which occur due to pressure, solvent flow, equipment etc. It should also be noted that as it was not possible to use a quaternary pump, the two liquids were simultaneously added to the solvent reservoir and so allowed to mix for a prolonged period before entering the reactor and eventually contacting the catalyst bed. Meaning that whilst this is a much clearer comparison than the glass vial tests, the bacteria still have a much larger contact time with the H_2O_2 compared with *in-situ* tests. The contact time for the *in-situ* tests was estimated earlier in this chapter to be approximately 75 seconds, for the *ex-situ* tests in the flow reactor the bacteria will be in contact with the H_2O_2 for much longer, as the two liquds are mixed in the solvent reservoir and then as they are passed through the first half of the reactor, before reaching the catalyst bed. Under the operating conditions listed, 12 ml of liquid will flow through the reactor to the sample bomb per hour, therefore as 2 ml of liquid is mixed for the *ex-situ* tests, it will take 10 minutes for that to flow completely through the reactor, however, the liquid will meet the catalyst bed approximately halfway through the reactor meaning an estimate of the additional contact time for the *ex-situ* tests in the flow reactor compared with the true *in-situ* reactions is 5 minutes. Figure 3.14 shows the results of these experiments:

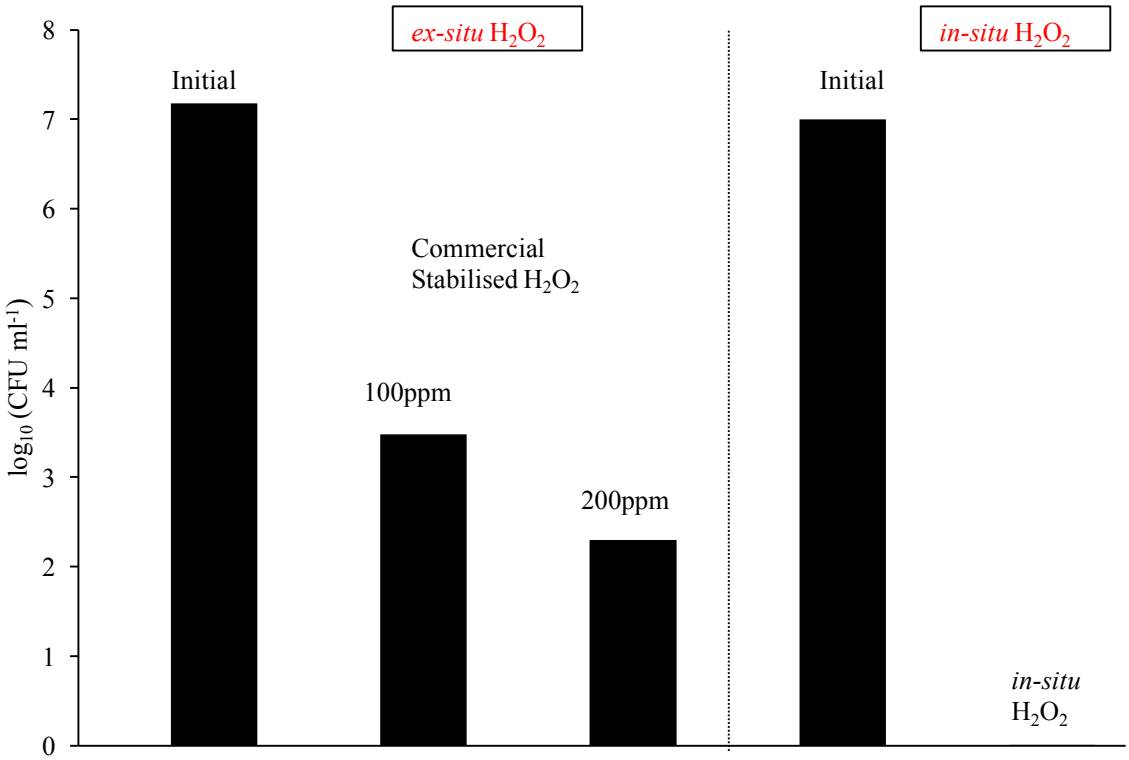

Figure 3.14: Measured cell density of reaction solutions after a single pass through the reactor with 100 and 200 ppm H_2O_2 solutions (stabilised) and after an *in-situ* experiment.

Reaction conditions: *10 bar pressure, 2 °C, 42 ml min^{-1} (synthetic air for ex-situ and 2% H_2/air for in-situ), solvent flow rate = 0.2 ml min^{-1}, 120 mg 1 wt.% AuPd/TiO_2 catalyst.*

These data show again that the *in-situ* generated H_2O_2 is acting far more effectively as an antimicrobial agent than the commercial, stabilised H_2O_2. After a single pass through the reactor the 100 ppm solution gave a 4-log reduction with approximately 10^3 CFU ml^{-1} *Escherichia Coli* measured in the reaction effluent. As is to be expected a further log reduction is achieved when the concentration of the H_2O_2 solution is doubled to 200 ppm. This is still clearly far less effective than the *in-situ* system, which is able to totally eliminate all of bacteria after a single pass, with a much shorter contact time. As was mentioned previously in this chapter, the amount of *in-situ* H_2O_2 produced under these conditions is approximately 140 ppm, meaning that this reaction and the resultant data obtained can be taken as a valid comparison between the two H_2O_2 sources.

These data coupled with the previous testing data from the experiments performed in glass vials conclusively show that *in-situ* > *ex-situ* for this application. Following on from this important observation it was decided to investigate whether H_2O_2 generated *in-situ* could be as effective when it is co-fed through the reactor system or whether the *in-situ* generation has to occur over the catalyst bed in the presence of the bacteria. To test this, a series of experiments was performed whereby H_2O_2 was synthesised using a standard experimental process reported in the experimental section of this work and also widely documented in the literature[25]. The catalyst used was the same as that in the flow system, a 1 wt.% AuPd/TiO_2 prepared via the modified impregnation technique[26]. It is known that this catalyst is highly stable under the aforementioned direct synthesis conditions and would therefore prevent traces of precious metal from leaching into the reaction solutions and potentially affecting the results. After a 30 minute direct synthesis reaction in the batch reactor the concentration of H_2O_2 in the reaction effluent was calculated via titration (500 – 550 ppm) dilutions were then made with HPLC grade H_2O to give the desired H_2O_2 concentrations of 100 and 200 ppm. The synthesised H_2O_2 was then co-fed through the reactor system as described in the prior test using stabilised H_2O_2 the results are shown below in figure 3.15:

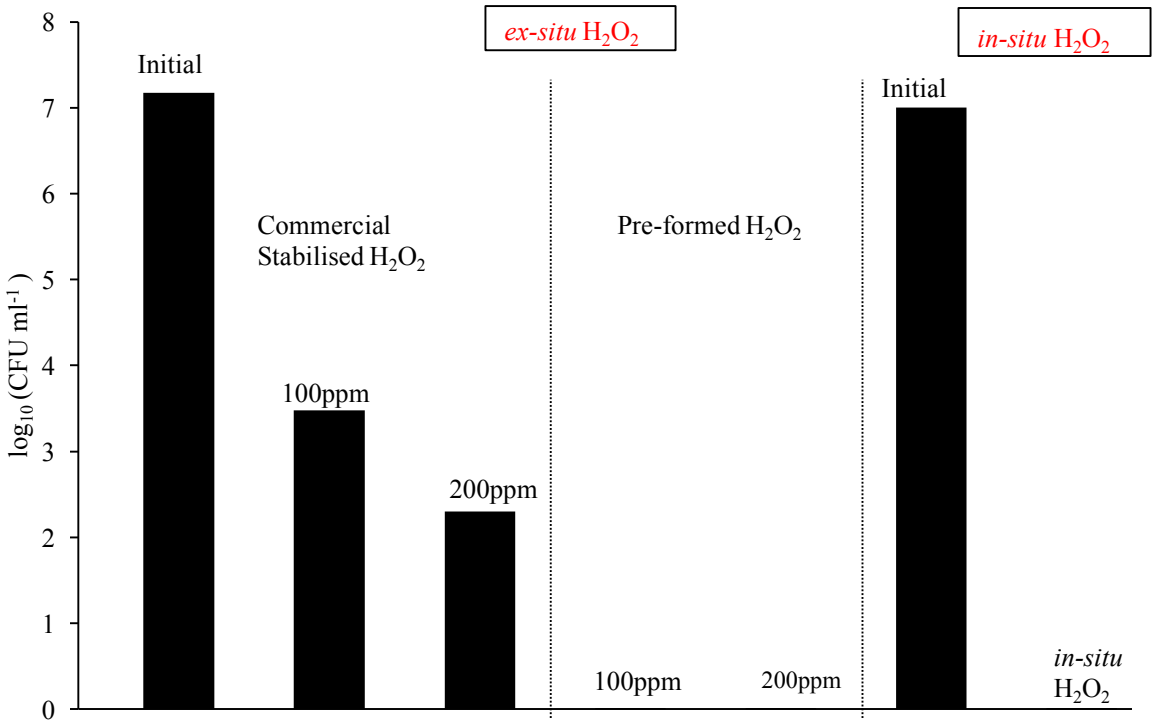

Figure 3.15: Measured cell density of reaction solutions after a single pass through the reactor with 100 and 200 ppm H_2O_2 solutions (unstabilised, synthesised and stabilised, commercial) and after an *in-situ* experiment.

Reaction conditions: *10 bar pressure, 2 °C, 42 ml min^{-1} (synthetic air for ex-situ and 2% H_2/air for in-situ), solvent flow rate = 0.2 ml min^{-1}, 120 mg 1 wt.% AuPd/TiO_2 catalyst.*
In addition, an analogous test was performed using synthesised H_2O_2 stirred in a glass vial. Earlier in this chapter it was shown that under such reaction conditions a contact time of 30 minutes with 200 ppm H_2O_2 was needed to remove all *Escherichia Coli* from the reaction solution. Figure 3.16 shows that when synthesised H_2O_2 is used the reaction is complete within 15 minutes with a 200 ppm solution, the results of the 100 and 50 ppm solutions are similar to those for commercial H_2O_2. At least 60 minutes is needed for the reaction to reach completion with a 100 ppm solution and only a 3-log reduction is achieved after 60 minutes with a 50 ppm solution.

Interestingly, the synthesised H_2O_2 performs on par with that of the *in-situ* reaction, with no bacteria detected in the post reaction solutions, even when plated neat. From this result, we can draw the conclusion that the unstabilised H_2O_2 formed either via the batch process or *in-situ* generation in the microreactor is superior to that of commercially available stabilised H_2O_2. This could be due to either the stabilisers present having a negative effect on the reaction or the inherent stability of the commercial solution preventing the formation of highly reactive oxidative intermediates which could potentially cause irreversible damage the cells of the bacteria. We can now draw the following conclusion:

In-situ generated H_2O_2 ≥ synthesised H_2O_2 > commercial stabilised H_2O_2

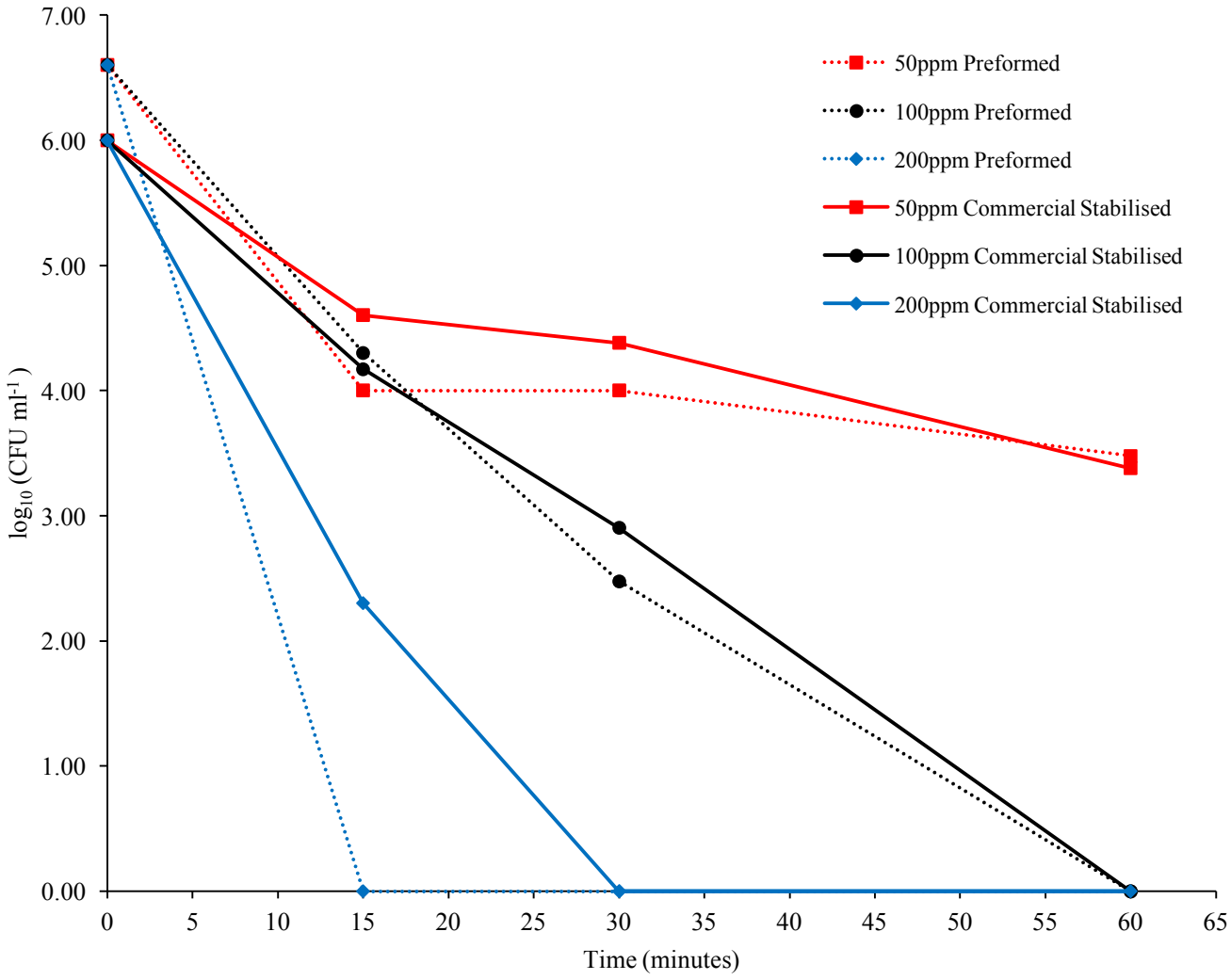

Figure 3.16: Removal of *Escherichia Coli* via the addition of H_2O_2 solutions of varying concentrations with varying contact times.

Reaction conditions: *2 ml H_2O_2 solution, 2 ml Escherichia Coli solution, varying reaction times, no catalyst or reaction gases, room temperature and constant agitation.*

One of the main questions that arises from these findings is why is the *in-situ* H_2O_2 so much more effective than the *ex-situ*? As was previously eluded to, the commercially available H_2O_2 contains stabilisers to ensure that the highly concentrated solutions do not decompose when transported or stored in a laboratory. The stabilising agents found in concentrated H_2O_2 solutions generally include:

- Colloidal stannate, concentrations typically range from 25 – 250 mg l^{-1}
- Sodium pyrophosphate, concentrations typically range from 25 – 250 mg l^{-1}
- Organo phosphonates
- Nitric and phosphoric acid

The most common and effective stabiliser is sodium stannate ($Na_2Sn(OH)_6$), the stannate solution is typically acidified between pH 1 and 5 depending on the concentration of the H_2O_2 solution which needs stabilising. Once added to the H_2O_2 solution, the stannate complex effectively inhibits the catalytic decomposition of H_2O_2 which may occur due to noble metal impurities, allowing the H_2O_2 to be stored for many months. The presence of such complexing agents may however play a role in the inhibition of the sterilisation of *Escherichia Coli* which has been observed in this work. It is possible to buy unstabilised H_2O_2 commercially and therefore compare the difference between stabilised and unstabilised H_2O_2 for this reaction. A series of experiments were performed through the microreactor using with 100 and 200 ppm concentrations of unstabilised commercial H_2O_2. The results are shown in figure 3.17 below:

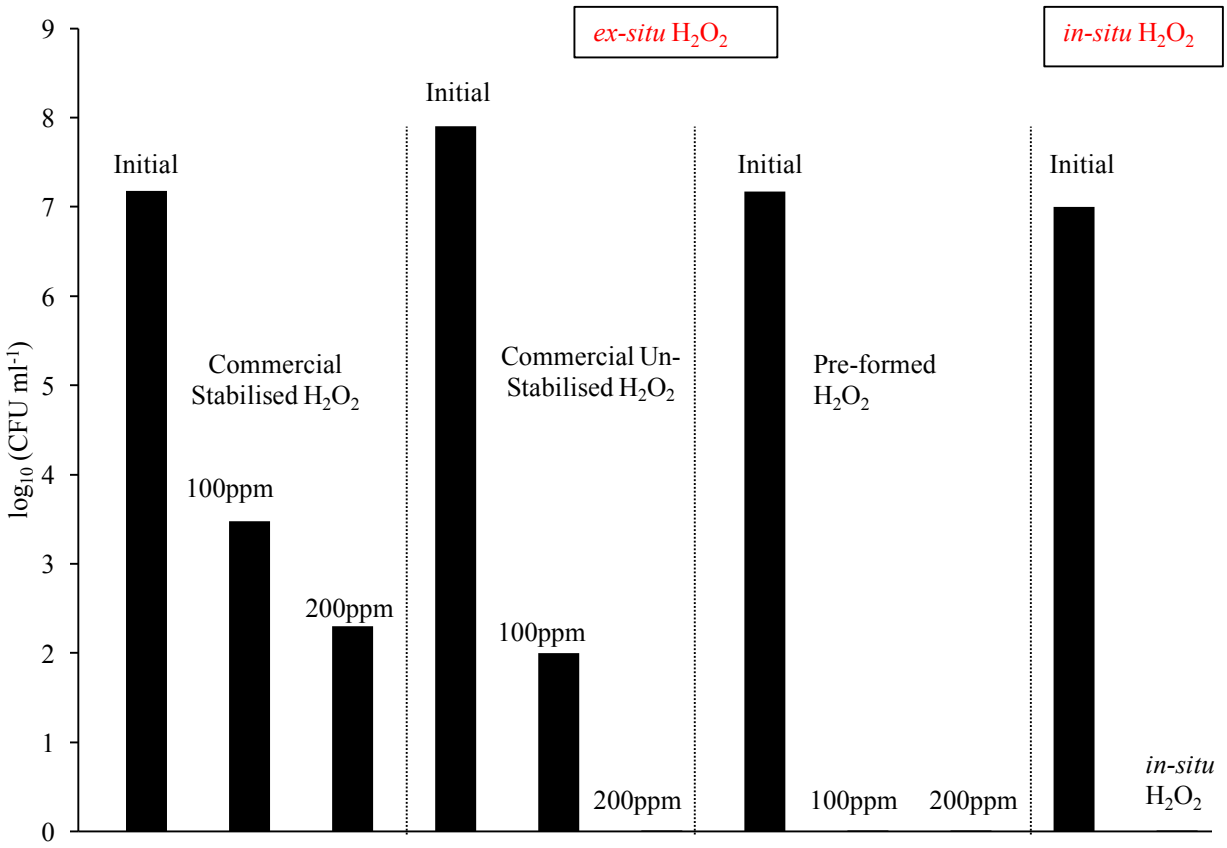

Figure 3.17: Measured cell density of reaction solutions after a single pass through the reactor with 100 and 200 ppm H_2O_2 solutions (varying sources) and after an *in-situ* experiment.

Reaction Conditions: *10 bar pressure, 2 °C, 42 ml min^{-1} (synthetic air for ex-situ and 2% H_2/air for in-situ), solvent flow rate = 0.2 ml min^{-1}, 120 mg 1 wt.% AuPd/TiO_2 catalyst.*

The results show that the unstabilised H_2O_2 is indeed more active than the stabilised solution. After a single pass through the reactor 200 ppm of the unstabilised H_2O_2 was sufficient enough to eliminate all of the bacteria present in the reaction solution. Whilst these results are better than the stabilised H_2O_2 they are still worse than both the synthesised H_2O_2 and *in-situ* generated H_2O_2. These data therefore indicate that the stabilisers present in the commercial H_2O_2 may be playing a role in the lower activity that is seen when compared to the *in-situ* and synthesised H_2O_2. Furthermore, the "shielding" of bacteria via particulate matter or organic loads is well documented in the literature[27] and results in a decrease in antimicrobial activity of many chemical disinfectants. The presence of stabilisers may also lead to such

diffusional effects, blocking the active sites on the catalyst surface and preventing further reaction with the bacteria.

Once it had been established that concentrations as low as 100 ppm of synthesised, unstabilised H_2O_2 were able to eliminate up to 10^7 CFU ml^{-1} after a single pass through the microreactor then lower concentrations were used to determine at what point a 100% conversion is no longer achieved. Concentrations of 50, 20 and 10 ppm H_2O_2 were investigated using the same reaction procedure as outlined previously in this chapter.

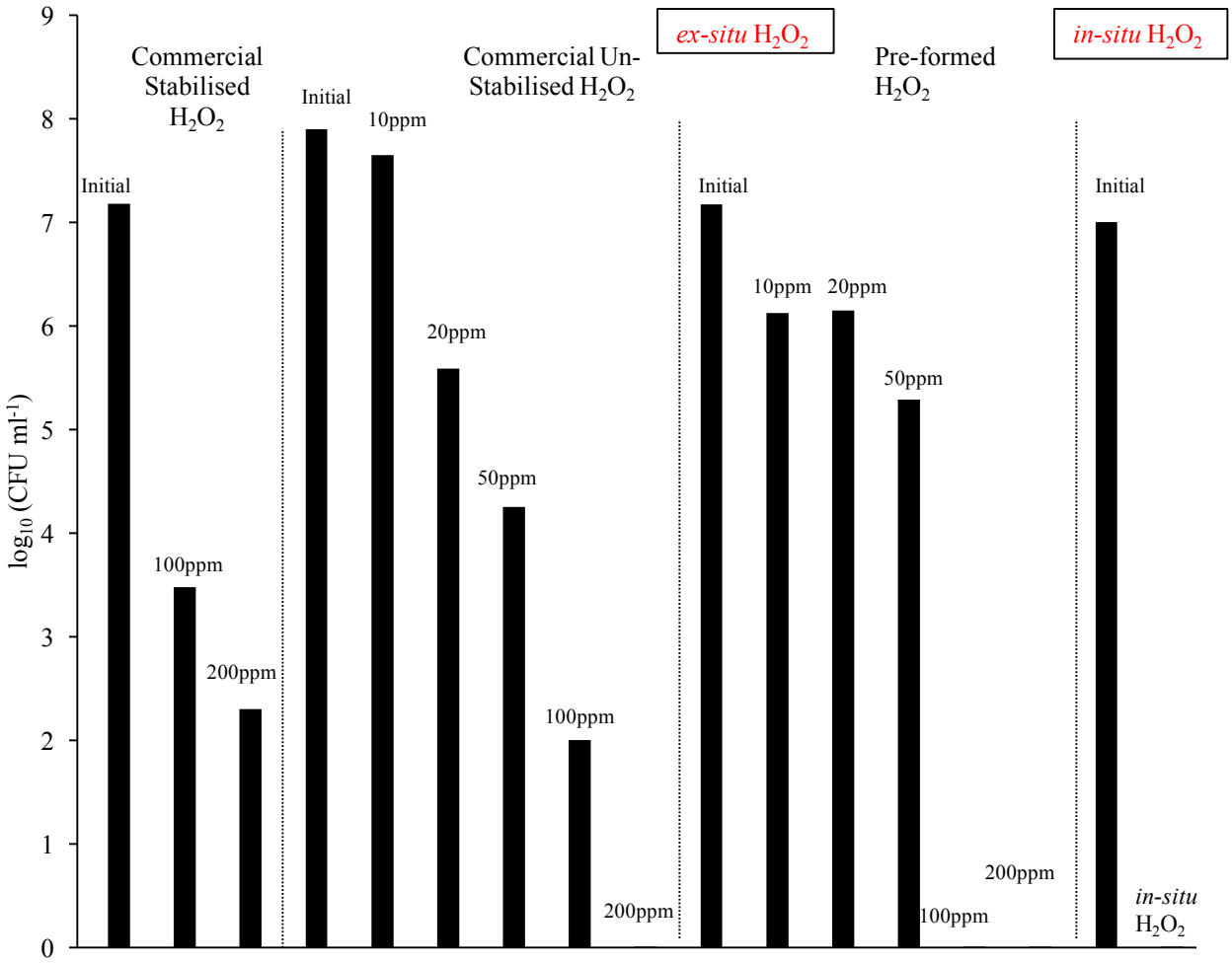

Figure 3.18: Measured cell density of reaction solutions after a single pass through the reactor with 10, 20, 50, 100 and 200 ppm H_2O_2 solutions (varying sources) and after an *in-situ* experiment.

Reaction conditions: *10 bar pressure, 2 °C, 42 ml* min^{-1} *(synthetic air for ex-situ and 2% H_2/air for in-situ), solvent flow rate = 0.2 ml* min^{-1}*, 120 mg 1 wt.% AuPd/TiO_2 catalyst.*

The results displayed above in figure 3.18 show that when the concentration of the pre-synthesised H_2O_2 is reduced to 50 ppm a dramatic reduction in the antimicrobial activation is observed. Only a 2-log reduction is achieved with a 50 ppm solution and a further decrease in activity is seen when using a 20 and 10 ppm solution, both of which gave only a 1-log reduction. Initial experiments showed that simply by pressurising the reaction solution and passing through the flow reactor in an absence of catalyst a 2-log reduction can be achieved and when the catalyst is introduced an extra log reduction is seen. This suggests that at very low concentrations the synthesised H_2O_2 is having essentially no antimicrobial effect. It should however be noted that those initial experiments involved the use of CO_2 in all gas streams and therefore promoted the formation of H_2CO_3 which may itself lead to a decrease in the concentration of *Escherichia Coli* in the reaction solution.

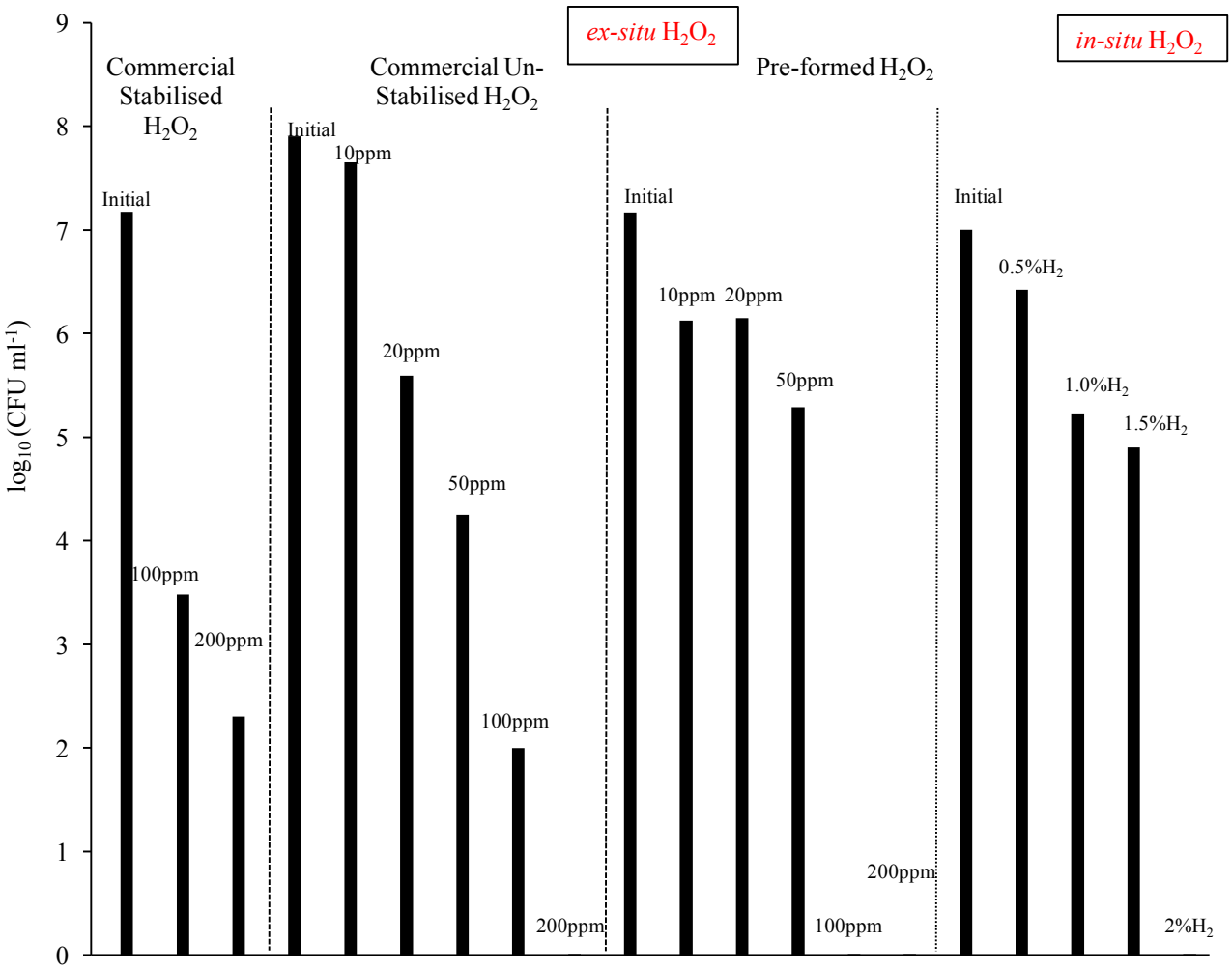

Figure 3.19: Measured cell density of reaction solutions after a single pass through the reactor with decreasing amounts of Hydrogen in the reactant gas stream.

Reaction conditions: *10 bar pressure, 2 °C, 42 ml min^{-1} (synthetic air for ex-situ and varying amounts of H_2/air for in-situ), solvent flow rate = 0.2 ml min^{-1}, 120 mg 1 wt.% AuPd/TiO_2 catalyst.*

To try and compare how lower amounts of *in-situ* H_2O_2 compared to the results just discussed for lower amounts of *ex-situ* H_2O_2, the amount of H_2 in the reactant gas stream was adjusted using the mass flow controllers on the reactor and flow rates were checked using a digital flow meter to ensure the experiments were as accurate as possible. The results are shown in figure 3.19, these data suggest that a minimum amount of H_2 is needed to generate enough H_2O_2 to inactivate the bacteria, with a sharp decrease in conversion seen when the amount of H_2 is reduced from 2% to 1.5%. The results seem to be comparable those of the experiments where lower concentrations of *ex-situ* H_2O_2 are used.

3.3 Conclusions

In this chapter, it has been shown that using a 1 wt.% $AuPd/TiO_2$ catalyst it is possible to synthesise H_2O_2 and utilise it *in-situ* to eradicate *Escherichia Coli* from a model wastewater stream in a continuous flow system. This represents a step forward in the direct synthesis of H_2O_2, as it has not been shown previously that *in-situ* generated H_2O_2 is effective for this application.

Under optimum conditions the catalyst is stable on stream for periods of 24 hours with no loss in activity and by the modification of the continuous reactor, it is possible to produce a H_2O_2 reservoir with no stabilisers and a concentration of greater than 1400 ppm. By operating under optimum conditions, full removal of up to 10^9 CFU ml^{-1} is achieved only when both H_2 and O_2 are fed into the reactor system. The potency of *in-situ* generated H_2O_2 as a disinfectant for the removal of bacterial contamination from wastewater streams has therefore also been shown. Furthermore, it stands that gas mixtures which can realistically be produced by electrolysis could potentially be used for this application and thus removing the need to store and transport concentrated H_2O_2 solutions for H_2O sterilisation.

It was observed that in the presence of a catalyst and under a reasonable working pressures removal by *in-situ* H_2O_2 production was more effective than using *ex-situ* H_2O_2 and it can be stated that for the bacteria investigated herein, the efficacy of H_2O_2 as a disinfectant follows order below:

In-situ ≥ pre-synthesised > commercial unstabilised > commercial stabilised.

3.4 References

1. Master Plumbers and Mechanical Services Association of Australia & Australia. National Water Commission, *Urban Greywater Design and Installation Handbook.*, **2008**, *National Water Commission, Canberra, A. C. T.*
2. D. Christova-Boal, R. E. Eden, S. McFarlane, *Desalation*, **1996**, *106*, 391 – 397.
3. J. G. March, M. Gual, F. Orozco, *Desalation*, **2004**, *164*, 241 – 247.
4. T. Itayama, M. Kiji, A. Suetsugu, A. Tanaka, T. Saito, N. Iwami, M. Muzochi, Y. Inamori, *Water Sci. Technol*., **2004**, *53*, 193 – 201.
5. K Sunada, Y. Kikuchi, K. Hashimoto, *Environ. Sci. Technol.*, **1998**, *32*, 726 – 728.
6. M. Cho, H. Chung, W. Choi, J. Yoon, *Water Res.,* **2004**, *38*, 1069 – 1077.
7. A. G. Rincon, C. Pulgarin, *Appl. Catal. B.*, **2003**, *44*, 263 – 284.
8. A. G. Rincon, C. Pulgarin, *Appl. Catal. B.*, **2004**, *49,* 99 – 112.
9. W. A. M. Hijnen, E. F. Beerendonk, G. J. Medema, *Water Res.*, **2006**, *40*, 3 – 22.
10. S. N. Frank, A. J. Bard, *J. Am. Chem. Soc.,* **1977**, *99*, 303 – 304.
11. S. N. Frank, A. J. Bard, *J. Phys. Chem*., **1977**, *81*, 1484 – 1488.
12. M. Pelaez, N. T. Nolan, S. C. Pillai, M. K. Seery, P. Falaras, A. G. Kontos, P. S. M. Dunlop, J. W. J. Hamilton, J. A. Byrne, K. O'Shea, M. H. Entezari, D. D. Dionysiou, *Appl. Catal. B.*, **2012**, *125*, 331 – 349.
13. M. N. Chong, B. Jin, C. W. K. Chow, C. Saint, *Water. Res.*, **2010**, *44*, 2997 – 3027.
14. S. J. Freakley, M. Piccinini, J. K. Edwards, E. N. Ntainjua, J. A. Mouljin, G. J. Hutchings, *ACS Catal.*, **2013**, *3*, 487 – 501.
15. D. A. Crole, S. J. Freakley, J. K. Edwards, G. J. Hutchings, *Proc. R. Soc. A*, **2016**, *472*, 1-9.
16. N. Gemo, P. Biasi, T. Salmi, P. Canu, *J. Chem. Thermodynamics*, **2012**, *54*, 1 – 9.
17. Z. Ronen, A. Guerrero, A. Gross, *Chemosphere*, **2010**, *78*, 61 – 65.
18. J. Koivenuen, H. Heinonen – Tanski, *Water Res.*, **2005**, *39*, 1519 – 1526.
19. L. Restaino, E. W. Frampton, J. B. Hemphill, P. Palnikar, *App. Environ, Microbiol.*, **1995,** *61*, 3471 – 3475.
20. P. A. Christensen, T. P. Curtis, T. A. Egerton, S. A. M. Kosa, J. R. Tinlin, *App. Catal. B.*, **2003**, *41*, 371 – 386.
21. R. Pedazuhr, O. Lev, B. Fattal, H. I. Shuval, *Wat. Sci. Tech.*, **1995**, *31*, 123 – 129.
22. R. Pedazuhr, H. I. Shuval, S. Ulitzur, *Wat. Sci. Tech.*, **1997**, *35*, 87 – 93.

23. M. Conte, H. Miyamura, S. Kobayashi, V. Chechik, *J. Am. Chem. Soc.*, **2009**, *131*, 7189 – 7196.
24. I. Huerta, P. Biasi, J. Garcia-Serna, M. J. Cocero, J. P. Mikkola, T. Salmi, *Green. Process. Synth.*, **2016,** *5*, 341 – 351.
25. J. K. Edwards, B. E. Solsona, P. Landon, A. F. Carley, A. Herzing, C. J. Kiely, G. J. Hutchings, *J. Catal.*, **2005**, *236*, 69 – 79.
26. M. Sankar, Q. He, M. Morad, J. Pritchard, S. J. Freakley, J. K. Edwards, S. H. Taylor, D. J. Morgan, A. F. Carley, D. W. Knight, C. J. Kiely, G. J. Hutchings, *ACS Nano*, **2012**, *6*, 6600 – 6613.
27. R. W. Emerick, F. J. Lodge, T. Ginn, J. L. Darby, *Water. Environ. Res.*, **2000**, *72*, 432 – 438.

Chapter 4

Utilisation of *In-situ* H_2O_2: Applications in Greywater Treatment Part 2

4.1 Introduction

Following the investigation of the feasabilty that the *in-situ* generation of H_2O_2 could eliminate *Escherichia Coli* (JM109) concentrations of up to 10^9 CFU ml^{-1} after a single pass through a flow reactor system the study was extended to investigate the antimicrobial efficiency against more resistant strains of bacteria. Moreover, *Escherchia Coli* is a gram negative bacterium, it is highly likely that household greywater (GW) will contain both gram negative and gram positive bacteria and it is therefore important to investigate whether or not *in-situ* generated H_2O_2 is effective against both gram negative and gram positive bacteria.

Gram positive and gram negative bacteria have different cell wall structures, illustrated below in figure 4.1. A simple test known as gram staining was developed by Hans Christian Joachim Gram[5] and allows bacteria to be easily identified as either gram positive or gram negative. The cells are heat fixed and stained with a triarylmethyl dye known as "crystal violet", the dye floods the cell walls and changes the appearance of the cells to a violet colour. Iodine is added as a trapping agent, forming a strong bond with the dye and preventing the cells from losing the violet colour. The cells are washed with ethanol (EtOH) for a period of approximately 20 seconds, gram negative bacteria will lose the violet colour after being washed with EtOH whereas gram positive bacteria will retain it. Finally, a counterstain, safranin, is added. The gram negative bacteria will take on the red colour of the safranin stain, whereas the gram positive bacteria will still retain the violet stain. The observed differences in staining can be explained due to the cell wall composition of the bacteria. Gram positive bacteria have a thick peptoglycan wall surrounding the plasma membrane, gram negative bacteria only have a thin peptoglycan wall which is surrounded by an outer membrane composed of lipopolysaccharides and proteins. When gram positive bacteria are stained with crystal violet the stain is tightly bound to the peptoglycan wall and so addition of alcohol does not affect the colour as it has no effect on the peptoglycan wall. In the case of gram negative bacteria, the stain is tightly bound to the lipopolysaccharide

surrounding the peptoglycan wall and when EtOH is added the lipopolysaccharide layer is dissolved and the bacteria lose the violet stain. As the EtOH treatment has been not been effective on the gram positive bacteria the safranin stain will have no effect. Gram negative bacteria will take on the red colour of the safranin stain.

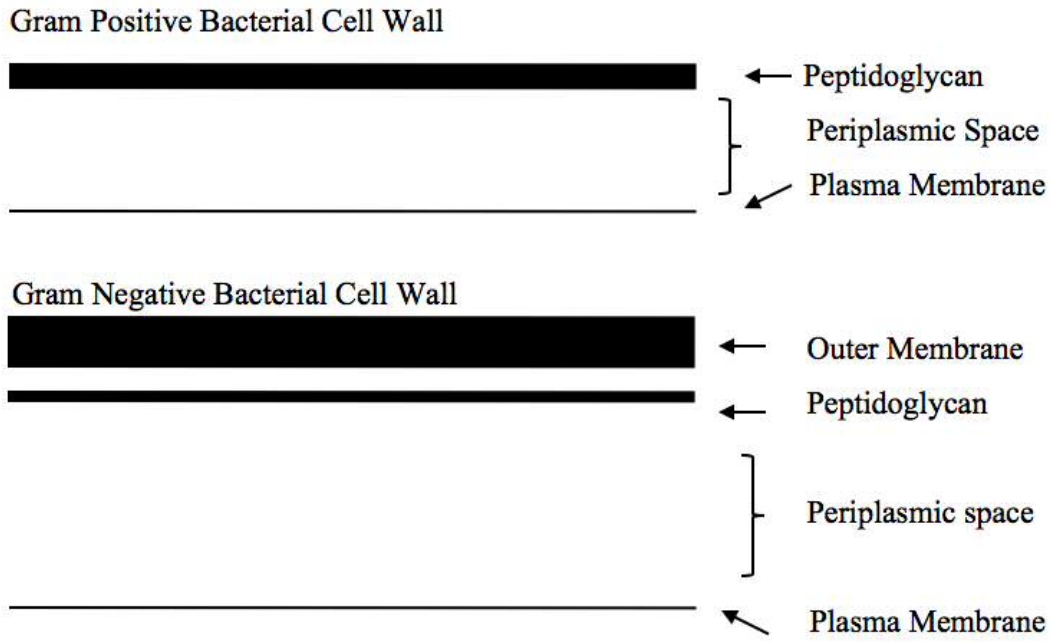

Figure 4.1: Schematic diagram showing the structural differences between cell walls of gram negative and gram positive bacteria

Staphylococcus Aureus was chosen as the target bacteria for the microbiological testing of *in-situ* generated H_2O_2 as a potential water disinfectant. There is a large amount of literature on the use of *Staphylococcus Aureus* as a target bacteria for the testing of disinfectants and antimicrobial agents[6-9]. It is important to show that the *in-situ* H_2O_2 generated in this system can be active against gram positive bacteria. *Staphylococcus Aureus* is a catalase positive bacterium[10] meaning it has an in-built defence against H_2O_2. Catalase is an enzyme present in aerobic organisms which catalyses the decomposition of H_2O_2 into water (H_2O) and oxygen (O_2). Catalase acts as an intra-cellular defence mechanism in catalase positive bacteria to prevent cell damage occurring due to H_2O_2 or peroxy radical ($OOH\bullet$) species. Disinfection of *Staphylococcus Aureus* is highly desirable for other applications including in public hospitals where *Methicillin Resistant Staphylococcus Aureus* (MRSA) has been a major problem and

to this day nosocomial infections are still an issue. The risk of transmitting nosocomial infections via contaminated hospital equipment is therefore high[11], if a disinfection procedure can be put in place which can effectively inactivate high concentrations of *Staphylococcus Aureus* without the use of potentially harmful chlorinated chemicals then it would be highly attractive and useful for such applications. Furthermore, alcohol based hand rubs commonly employed to prevent the transmission of MRSA are not without their pitfalls. Many alcohol products include low levels of additional biocidal agents such as chlorhexidine ($C_{22}H_{30}Cl_2N_{10}$) to boost their activity[12], again, introducing the use of chlorinated chemicals. The resistance of bacteria to antiseptics and disinfectants has been reviewed in detail[13] and it is noted that *Staphylococci* can develop high levels of resistance to a variety of commonly used antiseptics. The identification of EtOH as an effective germicide dates to 1936[14], however, it is not as effective as one might wish. Price[15] reported that a contact time of 5 minutes is needed to completely inactivate *Staphylococcus Aureus* in a test solution and that the germicidal activity is highly dependent upon the EtOH concentration, with 70 – 80% being the most effective at contact times of 5 minutes and 50% being the most effective at a contact time of 10 minutes. Therefore, the ability to inactivate high concentrations of *Staphyloccocus Aureus* using *in-situ* generated H_2O_2 would not only be advantageous for GW treatment, but also for a wide range of other applications such as the disinfection of surgical instruments.

This chapter builds upon the work performed in chapter 3 where the proof of concept of low concentrations of *in-situ* generated H_2O_2 are indeed efficient for the inactivation of *Escherichia Coli* (JM109) in H_2O solutions, the effectiveness against *Staphylococcus Aureus* is extensively investigated. The model conditions for the inactivation of this bacteria using a continuous flow reactor are established. The use of catalyst additives and promotors is explored and the effectiveness against other bacteria is explored.

4.2 Results

4.2.1 Introductory Experiments with *Staphylococcus Aureus*

It has been reported[16] that the rate limiting step involved in the inactivation of bacteria by H_2O_2 is the initial permeation of the cell wall into the plasma membrane. Initial reactions involving *Staphylococcus Aureus* were performed under the standard operating conditions presented in the experimental chapter of this work. If the cell wall structure does indeed have a significant effect on the rate of the inactivation of bacteria by H_2O_2, then the results between the previously investigated *Escherichia Coli* (JM109) and *Staphylococcus Aureus* (NCTC 10788) would be expected to be different. Furthermore, both *Escherichia Coli* and *Staphyloccocus Aureus* are catalase positive bacteria, providing further argument that any observed differences in the antimicrobial activity of *in-situ* generated H_2O_2 may be due to their different cell wall structures. The reactions were performed three times to ensure accuracy of the results and the reaction effluent was plated twice per experiment. The results in table 4.1 show that the log reduction is far less than was previously shown for *Escherichia Coli* (JM109), where a 7-log reduction was observed under identical operating conditions.

Bacteria	**Initial Concentration (CFU ml^{-1})**	**Final Concentration (CFU ml^{-1})**	**Log Reduction**
Staphylococcus Aureus. (NCTC 10788)	4 x 10^7	4 x 10^7	0
Staphylococcus Aureus. (NCTC 10788)	5 x 10^7	5 x 10^5	2
Staphylococcus Aureus. (NCTC 10788)	5 x 10^7	4 x 10^5	2
Staphylococcus Aureus. (NCTC 10788)	5 x 10^7	5 x 10^5	2

Table 4.1: Cell density in wastewater solution following a single pass through continuous flow reactor

Reaction conditions*: 10 bar pressure, 2 °C temperature, 42 ml min^{-1} gas flow rate, 2% H_2/air, 0.2 ml min^{-1} solvent flow rate, 120 mg 1 wt.% AuPd/TiO_2 catalyst.*

Although the cell structure of these bacteria is different, it was concluded that the main difference arises in the intended uses of the bacterial strains. *Escherichia Coli* (JM109) is designed to be used for general cloning and plasmid maintenance. Cloning can be achieved by using either a polymerase chain reaction (PCR), or restriction enzymes to "cut" and modifying enzymes to "paste" the desired DNA fragments into cloning vectors, which can then be replicated using live cells, usually *Escherichia Coli*. This means that the *Escherichia Coli* have modified DNA sequences[17] and are therefore already susceptible to attack from an antimicrobial agent, as it is believed that inactivation of *Escherichia Coli* via H_2O_2 is due to oxidative damage to the DNA of the cells. Whereas *Staphylococcus Aureus* (NCTC 10788) is a strain that is used for the testing and comparison of antimicrobial agents and is one of strains recognised by the british standards institution (BSI) for the testing of antimicrobial

agents. This can easily help to explain the observed difference in efficacy of the *in-situ* H_2O_2 for the inactivation of the two strains of bacteria.

After a single pass through the flow reactor under *in-situ* generating conditions a 2-log reduction is observed. A control reaction was also performed, whereby the catalyst bed was emptied and a blank tube was used, it can be seen that no log reduction was observed and as such the effect of pressure can be discounted. These data show that even against resilient bacterial strains, it is possible to remove 99.9% of the coliforms from a wastewater solution after a contact time of a matter of seconds. As was discussed in chapter 3 of this work, the approximate maximum concentration of H_2O_2 that can be expected to be produced under these conditions is 250 ppm, however, that is assuming that all of the H_2 is utilised to produce H_2O_2 and that the unwanted side reactions are suppressed. It is known that the competing hydrogenation and decomposition reaction pathways will lower the selectivity in the direct synthesis of H_2O_2 and as such we can assume that the amount of H_2O_2 that is actually produced is therefore less than 250 ppm. Baldry[18] investigated the bactericidal effect of H_2O_2, it was shown that H_2O_2 becomes bacteriostatic at concentrations above approximately 5 ppm, however it is poor as a bactericide, although H_2O_2 was actually shown to have greater sporicidal activity than peracetic acid (CH_3CO_3H). It is for this reason that many commercial disinfectant products use concentrations of H_2O_2 greater than 5000 ppm. It is clear that *in-situ* generated H_2O_2 using the continuous flow reactor is capable of inactivating significant amounts of bacteria after a very short contact time and only using relatively low concentration when compared to the concentrations traditionally used in commercial applications.

4.2.2 The Effect of Gas Flow Rate

After it had been shown that *in-situ* generated H_2O_2 was capable of inactivating *Staphylococcus Aureus*, the reaction conditions were investigaged to try and achieve a greater log reduction. It is desirable for a GW treatment system (GTS) to demonstrate a 4-log reduction in total coliforms, thus setting a benchmark for the *in-situ* generated H_2O_2.

In a continuous flow system, the reaction parameters can have a significant impact on the observed conversion and selectivity. In a typical chemical study using such a continuous flow system, there will be a desired target product and information on reaction kinetics.

Furthermore, reaction selectivities and conversions can be obtained in great detail through various analytical techniques. Monitoring of the reaction in such detail allows the researchers to then alter the reaction parameters and catalyst design to try and influence the reaction in favour of formation of the desired products or outcomes. Unfortunately, this is not the case for the wastewater treatment process. We are unable to monitor the exact amount of H_2O_2 produced during the reaction when bacteria is present and it is only speculative as to how this will interact with bacteria as they flow through the reactor and across the catalyst bed. It is however widely thought to be the formation of peroxy-type radicals, in particular hydroxyl (OH•) radicals that inactivate the bacteria by causing irreversible damage to the cell's DNA. Therefore, if the production of H_2O_2 can be increased through the flow reactor and the number of radical species which are thought to form on the catalyst surface is increased then the reduction in bacteria could be increased if radical species are responsible. Table 4.2 shows the effect of increasing and decreasing the gas flow for the inactivation of *Staphylococcus Aureus*:

Gas Flow Rate (ml min^{-1})	**Initial Concentration (CFU ml^{-1})**	**Final Concentration (CFU ml^{-1})**	**Log Reduction**
10.5	3×10^7	3×10^6	1.0
21	3×10^7	2×10^5	1.9
42	3×10^7	3×10^5	2.0
84	3×10^7	2×10^5	2.1
168	3×10^7	6×10^4	2.7

Table 4.2: Cell density measured in wastewater solution after a single pass of the flow reactor under varying gas flow rates.

Reaction conditions: *10 bar pressure, 2 °C temperature, varying gas flow rate, 2% H_2/air, 0.2 ml min^{-1} solvent flow rate, 120 mg 1 wt.% AuPd/TiO_2 catalyst.*

It was reported previously, decreasing the gas flow rate leads to a lower yield of H_2O_2 as the decomposition and hydrogenation reactions become more prominent, resulting in a reduced overall yield of H_2O_2. The results in table 4.2 echo this, as the gas flow is decreased from 42

ml min^{-1} to 10.5 ml min^{-1}, only a 1-log reduction is achieved, an order of magnitude less than the standard operating conditions. The opposite is seen as the gas flow is increased from 42 to 168 ml min^{-1} an extra 0.7-log reduction is observed. These results help to demonstrate that the amount of H_2 passed through the flow system per minute is an important factor in optimising the conditions of the flow reactor to obtain a higher antimicrobial activity from the *in-situ* generated H_2O_2. This can be expected as a greater amount of H_2 passing through the system per minute has been shown to lead to an increase in the concentration of H_2O_2 produced, ultimately leading to a greater log reduction.

4. 2. 3 The Effect of Liquid Flow Rate

Once it had been established that the reduction in bacteria was positively influenced by a higher flow rate and therefore a greater amount of H_2 passed through the catalyst reactor per minute, it was decided to investigate the effect of liquid flow rate in order to see if an increased contact time would be important. Reactions were carried out under the standard conditions set out in the experimental chapter of this work however the liquid flow rate was adjusted. The results displayed below in table 4.3 show that as is to be expected, slowing the flow of the liquid leads to a greater log reduction. When the liquid flow rate is quadrupled to 0.8 ml min^{-1} a 1-log reduction is achieved, an order of magnitude less than is achieved under a standard liquid flow rate of 0.2 ml min^{-1}. Moreover, as the standard liquid flow rate is then halved to 0.1 ml min^{-1} a log reduction of 2.3 is achieved. These results demonstrate that an increase contact time of the bacteria over the catalyst bed leads to a higher conversion provided the amount of H_2 passing through the catalyst bed per minute remains the same.

Liquid Flow Rate (ml min^{-1})	**Initial Concentration (CFU ml^{-1})**	**Final Concentration (CFU ml^{-1})**	**Log Reduction**
0.8	5 x 10^7	4 x 10^6	1.0
0.4	5 x 10^7	5 x 10^5	1.9
0.2	5 x 10^7	5 x 10^5	2.0
0.1	5 x 10^7	2 x 10^5	2.3

Table 4.3: Cell density measured in wastewater solution after a single pass of the flow reactor under varying liquid flow rates.

Reaction conditions: *10 bar pressure, 2 °C temperature, 42 ml min^{-1} gas flow rate, 2% H_2/air, varying solvent flow rate, 120 mg 1 wt.% AuPd/TiO_2 catalyst.*

An experiment was performed using the conditions that led to a greater log reduction from each of the flow rate experiments i.e. a higher flow rate of gas than is used in a standard reaction and half of the standard liquid flow rate. The results are shown below in table 4.4:

Liquid Flow Rate (ml min^{-1})	**Gas Flow Rate (ml min^{-1})**	**Initial Concentration (CFU ml^{-1})**	**Final Concentration (CFU ml^{-1})**	**Log Reduction**
0.1	84	6 x 10^7	3 x 10^4	2.7
0.1	168	6 x 10^7	6 x 10^4	3.0

Table 4.4: Cell density measured in wastewater solution after a single pass of the flow reactor under varying liquid flow rates.

Reaction conditions: *10 bar pressure, 2 °C temperature, 42 ml min^{-1} gas flow rate, 2% H_2/air, varying solvent flow rate, 120 mg 1 wt.% AuPd/TiO_2 catalyst.*

These data show that when the optimal results from both previous experiments are used there is an even greater log reduction observed. A gas flow rate of 84 ml min^{-1} gives a log reduction equal to that of the previously best seen result and when the gas flow rate is further

increased but the liquid flow rate is kept at 0.1 ml min^{-1} then an extra 0.3-log reduction is seen, a total of a 3-log reduction, which is 1-log greater than is achieved when using standard operating conditions. These data confirm the findings of the two previously reported sets of experiments and it can be deduced that a very low liquid flow rate and a high gas flow rate are effective at increasing the log reduction observed in *Staphyloccocus Aureus* (NCTC 10788) after a single pass through the continuous flow reactor under *in-situ* H_2O_2 generating conditions. Furthermore, it can be assumed that the higher concentrations of H_2O_2 that have been reported previously by Freakley *et al*[19] when altering the same reaction parameters, are responsible for the increased log reductions observed in these experiments. The mechanism of action by which *Staphylococcus Aureus* cells are killed by H_2O_2 is a widely disputed topic, although it is believed that the generation of OH• radicals that subsequently damage the DNA of the cells is the most important factor. The decomposition of H_2O_2 over AuPd surfaces is not widely reported in the literature, however many studies have been performed on the decomposition mechanism of H_2O_2 over Pd surfaces. Choudhary and Samanta[20] proposed a mechanism for the decomposition of H_2O_2 over a Pd/SiO_2 surface which includes the formation of OH• radicals via H_2O_2 dissociation followed by a surface reaction that leads to the formation of water. The mechanism was then modified by Voloshin *et al*[21] to include a third step that includes the formation of Oxygen. This mechanism is shown below in scheme 4.1:

$$\text{Step 1: } 2H_2O_2 + 4\bullet \longrightarrow 4OH\bullet$$

$$\text{Step 2: } 4OH\bullet \longrightarrow 2H_2O + 2O\bullet + 2\bullet$$

$$\text{Step 3: } 2O\bullet \longrightarrow O_2 + 2\bullet$$

Scheme 4.1: H_2O_2 decomposition pathway over Pd/SiO_2 catalysts as originally proposed by Choudhary and Samanta[20], later modified by Voloshin *et al*[21].

It can be seen from the above mechanism that the formation of OH• radicals is thought to be facilitated during the decomposition of H_2O_2 over a Pd surface. This would bode well for the antimicrobial effects of the in-situ H_2O_2 system due to the highly oxidising and destructive nature of OH•. The formation of such radicals are of course only assumed in this work as EPR studies would be required to identify the radicals formed during an in-situ H_2O_2 sterilisation reaction. Future studies will look to encoporate such techniques so as to elucidate

the intricacies of any free radical process that is occurring. As was mentioned previously, the decomposition pathway of H_2O_2 will be lower at lower liquid flow rates, therefore it can be expected that a lower amount of OH• radicals will be generated and it could therefore also be assumed that the log reduction would be greater when higher liquid flow rates are used. This is not reflected in the data, however, it is important to remember the extremely short lifetime of a OH• radical species. Repine *et al*[22] have shown that the OH• radicals that lead to the death of *Staphylococcus Aureus* cells may be generated after a reaction between the H_2O_2 and intrinsic Fe^{2+}, the authors demonstrate that not only was killing by H_2O_2 proportional to the intrinsic iron content of the cells but also that the killing of *Staphylococcus Aureus* was inhibited through the addition of OH• radical scavengers. It could be possible that the higher concentrations of H_2O_2 that have been reported to be synthesised under the optimal reaction conditions determined above is leading to a greater log reduction as there is more H_2O_2 present to react with the intrinsic Fe^{2+} of the *Staphylococcus Aureus* cells, ultimately leading to their death. Futhermore, an increased concentration of H_2O_2 would mean a greater liklehood of there being unscavanged H_2O_2 that has not been decomposed to H_2O by the catalase enzyme present in the *Staphylococcus Aureus* cells.

4.2.4 The Effect of Multiple Passes

It has become clear that whilst the *in-situ* generated H_2O_2 has demonstrated some antimicrobial activity against *Staphylococcus Aureus*, a greater log reduction is desirable and may still be possible. It is well documented in the literature that under the standard reaction conditions being used and with a 1 wt.% $AuPd/TiO_2$ catalyst prepared by modified impregnation, H_2O_2 can be generated on stream in a continuous flow system for several hours. This known catalyst stability coupled with previous results shown in this work and the work previously reported in the research group means that we can assume that if the bacteria was passed through the reactor multiple times, roughly the same of amount of H_2O_2 would be generated each time[23]. This could potentially lead to a greater total log reduction than has previously been seen. A reaction was carried out under the standard conditions and once all the liquid phase had been sampled and passed through the reactor it was sterilised and deionised H_2O was passed through the reactor, controls were then plated and the bacterial reaction solution was passed through the reactor for a second time, the process was then repeated for a third time. The results are presented below in table 4.5. The results show that a

2-log reduction is first seen upon passing the bacteria through the reactor, in keeping with the results previously stated in this chapter.

Interestingly, when the post reaction solution is passed through the reactor for a second time there is no change in the concentration of the bacteria in the solutions. This indicates that minimal H_2O_2 is present in the solution after each pass and that the bacteria are not being weakened as they pass through the flow reactor even though H_2O_2 is still being produced under *in-situ* generating conditions. Rather, the H_2O_2 that actually reacts with the *Staphylococcus Aureus* cells kills them and the rest of the H_2O_2 is either transformed via the unselective side reactions or via interaction with catalase to form H_2O. A third pass gives a slight improvement on the original results, however there is still only an additional 0.2-log reduction between the first and the third pass. All control plates showed no growth so it is clear that contamination of the reactor is not an issue.

Solution Composition	**Number of Passes**	**Initial Concentration (CFU ml^{-1})**	**Final Concentration (CFU ml^{-1})**	**Log Reduction**
Staphylococcus Aureus dispersed in sterile H_2O	1	4×10^7	3×10^5	2
Sterile H_2O control	N/A	0	0	0
Staphylococcus Aureus dispersed in sterile H_2O	2	3×10^5	3×10^5	0
Sterile H_2O control	N/A	0	0	0
Staphylococcus Aureus dispersed in sterile H_2O	3	3×10^5	1×10^5	0.2
Sterile H_2O control	N/A	0	0	0

Table 4.5: Cell density measured in different solutions after an increasing number of passes through the flow reactor.

Reaction Conditions: *10 bar pressure, 2 °C temperature, 42 ml min^{-1} gas flow rate, 2% H_2/air, 0.2 ml min^{-1} solvent flow rate, 120 mg 1 wt.% AuPd/TiO_2 catalyst.*

These data confirm that a limit is reached once the initial 2-log reduction has been observed and the same level of reduction is not possible. This observation leads to interesting conclusions, firstly, the remaining bacteria may be more resistant to treatment with *in-situ* generated H_2O_2 and therefore a higher concentration is required to kill these cells, meaning that passing them through the flow reactor under these conditions has no effect. Secondly, the

bulk of the remaining cells may be passing over the catalyst bed but not coming in to contact with the catalyst surface and therefore the H_2O_2 that is generated on the surface, meaning that they are avoiding the area where the H_2O_2 is directly generated and it is therefore far less likely that H_2O_2 or any radical species generated will react with the cells and kill them. It is difficult to know what exactly is causing this 2-log reduction limit that has been observed, however, it is widely known that as the concentration of H_2O_2 is increased its antimicrobial activity increases and furthermore increasing the concentration of H_2O_2 has a much more profound effect on log reduction of bacteria than increasing the contact time. It is therefore reasonable to assume that not enough H_2O_2 is being generated *in-situ* to give any more than the observed 2-log reduction.

4.2.5 The Effect of Starting Concentration

Using a higher starting concentration of bacteria can be used to simulate an organic loading in a wastewater stream, which is known to be one of the major issues with current wastewater treatment technologies. As was reported in the literature review of this work, an organic load can be detrimental for a number of reasons; the antimicrobial agent will often preferentially react with the organic load in the wastewater and this demand must first be overcome before any antimicrobial activity is observed, yielding a characteristic lag time before the disinfection begins properly. This lag time is then usually followed by a rapid inactivation of bacteria and more often than not a tailing effect.

Using a bacterial concentration that is much higher than is expected to be found in a typical GW stream means that the effects of an organic load can be simulated without the need to introduce various compounds which could potentially poison the catalyst or cause leaching issues, the introduction of a number of non-investigated variables is also avoided which would be highly undesirable at this stage of the investigation i.e. proof of concept stage.

Wastewater solutions were prepared using the method outlined in the experimental chapter of this work, in order to increase the starting concentration, the growth time and dilutions were adjusted accordingly. Bacterial concentrations were increased by an order of magnitude from the standard concentration of 10^7 CFU ml^{-1} up to 10^{10} CFU ml^{-1}. A reaction was then carried out under standard conditions; the post reaction solution was plated after a single pass and the bacteria were enumerated. The results are shown below in table 4.6:

Bacteria	**Initial Concentration (CFU ml^{-1})**	**Final Concentration (CFU ml^{-1})**	**Log Reduction**
Staphylococcus Aureus. (NCTC 10788)	7×10^8	5×10^6	2.2
Staphylococcus Aureus. (NCTC 10788)	4×10^9	8×10^6	2.6
Staphylococcus Aureus. (NCTC 10788)	2×10^{10}	1×10^7	3.1

Table 4.6: Cell density measured in post reaction solutions after a single pass through flow reactor with increasing starting cell density.

Reaction conditions: *10 bar pressure, 2 °C temperature, 42 ml min^{-1} gas flow rate, 2% H_2/air, 0.2 ml min^{-1} solvent flow rate, 120 mg 1 wt.% AuPd/TiO_2 catalyst.*

It can be seen that as the starting concentration of the bacteria in the solution is increased so does the observed log reduction after a single pass through the reactor. When the cell density is adjusted to approximately 10^8 CFU ml^{-1} there is a small increase in the log reduction, with the log reduction being 2.2-log as opposed to the 2-log reduction observed when a starting concentration of 10^7 CFU ml^{-1} is used. This trend continues as the starting concentration of bacteria is further increased and a 10^9 CFU ml^{-1} starting concentration yields a 2.6-log reduction, however when a 10^{10} CFU ml^{-1} starting concentration is used, there is a significant increase in the inactivation of the bacteria, with a log reduction of 3.1 being observed. This is slightly unexpected as a solution which contains a much higher cell density would be expected to be less susceptible to the small amounts of H_2O_2 produced in the flow reactor. However, this result may give an indication of the method of cell inactivation that is occurring. As the starting cell density is increased in the solution, the likelihood of bacteria encountering the catalyst surface increases, meaning that the generated radicals are more likely to interact with the DNA of these bacteria and lead to inactivation. In more dilute

solutions, there are less bacteria coming into contact with the catalyst and therefore the free radicals and so a smaller log reduction is seen.

In order to further test this, the same reaction was performed using a series of diluted reaction solutions. To prepare these solutions, the standard growth protocols outlined in the experimental section of this work were followed and then a sample of the culture was diluted appropriately in sterile deionised H_2O to give the desired cell density for the working culture. A reaction was then performed under the standard conditions mentioned throughout this work. The results are displayed below in table 4.7:

Bacteria	**Initial Concentration (CFU ml^{-1})**	**Final Concentration (CFU ml^{-1})**	**Log Reduction**
Staphylococcus Aureus. (NCTC 10788)	1 x 10^6	3 x 10^5	0.8
Staphylococcus Aureus. (NCTC 10788)	1 x 10^5	2 x 10^4	0.9
Staphylococcus Aureus. (NCTC 10788)	2 x 10^4	4 x 10^3	0.8
Staphylococcus Aureus. (NCTC 10788)	7 x 10^3	8 x 10^2	0.9

Table 4.7: Cell density measured in post reaction solutions after a single pass through the flow reactor with a decreasing starting cell density

Reaction conditions: *10 bar pressure, 2 °C temperature, 42 ml min^{-1} gas flow rate, 2% H_2/air, 0.2 ml min^{-1} solvent flow rate, 120 mg 1 wt.% AuPd/TiO_2 catalyst.*

These data show that as the starting concentration is diluted there is a significant decrease in the observed log reduction after a single pass through the reactor. All reactions failed to give a 1-log reduction and so substantially less of a log reduction compared with when a 10^7 CFU ml^{-1} starting concentration is used under the same conditions. Furthermore, this is greater than two orders of magnitude less of the log reduction observed when a 10^{10} CFU ml^{-1} cell density is used. These findings further indicate that the limiting factor in the observed log reductions could either be the amount of H_2O_2 generated or the lack of direct contact between the remaining bacteria in the higher concentrated solutions/the bacteria in the lower concentrated solutions and either the catalyst bed, the *in-situ* generated H_2O_2 or the free radicals which are generated on or close to the catalyst surface (due to their extremely short lifetime and small mean free path).

4.2.6 The Effect of Catalyst Pellet Size

The effect of catalyst pellet size has not been investigated for this flow reactor system. Freakley *et al*[19] reported the effect of total pressure, liquid and gas flow rates and total catalyst mass but the catalyst pellet size has never been changed. The standard pellet size that has been used throughout this work and that previously reported is 425 – 250 μm. Pellet sizes of 600 – 425 and 750 – 600 μm were prepared and packed into fresh catalyst bed tubes. A reaction was then carried out under standard conditions and the post reaction solution was enumerated after a single pass through the flow reactor. The results are shown below in table 4.8:

Catalyst Pellet Size Range (μm)	**Initial Concentration (CFU ml^{-1})**	**Final Concentration (CFU ml^{-1})**	**Log Reduction**
425 – 250	6×10^7	6×10^5	2.0
600 - 425	6×10^7	6×10^5	2.0
750 - 600	6×10^7	7×10^5	1.9

Table 4.8: Cell density measured in post reaction solutions after a single pass through the flow reactor with varying catalyst pellet sizes

Reaction conditions: *10 bar pressure, 2 °C temperature, 42 ml min^{-1} gas flow rate, 2% H_2/air, 0.2 ml min^{-1} solvent flow rate, 120 mg 1 wt.% AuPd/TiO_2 catalyst.*

It can be seen that increasing the pellet size has little to no effect on the observed log reduction after a single pass through the flow reactor. It is unknown what effect the increased pellet size has on the direct synthesis of H_2O_2, unlike the other reaction parameters that were previously investigated in this chapter, which have been extensively studied previously. The flow regime for this reactor set up is known to be that of a Taylor flow set up[19], whereby gas bubbles are followed by liquid slugs, these slugs are broken up by contact with the catalyst bed, this is illustrated below in figure 4.2:

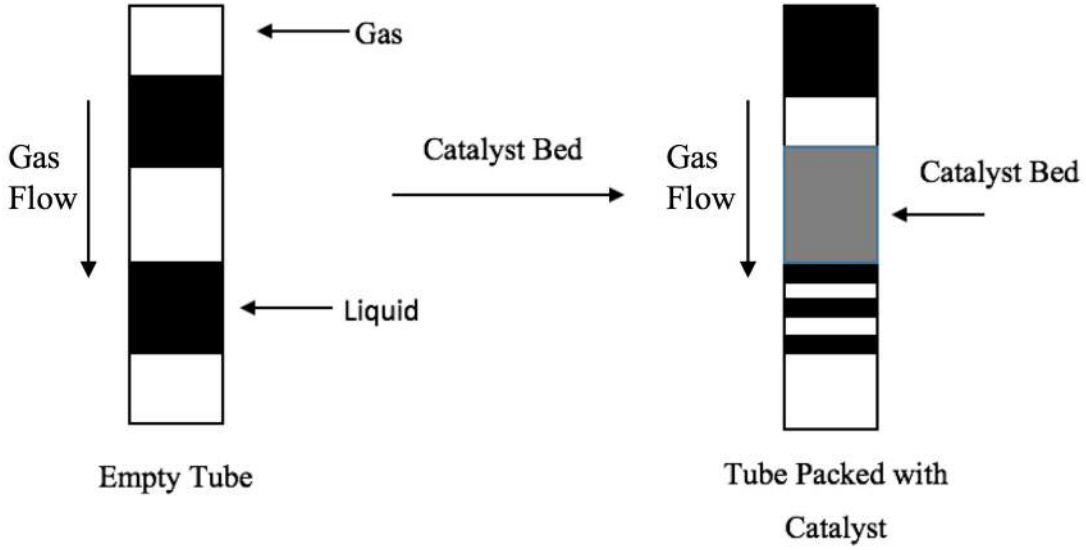

Figure 4.2: Schematic of the Taylor Flow scheme and the difference under operating conditions with and without a catalyst.

It can be assumed that the the larger catalyst particles allow for a greater amount of the liquid slugs to be broken up, however, the smaller surface area of the larger catalyst particles means there are greater voids between the pellets and the bacteria can pass through these voids. The resuts reflect this, as same log reduction is observed for both pellet sizes after a single pass through the flow reactor. In addition to the points mentioned above surrounding empty space in the catalyst bed, the effect that increasing the pellet size has on the concentration of H_2O_2 produced is unknown and therefore it is difficult to rationalise whether or not the log reduction could have been expected to be greater compared to when the standard pellet size is used. It can however be assumed that seeing as the increasing pellet size has no effect on the inactivation of *Staphylococcus Aureus* then there is no significant increase in the amount of H_2O_2 produced.

4.2.7 The Effect of Re-Culturing Post Reaction Solutions

A limit of the disinfection capabilities of *in-situ* generated H_2O_2 has clearly been reached using the current operating conditions. It is however unclear if this is a physical limit of the continuous flow process which would therefore require a re-design of the reactor to optimise it for the inactivation of bacteria or whether the remaining bacteria are just more resistant to the *in-situ* generated H_2O_2.

In order to test this a wastewater solution was prepared using the standard method outlined in the experimental chapter of this work, the solution was then passed through the flow reactor under standard reaction conditions and a small amount of the post-reaction solution was re-dispersed in tryptic soya broth and incubated overnight. A second wastewater solution was then prepared from this culture and again passed through the flow reactor under standard reaction conditions. Bacteria were enumerated before and after each of the aforementioned passes through the flow reactor. The results are presented below in table 4.9:

Solution Name	**Initial Concentration (CFU ml^{-1})**	**Final Concentration (CFU ml^{-1})**	**Log Reduction**
Initial *Staphylococcus Aureus*	5×10^7	6×10^5	1.9
Sterile Deionised H_2O Control	0	0	0
Re-cultured *Staphylococcus Aureus*	6×10^7	6×10^5	2

Table 4.9: Cell density measured in post reaction solutions after a single pass through the flow reactor using varying solutions

Reaction conditions: *10 bar pressure, 2 °C temperature, 42 ml min^{-1} gas flow rate, 2% H_2/air, 0.2 ml min^{-1} solvent flow rate, 120 mg 1 wt.% AuPd/TiO_2 catalyst.*

These data clearly show that the remaining bacteria do not have a greater resistance to the treatment with *in-situ* generated H_2O_2. Post reaction solutions showed essentially the same log reduction after a single pass through the flow reactor.

From the results presented throughout this chapter, it is clear that a limit has been reached using the current continuous flow reactor and catalyst set up where a 3-log reduction is the maximum that has been observed. The data has indicated that this limit has been reached due to the relatively low amount of H_2O_2 that is produced under even the most optimal conditions. Therefore, in order to futher increase the antimicrobial activity of the *in-situ* H_2O_2 flow system, the focus would need to shift to maximising the concentration of H_2O_2 that is produced and also to increase the contact time between the catalyst and the bacteria.

4.2.8 The Effect of Direct Contact with Catalyst Bed

The main advantage of using H_2O_2 in GW disinfection is the ability to generate highly oxidising radicals, such as OH• radicals, which are thought to be the most potent oxidising species for GW treatment, unfortunately these radicals are very shortlived and it is actually very unlikely that they will leave the catalyst surface. To investigate the effect of direct contact between the bacteria and the catalyst surface, a series of reactions was performed where varying concentrations of commercially available H_2O_2 was drip fed into the bacterial solution. It can be clearly seen from the data presented in table 4.10 when H_2O_2 is drip fed into the wastewater solution as opposed to directly passing the bacteria over the catalyst bed there is a significant decrease in the antibacterial activity.

Solvent	**Initial Concentration (CFU ml^{-1})**	**Final Concentration (CFU ml^{-1})**	**Log Reduction**
Sterile H_2O	1 x 10^7	2 x 10^6	0.9
500 ppm H_2O_2 in sterile H_2O	1 x 10^7	6 x 10^6	0.4
200 ppm H_2O_2 in sterile H_2O	1 x 10^7	7 x 10^6	0.3
100 ppm H_2O_2 in sterile H_2O	1 x 10^7	7 x 10^6	0.3

Table 4.10: Cell density measured in post reaction solutions after solvent solutions of varying compositions drip-fed into wastewater solution.

Reaction conditions: *10 bar pressure, 2 °C temperature, 42 ml min^{-1} gas flow rate, 2% H_2/air, 0.2 ml min^{-1} solvent flow rate, 120 mg 1 wt.% AuPd/TiO_2 catalyst for H_2O_2 solvents, blank tube for deionised H_2O solvent.*

When the reactor is operated under H_2O_2 generating conditions and the bacteria are positioned after the catalyst bed there is only a 0.9-log reduction, when the experiment is performed under identical conditions but the bacteria are passed over the catalyst bed then a

2-log reduction is seen. This clearly shows that the H_2O_2 must be generated *in-situ* on the catalyst bed and in the presence of the bacteria in order to attain a significant inactivation of *Staphylococcus Aureus*. Moreover, these data present significant evidence that the method of inactivation when using *in-situ* generated H_2O_2 in a continuous flow reactor is due to the formation of short lived radical species on the catalyst surface and their subsequent interaction with the DNA of *Staphylococcus Aureus*, this is in good agreement with the literature as was mentioned previously[22].

Interestingly, even when a H_2O_2 solution of 500 ppm, is drip-fed into the sample bomb that is positioned after the catalyst bed and containing the wastewater solution, there is only a 0.4-log reduction. This result is significant as it gives further evidence that the bacteria need to be passed over the catalyst bed in order for a significant log reduction to be achieved. This is in good agreement with the data presented earlier in the chapter as it further suggests that in order for the bacteria to be killed, it is likely to be imperative for them to be in direct contact with the catalyst surface. It is reasonable to assume that this is due to the fact that the catalyst surface is where the H_2O_2 and highly reactive radical species are formed.

4.2.8 Effect of Catalyst Additives

4.2.8.1 Addition of Iron Oxide

Following on from the important observation that a contact with between the catalyst surface and the bacteria under *in-situ* generating conditions is required to achieve a 2-log reduction or greater, it was decided to investigate the effect of catalyst additives. The generation of radical species either on the catalyst surface or inside the cells themselves is thought to be the most important factor in achieving a significant log reduction of *Staphylococcus Aureus*. The 1 wt.% AuPd/TiO_2 catalyst that has been used throughout this work is well known to selectively form H_2O_2 via the direct synthesis reaction, however, the increased selectivity towards H_2O_2 exhibited by this catalyst when compared with other supported metal catalysts may not be the most beneficial trait for the application to GW disinfection.

An area of chemistry which has been heavily documented in the literature[24] for wastewater treatment is that of Fenton's chemistry. Fenton's chemistry, named after H.J.H. Fenton,

involves the catalytic reaction of H_2O_2 with a metal catalyst, typically iron (Fe), to form OH• and OOH• racidal species, these reactions are summarised below in equation 1 and 2:

$$Fe^{2+} + H_2O_2 \longrightarrow Fe^{2+} + OH\bullet + OH^- \quad \text{Equation 1}$$

$$Fe^{3+} + H_2O_2 \longrightarrow Fe^{3+} + OOH\bullet + H^+ \quad \text{Equation 2}$$

Equation 1: Stoichiometric equation for the Fenton's reaction between an Fe^{2+} ion and H_2O_2.

Equation 2: Stoichiometric equation for the Fenton's reaction between an Fe^{3+} ion and H_2O_2.

It can be seen from the reaction equations shown above that the reaction of Fe^{2+} metal ions with H_2O_2 can effectively form OH• radical species, which as has been noted earlier is perhaps the most potent antimicrobial agent for bacteria such as *Staphylococcus Aureus*.

To investigate if this effect could be employed into the *in-situ* generation of H_2O_2 through the flow reactor, two batches of Fe modified catalyst were prepared by physically mixing 0.2 g of both iron(II) oxide (FeO) and iron(III) oxide (Fe_2O_3) with 1.8 g of 1 wt.% AuPd/TiO_2 using a pestle and mortar for a period of 10 minutes. The mixed powders were pressed following the same experimental procedure as is used for a standard pelleting of the 1 wt.% AuPd/TiO_2 catalyst. A series of reactions were then performed under standard conditions using the pellets produced by mixing Fe_2O_3 and FeO respectively with the 1 wt.% AuPd/TiO_2 as the catalyst, the post reaction solution was plated after a single pass through the reactor and the remaining bacteria were enumerated after a growth period of 12 hours. The results of the experiment are shown below in table 4.11. These data show that the addition of both iron oxides does indeed have a positive effect on the antimicrobial activity of the *in-situ* generated H_2O_2. Both the FeO and Fe_2O_3 catalyst additives show an increase in the log reduction compared to just the use of a 1 wt.% AuPd/TiO_2 under the same operating conditions. Interestingly, FeO seems to have a greater effect than Fe_2O_3 possibly due to the known generation of OH• radicals when FeO is reacted with H_2O_2.

Catalyst Bed Contents	**Initial Concentration (CFU ml^{-1})**	**Final Concentration (CFU ml^{-1})**	**Log Reduction**
1 wt.% $AuPd/TiO_2$ mixed with Fe_2O_3	4×10^7	2×10^4	3.2
1 wt.% $AuPd/TiO_2$ mixed with FeO	4×10^7	9×10^3	3.4

Table 4.11: Cell density measured in post reaction solutions after a single pass of wastewater solution through the flow reactor using a standard catalyst mixed with FeO and Fe_2O_3 additives.

Reaction conditions: *10 bar pressure, 2 °C temperature, 42 ml* min^{-1} *gas flow rate, 2%* H_2*/air, 0.2 ml* min^{-1} *solvent flow rate, 120 mg varying catalyst.*

However, whilst these results display a positive relationship between the Fe^{2+} and Fe^{3+} additives and antibacterial activity they must be treated cautiously. It is well known that Fe species will leach from the solid phase during such reactions[23] and although this has not been tested for this reaction, some observations point to this to being a possibility. Once the reaction was finished and the post reaction solution was sampled from the sample bomb, it was noted that the solutions had changed colour, in the case of Fe_2O_3, the solutions had a reddish-brown tint and FeO solutions displayed an orange-yellow tint. The introduction of trace amounts of metal ions into GW would be undesirable as it may no longer be fit for the intended re-use purposes. For example, the presence of Fe in water being used for laundry purposes can be an issue as it has been reported that concentrations greater than 0.3 mg l^{-1} of Fe can cause laundry and sanitary ware to stain as the dissolved aqueous metal ions will undergo oxidation to form a reddish-brown precipitate leading to rust coloured stains. It is for reasons such as this that catalyst stability becomes important for the treatment of GW using *in-situ* generated H_2O_2.

4.2.8.2 Use of a Supported PdFe Catalyst

Whilst the use of FeO and Fe_2O_3 in tandem with the supported catalyst has indeed yielded a greater log reduction the issue of stability must be addressed. Arends *et al*[25] reported that many reactions which have been thought to be heterogeneous in their mechanism are in fact unstable under the oxidising conditions in which they are used and therefore much of the activity can be attributed to a homogenous leachate. This is highly undesirable for any commercial application as a build-up of leaching over time will lead to catalyst deactivation.

The heterogeneous catalyst used throughout this work, 1 wt.% AuPd/TiO_2, is documented in the literature as a stable catalyst when used for the direct synthesis of H_2O_2 and it has been shown previously and in this work to perform on stream for several hours without losing any activity. The use of a PdFe bimetallic catalyst presents an interesting way to incorporate Fe into the reaction whilst reducing the risk of leaching as the two metals may be much more intimately mixed when compared to the physical mixture used earlier. It is well known that Pd is the active component in many supported metal catalysts for the direct synthesis of H_2O_2, if *in-situ* H_2O_2 formation can be effectively catalysed by the Pd present then the presence of Fe^{2+} or Fe^{3+} ions should lead to a rapid decomposition of the *in-situ* generated H_2O_2 yielding the desired oxygenated radical species.

A PdFe bimetallic catalyst was synthesised via the modified impregnation technique detailed in the experimental chapter of this work, using $PdCl_2$ and $FeCl_2$ as the metal precursors. Unlike the AuPd catalyst, the PdFe catalyst was reduced at 500 °C for 5 hours to try and prevent leaching of Fe species into the reaction effluent. A reaction was run under standard conditions using a 1 wt.% PdFe/TiO_2 catalyst and the post reaction solution was plated after a single pass through the flow reactor and the remaining bacteria were enumerated after a growth period of 12 hours. The results are shown below in table 4.12:

Catalyst	Initial Concentration (CFU ml^{-1})	Final Concentration (CFU ml^{-1})	Log Reduction
1 wt.% $PdFe/TiO_2$	2 x 10^7	1 x 10^4	3.1

Table 4.12: Cell density measured in post reaction solutions after a single pass of wastewater solution through the flow reactor using a supported 1 wt.% $PdFe/TiO_2$ catalyst.

Reaction conditions: *10 bar pressure, 2 °C temperature, 42 ml min^{-1} gas flow rate, 2% H_2/air, 0.2 ml min^{-1} solvent flow rate, 120 mg 1 wt.% $PdFe/TiO_2$ catalyst*

Like the use of Fe_2O_3 and FeO, the PdFe bimetallic catalyst gives a greater log reduction than the AuPd catalyst. In addition, the PdFe bimetallic catalyst is essentially on par with the added mixed Fe_2O_3/FeO-AuPd pellets, this result suggests that the Fe present in the bimetallic catalyst may be effective catalysing the decomposition of H_2O_2 once it has been formed *in-situ*, yielding radical species such as OH• radicals, something which the AuPd catalyst is not able to do as effectively and therefore the observed antibacterial activity of the PdFe catalyst is greater. It is however important again to stress that leaching may well be an issue with this catalyst, although the post reaction solutions did not exhibit the same change in colour as was seen with the mixed Fe_2O_3/FeO experiments, only very small amounts of Fe can have a significant effect on the reaction results and as mentioned earlier trace amounts of Fe in recycled H_2O can present problems for re-use applications.

4.2.10 Testing of Other Bacteria

4.2.10.1 Testing with *Escherichia Coli* (ATCC 10536)

Escherichia Coli is commonly employed as a target bacteria for the testing and benchmarking of antimicrobial agents for many household and commercial applications. *Escherichia Coli* is a gram negative bacterium which is rod-shaped in appearance, whilst most strains of *Escherichia Coli* are harmless, it can lead to severe gastrointestinal distress in humans and the as such the permitted amount of total *Escherichia Coli* coliforms in recycled GW is regulated. Effective removal of *Escherichia Coli* from any GW streams is therefore highly desirable for a GTS.

It was shown previously in this work that both *in-situ* generated and commercially available H_2O_2 can remove high concentrations of *Escherichia Coli* (JM109) from wastewater streams, however the strains present in GW are likely to be much more resistant than the strain which has been genetically weakened. Standard protocols include the testing of *Escherichia Coli* strains such as (ATCC 10536) which is designed for the comparison and benchmarking of antimicrobial agents.

To compare the effectiveness of the *in-situ* generated H_2O_2 with commercially available products and findings that are already present in the literature, recognised *Escherichia Coli* strains must be investigated. Therefore, an *Escherichia Coli* (ATCC 10536) liquid culture was prepared by growing the bacteria in a tryptic soya broth for 16-24 hours at 37 °C ± 1 °C. The test inocula were then prepared by centrifuging the bacteria at 5500 g for a period of 10 minutes, following this the bacteria were suspended in sterile deionised H_2O and diluted appropriately until the UV/Vis absorbance at 600 nm was in the range of 0.1 - 0.07, giving a starting concentration of approximately 10^7 CFU ml^{-1}. The results are shown below in table 4.13. The results of the *in-situ* H_2O_2 for the resistant *Escherichia Coli* strain are similar to those achieved under the same reaction conditions when *Staphylococcus Aureus* is used. That is, approximately a 2-log reduction is observed after a single pass through the flow reactor. This is however significantly lower than is seen for the *Escherichia Coli* (JM109) which was investigated in the previous chapter of this work, this is reasoned due to the nature of the bacterial strains, with the JM109 strain already being weakened meaning it is far more susceptible to the antimicrobial effect of the *in-situ* H_2O_2. These data show that whilst the effect is far less pronounced when investigating real world strains of bacteria, the *in-situ* H_2O_2 displays an intrinsic antimicrobial nature which is able to inactivate a range of bacterial strains that can be commonly found in GW and are deemed to be hazardous to human health.

Bacteria	**Initial Concentration (CFU ml^{-1})**	**Final Concentration (CFU ml^{-1})**	**Log Reduction**
Escherichia Coli (ATCC 10536)	9 x 10^7	7 x 10^5	2.2
Escherichia Coli (JM109)	1 x 10^7	0	7

Table 4.13: Cell density measured in post reaction solutions of different bacterial strains of *Escherichia Coli* after a single pass of wastewater solution through the flow reactor using a supported 1 wt.% AuPd/TiO_2 catalyst.

Reaction conditions: *10 bar pressure, 2 °C temperature, 42 ml min^{-1} gas flow rate, 2% H_2/air, 0.2 ml min^{-1} solvent flow rate, 120 mg 1 wt.% AuPd/TiO_2 catalyst*

Following on from this experiment it was decided to investigate the effectiveness of the PdFe catalyst which has shown to be more effective against *Staphylococcus Aureus* than the standard AuPd catalyst. An experiment was performed using the same procedure outlined above however the catalyst bed was filled with the 1 wt.% PdFe/TiO_2 catalyst pellets instead. The results are presented below in table 4.14:

Catalyst	**Initial Concentration (CFU ml^{-1})**	**Final Concentration (CFU ml^{-1})**	**Log Reduction**
1% $AuPd/TiO_2$, reduced at 400 °C (5% H_2/Ar atmosphere)	9×10^7	7×10^5	2.2
1% $PdFe/TiO_2$, reduced at 500 °C (5% H_2/Ar atmosphere)	7×10^7	8×10^4	2.9

Table 4.14: Cell density measured in post reaction solutions after a single pass of wastewater solutions, containing *Escherichia Coli* (ATCC 10536), through the flow reactor using a variety of supported metal catalysts.

Reaction conditions: *10 bar pressure, 2 °C temperature, 42 ml min^{-1} gas flow rate, 2% H_2/air, 0.2 ml min^{-1} solvent flow rate, 120 mg varying catalyst.*

Again, the results show trends like those observed with *Staphylococcus Aureus*, the PdFe catalyst is more effective for the inactivation of *Escherichia Coli* than the AuPd catalyst, the reason for this can be thought to be the same as that for *Staphylococcus Aureus*. That is, decomposition of H_2O_2 on the catalyst surface is being rapidly catalysed by the Fe species present, leading to the formation of radical species that are known to be highly active in the inactivation of a variety of bacteria. However, it must again be noted that it is not known whether the Fe which may be catalysing this radical formation is that of Fe nanoparticles on the catalyst surface or whether the reaction is being catalysed homogeneously by an Fe leachate that could be leaching from the catalyst during the reaction.

Another interesting observation from these experiments is that there is essentially no difference between the effectiveness of the *in-situ* generated H_2O_2 on gram negative and gram positive bacteria. The much thicker cell wall present in gram negative bacteria could present problems for the active component of the H_2O_2 which is leading to the bacterial inactivation and cell death. If, however this active component is indeed a radical species such

as OH• radicals then it would not be expected to observe a difference between the inactivation of gram positive and gram negative bacteria as the cell structural differences would be assumed to be negated by the extremely high oxidising ability of the radical. These results are also in keeping with those presented in the literature, as was discussed in the introduction chapter of this work, it is known that H_2O_2 displays a similar antimicrobial efficiency against both gram positive and gram negative bacteria, major differences are only noted when comparing the antimicrobial effect of H_2O_2 against bacteria versus that of spores and protozoans.

4.2.10.2 Testing with *Pseudomonas Aeruginosa* (NCTC 10662)

Pseudomonas Aeruginosa is a gram negative aerobic bacterium that is commonly found in wastewater streams and is an opportunistic human pathogen in hospital environments, where it is known to flourish. Although there is minimal evidence that *Pseudomonas Aeruginosa* leads to any significant problems with human health it can affect the turbidity and odour of water, making it an issue for recycled wastewater. Perhaps one of the most problematic characteristics of *Pseudomonas Aeruginosa* is its ability for form biofilms. Bjarnholdt[26] defines a biofilm as "A coherent cluster of bacterial cells embedded in a matrix, which is more tolerant of most antimicrobials and host defences compared with planktonic bacterial cells". The unique ability of biofilms to be able to attach to a surface and form a protective layer, usually consisting of proteins or polysaccharides which have been excreted by the bacteria, means that they can potentially demonstrate an extreme tolerance to even the most potent antimicrobial agents. It is therefore clear that inactivating bacteria such as *Pseudomonas Aeruginosa* which could be present in GW would be highly desirable.

A *Pseudomonas Aeruginosa* (NCTC 10662) liquid culture was prepared by growing the bacteria in a tryptic soya broth for 16-24 hours at 37 °C ± 1 °C. The test inocula were then prepared by centrifuging the bacteria at 5500 g for a period of 10 minutes, following this the bacteria were suspended in sterile deionised H_2O and diluted appropriately until the UV/Vis absorbance at 600 nm was in the range of 0.1 - 0.07, giving a starting concentration of approximately 10^7 CFU ml^{-1}. A disinfection test was then performed using the standard procedure set out in the experimental chapter of this work. The results of these experiments are displayed below in table 4.15:

Bacteria	**Initial Concentration (CFU ml^{-1})**	**Final Concentration (CFU ml^{-1})**	**Log Reduction**
Pseudomonas Aeruginosa (NCTC 10662)	1×10^7	6×10^6	0.5

Table 4.15: Cell density measured in post reaction solutions after a single pass of wastewater solutions, containing *Pseudomonas Aeruginosa* (NCTC 10662), through the flow reactor.

Reaction conditions: *10 bar pressure, 2 °C temperature, 42 ml min^{-1} gas flow rate, 2% H_2/air, 0.2 ml min^{-1} solvent flow rate, 120 mg 1 wt.% AuPd/TiO_2 catalyst.*

Only a small reduction is observed when using *Pseudomonas Aeruginosa*, a 0.5-log reduction is seen after a single pass through the flow reactor, which is significantly less than the 2-log reduction achieved under the same reaction conditions when using *Staphylococcus Aureus* and *Escherichia Coli*. This result demonstrates a greater resistance of *Pseudomonas Aeruginosa* to *in-situ* H_2O_2 than the other bacteria that have been investigated.

4.3 Conclusions

Following on from the findings of chapter 3, the effectiveness of H_2O_2 as a disinfectant of harmful bacteria including *Staphylococcus Aureus*, *Escherichia Coli* and *Pseudomonas Aeruginosa*. BSI strains of the bacteria were used so the results can be compared to well-known disinfectants.

Staphylococcus Aureus was used for much of the testing and to determine the optimum operating parameters. The previous testing performed in chapter 3 of this work did not require such testing as the standard operating conditions for H_2O_2 synthesis in the continuous microreactor were also found to be the optimum conditions for the disinfection of the *Escherichia Coli* (JM109). This was not the case for *Staphylococcus Aureus* (NCTC 10788), where it was found that slowing the liquid rate down to 0.1 ml min^{-1} and increasing the gas flow to 168 ml min^{-1} gave the greatest log reduction.

Catalyst additives were added to try and increase the disinfectant activity of the *in-situ* generated H_2O_2. Adding FeO and Fe_2O_3 to the catalyst bed led to an increase in the performance of the *in-situ* generated H_2O_2 and the same effect was observed when a PdFe bimetallic catalyst was used in the place of AuPd. This has led to the belief that the disinfection is occurring via a radical process and suggests that the ability of Fe species to breakdown H_2O_2 into radicals could be influencing the observed increase in activity. Moreover, it was determined that the bacteria must meet the catalyst bed under H_2O_2 generating conditions for a significant log reduction to be seen, further suggesting that radical species are playing a pivotal role in the inactivation of the bacteria under these reaction conditions.

Similar levels of log reduction to those of *Staphylococcus Aureus* (NCTC 10788) are also seen for *Escherichia Coli* (ACTC 10536), however, the system was ineffective against *Pseudomonas Aeruginosa* (NCTC 10662).

In conclusion, it has been shown that *in-situ* generated H_2O_2 can be used to effectively disinfect concentrated solutions of real-life strains of bacterial solutions. Whilst, the log reductions are not as significant as the observations of chapter 3 of this work, where a weakened strain of *Escherichia Coli* was used, the work presented in this chapter represents a significant step forward in the use of *in-situ* generated H_2O_2 for disinfection and GW treatment purposes. Ultimately, much work is needed to improve the activity and efficacy of the *in-situ* system, however the work presented here and in chapter 3 shows that not only is it possible but also a highly attractive alternative to current disinfection methods.

4.4 References

1. A. Ogston, *Arch. Klin. Chir*., **1880**, *25*, 588 – 600.
2. A. Ogston, *Br. Med. J.*, **1881**, *1*, 695 – 698.
3. A. Ogston, *J. Anat. Physiol.*, **1882**, *16*, 526 – 527.
4. A. J. Rosenbach, *Mikro-Organismen bei den Wund-Infections-Krankheiten des Menschen.*, **1884**, Wiesbaden, *J. F. Bergmann*, 18.
5. H. C. Gram, *Fortschr. Med.*, **1884**, *2*, 185 – 189.
6. W. L. Chou, D. G. Yu, M. C. Yang, *Polymer. Adv. Tech.*, **2005**, *16*, 600 – 607.
7. Q. Li, S. Mahendra, D. Y. Lyon, L. Brunet, M. V. Liga, D. Li, P. J. J. Alvarez, *Water Res.*, **2008**, *42*, 4591 – 4602.
8. C. Hu, J. Guo, J. Qu, X. Hu, *Langmuir*, **2007**, *23*, 4982 – 4987.
9. W-K. Liu, M. R. W. Brown, T. S. J. Elliot, *J. Antimicrob. Chemother.*, **1997**, *39*, 687 – 695.
10. G. L. Mandell, *J. Clin. Invest.*, **1975**, *55*, 561 – 566.
11. D. Pittet, S. Hugonnet, S. Harbarth, P. Mourouga, V. Sauvan, S. Touveneau, T. V. Perneger, *Lancet*, **2000**, *356*, 1307 – 1312.
12. L. E. Bush, L. M. Benson, J. H. White, *J. Clin. Microbiol.*, **1986**, *24*, 343-348.
13. G. L. Mcdonnell, A. D. Russell, *Clin Microbiol. Rev.*, **1999**, 147 – 179.
14. C. E. Coulthard, G. Skyes, *Pharm. J.*, **1936**, *137*, 79 – 81.
15. P. B. Price, *Arch. Surg.*, **1950**, *60*, 492 – 502.
16. M. J. Flores, R. J. Brandi, A. E. Cassano, M. D. Labas, *Water Sci. Technol.*, **2016**, *73*, 275 – 282.
17. K. A. Datsenko, B. L. Wanner, *Proc. Natl. Acad. Sci. USA*, **2000**, *97*, 6640 – 6645.
18. M. G. C. Baldry, *J. Appl. Bacteriol*., **1983**, *54*, 417 – 423.
19. S. J. Freakley, M. Piccinini, J. K. Edwards, E. N. Ntainjua, J. Moulijn, G. J. Hutchings, *ACS Catalysis*, **2013**, *3*, 487 – 501.
20. V. R. Choudhary, C. Samanta, *J. Catal.*, **2006**, *238*, 28 – 38.
21. Y. Voloshin, J. Manganaro, A. Lawal, *Ind. Eng. Chem. Res.*, **2008**, *47*, 8119 – 8125.
22. J. E. Repine, R. B. Fox, E. M. Berger, *J. Biol. Chem.*, **1981**, *256*, 7094 – 7096.
23. M. Sankar, Q. He, M. Moataz, J. C. Pritchard, S. J. Freakley, J. K. Edwards, S. H. Taylor, D. J. Morgan, A. F. Carley, D. W. Knight, C. J. Kiely, G. J. Hutchings, *ACS Nano*, **2012**, *6*, 6600 – 6613.
24. E. Neyens, J. Baeyens, *J. Hazard. Mater.*, **2003**, *98*, 33-50.

25. I. W. C. E Arrends, R. A. Sheldon, *Appl. Catal. A.*, **2001**, *212*, 175- 187.

26. T. Bjarnholdt, *APMIS*, **2013**, *121*, 1 – 54.

Chapter 5

Synthesis of Novel Pd-SnO_2 Materials and Their Use as Catalysts for the Direct Synthesis of H_2O_2

5.1 Introduction

Strong metal support interactions (SMSI) have long been shown in the literature to be present in catalysts containing a bulk metal oxide support and reduced precious metal nanoparticles. Tauster *et al*[1] reported the first observations of SMSI's between group 8 metals supported on titanium dioxide (TiO_2) that were reduced at varying temperatures between 200 °C and 500 °C. When reduced at 200 °C the authors noted that the chemisorption properties of the catalysts were indicative of a high metal dispersion. Upon increasing the reduction temperature to 500 °C, the uptake of hydrogen (H_2) and carbon monoxide (CO) decreased to essentially zero. This observed decrease in the uptake of H_2 and CO could not be attributed to metal nanoparticle agglomeration and so the authors concluded that the TiO_2 was covering the nanoparticles giving rise to a SMSI occurring between the metal nanoparticles and the TiO_2 support. SMSI's were deemed to be destroying the interactions of the nanoparticles with H_2 and CO molecules, although due to the only evidence coming from macroscopic adsorption studies it was unknown how the SMSI was occurring. Later studies[2] confirmed that a direct interaction between the metal atoms and reduced Ti ions leading to either an encapsulation of the metal nanoparticles or a change in their morphology can result in a change in the catalytic activity of said nanoparticles.

Many techniques for the preparation of heterogeneous catalysts have been reported in the literature with the main procedures including impregnation[3,4], co-precipitation[5,6], deposition-precipitation[7,8] and ion-exchange[9,10]. However, there has been little in the literature on the use of novel catalysts for the direct synthesis of H_2O_2 in recent times. The sol-gel technique for the preparation of heterogeneous catalysts is known to give control over a variety of properties of the resultant catalyst materials, such as homogeneity, surface area and composition[11]. Nicolaon *et al*[12] reported the breakthrough synthesis procedure of a silica

aerogel via the controlled hydrolysis of alkoxides in an alcohol solvent, following this, the sol-gel method has been used in large scale applications. The preparation of precious metal catalysts via sol-gel supported on metal oxides such as Pt-SiO_2[13], Pd-Al_2O_3[13] and Pt-Sn-Al_2O_3[14] has been reported in the literature. Gomez *et* al[15] reported the use of Pt-Sn/Al_2O_3 catalysts prepared via sol-gel for the dehydrocyclsation of n-heptane. Catalysts that were prepared via sol-gel had a higher metal dispersion (90%) compared to those prepared via impregnation (50%), the sol-gel catalysts also had a smaller particle size than the impregnation catalysts. Furthermore, sol-gel catalysts exhibited a higher selectivity towards gasolines and a lower selectivity towards benzene and were more resistant to catalyst deactivation as a consequence of coke formation.

A study by Boskovic *et al*[16] investigated Pd/SnO_2 catalysts prepared via sol-gel for the denitration of H_2O, the Pd was incorporated by two methods, firstly via impregnation of the SnO_2 with palladium chloride ($PdCl_2$) solution and secondly via the simultaneous addition of both Pd and support precursors for a sol-gel catlayst. It was found that the modified sol-gel technique whereby the Pd undergoes simultaneous hydrolysis with the support leads to the distribution of well formed Pd particles on a SnO_2 support that are intimately mixed, thus providing a platform for SMSI's to occur. The catalyst testing results further demonstrate the superiority of the modified sol-gel sample, the higher BET surface area and Pd distribution present in this sample compared to the Pd impregnation sample leads to a greater catalyst activity and more favourable, lower selectivity towards undesirable NH_3. Interestingly, the authors postulate that the "partial distribution of Pd species into the SnO_2 lattice results in a higher number of surface defects" which may lead to the presence of active sites on the support.

The unique and intimate interactions between Pd and Sn pose discussed above pose an interesting area of research in the development of selective Pd catalysts with the generation of intermetallic species and strongly bound alloys known to influence the activity of these heterogeneous catalysts. Furthermore, the SMSI that has been displayed between Pd nanoparticles and SnO_2 and its influence on the selectivity of the catalyst species towards H_2O_2 in the direct synthesis reaction makes the topic worthy of further research. Therefore, this chapter of work is split into two sections, firstly, the catalytic activity of supported Pd/SnO_2 catalysts is investigated for the direct synthesis of H_2O_2 and the effect of an oxidation-reduction-oxidation (ORO) heat treatment that was previously used by the group to

selectively switch off the sequential hydrogenation and decomposition in PdSn bimetallic catalysts is reported. The interactions generated by the heat treatment cycle are then analysed by STEM and EELS analysis were then carried out by Dr Qian He at the Oak Ridge National Laboratory. The goal of this was to build on the previous work of the research group, which revealed that layers of SnO_2 can be formed as a result of a SMSI following the ORO heat treatment. By using a sol-gel technique where the Pd and SnO_2 precursors undergo simultaneous hydrolysis, we aim to embed the Pd nanoparticles into the SnO_2 layers/lattice and investigate the effect this has on the interactions between Sn and Pd species and how this is reflected in the catalytic activity when the materials are employed for the direct synthesis of H_2O_2. Characterisation is performed by the use of XRD, TPR, TGA, BET, STEM and EELS to provide electronic and structural information on the catalyst materials and insight towards the objectives mentioned above.

5.2 Results

5.2.1 Pd/SnO_2 Catalysts Synthesised by Impregnation

5.2.1.1 Catalyst Testing

Supported Pd catalysts were prepared by impregnating a SnO_2 (Sigma Aldrich, >99.99% trace metal basis) support with $PdCl_2$ (Sigma Aldrich, >99.9%) following the catalyst preparation procedures outlined in detail in chapter 2 of this work. H_2O_2 direct synthesis reactions were performed using the experimental procedure outlined in chapter 2 of this work and any variations from this standard procedure will be explicitly stated. The same is true for H_2O_2 hydrogenation reactions. A brief outline of the experimental conditions is given below:

- Direct synthesis of H_2O_2 in a Parr stainless steel 100 ml high pressure autoclave: H_2O (2.9 g)/MeOH (5.6 g) solvent, 5% H_2/CO_2 (420 psi), 25% O_2/CO_2 (160 psi), 10 mg catalyst, 2 °C, 1200 rpm stirrer speed, 30 minutes.
- Hydrogenation of H_2O_2 in a Parr stainless steel 100 ml high pressure autoclave: H_2O_2 (0.68 g) H_2O (2.22 g)/MeOH (5.6 g) solvent, 5%H_2/CO_2 (420 psi), 10 mg catalyst, 2 °C, 1200 rpm stirrer speed, 30 minutes.

5.2.1.2 H_2O_2 Synthesis Testing of Pd/SnO_2 Catalysts

Supported Pd catalysts were prepared by impregnating a commercially available TiO_2 support with the requisite amount of a $PdCl_2$ solution and calcining the samples at 500 °C in static air for 3 hours. Catalysts were prepared to determine if the Pd supported on SnO_2 samples were active for H_2O_2 synthesis and if so, allow comparison to other well documented catalyst supports such as TiO_2, silica (SiO_2) and activated carbon (C). Table 5.1 shows that the 2.5 wt.% Pd/SnO_2 catalyst was indeed active for H_2O_2 synthesis under the reaction conditions stated earlier, these reaction conditions shall be denoted as standard conditions throughout the rest of this chapter and any variations from said conditions will be explicitly stated. A productivity value of 4 mol_{H2O2} kg_{cat}^{-1} h^{-1} was observed after a 30 minute reaction under standard conditions. This result was verified by repeating the reaction a further two times and carrying out the same procedure with another two batches of catalyst. When comparing the productivity of the 2.5 wt. %Pd/SnO_2 catalyst with other supports, whilst the productivity is not as good, it is indeed in the same region as the SiO_2 supported catalyst, showing that the supported Pd is not being completely inhibited by the SnO_2 support.

Catalyst	**Productivity (mol_{H2O2} kg_{cat}^{-1} h^{-1})**
2.5 wt.% Pd/SnO_2 (1)	4
2.5 wt.% Pd/SnO_2 (2)	4
2.5 wt.% Pd/SnO_2 (3)	5
2.5 wt.% Pd/TiO_2	20
2.5 wt.% Pd/SiO_2	8

Table 5.1: H_2O_2 productivity of monometallic Pd catalysts with a total weight loading of 2.5 wt.% on a variety of oxide supports. Data on TiO_2 and SiO_2 supported catalysts taken from Freakley *et al*[17]

Reaction conditions: *H_2O (2.9 g)/MeOH (5.6 g) solvent, 5% H_2/CO_2 (420 psi), 25% O_2/CO_2 (160 psi), 10 mg catalyst, 2 °C, 1200 rpm stirrer speed, 30 minutes.*

Following this a catalyst with double the weight loading, 5 wt.%, was synthesised using the same impregnation method and tested for H_2O_2 synthesis. These higher loaded catalyst were produced in line with the total weight loading that is widely observed in the literature for supported Pd heterogeneous catalysts, including those that have been investigated for the direct synthesis of H_2O_2[6]. Testing these higher loaded catalysts give the opportunity for a comparison between other well-known mono metallic Pd catalysts as well as bimetallic Pd catalysts that have a total weight loading of 5%. As with the lower loaded catalysts above, three batches of the catalyst were made and tested multiple times for reproducibility and determination of errors in the measurements. It can be seen from the results in table 5.2 that the productivity of the catalysts has increased as the Pd weight loading is increased from 2.5 to 5 wt.%. The turnover numbers (TON's) of the 2.5 wt.% catalyst and the 5 wt.% catalyst are calculated as 22.3 and 23.5 $mol_{(H2O2)}$ $mol_{(Pd)}^{-1}$ h^{-1} respectively. This is slightly unexpected as a greater metal dispersion that is observed with lower loaded catalysts generally leading to higher TON values. Lopez-Sanchez *et al*[18] report that for a 1 wt.% AuPd/C prepared via sol-immobilsation the average particle size of 4 – 7 nm with no large nanoparticles (20nm or greater). A counterpart 5 wt.% AuPd/C prepared by impregnation previously reported by Edwards *et al*[19] displayed a larger particle size distribution and approximately 20% of the nanoparticles were reported to be >20 nm in diameter. Chary *et al*[20] investigated the use of Pd/C catalysts prepared by impregnation for the hydrogenation of phenol, they observed a sharp decrease in the Pd dispersion and metal area per gram of Pd as the weight loading is increased from 0.5 wt.% to 6 wt.%. Interestingly however, this is met with an increase in the turnover frequency (TOF), similar to the results seen for the Pd/SnO_2 catalysts above, although CO chemisorption data would be required to confirm the Pd dispersion of the Pd/SnO_2 catalysts. Therefore, from the productivity data rationalised per moles of Pd it can be assumed that the metal dispersion is not hindering the catalyst performance when increasing the weight loading from 2.5 to 5 wt.%.

SnO_2 supported catalysts demonstrate a near identical H_2O_2 productivity value to the SiO_2 supported catalysts. These results further demonstrate that whilst the H_2O_2 productivity values for SnO_2 supported catalysts are low when compared with the TiO_2 supported catalysts, the catalysts are indeed still active for the direct synthesis reaction. To our knowledge, there are no studies in the literature on the use of Pd/SnO_2 catalysts for the direct synthesis of H_2O_2, however, a range of literature exists on the use of Pd/SnO_2 catalysts for other reactions and the influence of a strong interaction between the Pd species and the SnO_2

support on the catalytic activity is often reported. Takeguchi *et al*[21] reported that Pd/SnO_2 catalysts are active for the combustion of methane (CH_4) and outperformed Pd/Al_2O_3 and Pd/ZrO_2 catalysts, the authors also note that an increase in the activity is observed with an increase in the Pd content and loadings as high as 11 wt.% lead to a 100% conversion of CH_4. A strong interaction between the Pd species and the support is thought to lead to a high dispersion of small Pd nanoparticles, even at high loadings. Given the results of the preliminary H_2O_2 synthesis experiments and the interesting effects observed on these catalysts in the literature for other reactions. It would therefore be of interest to further investigate Pd/SnO_2 catalysts for the direct synthesis of H_2O_2 for the first time. The ORO heat treatment process referenced earlier in this chapter is therefore to be used to try and generate a strong interaction between the Pd and SnO_2 and see how this affects the catalytic performance.

Catalyst	**Productivity (mol_{H2O2} kg_{cat}^{-1} h^{-1})**
5 wt.% Pd/SnO_2 (1)	10
5 wt.% Pd/SnO_2 (2)	12
5 wt.% Pd/SnO_2 (3)	10
5 wt.% Pd/TiO_2	41
5 wt.% Pd/SiO_2	12

Table 5.2: H_2O_2 productivity of monometallic Pd catalysts with a total weight loading of 5 wt.% supported on a variety of metal oxides. Data on TiO_2 and SiO_2 supported catalysts taken from Freakley *et al*[17]

Reaction conditions: *H_2O (2.9 g)/MeOH (5.6 g) solvent, 5% H_2/CO_2 (420 psi), 25% O_2/CO_2 (160 psi), 10 mg catalyst, 2 °C, 1200 rpm stirrer speed, 30 minutes.*

5.2.1.3 H_2O_2 Hydrogenation Testing of Pd/SnO_2 Catalysts.

The hydrogenation activity of supported Pd/SnO_2 catalysts was analysed to gain an insight into their selectivity. H_2O_2 hydrogenation reactions were performed under the standard

conditions and the H_2O_2 concentrations were analysed before and after reaction to give an overall hydrogenation activity with respect to H_2O_2. The results are shown in table 5.3 below:

Catalyst	**Hydrogenation Activity (mol_{H2O2} kg_{cat}^{-1} h^{-1})**
5 wt.% Pd/SnO_2	117
2.5 wt.% Pd/SnO_2	93
5 wt.% Pd/TiO_2	126
5 wt.% Pd/SiO_2	113

Table 5.3: H_2O_2 hydrogenation activity of monometallic Pd catalysts with a total weight loading ranging from 2.5 wt.% - 5 wt.% supported on a variety of metal oxides. Data on TiO_2 and SiO_2 supported catalysts taken from Freakley *et al*[17].

Reaction conditions: *H_2O_2 (0.68 g), H_2O (2.22 g)/MeOH (5.6 g) solvent, 5% H_2/CO_2 (420 psi), 10 mg catalyst, 2 ℃, 1200 rpm stirrer speed, 30 minutes.*

The results show that the Pd/SnO_2 catalysts are also active for the degradation of H_2O_2 and as was observed with the direct synthesis reaction, there is a very similar activity between the SnO_2 and SiO_2 supported catalysts. From these data it is clear that the low amounts of H_2O_2 being produced by the Pd/SnO_2 is due in part to over hydrogenation of the H_2O_2 formed.

5.2.1.4 Effect of the ORO Heat Treatment

As has been discussed previously in this chapter, the ORO heat treatment has been shown to induce a strong metal support interaction in the case of bimetallic SnPd catalysts. Moreover, this interaction can influence the catalytic performance of the material, drastically increasing the selectivity towards H_2O_2 selectivity. The 2.5 wt.% and 5 wt.% Pd/SnO_2 catalysts were subjected to an ORO heat treatment cycle at the temperatures previously reported by Freakley *et al*[17] and the activity of the catalysts was measured after each stage of the heat treatment cycle by performing a direct synthesis reaction under standard conditions and recording the productivity. The results are shown below in table 5.4:

Catalyst	**H_2O_2 Productivity (mol_{H2O2} kg_{cat}^{-1} h^{-1})**	**Heat Treatment**
5 wt.% Pd/SnO_2	10	Calcination in static air @ 500 °C, 3 hours
2.5 wt.% Pd/SnO_2	4	Calcination in static air @ 500 °C, 3 hours.
5 wt.% Pd/SnO_2	51	As above, followed by reduction under 5% H_2/Ar, 2 hours.
2.5 wt. % Pd/SnO_2	20	As above, followed by reduction under 5% H_2/Ar, 2 hours.
5 wt. % Pd/SnO_2	13	As above, followed by re-calcination in static air @ 400 °C, 3 hours.
2.5 wt. % Pd/SnO_2	5	As above, followed by re - calcination in static air @ 400 °C, 3 hours.

Table 5.4: H_2O_2 productivity of monometallic Pd catalysts with a total weight loading ranging from 2.5 wt.% - 5 wt.% supported on SnO_2 with varying heat treatments.

Reaction conditions: *H_2O (2.9 g)/MeOH (5.6 g) solvent, 5% H_2/CO_2 (420 psi), 25% O_2/CO_2 (160 psi), 10 mg catalyst, 2 °C, 1200 rpm stirrer speed, 30 minutes.*

These data show that upon reduction after calcination the catalysts are far more active, with the 5 wt.% Pd/SnO_2 catalyst giving a H_2O_2 productivity of 51, this is a comparable value to other supported Pd catalysts which have been reported in the literature under the same reaction conditions, the same effect is seen for the lower loaded Pd catalyst, although the difference is not as great. Upon re-calcination both the 2.5 wt.% and 5 wt.% catalysts drop back down to near the original H_2O_2 productivities that were observed in samples only subjected to an initial calcination. There are many examples in the literature which report that a reduced Pd/SnO_2 is active for a range of reactions, including the selective hydrogenation of

2, 4-difluoronitrobenzene[22], electroreduction of H_2O_2[23], CO oxidation[24], CH_4 oxidation[21] and nitrate hydrogenation[19]. It should therefore not be surprising that the reduced Pd/SnO_2 is the most active for both the direct synthesis of H_2O_2 and the undesired degradation reactions. Gavagnin *et al*[25] showed that Pd/SnO_2 offered the best mix of selectivity and hydrogenation activity for the hydrogenation of nitrates. Interestingly, the authors also suggest that reduced SnO_x in the local vicinity of the Pd surface species may be acting as a promotor, yielding the impressive catalytic activity. It can therefore be expected that the reduced Pd/SnO_2 catalysts are also active for the degradation of H_2O_2, given that reduced SnO_x or Sn metal may be actively promoting hydrogenation reactions. Whilst there is no XPS data to confirm that there is an increase in the amount of reduced Sn species in those samples subjected to a 200 °C reduction compared with the calcined only samples, it is logical to think this is the case.

5.2.2 Catalyst Characterisation

5.2.2.1 Scanning Transmission Electron Microscopy

The Pd/SnO_2 catalysts were analysed by high resolution scanning transmission electron microscopy (STEM) and electron energy loss spectroscopy (EELS) by Dr Qian He at the Oak Ridge National Laboratory, Tennessee. These techniques were used to image 5 wt.% Pd/SnO_2 catalysts at each stage of the ORO heat treatment cycle to observe any key changes that happen to either the supported Pd nanoparticles or the SnO_2 support surface during the ORO process. The images are shown below in figures 5.1 – 5.3.

Figure 5.1 shows a 5 wt.% Pd/SnO_2 catalyst after an initial calcination of 500 °C in static air for 3 hours. The first STEM images shown in figures 5.1a and 5.1b show that the SnO_2 support particles are large, in the region of 100 nm and well faceted. Both the bright field and annular dark field images indicate that there are no large Pd particles visible under this level of magnification. As the resolution is increased we can identify the Pd nanoparticles, which appear to be well ordered, spherical-like and sitting on the SnO_2 surface, these features are highlighted in the bright field and annular dark field images shown in figures 5.1c and 5.1d. The Pd nanoparticles appear to be in the size range of 8 – 10 nm, which is in keeping with that of other supported Pd catalysts prepared via the impregnation technique. EELS was used to identify the species present in the microscopy images and the spectroscopic data was

acquired in tandem with the annular dark field images. It can be seen in the image shown in figure 5.1e, as is expected, Pd nanoparticles are "sitting" on the SnO_2 surface. It appears that there is an interaction occurring between the Pd particles and the SnO_2 surface as they are in contact, however the interaction can be assumed to be relatively weak as there is no evidence of alloying or particle encapsulation. This reflects the observations of Kamiuchi *et al*[26] who reported that a 1 wt.% Pd/SnO_2 catalyst prepared by impreganation and subjected to a calcination in static air at 400 °C for 30 minutes contained both amorphous and fine Pd nanoparticles that were weakly interacting with the SnO_2 support and showed no signs of encapsulation.

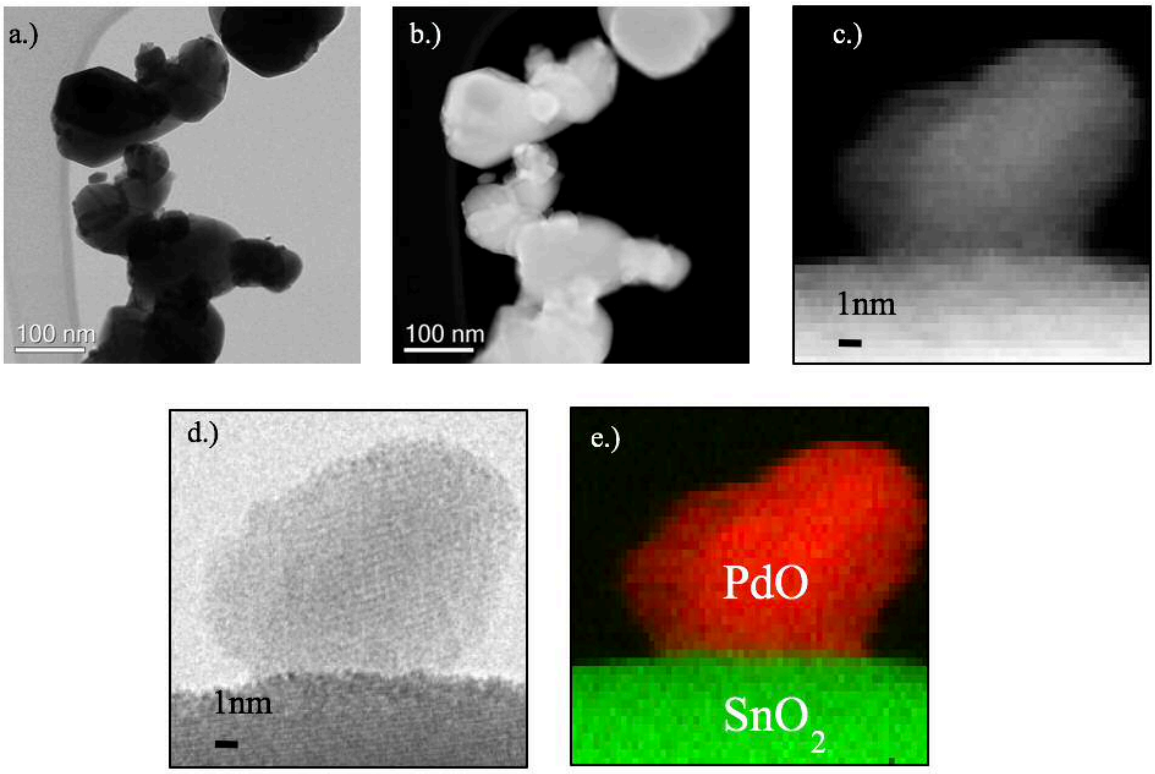

Figures 5.1a – 5.1e: Representative STEM images, including annular dark field (b. and d.), bright field (a. and c.) and EELS (e.) images of a 5 wt.% Pd/SnO_2 catalyst prepared by impregnation and heat treated at 500 °C in static air for 3 hours. The scale bars represent 100 nm on images a. and b. and 1 nm on images c and d.

Following these results, analysis of a 5 wt. % Pd/SnO_2 catalyst which had been subjected to the full ORO cycle was performed. STEM images of the aforementioned sample are shown in figures 5.2a – 5.2e. The first images, shown in figures 5.2a and 5.2b are the bright field and annular dark field images respectively. The Pd nanoparticles again appear to have a spherical-like morphology and are "sitting" on the SnO_2 surface. There appears to be a faint

outline of a somewhat amorphous layer on the Pd particle but it is difficult to confirm this using only these images. EELS spectrum images are shown in figures 5.2c – 5.2e, interestingly with these images it is possible to see that the SnO_2 is interacting with the Pd nanoparticle and there is some sort of encapsulation occurring, indicating an SMSI after this heat treatment cycle. This is in keeping with the findings of Freakley *et al*[17] who investigated the same heat treatment for a range of PdSn supported catalysts.

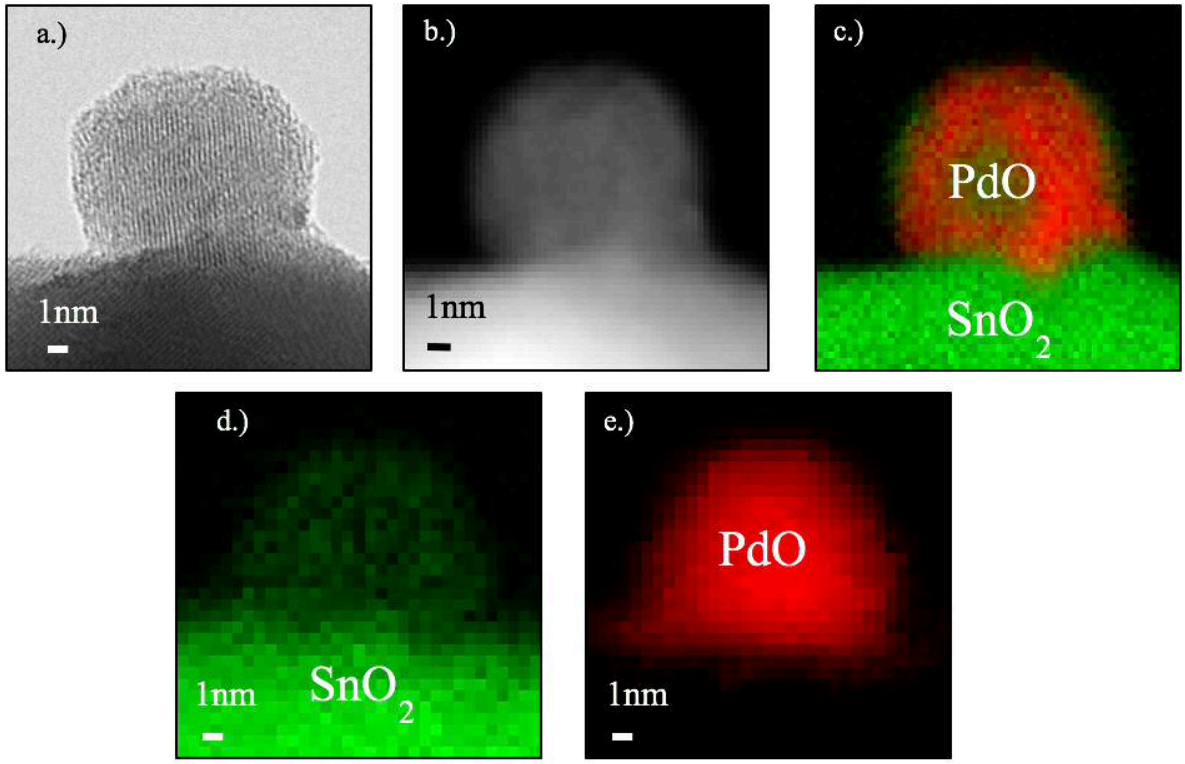

Figures 5.2a – 5.2e: Representative STEM images, including annular dark field (b.), bright field (a.) and EELS (c., d. and e.) images of a 5 wt.% Pd/SnO_2 catalyst prepared by impregnation and heat treated at 500 °C in static air for 3 hours, followed by reduction in 5% H_2/Ar at 200 °C for 2 hours and re-calcination at 400 °C in static air for 3 hours. The scale bars represent 100 nm on images a. and b. and 1 nm on images d. and e.

It cannot be said whether alloying is occurring, however there is an interaction between the Pd nanoparticles and the SnO_2 following the ORO heat treatment cycle and there appears to be encapsulation occurring. After subjecting Pd catalysts to a similar ORO heat treatment cycle Kamiuchi *et al*[26] reported a strong interaction between the Pd species and the SnO_2 support which led to a series of different particle morphologies including core-shell and particle intrusion structures. The authors claimed that this was not due to the migration of

SnO_2 but due to the phase separation of a Sn species from a PdSn intermetallic compound which is formed upon reduction at 400 °C. It is reasonable to assume that the encapsulation occurring, displayed in figures 5.2a – 5.2e, after the ORO heat treatment cycle is due to the migration of the metal oxide support onto the Pd surface species as the reduction temperature may not have been high enough to form the intermetallic species observed by Kamiuchi *et al*[26] hence why no core-shell or completely encapsulated particles are observed. This may also explain why the reduced samples are the most active, as the reduction temperature should be enough to reduce the Pd species to Pd metal (although XPS or XRD further analysis would be required to prove this) which has been noted in the literature to be highly active for the direct synthesis and degradation of H_2O_2. Moreover, the reduction temperature may not be high enough to induce the formation of core-shell or other particle structures usually observed as a consequence of a very strong interaction between the metal and the support material and such particle types can lead to a blocking of the active sites and therefore a reduced catalyst activity. When the catalyst is then re-calcined it is plausible to think that the SnO_2 species that has migrated during the reduction is simply re-oxidised back to SnO_2 and the Pd species is oxidised back to its state as in the calcined sample, leading to a negiglible difference in the observed catalytic activity of the direct synthesis of H_2O_2 and the subsequent degradation.

When performing the STEM analysis of the sample which had undergone the ORO heat treatment cycle, an interesting anomaly was spotted. A carbon contaminate was noticed with a Pd nanoparticle “sitting” on it and therefore not directly upon the surface of the SnO_2 support. When EELS analysis was conducted on this particle it was found that there is no strong metal support interaction between the Pd and the SnO_2. Therefore, the Pd particles must be directly touching the SnO_2 surface to observe an encapsulation and interaction with the SnO_2. These images are shown below in figures 5.3 a– 5.3e

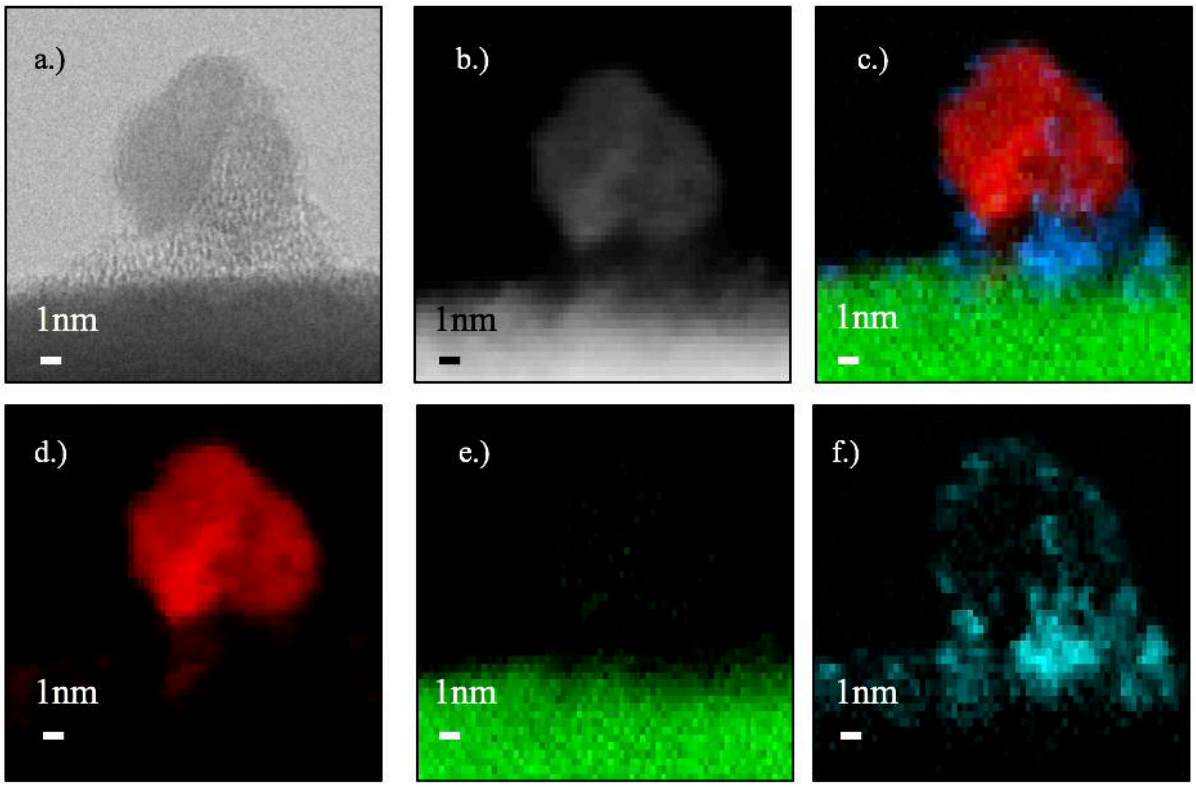

Figures 5.3a – 5.3e: Representative STEM images, including annular dark field (b.), bright field (a.) and EELS (c., d., e. and f.) images of a 5 wt.% Pd/SnO_2 catalyst containing a carbon contaminant, prepared by impregnation and heat treated at 500 °C in static air for 3 hours, followed by reduction in 5% H_2/Ar at 200 °C for 2 hours and re-calcination at 400 °C in static air for 3 hours. The scale bars represent 1 nm.

These findings further compound the hypothesis that there is a SMSI occurring as a consequence of the ORO heat treatment and that the PdO_x surface species become encapsulated as a consequence of migration of the support metal oxide. However, it is reasonable to assume that this encapsulation may not be significant as there is no real change observed in the activity of the catalysts after undergoing the heat treatment cycle.

5.2.3 Pd-SnO_2 Catalysts Synthesised via Sol-Gel.

5.2.3.1. Catalyst Testing

Supported Pd catalysts were prepared via a sol-gel method which has been previously described in the literature for the preparation of SnO_2 with a high surface area[27]. This method was modified by including the addition of $PdCl_2$ (Sigma Aldrich, >99.9 %) with the tin(iv)

chloride pentahydrate ($SnCl_4$. $5H_2O$) (Sigma Aldrich, >98 %) precursor so as to try and form an intimately mixed Pd-SnO_2 catalyst in which the whole surface contains the small Pd oxide species that are thought to be the main active component of supported Pd catalysts for the direct synthesis of H_2O_2. A detailed description of the sol-gel preparation technique is outlined in chapter 2 of this work. H_2O_2 direct synthesis reactions were performed using the experimental procedure outlined in chapter 2 of this work and any variations from this standard procedure will be explicitly stated. The same is true for H_2O_2 hydrogenation reactions. A brief outline of the experimental conditions is given below:

- Direct synthesis of H_2O_2 in a Parr stainless steel 100 ml high pressure autoclave: H_2O (2.9 g)/MeOH (5.6 g) solvent, 5% H_2/CO_2 (420 psi), 25% O_2/CO_2 (160 psi), 10 mg catalyst, 2 °C, 1200 rpm stirrer speed, 30 minutes.
- Hydrogenation of H_2O_2 in a Parr stainless steel 100 ml high pressure autoclave: H_2O_2 (0.68 g) H_2O (2.22 g)/MeOH (5.6 g) solvent, 5%H_2/CO_2 (420 psi), 10 mg catalyst, 2 °C, 1200 rpm stirrer speed, 30 minutes.

5.2.3.2 H_2O_2 Synthesis Testing of Pd-SnO_2 Catalysts

Initial reactions were performed to establish whether the sol-gel catalysts were active for the direct synthesis of H_2O_2. An initial batch of catalysts was made using a 1 wt.% total Pd weight loading and the catalysts were subjected to the standard calcination of 500 °C in static air for 3 hours, as has been used for the supported Pd catalysts previously investigated in this chapter. 1 wt.% was chosen as the initial weight loading as the nature of the sol-gel technique means that high metal dispersions and surface areas of both the active metal and the support material are easily achieved and controlled. Therefore a relatively low Pd loading was decided upon to try and achieve a high metal dispersion and catalyst activity, whilst minimising the amount of active metal required. The results of these initial experiments are shown in table 5.5:

Catalyst	**H_2O_2 Productivity (mol_{H2O2} kg_{cat}^{-1} h^{-1})**
1 wt.% Pd-SnO_2 (1)	26
1 wt.% Pd-SnO_2 (2)	26
1 wt.% Pd-SnO_2 (3)	22
1 wt.% Pd/SnO_2 (Impregnation, SnO_2 not synthesised via sol-gel)	3

Table 5.5: H_2O_2 productivity of monometallic Pd-SnO_2 catalysts with a total weight loading of 1 wt.% prepared by a novel sol-gel technique and impregnation.

Reaction Conditions: *H_2O (2.9 g)/MeOH (5.6 g) solvent, 5%H_2/CO_2 (420 psi), 25%O_2/CO_2 (160 psi), 10 mg catalyst, 2 °C, 1200 rpm stirrer speed, 30 minutes.*

These data show that the sol-gel technique is indeed an effective way of preparing supported Pd catalysts, when compared with the results presented previously in this chapter, whilst the total weight loading of the sol-gel catalysts is 5 times less, the H_2O_2 productivity observed is in fact 2 times greater. To further explore this observation, an analogous 1 wt.% Pd/SnO_2 catalyst was prepared via impregnation and the H_2O_2 productivity of said catalyst was investigated. Table 5.5 shows that the productivity of this catalyst is nearly 10 times less than the sol-gel catalyst with the same Pd metal loading. It must also be noted that the SnO_2 support of the impregnation sample was not synthesised via the sol-gel route, rather the SnO_2 for this catalyst was purchased (Sigma Aldrich, >99.99% trace metal basis). Adnan *et al*[27] report that a high surface area can be achieved through this sol-gel synthesis (111 m^2 g^{-1}). Furthermore, the authors also show that the high surface area and small SnO_2 nanoparticles (4.5 nm average size) lead to an increased activity in the hydrogenation of styrene. It can therefore be expected that the catalyst samples prepared via sol-gel will have a higher surface area than those prepared via impregnation and This result helps to further highlight how much more active the catalysts prepared via sol-gel are.

5.2.3.3 H_2O_2 Hydrogenation Testing of Pd-SnO_2 Catalysts.

The H_2O_2 hydrogenation activity of the Pd-SnO_2 sol-gel catalysts were investigated to assess the selectivity towards H_2O_2. Having established that the H_2O_2 productivity is much greater than the analogous catalysts prepared by impregnation it was necessary to check if the H_2O_2 hydrogenation activity is also much higher, therefore making the catalysts highly unselective, or whether the catalysts prepared via sol-gel simply demonstrate a greater affinity towards H_2O_2 production as is highly desirable. The results of the hydrogenation experiments are given below in table 5.6:

Catalyst	**H_2O_2 Hydrogenation Activity (mol_{H2O2} kg_{cat}^{-1} h^{-1})**
1 wt.% Pd-SnO_2 (1)	122
1 wt.% Pd-SnO_2 (2)	121
1 wt.% Pd-SnO_2 (3)	125
1 wt.% Pd/SnO_2 (Impregnation, SnO_2 not synthesised via sol gel)	90

Table 5.6: H_2O_2 hydrogenation activity of monometallic Pd-SnO_2 catalysts with a total weight loading of 1 wt.% prepared by a novel sol-gel technique and impregnation.

Reaction conditions: *H_2O_2 (0.68 g), H_2O (2.22 g)/MeOH (5.6 g) solvent, 5%H_2/CO_2 (420 psi), 10 mg catalyst, 2 °C, 1200 rpm stirrer speed, 30 minutes.*

Catalysts prepared by sol-gel also exhibit a greater activity towards H_2O_2 hydrogenation. The hydrogenation activity of the sol-gel catalysts is approximately 1.5 times that of the 1 wt.% Pd/SnO_2 catalysts prepared via impregnation. This is to be expected given the enhanced rate of H_2O_2 synthesis observed with the sol-gel catalysts and it must also be noted that whilst the H_2O_2 hydrogenation activity is greater than that of the impregnation catalysts, it is less than the hydrogenation activity reported in the literature for established H_2O_2 synthesis catalysts such as 5 wt.% AuPd/TiO_2. Furthermore, although the hydrogenation activity is 1.4 times greater for the sol-gel prepared catalysts, the synthesis activity is 8.2 times greater, these results show that the sol-gel method is a highly effective way of preparing Pd-SnO_2 catalysts

for the direct synthesis of H_2O_2. Moreover, the results indicate that the catalysts prepared via sol-gel may contain many active sites that produce H_2O_2 and not as many that catalyse the degradation pathways, whereas the catalysts prepared via impregnation may have a greater amount of sites that catalyse degradation pathways or a lower amount of sites that catalyse the synthesis of H_2O_2, leading to an overall observed decrease in the synthesis of H_2O_2. Boskovic *et al*[16] reported similar findings for the hydrogenation of nitrates in an aqueous solution, hydrogenation activity was greater for a catalyst prepared via a sol-gel method, with the reaction coming to completion after only 2 hours whilst the equivalent catalyst prepared via impregnation of Pd onto the SnO_2 support did not achieve a suitable level of nitrate concentration, even after 200 minutes reaction time.

5.2.3.4 The Effect of Weight Loading

Having established that the sol-gel technique is more effective for producing Pd catalysts supported on SnO_2 for the direct synthesis of H_2O_2, a series of catalyst with an increasing total weight loading of Pd were synthesised to investigate this effect. To achieve this the amount of $PdCl_2$ added was simply adjusted to give the desired total weight loading, the remainder of the catalyst preparation procedure remained identical to that used for the preparation of the initial 1 wt.% Pd-SnO_2 catalyst (detailed experimental procedure outlined in chapter 2 of this work). Following a calcination at 500 °C the resultant catalysts were tested for H_2O_2 productivity. The results are shown below in figure 5.4:

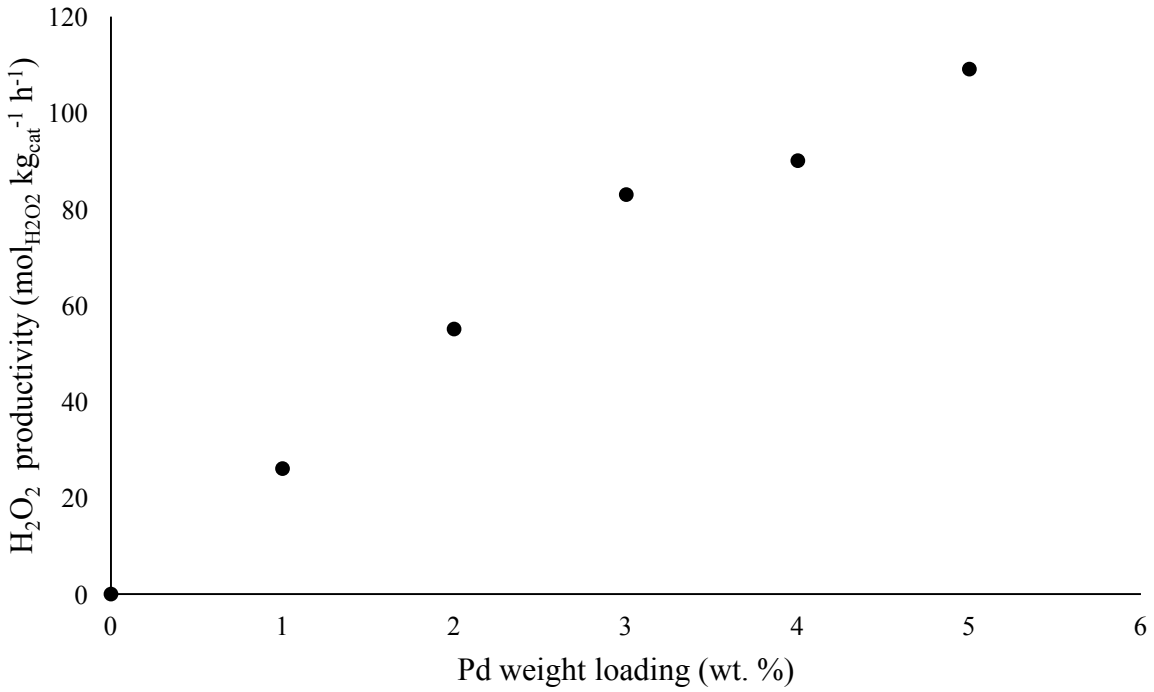

Figure 5.4: H_2O_2 productivity of monometallic Pd-SnO_2 catalysts with a total weight loading between 1 – 5 wt.% prepared by a novel sol-gel technique.

Reaction Conditions: *H_2O (2.9 g)/MeOH (5.6 g) solvent, 5% H_2/CO_2 (420 psi), 25% O_2/CO_2 (160 psi), 10 mg catalyst, 2 ℃, 1200 rpm stirrer speed, 30 minutes.*

There is a near linear increase in H_2O_2 productivity as the total Pd weight loading is increased from 1 – 3%, with the 3 wt.% Pd-SnO_2 catalyst giving a H_2O_2 productivity of 83 mol_{H2O2} kg_{cat}^{-1} h^{-1}. Interestingly, as the total Pd weight loading is increased to 4 wt.% the activity levels off slightly and deviates from the linear relation, upon increasing the weight loading to 5 wt.% there is a further increase in H_2O_2 productivity and the trend reverts to a near-linear relation, with a productivity of 109 mol_{H2O2} kg_{cat}^{-1} h^{-1} observed. These data show that the sol-gel catalysts are highly active for the direct synthesis of H_2O_2, outperforming other Pd catalysts in the reported in the literature, prepared by both impregnation[28] and modified impregnation techniques[29].

The effect of weight loading was also investigated for the hydrogenation of H_2O_2 , using the same catalyst samples as those for the direct synthesis investigations. The results of the H_2O_2 hydrogenation experiments are shown below in figure 5.5:

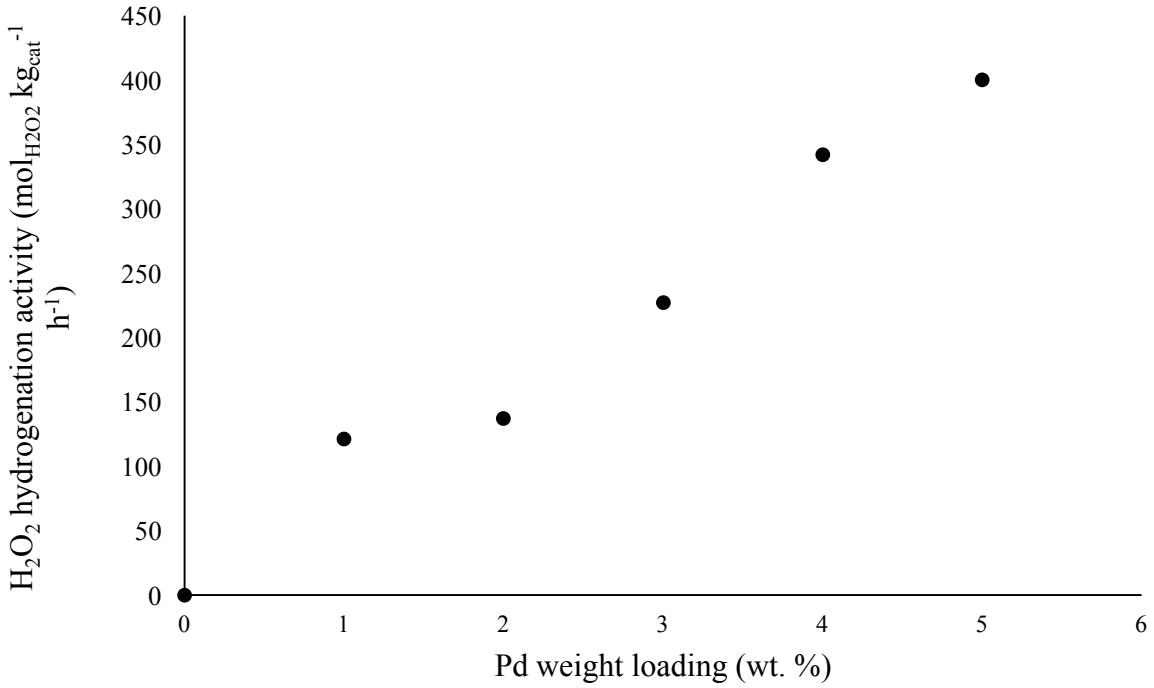

Figure 5.5: H_2O_2 hydrogenation activity of monometallic Pd-SnO_2 catalysts with a total weight loading between 1 – 5 wt.% prepared by a novel sol-gel technique.

Reaction Conditions: *H_2O (2.9 g)/MeOH (5.6 g) solvent, 5% H_2/CO_2 (420 psi), 10 mg catalyst, 2 ℃, 1200 rpm stirrer speed, 30 minutes.*

The results in figure 5.5 show that as is to be expected, as the Pd weight loading increases, so does this hydrogenation activity and the trend appears to echo that of the H_2O_2 productivity data. From this data it can therefore be said that the increase in H_2O_2 production with increasing Pd loading is not due to a greater selectivity and is likely to be caused by a larger number of Pd active sites on the catalyst surface, as a consequence of this, there is also an increase in the undesired over hydrogenation reaction. Again, it should be noted that the hydrogenation activity of the sol-gel catalyst with a similar Pd weight loading is comparable to that of well-known H_2O_2 synthesis catalysts such as 5 wt.% AuPd/TiO_2, whilst the H_2O_2 productivity value is higher, with the 3 wt.% Pd sol-gel catalyst having a productivity of 83 mol_{H2O2} kg_{cat}^{-1} h^{-1} compared with 64 mol_{H2O2} kg_{cat}^{-1} h^{-1} and for the 5 wt.% AuPd/TiO_2 catalyst[24], highlighting the performance of these catalysts.

5.2.3.5 The Effect of Calcination Temperature

A key consideration in the design of a heterogeneous catalyst is its stability, it is known that increasing the calcination temperature can improve the stability of heterogeneous catalysts. To investigate the effect that calcination temperature has on both the stability and activity of the Pd-SnO_2 sol-gel catalysts, the most active sol-gel catalyst (5 wt.% Pd-SnO_2) was subjected to calcination at a temperature range of 400 – 600 °C. The resultant catalysts were then tested for the direct synthesis of H_2O_2 under the established standard conditions, however a greater catalyst amount of 70 mg was used to ensure that enough sample could be recovered post reaction, dried in a vacuum desiccator for a period of 48 hours and then re-tested. This testing protocol allowed for the study of the reusability of the catalysts. The effect of calcination temperature on catalyst activity was investigated by simply performing a standard direct synthesis reaction on each of the samples, this data is presented below in figure 5.6. From the graph, it is clear to see that the activity does indeed vary as a function of calcination temperature. Between the temperatures of 400 – 500 °C there is an increase in the H_2O_2 productivity of the catalysts, with a maximum value of 109 mol_{H2O2} $kg_{cat}^{-1}h^{-1}$ seen at a calcination temperature of 500 °C. Then as the calcination temperature is further increased to 600 °C there is a distinct drop in the H_2O_2 productivity and the sample that was calcined at 600 °C gives the lowest H_2O_2 productivity. These data lead to the conclusion that 500 °C represents the optimal temperature for calcination of the sol-gel prepared Pd-SnO_2 catalysts in terms of H_2O_2 productivity. It is however crucial to test the re-usability of these catalysts as an increase in catalyst activity can be due to leached species in the reaction solution and whilst the samples subjected to a higher calcination temperature may exhibit lower productivity values, they may have an increased stability.

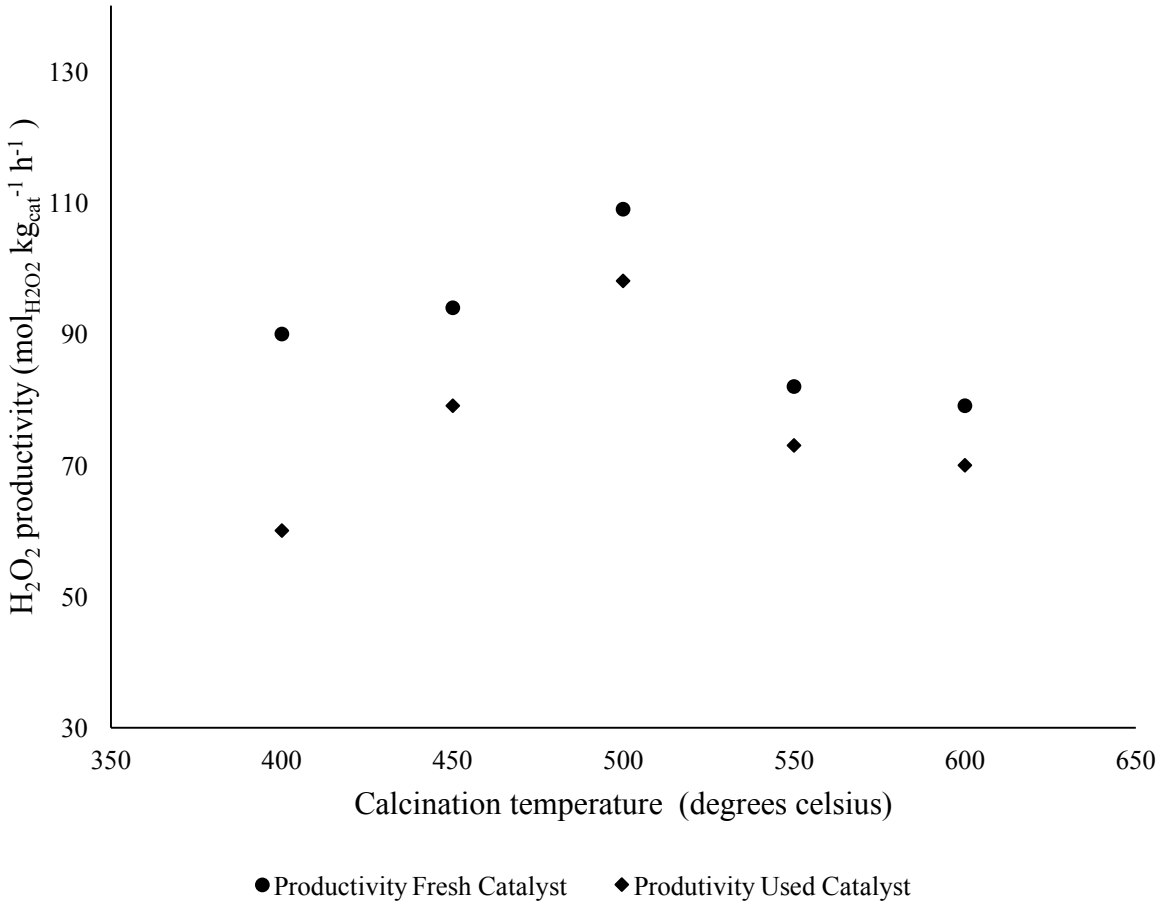

Figure 5.6: H_2O_2 productivity of fresh and re-used monometallic Pd-SnO_2 catalysts with a total weight loading of 5 wt.% and varying calcination temperatures, prepared by a novel sol-gel technique.

Reaction conditions: *H_2O (2.9 g)/MeOH (5.6 g) solvent, 5% H_2/CO_2 (420 psi), 25% O_2/CO_2 (160 psi), 10 mg catalyst, 2 ℃, 1200 rpm stirrer speed, 30 minutes*.

Figure 5.6 shows the results of the re-use experiments. All catalysts lose some activity upon re-use, leading to the conclusion that none of the catalysts are completely stable. Even when exposed to higher calcination temperatures of 600 °C, there is still a 10% drop in catalytic activity towards H_2O_2 synthesis. At lower calcination temperatures of 400 °C and 450 °C the instability is more pronounced and the greatest difference in productivity on re-use is observed for the sample calcined at 400 °C, with a 33% difference in productivity between the fresh and re-used samples. As the calcination temperature is increased to 500 °C, the difference drops to approximately 11% and interestingly, remains at 11% even as the

calcination temperature is increased to 550 and finally 600 °C. This observation leads to the conclusion that there is some inherent instability for the sol-gel catalysts. The re-use data helps to explain the trends observed in the performance of the fresh catalyst upon increasing calcination temperature. Upon calcination at 400 °C the catalyst is least stable of all the calcination temperatures, therefore suggesting that metal leaching is occurring, whilst it has been reported by Lunsford *et al*[30] that leached Pd will lead to an increase in productivity of the catalyst towards H_2O_2 synthesis, it will also lead to a large increase in the degradation of the H_2O_2. As the calcination temperature is increased towards 500 °C, the productivity increases but the catalysts become far more stable, suggesting that less Pd is leached into the reaction solution, this could lead to an increase in the productivity but also less of an increase in the unwanted degredation, meaning the observed productivity is actually greater than that of the least stable catalyst. Finally, as the calcination temperature increases beyond 500 °C the well known sintering affects of Pd occur and the particle sizes increase meaning that both observed difference in productivity of the catalyst upon re-use decreases but the overall productivity is actually less.

5.2.3.6 The Effect of an ORO Heat Treatment

The reduction of heterogeneous Pd catalysts is well reported in the literature, subjecting such catalysts to a high temperature reduction is known to lead to an increased metal-support interaction as was discussed in the introduction section of this chapter. Tauster *et al*[1] revealed that H_2 and CO adsorption values for a supported Pd catalyst drastically decreased upon reduction at an elevated temperature of 500 °C. Subjecting the catalyst to a further oxidation step can restore the metal nanoparticles to a higher oxidation state and help to increase the H_2 and CO adsorption values back to those of the calcined only sample, whilst maintaining some of the benefits of the SMSI such as alloying and modification of the nanoparticle structure. It was shown earlier in this chapter and in a recent publication, that a strong interaction between Pd and Sn can be induced by performing an oxidation-reduction procedure, following this with a secondary oxidation then allows the Pd nanoparticles to return to a higher Pd oxidation state whilst maintaining an encapsulation with SnO_2. It was decided to see if this is the case for the sol-gel catalysts and if like the PdSn supported catalysts reported by Freakley *et al*[17], there is a positive effect on the H_2O_2 synthesis activity after an ORO heat treatment. A 5 wt.% Pd-SnO_2 sol-gel catalyst was subjected to the same ORO heat treatment as the PdSn

bimetallic catalysts of Freakley *et al*[17] and the H_2O_2 productivity and hydrogenation activity was tested after each stage of the heat treatment. The results of these experiments are shown below in table 5.7:

Catalyst	**H_2O_2 Productivity (mol_{H2O2} kg_{cat}^{-1} h^{-1})**	**H_2O_2 Hydrogenation Activity (mol_{H2O2} kg_{cat}^{-1} h^{-1})**	**Heat Treatment**
5 wt.% Pd-SnO_2	109	400	Calcination in static air @ 500 °C, 3 hours
5 wt.% Pd-SnO_2	11	665	As above, followed by reduction under 5% H_2/Ar, 2 hours.
5 wt. % Pd-SnO_2	101	366	As above, followed by re - calcination in static air @ 400 °C, 3 hours.

Table 5.7: H_2O_2 productivity of monometallic Pd catalysts with a total weight loading 5 wt.% prepared by a novel sol-gel technique and subjected to varying heat treatments.

Reaction conditions: *H_2O (2.9 g)/MeOH (5.6 g) solvent, 5% H_2/CO_2 (420 psi), 25% O_2/CO_2 (160 psi), 10 mg catalyst, 2 °C, 1200 rpm stirrer speed, 30 minutes. For hydrogenation experiments, only 5% H_2/CO_2 present and 0.68 g of H_2O_2 in the solvent.*

These data show that after a reduction, the catalytic activity towards H_2O_2 synthesis is greatly diminished and furthermore, the activity towards H_2O_2 hydrogenation is greatly increased. These results are the opposite of those for the Pd/SnO_2 catalysts investigated previously in this chapter, where H_2O_2 productivity increased upon reduction. These data suggest that an oxidised Pd species is the active catalyst species for the sol-gel catalysts in the case of H_2O_2

synthesis. This is not the case for H_2O_2 hydrogenation, which increases dramatically upon reduction, this result clearly explains the low H_2O_2 synthesis activity of the OR Pd-SnO_2 catalyst sample. Once the H_2O_2 is formed on the catalyst surface, it is over hydrogenated to form H_2O and so the concentration of H_2O_2 present after a 30 minutes reaction is greatly diminished. Once the catalyst has been re-calcined, the H_2O_2 synthesis activity returns to near that of the catalyst which has only been calcined, the H_2O_2 hydrogenation activity of the ORO sample is slightly less but not to the extent of the PdSn bimetallic catalysts of Freakley *et al*[20] which show a complete switch off in H_2O_2 hydrogenation. These data therefore show that the ORO treatment conditions are not an effective method for tailoring the selectivity and activity of Pd-SnO_2 catalysts in the direct synthesis of H_2O_2. Boskovic *et al*[16] found that after reduction of a low temperature reduction of a modified sol-gel catalyst, prepared in a similar method whereby the metal and support precursor were simultaneously hydrolysed, there was only one Pd state present after subjecting the catalyst sample to a high temperature calcination followed by a low temperature reduction. The authors postulate that a small shift in the binding energy of the Pd 3d 5/2 peak indicated a partial reduction but not to metallic Pd and so the Pd species exists in a partially oxidised state that is stabilised due to the intimate contact with SnO_2. This may explain the results of the ORO experiments discussed above, Pd may be partially reduced upon the reduction step of the 5 wt.% Pd-SnO_2 catalysts but not completely reduced to metallic Pd, the partially reduced Pd species may be inactive for the direct synthesis reaction and highly active for the degredation, as is demonstrated in the testing results. Once the catalyst sample is then re-calcined the Pd is reoxidised to a higher oxidation state and the catalyst becomes active towards the direct synthesis reaction again. Whilst there is no XPS at present to support this theory, XRD analysis given in the characterisation section provides some support of this.

It was decided to slightly alter the reduction step of the ORO heat treatment to see if any beneficial changes in catalyst activity could be induced by using a higher reduction temperature. A fresh batch of 5 wt. % Pd-SnO_2 catalyst was subjected to a modified ORO heat treatment cycle, where the reduction temperature was increased to 300 °C. H_2O_2 synthesis and hydrogenation reactions were then performed and the results are displayed below in table 5.8. The results show that the trend is very much the same as was observed for the sample that was reduced at 200 °C. The catalyst appears to be more selective towards H_2O_2 synthesis with a 25% decrease in H_2O_2 hydrogenation activity observed, suggesting that

some subtle changes may have occurred during the higher reduction step. Freakley *et al*[15] have previously shown that when PdSn supported bimetallic catalysts are reduced at both 200 °C and 300 °C after an initial calcination, the H_2O_2 degradation increased dramatically, this provides further evidence that a reduced Pd species is far more active for the degradation of H_2O_2 than the PdO. Furthermore, Freakley *et al*[17] found that the reduction of Pd^{2+} to metallic Pd occurs at a reduction of 100 °C for the supported PdSn catalysts, this may explain why these catalysts are still therefore active towards the direct synthesis of H_2O_2 as well as the degradation after being subjected to a reduction, unlike the sol-gel catalysts. Which, as eluded to previously may not have metallic Pd present after a reduction at 200 or 300 °C.

Catalyst	**H_2O_2 Productivity (mol_{H2O2} kg_{cat}^{-1} h^{-1})**	**H_2O_2 Hydrogenation Activity (mol_{H2O2} kg_{cat}^{-1} h^{-1})**	**Heat Treatment**
5 wt.% Pd-SnO_2	109	400	Calcination in static air @ 500 °C, 3 hours
5 wt.% Pd-SnO_2	16	541	As above, followed by reduction under 5% H_2/Ar, 2 hours.
5 wt. % Pd-SnO_2	99	308	As above, followed by re -calcination in static air @ 400 °C, 3 hours.

Table 5.8: H_2O_2 productivity of monometallic Pd catalysts with a total weight loading 5 wt.% prepared by a novel sol-gel technique and subjected to varying heat treatments.

Reaction conditions: *H_2O (2.9 g)/MeOH (5.6 g) solvent, 5% H_2/CO_2 (420 psi), 25% O_2/CO_2 (160 psi), 10 mg catalyst, 2 °C, 1200 rpm stirrer speed, 30 minutes. For hydrogenation experiments, only 5%H_2/CO_2 present and 0.68 g of H_2O_2 in the solvent.*

5.2.4 Catalyst Characterisation

5.2.4.1 X-ray Diffraction

X-ray diffraction (XRD) was used to analyse the sol-gel catalysts directly after the synthesis process was completed to investigate the material and identify if the synthesis procedure had been successful. The bright orange 5 wt.% Pd-SnO_2 powder was first analysed via XRD, the pattern of which is shown below in figure 5.8. The pattern contains many sharp intense reflections which were attributed to two crystallite phases. Firstly, ammonium chloride also known as sal ammoniac (NH_4Cl) and secondly ammonium hexachlorostannate(IV) also known as panichiite ($(NH_4)_2SnCl_6$). The reflections for these crystallite phases are indicated on the XRD profile. These XRD profiles show that after drying an intermediate material has been made still containing some of the unwanted precursors and that these precursor materials are not being removed during the washing phase. Moreover, there are no reflections present which can be attributed to any Pd species, suggesting that the Pd is below the XRD detection limit, which can be expected given that the Pd has been intimately mixed into the metal oxide material and no calcination has taken place. The reflections present in the diffraction pattern of the Sn only sample are significantly less intense than the 5 wt.% Pd-SnO_2 sample suggesting that the Pd-SnO_2 crystallite particles have a slightly different morphology to the SnO_2 particles.

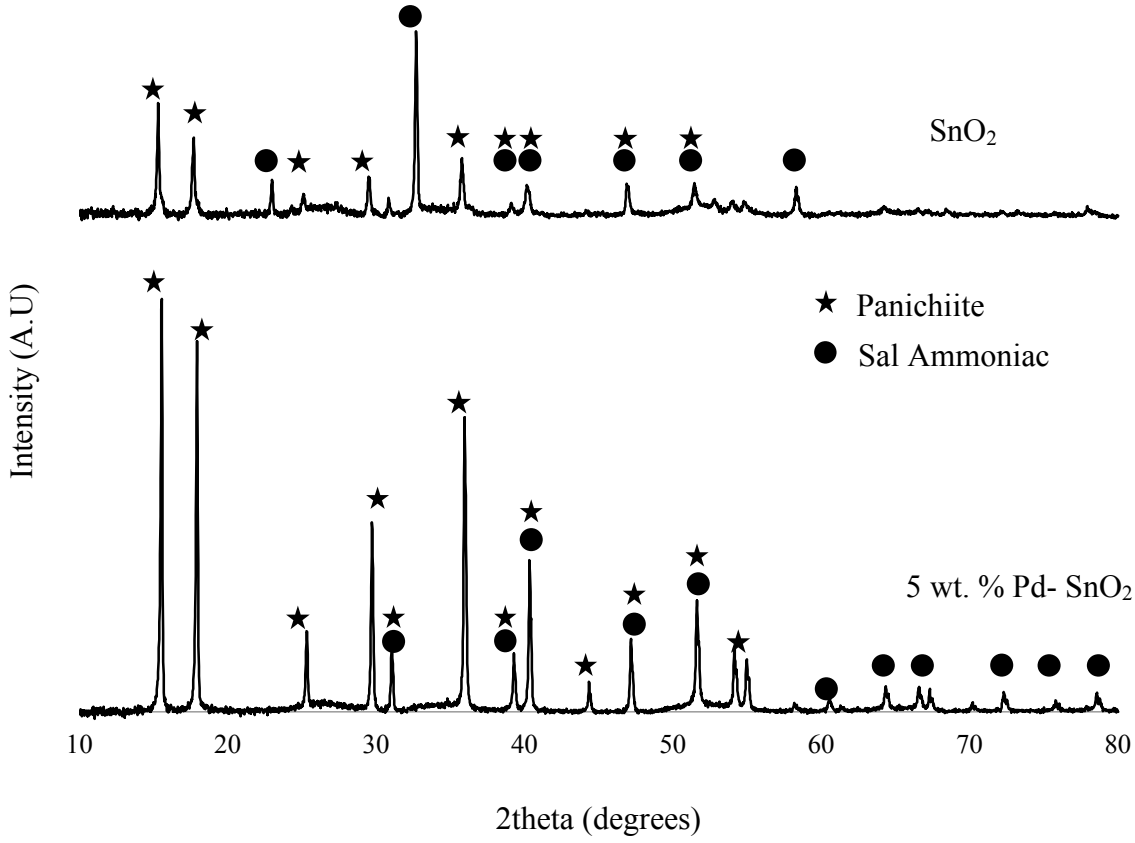

Figure 5.8: XRD patterns of SnO_2 and 5 wt. % Pd-SnO_2 materials prepared via sol-gel before calcination.

The same samples were analysed via XRD after a calcination procedure of 500 °C for 3 hours in static air. The patterns shown in figure 5.9 are completely different to the patterns of the dried only materials previously discussed in figure 5.8. After calcination, the remaining precursor materials are no longer present and nearly all reflections in the diffraction patterns of both samples are attributed to SnO_2, also known as cassiterite. The diffraction pattern of the 5 wt.% Pd-SnO_2 does however show some features that are not present in the SnO_2 only sample. There is a sharp reflection at 40 degrees and another reflection at 46 degrees, both of these can be attributed to either metallic Pd or a PdSn intermetallic species, seeing as the catalyst has not been subjected to any sort of reduction and the Pd and Sn precursors have been intimately mixed it is logical to assign both the reflections at 40 and 46 degrees as a PdSn ($Pd_{3.4}Sn_{0.6}$)[31] species.

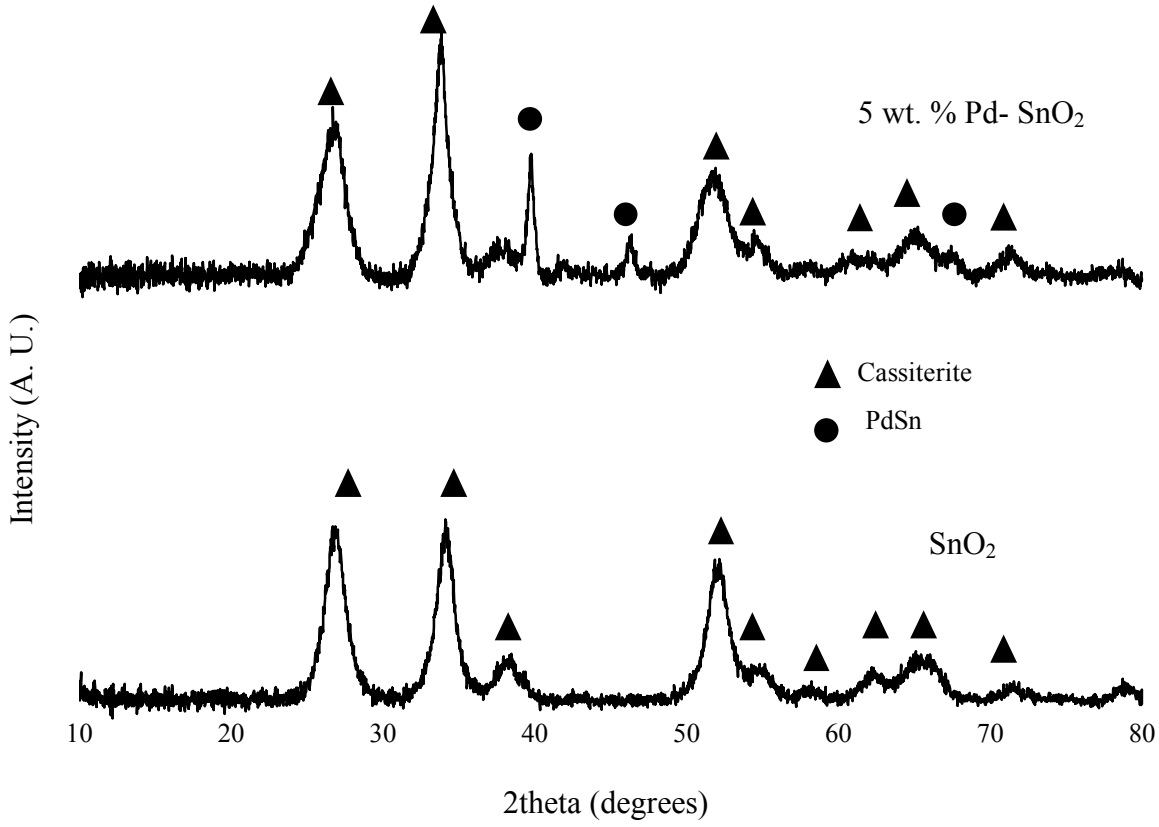

Figure 5.9: XRD patterns of SnO_2 and 5 wt. % Pd-SnO_2 materials after calcination at 500 °C for 3 hours in static air.

The reflections are broader and of lower intensity suggesting that the crystallite size has decreased upon calcination. This is consolidated by the crystallite size calculations of SnO_2 samples before and after calcination shown below in table 5.9:

Material	**Crystal Phases Present**	**Average Crystallite Size (Angstroms)**
SnO_2 prepared via sol gel, dried 80 °C only	Panichiite ($(NH_4)_2SnCl_6$) Sal Ammoniac (NH_4Cl)	773
SnO_2 prepared via sol gel, dried at 80 °C then calcined at 500 °C for 3 hours in static air	Cassiterite (SnO_2)	508

Table 5.9: Average crystallite size of SnO_2 materials prepared via sol-gel, before and after calcination.

Figure 5.10 shows the XRD patterns of a 5 wt.% Pd-SnO_2 catalyst after a reduction at both 200 °C and 300 °C. Both samples show the disappearance of the reflection at 46 degrees, suggesting that upon reduction the intermetallic species has been affected by the reductive heat treatment. Interestingly, when the reduction temperature is increased to 300 °C there are is a subtle new feature in the XRD pattern of the Pd-SnO_2 catalyst, a reflection at 41 degrees, this is characteristic of another PdSn intermetallic species, Pd_3Sn_2. Lorenz *et al*[31] also report the formation of a Pd_3Sn_2 species after subjecting a Pd/SnO_2 to reduction temperatures of 300 °C and above, the authors report that this intermetallic species was not present for samples reduced below 300 °C.

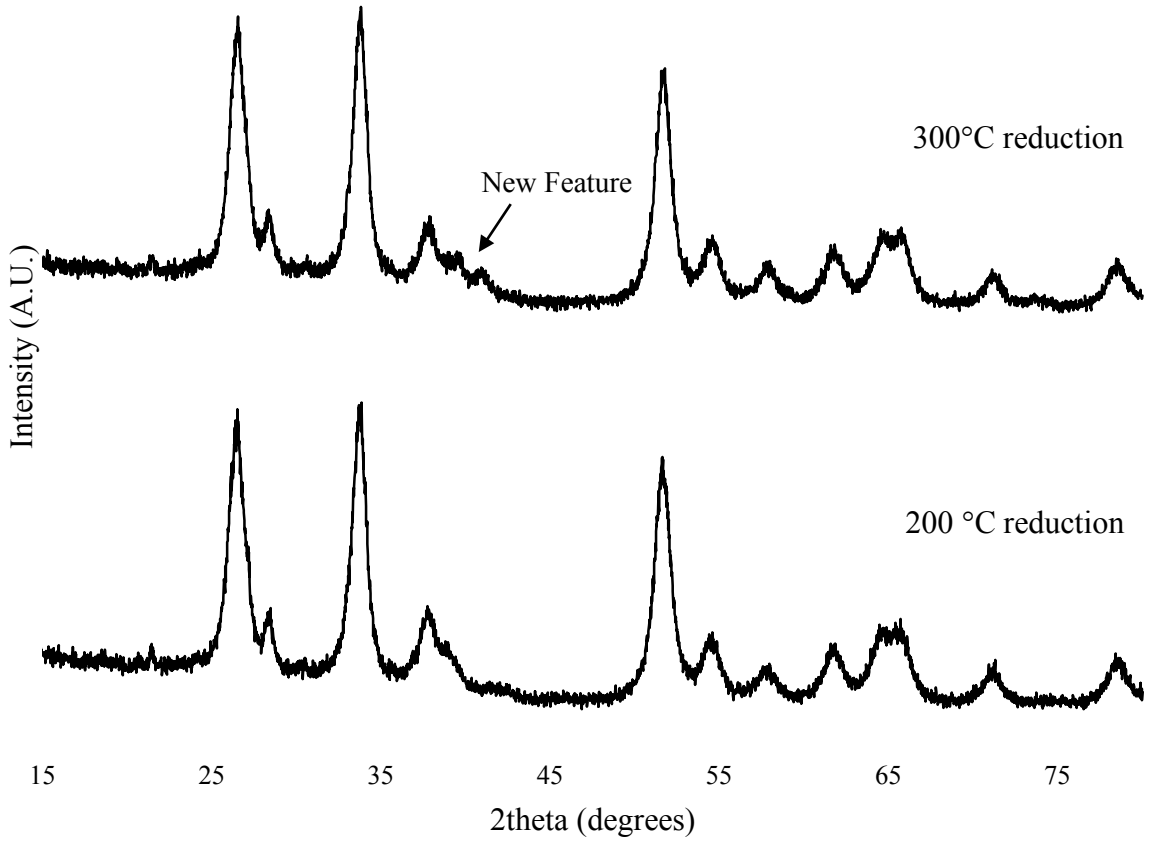

Figure 5.10: XRD Patterns of 5 wt.% Pd-SnO_2 materials after calcination at 500 °C for 3 hours in static air, followed by reduction at both 200 and 300 °C for 2 hours in 5% H_2/Ar. Reflections are as assigned in figure 5.9.

Moreover, it should be noted that no metallic Pd is observed in the XRD diffraction profiles of both the reduced catalysts, this further supports the theory that reduction of the sol-gel catalysts leads to a partially reduced Pd species and not metallic Pd that is in turn leading to the observed decrease in H_2O_2 synthesis and increase in degradation.

5.2.4.2 *In-situ* X-ray Diffraction

In-situ XRD was used to analyse the change of the crystal structure as the catalyst material is subjected to the calcination procedure and observe how the SnO_2 crystal structure forms throughout the calcination. Analysis of the *in-situ* XRD patterns shows that both sal ammoniac and panichiite are present up to a temperature of 200 °C after which the sal ammoniac is no longer present. We then see the underlying broader cassiterite peaks start to

appear and the sharp panichiite peaks decrease in intensity, when a temperature of 300 °C is reached then the XRD profile only shows peaks attributable to cassiterite and this is the case from 300 – 500 °C with no clear peaks shifts or change in shape/intensity.

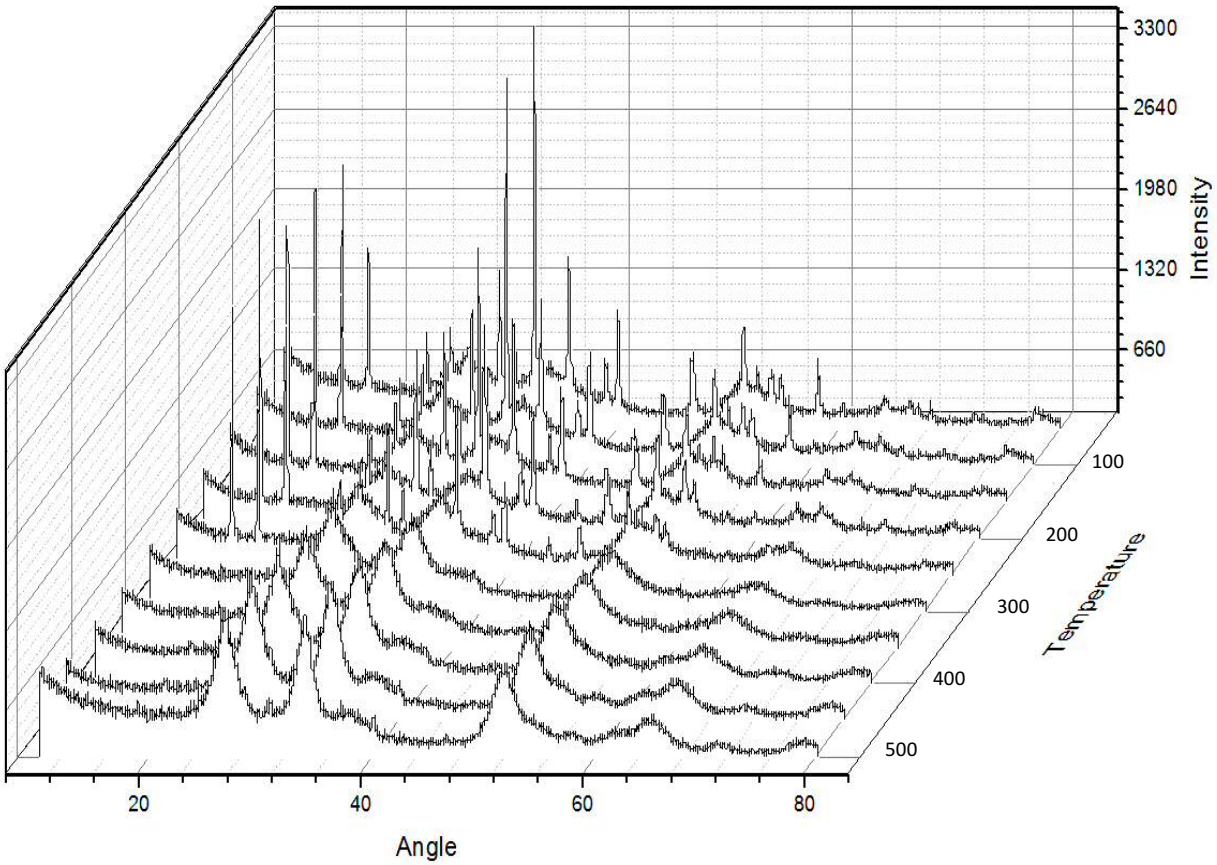

Figure 5.11: *In-situ* XRD pattern of 5 wt.% Pd-SnO_2 material synthesised via sol-gel during calcination process at 500 °C for 3 hours in static air.

5.2.4.3 Temperature Programmed Reduction

An ORO heat treatment cycle has been shown by Freakley *et al*[17] to switch off the hydrogenation activity in an active 5 wt.% SnPd/TiO_2 catalyst. In addition, work previously discussed in this chapter demonstrated that when a 5 wt.% Pd/SnO_2 catalyst is subjected to the same ORO heat treatment, the SnO_2 interacts with the Pd nanoparticles. However, we have seen that reduction of the sol-gel catalysts leads to a substantial reduction in the catalytic activity towards H_2O_2 synthesis and an increase in the H_2O_2 hydrogenation activity. Temperature programmed reduction was used to study the effect of a reduction step on two catalysts. Firstly, a 5 wt.% Pd-SnO_2 catalyst prepared via sol-gel (calcined at 500 °C for 3

hours in static air) and secondly a 5 wt.% Pd/SnO_2 catalyst prepared via impregnation (calcined at 500 °C for 3 hours in static air, SnO_2 support synthesised via sol-gel). The TPR profiles are shown below in figure 5.12:

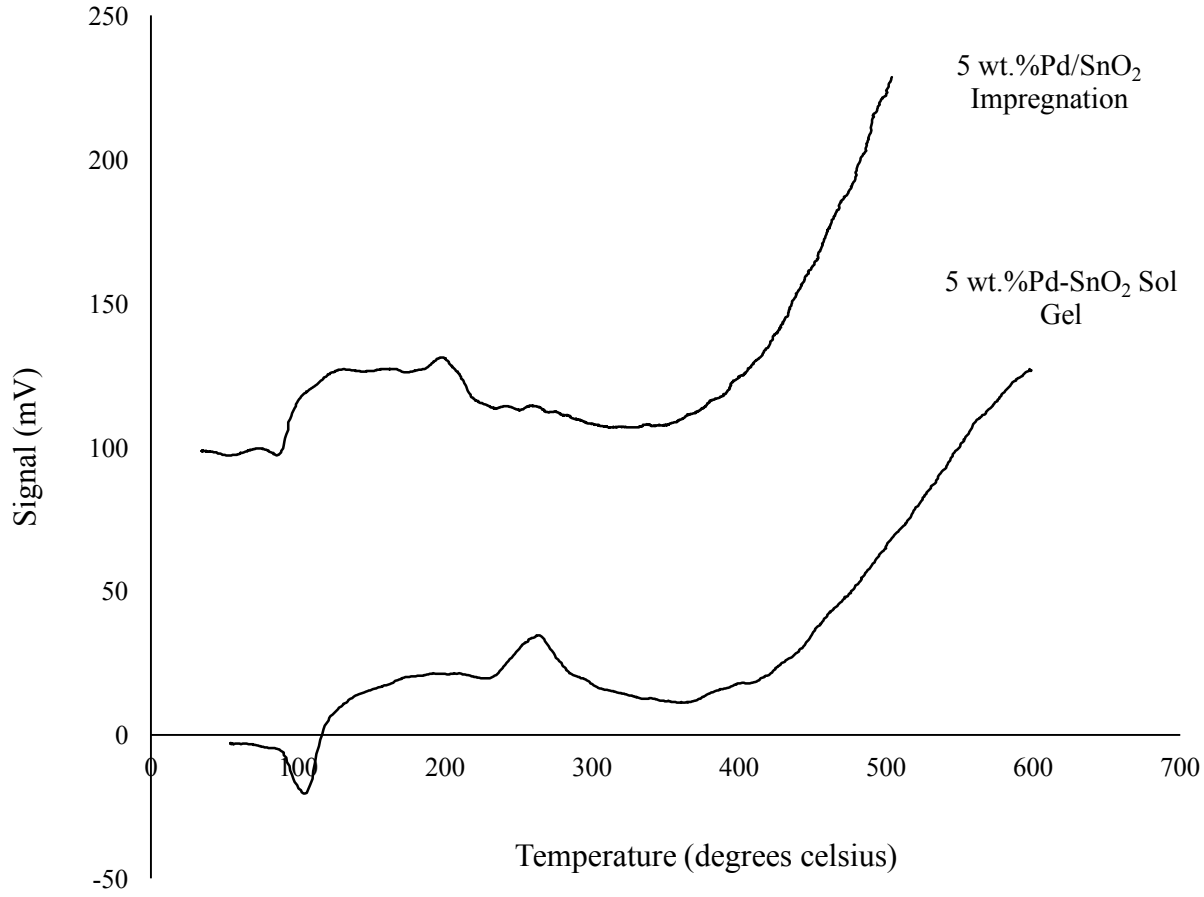

Figure 5.12: TPR profiles of 5 wt.% Pd-SnO_2 and 5 wt.% Pd/SnO_2 materials prepared via sol-gel and impregnation respectively.

In the profile of the 5 wt.% Pd-SnO_2 sol-gel catalyst there is a negative signal observed at approximately 100 °C, this feature is typically seen in the TPR profiles Pd containing materials and can be attributed to the decomposition of Pd beta-hydride. Whilst this feature is also present in the 5 wt.% Pd/SnO_2 catalyst prepared via impregnation, it has been greatly supressed, indicating that the Pd present in this catalyst material is in some way interacting with the SnO_2 support, however it cannot be said for certain that this is due to an alloy formation. There is a second feature in the profile of the 5 wt.% Pd-SnO_2 sol-gel catalyst, centred at approximately 270 °C likely due to the reduction of SnO_2 before the onset of a

bulk reduction. Interestingly, this correlates well with the XRD pattern of the same material after a 300 °C reduction, where a new Pd feature is present after a reduction at 300 °C but not at 200 °C, this may indicate that the reduction is leading to an interaction between the Pd metal particles and the SnO_2 support. This feature is present at a much lower temperature in the TPR profile of the impregnation catalyst, centred at around 200 °C, this may be due to the Pd interacting with the SnO_2 and lowering one of the SnO_2 reduction bands compared to the sol-gel catalyst. This lower reduction temperature also supports the work of Freakley *et al*[17] who showed that a reduction temperature of 200 °C is sufficient to induce a structural change in $PdSn/TiO_2$ catalysts prepared via impregnation. Finally, we see the onset of a bulk reduction at approximately 400 °C in both samples.

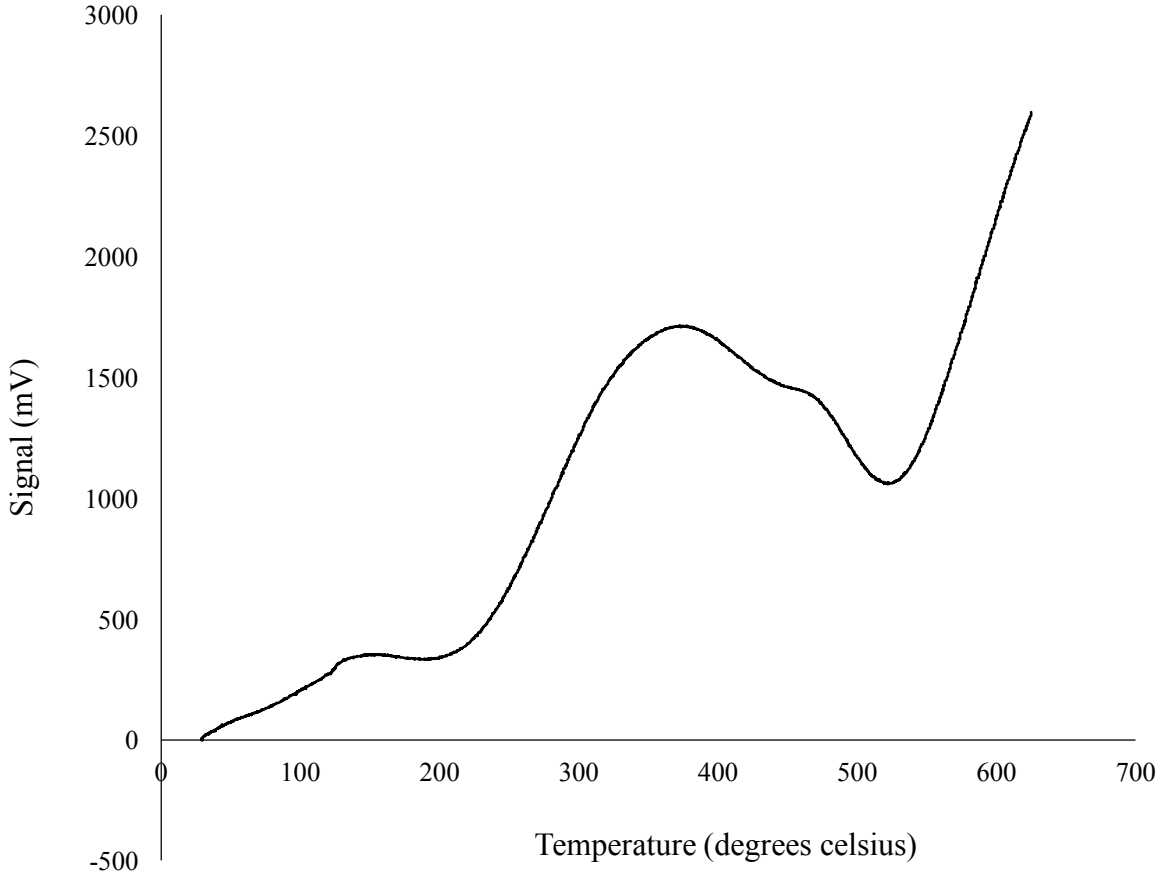

Figure 5.13: TPR profile of SnO_2 material prepared via sol-gel

TPR analysis of the SnO_2 support, prepared via sol-gel, was also conducted for a comparison with the Pd containing samples. The profile, shown in figure 5.13 is distinctly different to the Pd containing samples. There are two large features in the profiles, firstly at approximately

250 – 300 °C which is attributed to the reduction of Sn^{IV} to Sn^{II} and secondly, at approximately 525 – 550 °C which is attributed to the reduction of Sn^{II} to metallic Sn.

5.2.4.4 Thermogravimetric Analysis

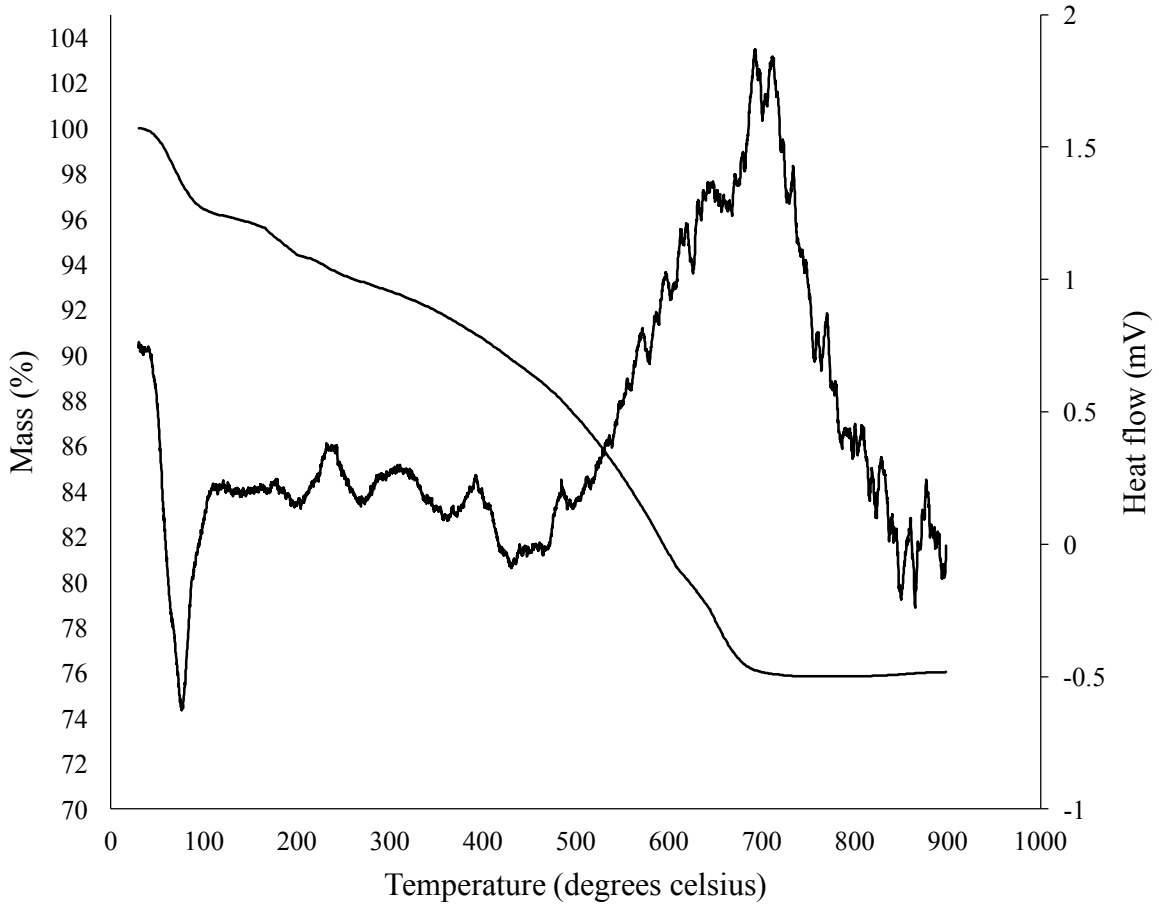

Figure 5.14: TGA profile of 5 wt.% Pd-SnO_2 material prepared via sol-gel and calcined at 500 °C for 3 hours. TGA analysis performed under a 5% H_2/Ar atmosphere.

The results of the TPR experiments yielded some interesting results for the 5 wt.% Pd-SnO_2 sol-gel catalyst, the data showed that reduction of this catalyst material may need to be conducted at above 200 °C to induce an interaction between the Pd particles and the SnO_2 support. To establish more information about this, TGA analysis was performed in a 5% H_2/Ar atmosphere. An initial mass loss is seen due to H_2O evaporation, following this there are 3 small positive features, in the heat flow between 200 and 400 °C and interestingly the first is in the temperature range of 220 – 260 °C, like that seen in the TPR profile of the same

material, further suggesting that the SnO_2 is being modified by the Pd particles, leading to a lowering in the Sn reduction. As bulk reduction of SnO_2 occurs, there is a large positive heat flow seen between 500 and 700 °C, this is also correlated with a large mass loss. Once reduction is complete, there is no further mass loss and a large negative feature is seen in the heat flow.

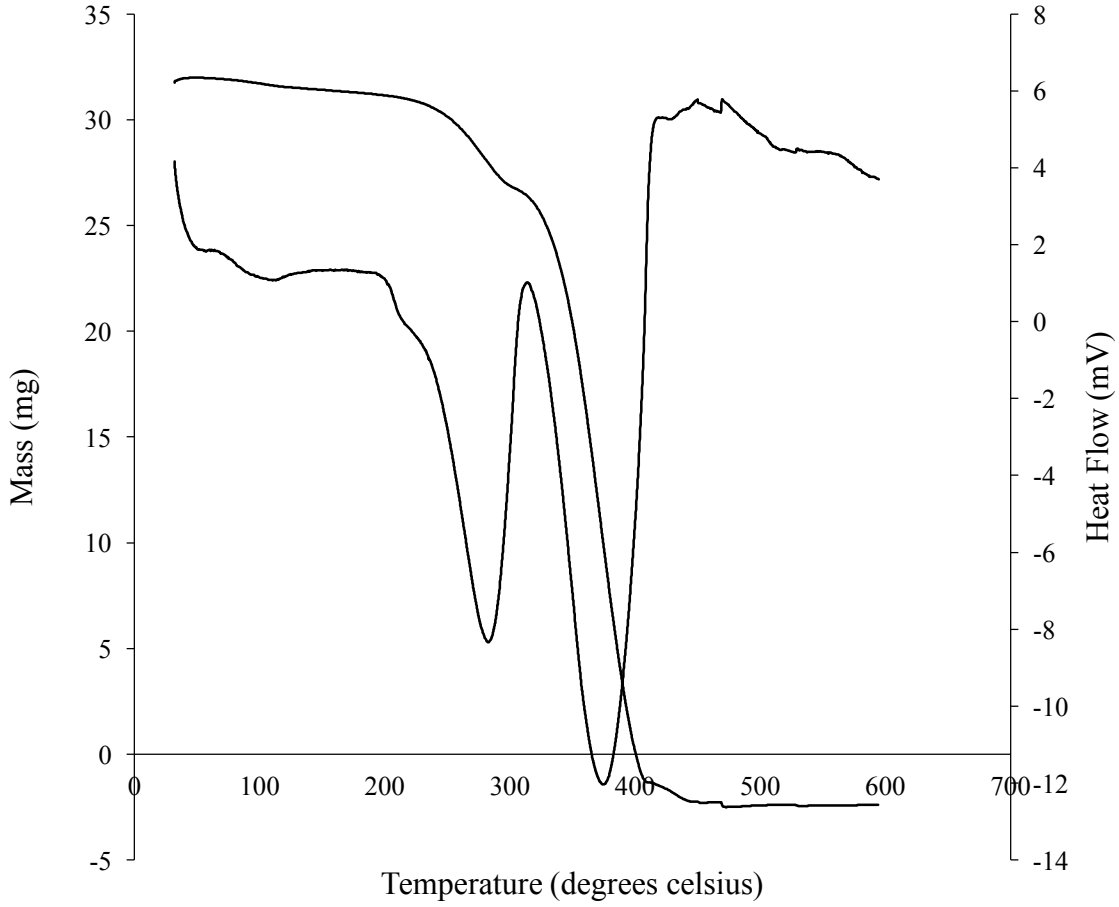

Figure 5.15: TGA profile of SnO_2 material prepared via sol-gel.

For completeness and to ensure the calcination temperature was at a high enough temperature, a TGA of bare SnO_2 was performed. There are two distinct mass losses in the TGA profile, firstly between 220 and 300 °C and secondly between 320 and 400 °C. The first mass loss can be attributed to the loss of ammonium-and chlorine-based precursors, as this correlates well with the *in-situ* XRD data. The second mass loss is much larger than the first and can be attributed to the loss of the remaining precursors as SnO_2 formation is completed, again, this correlates well with the *in-situ* XRD data. Both mass losses also show a large

negative heat flow, indicating an endothermic process. This data confirms the testing data shown earlier in this chapter, that calcination temperatures greater than 400 °C are needed to lead to a greater catalyst stability, after which, catalyst stability and activity can be attributed to factors such as precious metal leaching and sintering. It should be noted that a negative mass loss is seen at the end of the analysis, this is attributed to an error in the experimental run and weighing of the sample, however this error does not affect the outcome of the experiment.

5.2.4.5 BET Surface Area Analysis

Catalyst Name	**Surface Area (m^2 g^{-1})**
SnO_2 (sol –gel)	125
5 wt.% Pd-SnO_2 (sol-gel)	96
SnO_2 (literature value)[27]	111

Table 5.8: BET surface areas of 5 wt.% Pd-SnO_2 and SnO_2 materials prepared via sol-gel. Literature value for SnO_2 is also given.

BET surface area analysis was performed to investigate how similar the SnO_2 materials prepared via sol-gel were to the literature value. The literature value shown is 110 m^2 g^{-1} and the bare SnO_2 synthesised via the same sol-gel technique is 125 m^2 g^{-1}, the results are therefore in good agreement. The 5 wt.% Pd-SnO_2 catalyst does have a slightly lower surface area, 96 m^2 g^{-1}, however this is relatively a high surface area. High surface areas are typical of materials prepared via sol-gel as the rate of hydrolysis and condensation can be controlled by adjusting the concentration and addition rate of the hydrolysing agent, NH_3OH in this case. Using a relatively low concentration of NH_3OH and a slow addition rate leads to a retarded rate of hydrolysis and particle growth, meaning less particle aggregation occurs, this is also in good agreement with the XRD particle size data, which showed that SnO_2 crystallite particle size was only approximately 50 nm.

5.2.4.6 Scanning Transmission Electron Microscopy

STEM analysis was performed on two different catalysts samples, a 5 wt.% Pd/SnO_2 catalyst prepared via impregnation (SnO_2 support prepared via sol-gel) and a 5 wt.% $Pd\text{-}SnO_2$ catalyst prepared via sol-gel. The STEM images of the impregnation catalyst are shown below in figures 5.16 a - d:

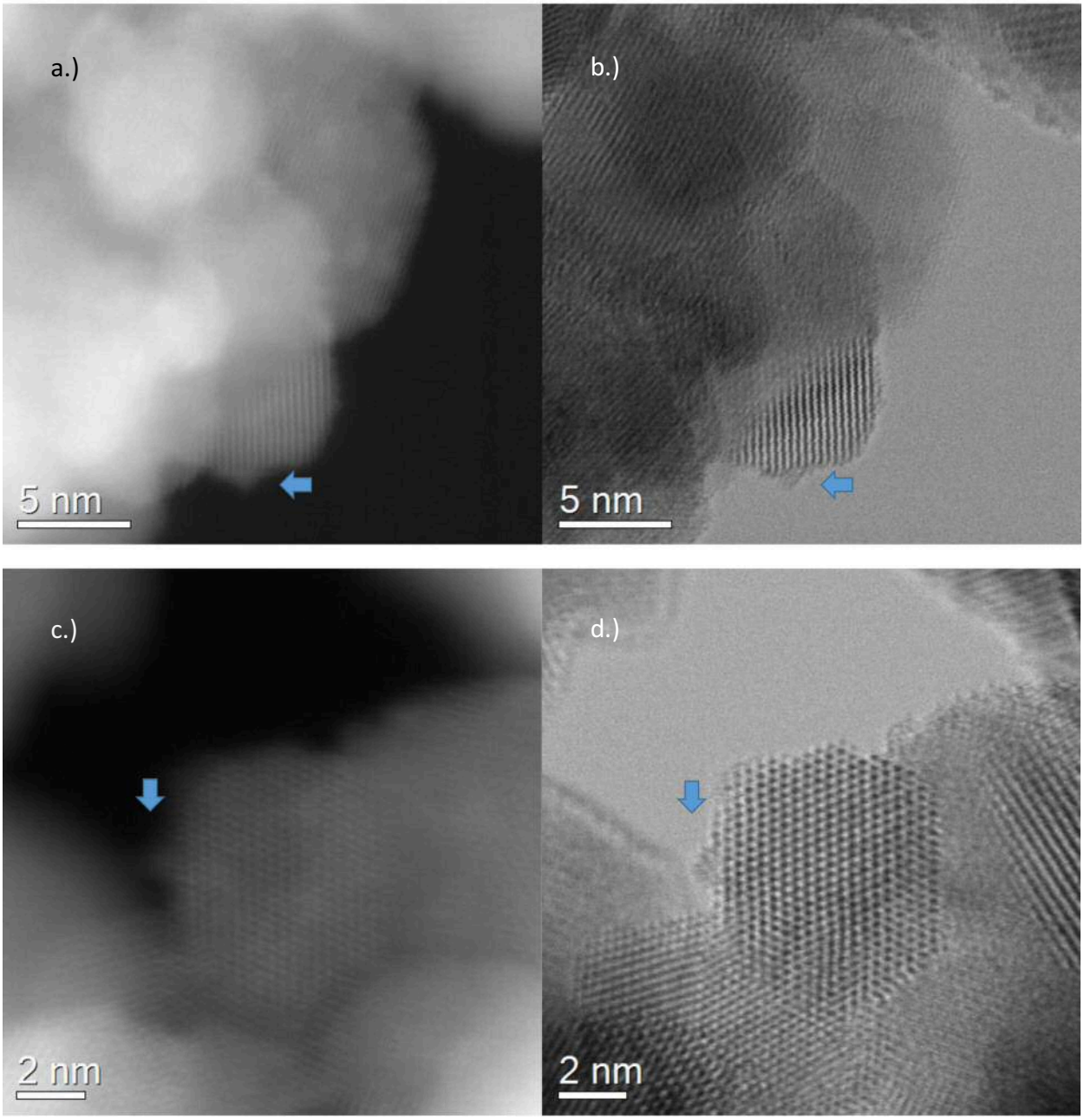

Figure 5.16a - d: STEM images of a 5 wt.% Pd/SnO_2 catalyst prepared via impregnation (SnO_2 support prepared via sol-gel), calcined at 500 ° C for 3 hours in static air.

The images show that the SnO_2 particles are small and a well-ordered crystal lattice can be seen, particularly in the bright field images. The Pd nanoparticles are indicated by the blue arrows and can be seen on the surface of SnO_2 support particles, they are approximately 1 nm in diameter and are "sitting" on the SnO_2 support surface similarly to the 5 wt.% Pd/SnO_2 catalyst investigated earlier in this chapter. EELS spectrum images of the same sample are shown below in figure 5.17:

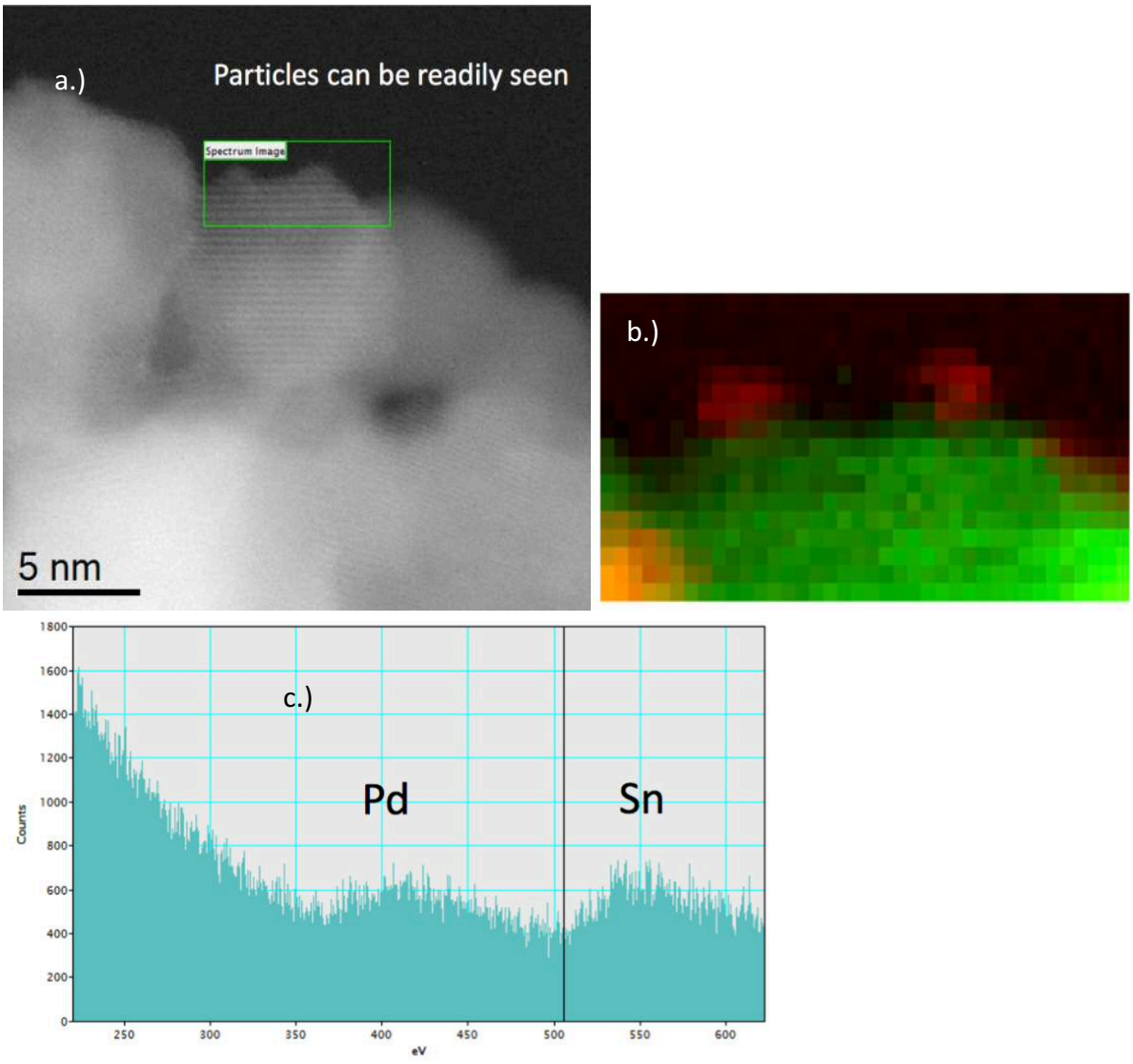

Figure 5.17a - c: STEM image and EELS spectrum of 5 wt.% Pd/SnO_2 material prepared via impregnation (SnO_2 support prepared via sol-gel), calcined at 500 °C for 3 hours in static air.

The EELS spectrum images shown in figures 5.17b and 5.17c show that the Pd nanoparticles are visible on the SnO_2 surface and that there is a Sn edge presence with Pd, which is

indicative of alloying. These images confirm that the sol-gel method is an effective way of synthesising SnO_2 and if the parameters are controlled correctly during the synthesis then the SnO_2 particles are small with a well-ordered crystal lattice and that small Pd nanoparticles can be easily impregnated onto the surface and potentially form alloys.

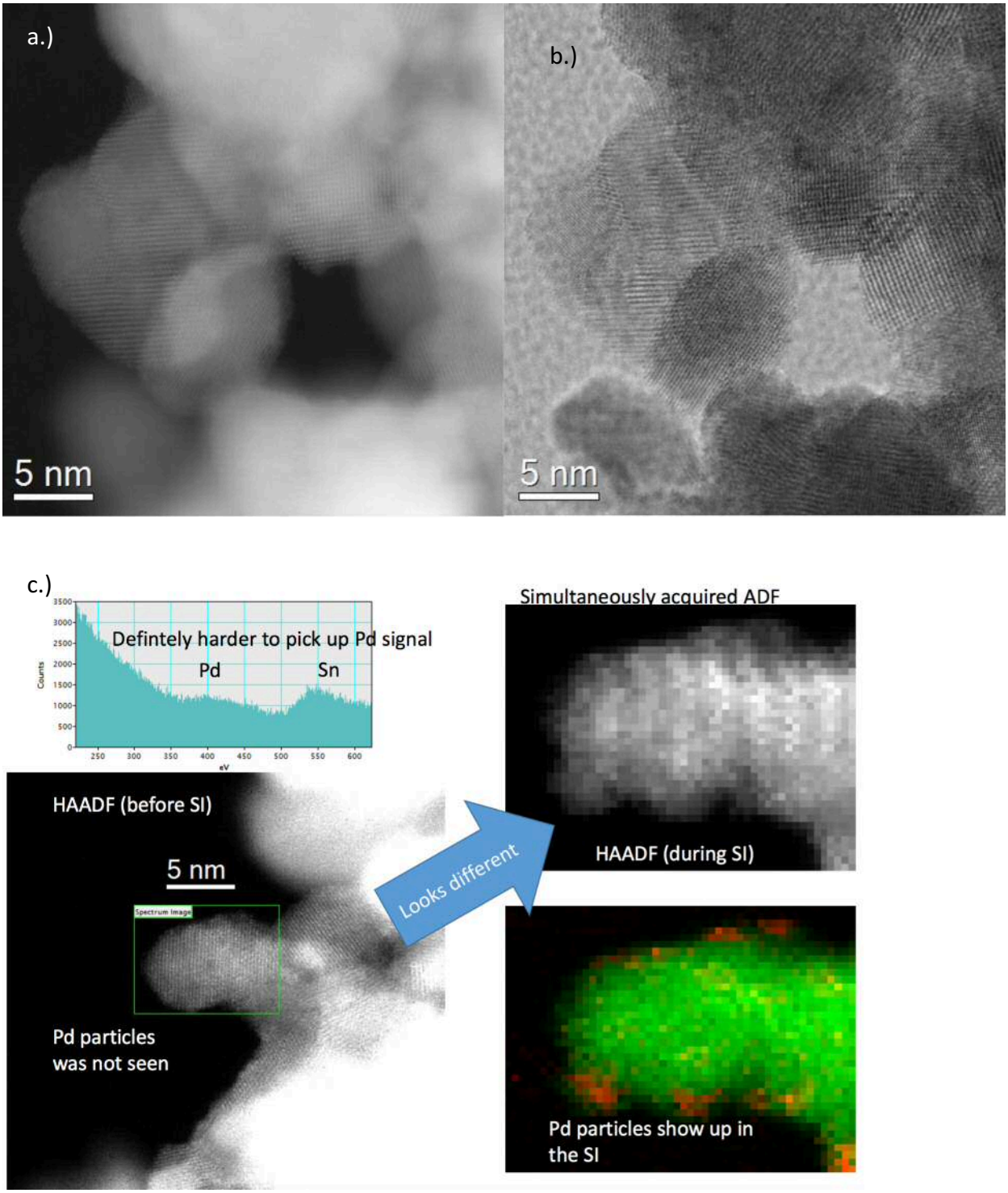

Figure 5.18a - c: STEM images and EELS spectrum of 5 wt.% Pd-SnO_2 material prepared via sol-gel and calcined at 500 °C for 3 hours in static air.

STEM analysis of the sol-gel 5 wt.% Pd-SnO_2 was then performed to compare the preparation methods and check if any differences in the Pd particles could be seen. The bright field and high annular dark field images shown in figure 5.18a and 5.18b show that the SnO_2 particles are essentially identical to the impregnation catalyst, however in the sol-gel sample the Pd particles can't be readily seen. Indeed, even after close inspection it is difficult to confirm the presence of Pd particles. Analysis with EELS was performed and led to an interesting observation, Pd nanoparticles are visible after the beam damage caused by the EELS analysis, this is shown in figure 5.17c, this observation suggests that the Pd nanoparticles are intimately mixed with the SnO_2 and are dispersed in a finer form. These images provide further evidence that the intimate mixing of the SnO_2 and Pd precursors during the sol-gel process leads to the potential formation of PdSn bimetallic species which may influence the activity of the catalyst for the direct synthesis of H_2O_2. The reduced visibility of the Pd nanoparticles in the STEM images in contrast with the impregnated sample and the reduced Pd signal in the EELS spectra help to confirm the structural differences in the catalysts prepared via the sol-gel method.

5.3 Conclusions

A new catalyst preparation method for the synthesis of supported Pd heterogeneous catalysts and their use in the direct synthesis of H_2O_2 has been investigated. It has been found that the sol-gel technique can be used to prepare a Pd-SnO_2 catalyst that is highly active towards the direct synthesis of H_2O_2, out performing well established catalysts such as 5 wt.% $AuPd/TiO_2$, which is thought to be a yardstick for comparing heterogeneous Pd catalysts.

The relationship between Pd and Sn in heterogeneous catalysts has been further examined and it has been shown that a strong interaction between supported Pd nanoparticles and a SnO_2 support can be induced by performing a simple reduction of an already calcined catalyst. Unlike PdSn bimetallic catalysts, only a marginal selectivity increase towards H_2O_2 synthesis is induced by performing an ORO heat treatment, suggesting that the interactions induced between a SnO_2 support and Pd nanoparticles are different to those in the PdSn bimetallic catalysts.

Moreover, this work leads to the conclusion that by selective design of the preparation method, a strong interaction between Pd surface species and a bulk SnO_2 support can be

easily produced. Indeed, it has been shown that by using a sol-gel technique Pd nanoparticles can be intimately mixed within a high surface area SnO_2 material and a simple calcination leads to a highly active catalyst for the direct synthesis of H_2O_2. The sol-gel technique has been shown to be superior to the impregnation technique for the preparation of SnO_2 supported Pd as a catalyst for the direct synthesis of H_2O_2. In the context of the direct synthesis of H_2O_2 and potentially, selective hydrogenations, this represents a step forward in the design of heterogeneous Pd catalysts.

5.3 References.

1. S. J. Tauster, *Acc. Chem. Res.*, **1987**, *20*, 389 – 394.
2. S. J. Tauster, S. C. Fung, R. T. K. Baker, J. A. Horsley, *Science*, **1981**, 211, 1121 – 1125.
3. R. Burch, P. R. Ellis, *Appl. Catal. B.*, **2003**, *42*, 203-211.
4. V. R. Choudhary, S. D. Sansare, A. G. Gaikwad, *Catal. Lett.*, **2002**, *84*, 81-87.
5. M. J. Maraschino, US Patent No. 5, **1992**, *169*, 618.
6. J. K. Edwards, B. Solsona, P. Landon, A. F. Carley, A. Herzing, M. Wanatabe, C. J. Kiely, G. J. Hutchings, J. Mater. Chem., **2005**, *15*, 4595 – 4600.
7. T. Miyahara, H. Kanzaki, R. Hamada, S. Kuroiwa, S. Nishiyama, S. Tsuruya, *J. Mol. Catal. A.*, **2001**, *176*, 141-150.
8. B. S. Uphade, T. Akita, T. Nakamura, M. Haruta, *J. Catal.*, **2002**, *209,* 331-340.
9. D. I. Enache, D. W. Knight, G. J. Hutchings, *Catal. Lett.*, **2005**, *103*, 43 – 52.
10. I. W. C. E. Arends, R. A. Sheldon, *Appl. Catal. A.*, **2001**, *212*, 175 – 187.
11. Y. Wang, Q. H. Zhang, T. Shishido, K. Takehira, **2002**, *J. Catal.*, **209**, 186 – 196.
12. J. A. Schwartz, *Chem. Rev*., **1995**, *95*, 477 – 510.
13. G. A. Nicolaon, S. J. Teichner, *Bull. Soc. Chim. Fr*., **1968**, *5*, 1906 – 1911.
14. M. A. Cauqui, J. M. J. Rodriguez-Izquidero, *J. Non-Cryst. Solids*., **1992**, *14*, 724 – 738.
15. R. Gomez, V. Bertin, M. A. Ramirez, T. Zamudio, P. Bosch, I. Schifter, T. Lopez, *J. Non-Cryst. Solids.*, **1992**, *147/148*, 748-752.
16. G. Boskovic, M. Kovacevic, E. Kiss, J. Radnik, M. Pohl, M. Schneider, U. Bentrup, A. Bruckner, *Int. J. Environ. Sci. Technol.*, **2012**, *9*, 235 – 246.
17. J. A. Lopez-Sanchez, N. Dimitratos, P. Medziak, E. Ntainjua, J. K. Edwards, D. J. Morgan, A. F. Carley, R. Tiruvalam, C. J. Kiely, G. J. Hutchings, *Phys. Chem. Chem. Phys.*, **2008**, *10*, 1921 – 1930.
18. J. K. Edwards, B. Solsona, E. Ntainjua, A. F. Carley, A. A. Herzing, C. J. Kiely, G. J. Hutchings, *Science*, **2009**, *23*, 1037 – 1041.
19. K. V. R. Chary, D. Naresh, V. Vishwanathan, M. Sadakane, W. Ueda, *Cat. Comm.*, **2007**, *8*, 471 – 477.
20. S. J. Freakley, Q. He., J. H. Harrhy, L. Liu, D. A. Crole, D. J. Morgan, E. N. Ntainjua, J. K. Edwards, A. F. Carley, A. Y. Borisevich, C. J. Kiely, G. J. Hutchings, *Science*, **2016**, *351*, 965 – 968.

21. T. Takeguchi, O. Takeoh, S. Aoyama, J. Ueda, R. Kikuchi, K. Eguchi, *Appl. Catal. A.*, *252*, **2003**, 205 – 214.
22. J. Zhao, L. Ma, X. L. Xu, F. Feng, X. N. Li, *Chin. Chem. Lett.*, **2014**, *25*, 1137 – 1140.
23. L. Sun, Z. Liu, Y. Bao, H. Xi, W. Bao, *Int. J. Mat. Res.,* **2014**, *105*, 584 – 587.
24. B. Mirkelamoglu, G. Karakas, *Appl. Catal. A.*, **2005**, *281*, 275 – 284.
25. R. Gavagnin, L. Biasetto, F. Pinna, G. Strukul, *Appl. Cat. B.*, **2002**, *38*, 91 – 99.
26. N. Kamiuchi, H. Muroyama, T. Matsui, R. Kikuchi, K. Eguchi, *Appl. Catal. A.*, **2010**, *379*, 148 – 154.
27. R. Adnan, N. A. Razana, I. A. Rahman, M. A. Farrukh, *J. Chin. Chem. Soc.*, **2010**, *57*, 222 – 229.
28. J. K. Edwards, B. E. Solsona, P. Landon, A. F. Carley, A. Herzing, C. J. Kiely, G. J. Hutchings, *J. Catal.*, **2005**, *236*, 69 – 79.
29. M. Sankar, Q. He, M. Morad, J. Pritchard, S. J. Freakley, J. K. Edwards, S. H. Taylor, D. J. Morgan, A. F. Carley, D. W. Knight, C. J. Kiely, G. J. Hutchings, *ACS Nano,* **2012**, *6*, 6600 – 6613.
30. D. P. Dissanayake, J. H. Lunsford, *J. Catal.*, **2002**, *206*, 173 – 176.
31. H. Lorenz, Q. Zhao, S. Turner, O. I. Lebdev, G. V. Tendeloo, B. Klotzer, C. Rameshan, K. Pfaller, J. Konzett, S. Penner, *Appl. Catal. A.*, **2010**, *381*, 242 – 252.

Chapter 6

Conclusions and Future Work

It was discussed in chapter 1 how there is currently many uses for H_2O_2 and hence why it is produced on a global scale in huge quantities, predominantly via the anthraquinone process. In recent years, the direct synthesis of H_2O_2 from H_2 and O_2 has been widely researched however this is yet to make the shift from laboratory research to real-world application. A key issue with the anthraquinone process is that it is only economically viable to produce very concentrated solutions, typically 40 wt.%. The transportation of such concentrated solutions poses serious health and safety risks and moreover, H_2O_2 is regularly diluted down to much more dilute concentrations at the point of use. An application that may present the opportunity for the direct synthesis of H_2O_2 to make the jump from academic research to real-world application is wastewater sterilisation, yet to our knowledge there is no literature or industrial product that utilises *in-situ* derived H_2O_2 for this application. This is addressed in chapter 3 and it is reported for the first time that *in-situ* derived H_2O_2 generated in a small flow reactor is capable of sterilising model wastewater solutions. Furthermore, *in-situ* derived H_2O_2 shows superior antimicrobial properties when compared with *ex-situ* commercially available H_2O_2, the work in this thesis has demonstrated that *in-situ* derived H_2O_2 can eliminate solutions of *Escherichia Coli* (JM109) that are several orders of magnitude more concentrated when compared with the antimicrobial activity of analogous concentrations of *ex-situ* commercially available H_2O_2 for the same bacteria. Research was then extended to encompass both stabilised and unstabilised commercially available H_2O_2 and whilst it was found that the stabilisers present were contributing to the lower observed activity of the *ex-situ* H_2O_2, *in-situ* H_2O_2 still demonstrated greater antimicrobial activity towards *Escherichia Coli* (JM109). Finally, the comparison between H_2O_2 synthesised via the direct synthesis process in a batch reactor and the *in-situ* H_2O_2 generated in the flow reactor was investigated, it was established that synthesised H_2O_2 was as effective as *in-situ* generated H_2O_2, however the difference in contact time between the two led to the conclusion that *in-situ* generated H_2O_2 could be considered the more favourable approach. This work and conclusions presented in chapter 3 therefore represent an important

step forward in the direct synthesis of H_2O_2, providing a platform for a new area of research in that area.

The work performed in collaboration with Prof. Jean-Yves Maillard in the school of pharmacy presented in chapter 4 extends the research detailed in chapter 3, to make the step from a proof of concept study through to a process development that has the end goal of being put into real-life applications. This was done by investigating the antimicrobial activity of *in-situ* generated H_2O_2 on strains of *Staphylococcus Aureus*, *Escherichia Coli* and *Pseudomonas Aeruginosa* that are recognised by the British Standards Industry (BSI). It was found that by optimising the reaction conditions in the continuous flow system and altering the catalyst composition, a maximum reduction of 99.99% of the *Staphylococcus Aureus* and *Escherichia Coli* bacteria could be removed from the wastewater solutions after a single pass through the reactor under *in-situ* generating conditions. The mechanism of cell inactivation is reasoned to occur due to the interaction of free radicals with the bacteria, however, the exact mechanism of cell inactivation is still largely unknown. The future work therefore falls into two parts. Firstly, continuing to optimise the flow reactor system to enable greater concentrations of H_2O_2 to be generated under similarly mild conditions, in the hope of eliminating greater concentrations of bacteria, as would be required for a real-life application. Secondly, investigative work should be performed into understanding the mode of cell inactivation for *in-situ* and *ex-situ* H_2O_2, thus giving a better understanding of the antimicrobial properties which could lead to a more effective system for the treatment of wastewater. Whilst this work has proven for the first time that it is possible to use *in-situ* generated H_2O_2 as an antimicrobial agent, particularly in the case of water treatment, a detailed understanding of the chemistry taking place during such disinfection processes is required. The future work should therefore aim to elucidate the reaction mechanism involving *in-situ* generated H_2O_2 and target bacteria such as *staphylococcus aureus*. EPR experiments should be performed to gain an understanding of the free radicals generated during the *in-situ* and *ex-situ* sterilisation reactions.

The direct synthesis of H_2O_2 may be one of the most studied reactions in heterogeneous catalysis, however there has been little progress in the development of new heterogeneous catalysts in recent years. Chapter 5 focuses on developing Pd/SnO_2 and $Pd\text{-}SnO_2$ catalysts prepared by impregnation and sol-gel techniques respectively. It was found that a sol-gel technique can yield a more active heterogeneous catalyst than the traditional impregnation technique. It was shown that the $Pd\text{-}SnO_2$ sol-gel catalysts allowed for the formation of very

small Pd nanoparticles that were finely dispersed in the SnO_2 lattice. In comparison, Pd/SnO_2 catalysts prepared via impregnation were found to have larger Pd nanoparticles that were weakly interacting with the SnO_2 support. In performing an ORO heat treatment, subtle changes in the catalyst morphology can be induced and this was observed through detailed STEM and EELS analysis performed by Dr Qian He at the Oak Ridge National Laboratory. Future work should focus on further developing this sol-gel process to fine tune the synthesis method as the list of variables with such a preparation method are vast and it is well known that by changing each of these variables it is possible to change the features of the resultant catalyst material. In addition, the heat treatment process can be further investigated and the electronic effects on the Pd and Sn catalyst species that are induced by such a heat treatment should be investigated, with the goal of using these investigations to design a more active and selective catalyst for the direct synthesis of H_2O_2. A detailed catalyst characterisation investigation using techniques such as XPS should also be performed, particularly paying attention to the oxidation state of the Pd and Sn species in both sol-gel and impregnation catalysts. Further characterisation techniques that can give detail on metal dispersion, such as CO chemisorption would also be highly beneficial.

Overall, future work should focus on a more detailed understanding of the underlying chemistry for both greywater sterilisation using *in-situ* generated H_2O_2 and the direct synthesis of H_2O_2 via Pd-SnO_2 catalysts.